UNCLASSIFIED

AD NUMBER
AD024362
CLASSIFICATION CHANGES
TO: unclassified
FROM: confidential
LIMITATION CHANGES
TO: Approved for public release, distribution unlimited
FROM: Distribution authorized to DoD only; Administrative/Operational Use; MAY 1953. Other requests shall be referred to Bureau of Aeronautics, Department of the Navy, Washington, DC 20350. Pre-dates formal DoD distribution statements. Treat as DoD only.
AUTHORITY
NAVAIR ltr dtd 22 Apr 1980; NAVAIR ltr dtd 22 Apr 1980

THIS PAGE IS UNCLASSIFIED

CONFIDENTIAL

AD 24 362

BuAer Report AE-61-4

Fundamentals of Design of Piloted Aircraft Flight Control Systems

Volume IV

THE HYDRAULIC SYSTEM

Reproduction of this document in any form by other than naval activities is not authorized except by special approval of the Secretary of the Navy or the Chief of Naval Operations, as appropriate

PUBLISHED BY DIRECTION OF
THE CHIEF OF THE BUREAU OF AERONAUTICS

NOTICE—This document contains information affecting the national defense of the United States within the meaning of the Espionage Laws, Title 18, U. S. C., Sections 793 and 794. The transmission or the revelation of its contents in any manner to an unauthorized person is prohibited by law.

CONFIDENTIAL

MAY 1953

IMPORTANT NOTE

This volume was written by and for engineers and scientists who are concerned with the analysis and synthesis of piloted aircraft flight control systems. The Bureau of Aeronautics undertook the sponsorship of this project when it became apparent that many significant advances were being made in this extremely technical field and that the presentation and dissemination of information concerning such advances would be of benefit to the Services, to the airframe companies, and to the individuals concerned.

A contract for collecting, codifying, and presenting this scattered material was awarded to Northrop Aircraft, Inc., and the present basic volume represents the results of these efforts.

The need for such a volume as this is obvious to those working in the field. It is equally apparent that the rapid changes and refinements in the techniques used make it essential that new material be added as it becomes available. The best way of maintaining and improving the usefulness of this volume is therefore by frequent revisions to keep it as complete and as up-to-date as possible.

For these reasons, the Bureau of Aeronautics solicits suggestions for revisions and additions from those who make use of the volume. In some cases, these suggestions might be simply that the wording of a paragraph be changed for clarification; in other cases, whole sections outlining new techniques might be submitted.

Each suggestion will be acknowledged and will receive careful study. For those which are approved, revision pages will be prepared and distributed. Each of these will contain notations as necessary to give full credit to the person and organization responsible.

This cooperation on the part of the readers of this volume is vital. Suggestions forwarded to the Chief, Bureau of Aeronautics (Attention AE-612), Washington 25, D. C., will be most welcome.

L. M. Chattler
Head, Actuating & Flight Controls Systems Section
Airborne Equipment Division
Bureau of Aeronautics

PREFACE

This volume, The Hydraulic System, has been written under BuAer Contract NOas 51-514(c) to present to those concerned with the problems of designing integrated aircraft control systems certain basic information regarding hydraulic systems used to position aircraft control surfaces.

The purpose of the volume is to develop mathematical models of typical aircraft hydraulic control systems. The analyses are used to show the effects of various system parameters on stability where aeroelastic behavior of the airframe is not a prominent factor. Portions of the analyses are used to outline possible flutter systems including the aeroelastic airplane, the hydraulic actuator, and other servomechanisms of flight controller loops.

It is mathematically expedient, though somewhat artificial, to treat the flutter problem as a separate entity. This separation corresponds to current practice in the study of the control of aircraft. The material of this volume is therefore presented in two parts.

Part I, composed of eight chapters, is primarily concerned with derivation of the controlling equations of typical actuators and with stability of typical systems embracing an actuator and a simplified control surface. The problem of instability is given heavy emphasis, and several methods for overcoming this difficulty are presented. Details of design have been considered only where the reader may be aided in a physical understanding of the behavior of typical systems. The hydraulic actuator configurations which are discussed have been chosen as most nearly representing current design practice.

Part II of the volume is composed of two chapters. The first deals with the conceptual modification of the classical flutter system to account for the effect on flutter of a complex control system embracing several servomechanisms. A second chapter presents certain techniques for effecting a solution of the complete servo-flutter system.

Among those who have helped in the preparation of this volume, special reference should be made to R. E. Gaskill for his skilful work in transcribing the many equations, and to Shirley Keys who typed the manuscript.

D. T. McRuer, Supervisor
Servomechanisms Section

CONTRIBUTING AUTHORS
G. E. Click
A. P. Henry
R. L. Rishel
J. W. Hager
D. T. McRuer
D. Benun

EDITORIAL BOARD
K. B. Tuttle
E. Moness
F. B. Bacus
J. E. Moser

TABLE OF CONTENTS

PART I

HYDRAULIC ACTUATING SYSTEMS

CHAPTER I

INTRODUCTION

Part I of this volume is concerned specifically with the problems and the general design criteria associated with hydraulically powered aircraft surface controls. The early sections deal with general considerations relating to this subject, and the later chapters discuss more specific applications of particular systems. It should be emphasized that throughout the volume the basic analytical approach rests upon the mathematical models of the transfer functions of interest. The effects of parameter variations upon these transfer functions and upon over-all performance are discussed in the final chapters.

A primary consideration in the design of any type of servomechanism, or of control systems in general, is the ease with which the flow of power is controlled. Among other things which a servo does, it operates as a power amplifier, and therefore the facility with which the power may be metered into some dynamical system determines to a large degree the choice of various components comprising the system. Nearly all the difficulties encountered in the design of any device arise from a misapplication of the most fundamental engineering concepts. In the particular case of a hydraulic control device, certain design shortcomings may be attributed to improper applications of such basic concepts as fluid flow and system dynamics, and to other simpler considerations, mechanical in nature.

With these introductory thoughts in mind, the more general considerations entailed in hydraulics analysis will now be presented.

CHAPTER II

GENERAL CONSIDERATIONS

SECTION 1 - THE NATURE OF THE HYDRAULIC MEDIUM

The hydraulic medium is considered to be a (relatively) incompressible fluid. In addition it is considered to be completely continuous and homogeneous. This implies that, in the hydraulic system, there are no discontinuities, such as cavitation, free air, etc. The hydraulic medium is thus capable of completely filling any cavity or chamber. This hydraulic medium, which will be referred to hereafter as a "liquid," is capable of withstanding compressive loading only. The column of liquid comprising the hydraulic system can be considered as a fluid piston. Therefore a displacement of a volume of liquid anywhere in the hydraulic system will result in an equivalent displacement elsewhere in the system.

Consider a system made up of two movable pistons connected by means of external plumbing.

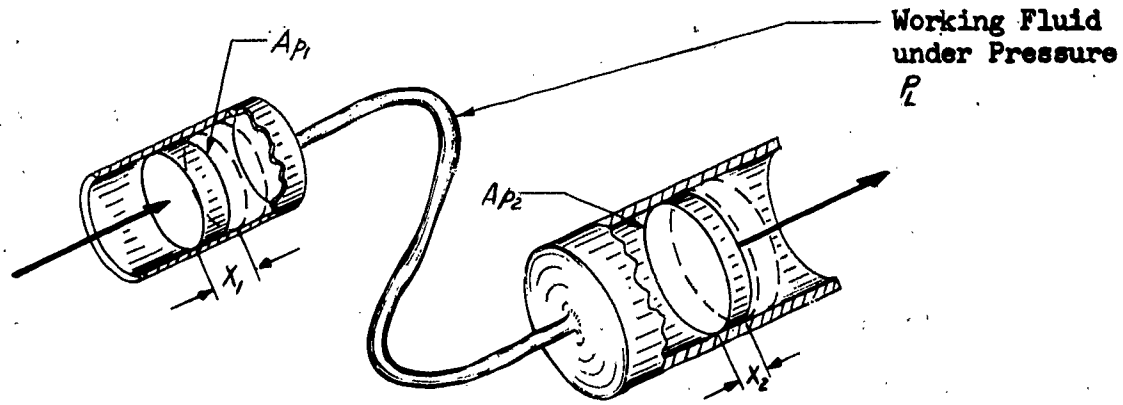

$$P_L = \frac{\text{Output Load}}{A_{P_2}} \qquad X_2 = X_1 \frac{A_{P_1}}{A_{P_2}}$$

Figure II-1. Simple Hydraulic System

The chambers formed by the two pistons and the bores in which they operate and also the interconnecting plumbing are completely filled with liquid. Disregarding the transient state, if one piston is displaced, the entire

column of liquid undergoes an identical volumetric displacement. The linear displacement of the second piston is equal to that of the first piston modified by a proportionality factor which is the ratio of the areas of the two pistons exposed to the hydraulic fluid, A_{P_1}/A_{P_2}. If the output piston operates against a load, the liquid contained in the system is subjected to a compressive loading. The intensity of this loading is the magnitude of the output load divided by the area of the output member as seen by the fluid under compression. The intensity of the compressive stress so generated is referred to as "pressure," which is generally expressed in pounds per square inch. If the velocities encountered in a system are not high, this compressive stress is uniform throughout the system.

The product of the volumetric flow rate (corresponding to the output piston velocity) and the generated pressure yields a time rate of work performed, or power output. In the hydraulic system described above, if the load on the output member is such that a pressure of 1714 pounds per square inch is induced throughout the system, and if the input member is moved so that the fluid is displaced at the rate of one gallon per minute, the system is transmitting one horsepower.

SECTION 2 - GENERATION OF HYDRAULIC POWER

Since the main function of the hydraulic control system is to meter hydraulic power into a dynamical system, a brief discussion of how this power is generated is pertinent. The source of the hydraulic power is a fluid pump of some type, usually driven by the main propulsion unit of the aircraft.

In general, two types of pumps are available: these are classified as hydrokinetic and hydrostatic.

The hydrokinetic type pump involves the handling of relatively large volumes of fluid at fairly low pressures. An example of this type of hydraulic power generator is the well-known centrifugal pump. In a device of this sort, large volumes of fluid are received in a central chamber. This fluid is accelerated in a radial direction and attains high velocity. The momentum thus imparted to the fluid is delivered to the high pressure outlet of the pump as the fluid is decelerated in the outlet chamber. Since this type of fluid power generator is not normally used in aircraft hydraulic systems, only passing mention of the device is made here.

Because minimization of the weight and volume of components used in aircraft systems is of prime importance, the hydrostatic, or positive displacement, type pump is almost universally used. The simplest type of pump (see Figure II-2) is a simple reciprocating piston.

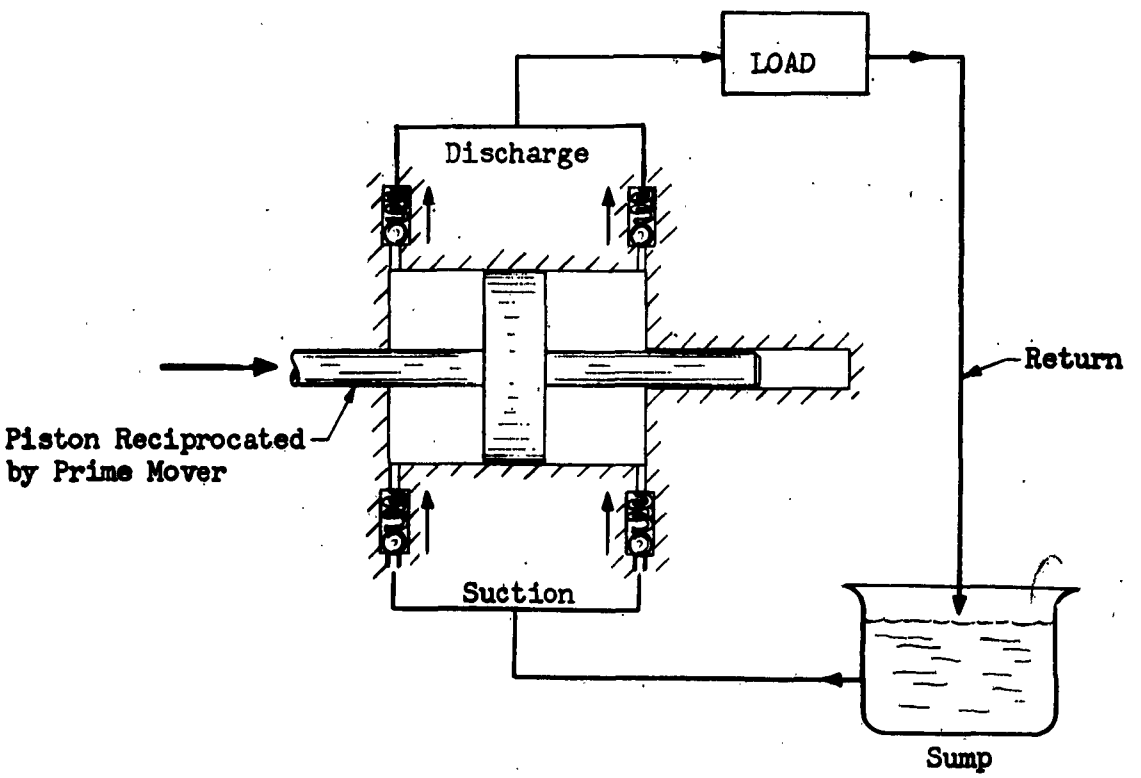

Figure II-2. Simple Reciprocating Piston

The piston is connected to suction and discharge ports by means of appropriate valving such that on the suction part of the stroke the chamber formed by the piston and the bore in which it operates is completely filled with fluid taken from the suction line. During the reverse, or discharge, stroke this volume of fluid is delivered to the discharge line at a somewhat higher pressure. If the piston is driven continuously in an approximately sinusoidal manner by means of a crank mechanism, a simple positive displacement pump is the result.

A device of this type is suitable for use with a compressible fluid; an example is its use as an air compressor. However, this kind of pump cannot be used as a hydraulic power generator since the discharge rate throughout the cycle is not constant, or even approximately so. In order to provide a satisfactory hydraulic power generator, a multiplicity of such pistons must be provided. In addition, the angular phasing of the pistons should be such that each piston performs its suction and discharge functions in a fixed phase relationship to the piston which follows it. To minimize pump output ripple, an uneven number of pistons is employed.

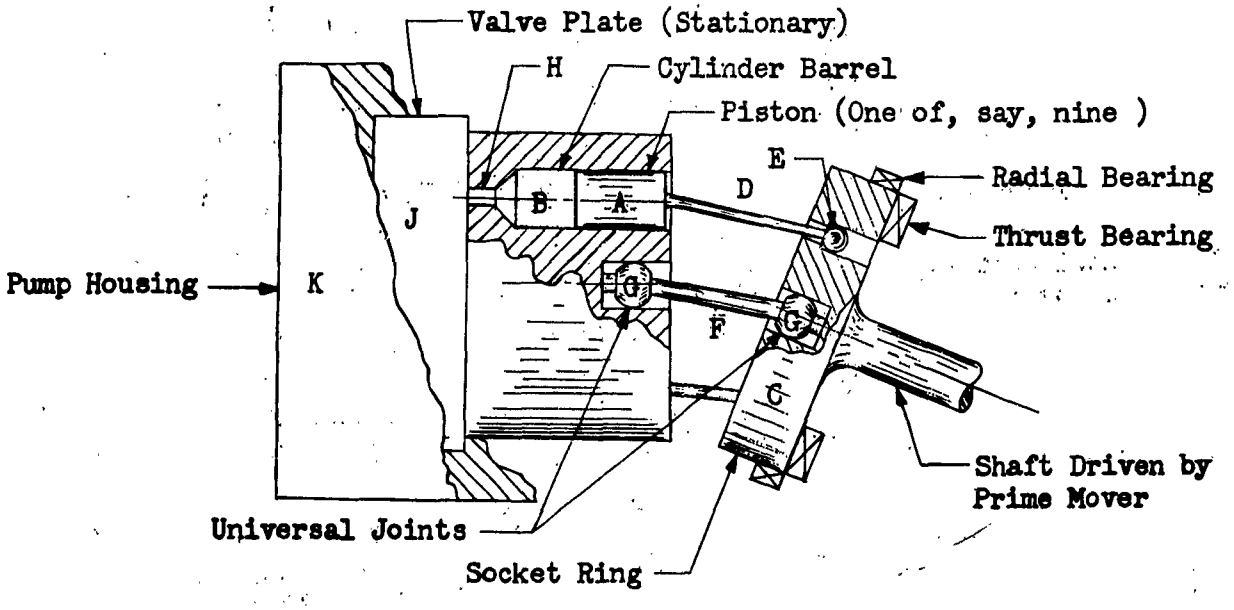

Figure II-3(a). Positive Displacement Hydraulic Pump

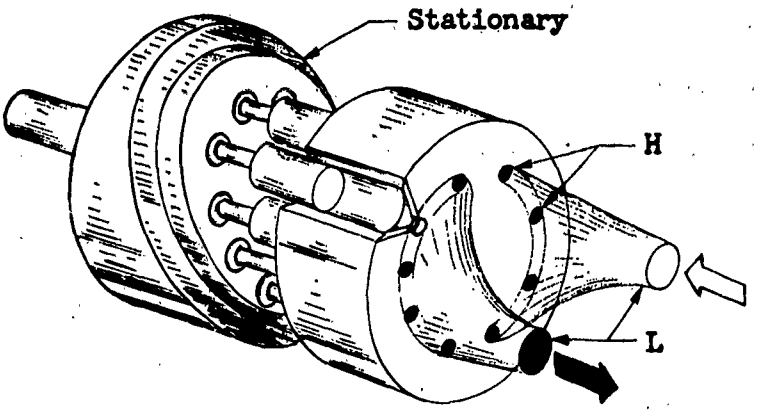

Note: Socket ring thrust and radial bearing not shown.

Figure II-3(b). Positive Displacement Hydraulic Pump

A typical configuration (see Figure II-3) consists of, say, seven or nine pistons (A) operating in the bores of a rotatable cylinder barrel (B). The pistons are connected to a rotatable socket ring (C) by means of short connecting rods (D) and ball and socket joints (E). The socket ring and the cylinder barrel are synchronized by means of a small connecting shaft (F) and universal joints (G) as required. Consider that the socket ring is rotated by some prime mover such as the main propulsion plant. Therefore, the cylinder barrel and the pistons also rotate about a longitudinal axis. If the socket ring is displaced angularly about a transverse axis normal to the axis of rotation, continuous reciprocation of the pistons relative to the cylinder barrel results as the socket ring is driven by the prime mover. Because the bores in which the pistons operate are arranged parallel to the axis of rotation of the cylinder barrel and are located at the same radial distance from the axis of rotation, and since the angular spacing of the bores is equal in each case, the desired fixed phase relationship between the individual pistons is achieved. The remaining necessary feature is the valving means which alternately connects

the pistons, as they reciprocate, to the suction and discharge lines of the hydraulic system. The cylinder barrel is provided with a flat surface normal to the axis of its rotation. The chambers of variable volume, formed by the piston heads and the parallel bores in the cylinder barrel, communicate with the flat surface of the base of the cylinder barrel by means of drilled holes (H) of reduced diameter. These holes, of course, move through a circular path as the cylinder barrel rotates in synchronism with the socket ring. Rotation of the cylinder barrel through 180° moves some reference piston into the cylinder barrel, thereby reducing the volume of fluid within the cylinder. During the remaining half cycle, the piston travels in the reverse direction, drawing fluid into the cylinder. All that remains to be provided is means to isolate these two regions of operation from each other and to connect them respectively to the discharge and suction lines of the hydraulic system.

The flat base of the cylinder barrel rotates against a flat surface which forms a valve plate (J) fixed to the pump housing (K). The valve plate is equipped with two kidney shaped ports (L). These two ports are so arranged that one of them communicates through the holes (H) with the chambers in which the pistons are advancing and for which the volume of the chambers is therefore decreasing; and the other port gives access to the chambers in which the volume is increasing.

At the two dead center positions, corresponding to the point where any piston reverses direction, commutating lands separate the two ports of the valve plate. The width of these two commutating lands is approximately equal to the diameter of the holes in the flat surface of the cylinder barrel. The two ports of the valve plate are connected directly with the suction and discharge lines of the hydraulic system. The configuration of the cylinder bores,

the reduced diameter holes, and the semi-circular ports of the valve plate are arranged by means of careful design so that the system is in a state of hydraulic balance. Thus internal pressure has no tendency to disturb the intimate surface contact of the rotating cylinder barrel with the stationary valve plate.

If the angular relationship of the socket ring to the cylinder barrel about the transverse axis is fixed, the pump is a constant displacement type. If this angular relationship can be changed during the normal operation of the pump, it becomes a variable displacement type. Both are widely used in aircraft installations.

The type of equipment just described when driven by a prime mover is a hydraulic pump. The same basic unit when supplied by a source of hydraulic fluid under pressure can be used as a motor. The combination of a variable displacement pump driving a constant displacement motor constitutes the basic configuration of a positive displacement hydraulic transmission. This device is widely used and is to be considered in some detail in this chapter.

SECTION 3 - FUNCTION OF THE HYDRAULIC SERVOMECHANISM

The function of the hydraulic servomechanism is to control the flow of hydraulic power. This power is in the form of a volumetric flow rate of a (relatively) incompressible fluid operating, generally, against an appreciable load-induced pressure. This volumetric flow is used to actuate some type of servo motor. The servo motor or actuator is used to control the position, velocity, or acceleration of some dynamical system which is made up of lumped or distributed elements of inertia, damping, and elasticity. Therefore, the dynamical nature of the load and the attendant coupling of the dynamics of the load to those of the servo actuator with its associated control elements, present a problem of some complexity. Generally the power level of the output

of the hydraulic servo is many times greater than the power level of the input signal. Thus the hydraulic servomechanism operates as a power amplifier.

Because the unit is actuated by the existence of an error, generally appearing as a valve displacement, a feedback loop and an error sensing element are necessary parts of the system. The hydraulic servomechanism must control the position, velocity, and acceleration (and sometimes higher derivatives) of the output control member in a stable fashion throughout the entire frequency spectrum. Marginal instability exhibited by a condition of incipient hunting is sufficient reason for rejecting any specific servo design.

The functions and performance requirements of the hydraulic servomechanism are of course identical to those of any other type of servomechanism. In the functional consideration of the hydraulic servomechanism it is necessary to study those particular features which make the use of hydraulic components particularly attractive to the controls designer. Those features which are worthy of consideration are enumerated as follows:

1. Size
2. Weight
3. Power level
4. Speed of response (torque to inertia ratio)
5. Reliability
6. Cost
7. Ease of control

The first four items of this list are those in which the hydraulic servo has an advantage over other types through a certain range of power levels. The data in Table II-1 indicate the important features of several commercially available hydraulic motors adaptable directly for use as servo actuators. Most

MOTOR CHARACTERISTICS	UNITS	VICKERS INC. MOTOR NO.		
		MF-24-3906-30BC-2	MF-36-3908-30Z-2	MF-3909-30Z-2
Maximum Operating Pressure	psi	3000	3000	3000
Maximum R.P.M. Continuous	rpm	6000	3750	3750
Displacement	$in.^3$ / rev.	0.095	0.240	0.367
Torque at Maximum Pressure	in.-lb.	45.4	115	175
Horsepower at Maximum Pressure & R.P.M.	h.p.	4.3	6.8	10.4
Moment of Inertia	$lb.in.sec.^2$	1.09×10^{-4}	4.95×10^{-4}	1.02×10^{-4}
Volume of Oil Under Compression	$in.^3$	0.12	0.35	0.42
Approximate Volumetric Efficiency	%	96	96	96
Weight	lbs.	1.75	2.75	4.5
Torque to Pressure Ratio	$in.^3$	0.015	0.038	0.058
Torque to Inertia Ratio	rad. / $sec.^2$	410,000	230,000	171,000
Hydraulic Compliance*	rad./lb.in.	53.3×10^{-6}	24.3×10^{-6}	13.16×10^{-6}

Table II-1. Rotary Hydraulic Motor Data

*Based on a bulk modulus for the hydraulic fluid of 250,000 psi. (Compliance is reciprocal of "stiffness.")

of the features listed are from the manufacturers' catalog data. Some of the others are calculated from these data.

For a high performance servo, the most important item on the list is the torque to inertia ratio. This ratio is often given as a figure of merit for a servo motor and is a direct measure of the available acceleration. Of almost equally great importance is the low weight (and corresponding small size) of any of the motors listed for the given power rating. Comparison of the items of this list with those for an equivalent electric servo actuator clearly demonstrates the superiority of the hydraulic servo.

The cost of hydraulic components is generally fairly high because of the necessary precision of the manufacturing techniques. Even so, the cost of hydraulic components compares favorably with that of equivalent components of other types. This is especially true in the field of aircraft control systems.

In general, the reliability of hydraulic components is excellent. The flexibility and ease of control further enhance the over-all excellence of the hydraulic servo. It is believed that the ease with which hydraulic power can be controlled will become evident later in this chapter when the control of hydraulic power is more specifically considered.

SECTION 4 - TYPES OF HYDRAULIC SERVOMOTORS

Hydraulic servomotors can be classified under two generic headings; they are the linear and the rotary types. The former of these is the direct acting hydraulically controlled piston actuator. This type of actuator generally operates with the chambers at each side of the piston head pressurized. (An exception to this is the use of this kind of actuator in the so-called "open center" system.) The piston may be of the balanced area type in which the

areas exposed to the respective pressures at the two sides of the piston head are approximately equal. With such an actuator, the pressures on both sides of the piston head, and the resulting fluid flows, are precisely controlled by complementary servo elements. (See Figure II-4(a).)

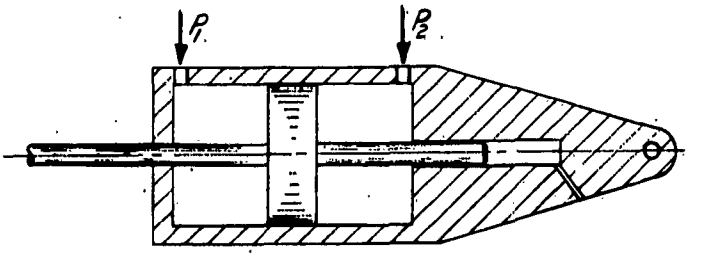

(a) Balanced area piston type actuator. (Pressures P_1 and P_2 at each side of piston head both controlled by valving means.)

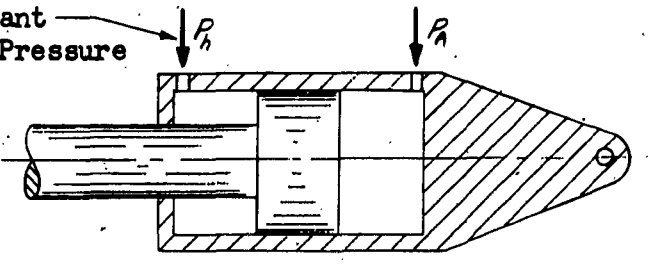

(b) Differential area piston type actuator. (Only one pressure, P_A, controlled by valving means.)

Figure II-4. Types of Servo Actuator

An alternate type of linear servo actuator is the piston type in which the ratio of the areas of either side of the actuator piston head is approximately two to one. (See Figure II-4(b).) In such a device, the small area chamber is ported directly to the constant pressure system supply. The pressure and the flow rate to the larger area chamber control the actuator performance.

The rotary type actuator assumes a variety of forms. Practically any type of positive displacement hydraulic pump can be adapted for use as a rotary servo actuator. These include axial and radial multiple piston actuators as well as gear and vane type actuators.

In general, any hydraulic servo actuator, linear or rotary, can be controlled either by the use of conventional valving or by the use of a servo controlled variable displacement pump.

SECTION 5 - POSITIVE DISPLACEMENT HYDRAULIC TRANSMISSION

The positive displacement hydraulic transmission consists basically of a variable displacement pump and a fixed displacement motor hydraulically interconnected in such a way that the volumetric output of the pump drives the hydraulic motor. The variable displacement pump is driven at a constant speed by some type of prime mover. The angular velocity of the motor is proportional to the volumetric flow rate to it; the latter is proportional to the angle of tilt of the socket ring in the pump if the device is of the same type as that described earlier in this chapter. Therefore, servo control of the output member, that is, of the fixed displacement motor, is achieved by control of the tilt angle of the variable displacement pump. Generally the variable displacement pump is referred to as the "A-end," and the fixed displacement motor is referred to as the "B-end." The simple system is as shown:

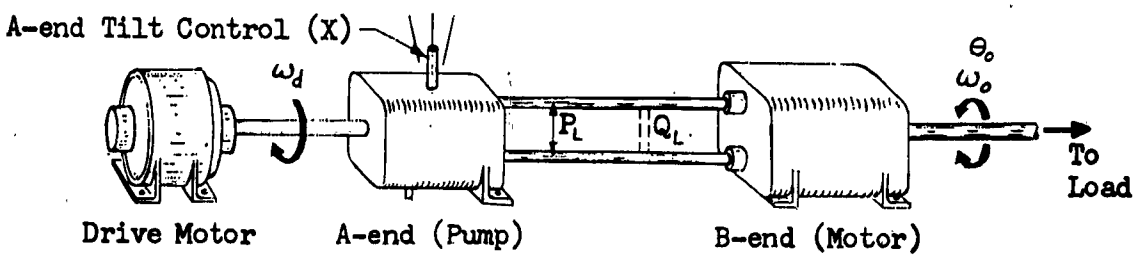

Figure II-5. Hydraulic Transmission

The basic equation involved can be expressed as:

(II-1) $$Q_P = Q_M + Q_L + Q_C$$

where

Q_P is the total volumetric flow rate from the pump

Q_M is the flow rate consumed by motor rotation

Q_L is the leakage flow rate

Q_C is the compressibility "flow rate"

It is possible to define each of the quantities above in terms of known system characteristics.*

Q_P varies from zero to a maximum in stepless increments as controlled by the A-end stroke (X). X varies from zero to $\pm$ 1.0. Therefore

(II-2) $$Q_P = X d_p \omega_d \quad (\text{in}^3 / \text{sec.})$$

where

d_p is the volumetric displacement of the A-end at full stroke $(X = 1.0)$ per unit of angular displacement (in^3 / radian).

ω_d is the (constant) angular velocity at which the A-end is driven.

Also:

(II-3) $$Q_L = L P_L \quad (\text{in}^3 / \text{sec.})$$

where:

L is the system leakage factor of the complete transmission. (This is derivable from catalog curves of volumetric efficiency versus pressure drop across the motor. This is very nearly a linear function.)

*The following derivation of (II-6) is essentially that given in Brown, G. S., and Campbell, D. P., Principles of Servomechanisms, John Wiley & Sons, New York, 1948.

P_L is the pressure drop (psi) across the motor. (This is entirely a load induced pressure.)

Further:

$$(II\text{-}4) \qquad Q_c = \frac{\gamma_c}{N} \frac{dP_L}{dt} \quad (in.^3 / sec.)$$

where:

γ_c is the total volume of liquid under compression in the active system. (This is a constant and does not vary with motor position.)

N is the bulk modulus of the liquid. (See Chapter III, Section 2.)

Finally:

$$(II\text{-}5) \qquad Q_M = d_m \omega_o \quad (in.^3 / sec.)$$

where:

d_m is the volumetric displacement of the B-end per unit angular displacement.

ω_o is the angular velocity (variable) of the B-end.

Combining (II-2), (II-3), (II-4), and (II-5):

$$(II\text{-}6) \qquad X d_p \omega_d = d_m \omega_o + L P_L + \frac{\gamma_c}{N} \frac{dP_L}{dt}$$

At this point, it is convenient to introduce the quantity Z_L, which is referred to as "load impedance."

By definition,

$$Z_L = \frac{P_L}{Q_m}$$

therefore, from (II-5):

$$P_L = Z_L d_m \omega_o$$

Substituting this value of P_L into Equation (II-6):

$$(II\text{-}7) \qquad X d_p \omega_d = d_m \omega_o + Z_L d_m \omega_o \left(L + \frac{\gamma_c}{N} s \right)$$

The Laplace transform is introduced at this point to simplify presentation of the equations.

The open loop transfer function of the hydraulic transmission is then:

$$(II\text{-}8) \qquad \frac{\omega_o}{X}(s) = \frac{d_p \omega_d}{d_m} \frac{1}{1 + Z_L \left(L + \frac{\gamma_c}{N} s \right)}$$

For the relationship between the angular output position (θ_o) of the B-end and the control input (X), there results:

$$(II\text{-}9) \qquad \frac{\theta_o}{X}(s) = \frac{K}{s} \frac{1}{1 + Z_L \left(L + \frac{\gamma_c}{N} s \right)}$$

where

$$K = \frac{d_p \omega_d}{d_m}$$

Several simple cases of specific types of loading are considered:

Case (a)

The case where an inertia element is rigidly coupled to the B-end output shaft.

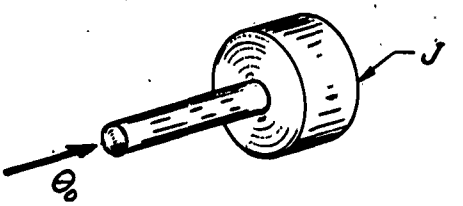

The load torque,

$$T = J s^2 \theta_o$$

Since

$$Z_L = \frac{P_L}{Q_m}$$

$$Z_L = \frac{P_L}{d_m s \theta_o}$$

Also, the torque,

$$T = c P_L$$

where c (in^3) is the motor torque per unit pressure (inch pounds per psi active system pressure differential). This value is often given as part of the manufacturer's model designation.

Therefore, in this case,

$$Z_L = \frac{J s^2 \theta_o}{c d_m s \theta_o}$$

or

$$Z_L(s) = \frac{Js}{c d_m}$$

and the system (open loop) transfer function becomes

(II-10) $$\frac{\theta_o}{X}(s) = \frac{d_p \omega_d}{d_m s} \frac{c d_m}{\left(c d_m + JLs + \frac{J \gamma_c}{N} s^2\right)}$$

or

(II-10a) $$\frac{\theta_o}{X}(s) = \frac{K}{s} \frac{1}{\left(\frac{J \gamma_c}{c d_m N} s^2 + \frac{JL}{c d_m} s + 1\right)}$$

Case (b)

The case where an inertia element is coupled to the B-end output shaft by means of an elastic member and with output damping.

As before,

$$Z_L = \frac{Torque}{cd_m s\,\theta_o}$$

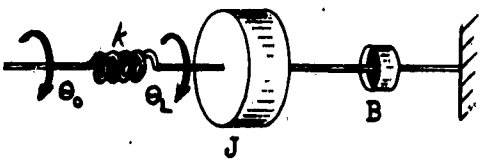

The load torque,

$$T = k(\theta_o - \theta_L) = Js^2\theta_L + Bs\theta_L$$

from which

$$\theta_L = \frac{k\,\theta_o}{Js^2 + Bs + k}$$

Then the torque,

$$T = (Js^2 + Bs)\frac{k\,\theta_o}{Js^2 + Bs + k}$$

Since

$$Z_L = \frac{Torque}{cd_m s\,\theta_o}$$

$$Z_L(s) = \frac{k(Js + B)}{cd_m(Js^2 + Bs + k)}$$

and the system transfer function becomes

(II-11)
$$\frac{\theta_o}{X}(s) = \frac{d_p\,\omega_d}{d_m s}\,\frac{cd_m(Js^2 + Bs + k)}{cd_m(Js^2 + Bs + k) + kL(Js + B) + \frac{k\gamma_c}{N}(Js^2 + Bs)}$$

$$= \frac{K}{s}\,\frac{(Js^2 + Bs + k)}{\left[\left(J + \frac{Jk\gamma_c}{cd_mN}\right)s^2 + \left(B + \frac{JkL}{cd_m} + \frac{Bk\gamma_c}{cd_mN}\right)s + \left(k + \frac{BkL}{cd_m}\right)\right]}$$

Case (c)

This system is the same as (b) but with zero damping $(B=0)$.

$$(II\text{-}12) \qquad \frac{\theta_o}{X}(s) = \frac{k}{s} \frac{\frac{J}{k}s^2 + 1}{\left[\left(\frac{J}{k} + \frac{\gamma_c J}{c d_m N}\right)s^2 + \frac{L J}{c d_m}s + 1\right]}$$

In a similar manner, load dynamics of any degree of complexity can be included in the over-all system transfer function. Study of the transfer function above yields the design requirements of the servo device which controls the stroke (X) of the A-end.

SECTION 6 - SEPARATION OF LOAD DYNAMICS

In the preceding section, the concept of load impedance was introduced. This was done in order to establish a means whereby the load dynamics of a system may be separated from the dynamics of the unloaded servo device. Although it is not necessary to separate the load dynamics in this manner, doing so sometimes yields a better physical insight. The techniques involved may appeal to certain engineers, and this section is presented for that reason.

In general the dynamics of the unloaded servo element are fairly easy to define. If no other means are available, a series of simple bench tests will suffice, in many cases, to establish the important parameters applicable to the unloaded servo element. If the dynamics of the load can be handled as a separate entity, the over-all problem of determining system behavior becomes somewhat simplified.

In order to clarify this idea, the block diagram below is considered.

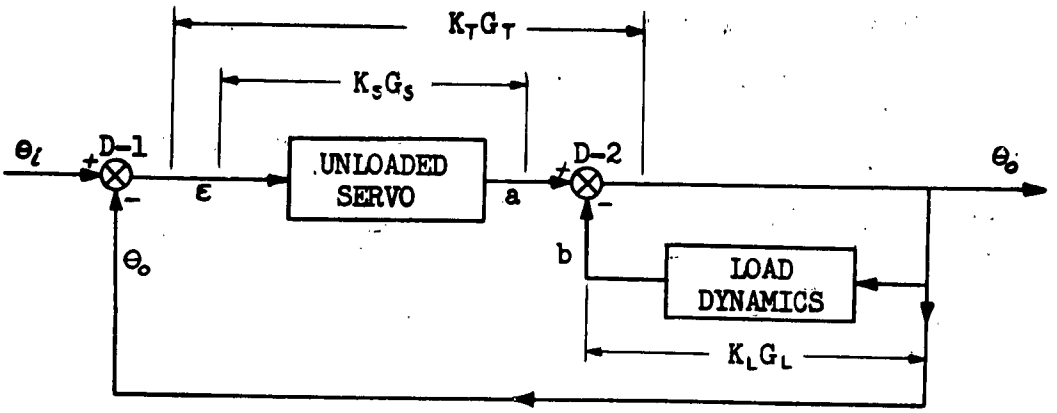

Figure II-6. Load Block Diagram

In the diagram the transfer function of the unloaded servo system is designated by $K_S G_S$. For a condition of no load the system output (a) is identical with θ_o , since the contribution of the load dynamics is zero. For the system operating under an appreciable load, the unloaded system output (a) differs from the actual output (θ_o) by the amount (b) supplied by the load dynamics. It is well to keep in mind that the diagram does not necessarily represent any actual physical array of hardware. Parts of the diagram may be purely fictitious, and such an arrangement is used here only to provide a means of understanding the over-all problem.

If the diagram is accepted as such, the following relationships are apparent.

(I) $\theta_o = a - b$

b is subtracted from a by the fictitious differential device D-2.

(II) $\varepsilon = \theta_i - \theta_o$

ε can be considered the instantaneous error and is formed by comparing system output (θ_o) to the input (θ_i) at the differential device D-1.

(III) $a = (K_S G_S)\varepsilon$

$K_S G_S$ is the open loop transfer function of the unloaded system.

(IV) $b = (K_L G_L)\theta_o$

$K_L G_L$ is the "transfer function" of the load dynamics.

(V) $\theta_o = (K_T G_T)\mathcal{E}$

$K_T G_T$ is the actual open loop system transfer function under load.

Combining (I), (III), and (IV),

$$\theta_o = (K_s G_s)\mathcal{E} - (K_L G_L)\theta_o$$

and

$$\frac{\theta_o}{\mathcal{E}} = K_s G_s \left(\frac{1}{1 + K_L G_L}\right)$$

Since $\frac{\theta_o}{\mathcal{E}}$ is by definition $K_T G_T$,

(II-13) $$K_T G_T = K_s G_s \left(\frac{1}{1 + K_L G_L}\right)$$

This last expression relates the over-all system transfer function to the transfer function of the unloaded system and that of the load dynamics as a separate entity. This may be compared with the general expression for the over-all system transfer function of the positive displacement hydraulic transmission, Equation (II-9), which is repeated below as:

(II-14) $$\frac{\theta_o}{X}(s) = \frac{K}{s}\left[\frac{1}{1 + Z_L\left(L + \frac{\gamma_c}{N}s\right)}\right]$$

In this expression the unloaded system transfer function is that part of the right hand side not enclosed in the brackets. Therefore, in this case:

$$K_s G_s = \frac{K}{s}$$

This indicates that the unloaded positive displacement hydraulic transmission acts as a perfect integrator, as indeed it does. That is, for a fixed position of A-end tilt, a proportional B-end output velocity results.

Further comparison of Equations (II-13) and (II-14) shows that the transfer function of the load dynamics is:

$$K_L G_L = Z_L\left(L + \frac{\gamma_c}{N}s\right) \qquad \text{(II-15)}$$

The performance of a well-designed servo system employing a positive displacement hydraulic transmission will be such that in the range of frequencies covered by the input signal, the device will operate very nearly like a perfect integrator. In the higher frequency range where the effects of the load dynamics become more pronounced, there must be no evidence of incipient instability. In addition, of course, the device must be capable of meeting whatever performance specifications are applicable.

These last comments apply, in a general sense, to the valve controlled actuator servo device. This type of servo element is discussed in the following section. An attempt is made to show the similarity of the valve controlled servo, which is basically a non-linear device, to the positive displacement type, which is essentially a linear device.

SECTION 7 - VALVE CONTROLLED SERVO ELEMENT

The valve controlled hydraulic actuator is probably more widely used as a servo element in aircraft control surface actuation than any other device. A typical configuration employing a closed center four-way control valve with unity feedback is shown in Figure II-7.

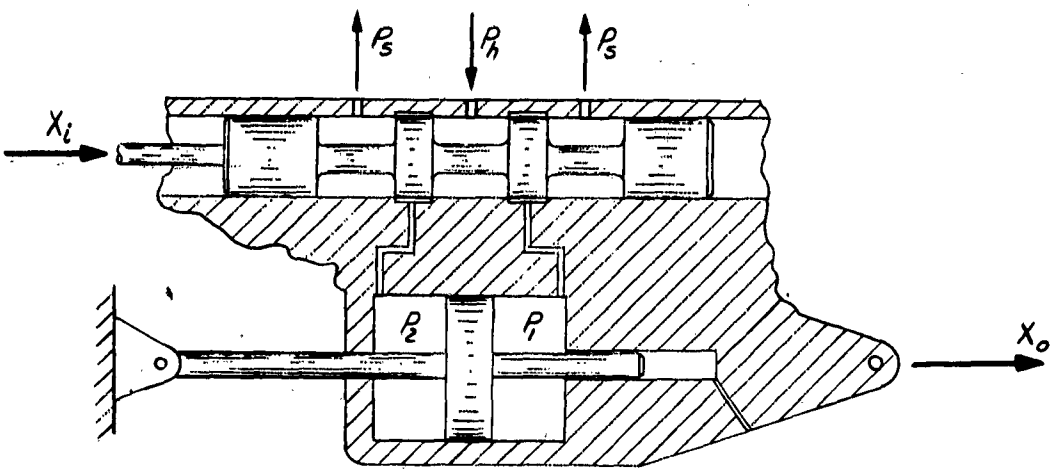

Figure II-7. Valve Controlled Hydraulic Actuator

In the figure, P_h is system supply pressure, and P_s is system return pressure. For the purpose of the present discussion, P_s is assumed to be zero and P_h a constant.

Control of the actuator is accomplished by simultaneously controlling the volumetric flow to and from the two chambers adjacent to the two sides of the piston head. The flow to the cylinder through an inlet orifice is given by the basic relationship:

$$Q = Ca\sqrt{2g\frac{\Delta p}{\omega}} \qquad \text{(II-16)}$$

(This equation can be readily derived from Bernoulli's equation. See, for example, Vennard, J. K., Elementary Fluid Mechanics, John Wiley & Sons, New York, 1940.)

where

C is the orifice coefficient

a is the orifice area

ω is the specific weight of the fluid

Δp is the pressure drop across the orifice

g is the acceleration due to gravity

Assuming an essentially closed-center valve configuration, i.e., negligible leakage flow past the valve lands at a centered valve position, the flow relationship above also expresses the volumetric time rate of cylinder displacement. Further, the pressure drop, Δp, across the orifice becomes a simple function of the system pressure P_h and the load induced pressure P_L $(P_L = P_1 - P_2)$. Since the inlet orifice area is a direct function of the instantaneous system error E (or valve displacement from neutral), it follows that the effective flow tending to move the cylinder is a function of the three variables just named, i.e.,

$$Q = f(E, P_L, P_h)$$

If it is assumed that the total flow Q consists of a steady flow Q^* and a perturbation, q, about this steady value: $Q = Q^* + q$; then the perturbed flow can be approximated as the first-order Taylor's series expansion of q as a function of E, P_L, and P_h:

$$q = \frac{\partial Q}{\partial E} E + \frac{\partial Q}{\partial P_L} P_L + \frac{\partial Q}{\partial P_h} P_h \qquad \text{(II-17)}$$

but since the system supply pressure has been assumed constant:

$$q = C_\epsilon \epsilon - C_p P_L \qquad \text{(II-18)}$$

where, by definition,

$$C_\epsilon \equiv \frac{\partial Q}{\partial E} \quad ; \qquad C_p \equiv -\frac{\partial Q}{\partial P_L} \qquad \text{(II-19)}$$

The perturbation flow rate q may also be thought of as the sum of two components:

(1) An incompressible component, q_o, which causes motion of the cylinder relative to the piston.

(2) A compressible component, q_c, due to the compliance of the fluid within the cylinder; this component causes no actuator motion.

Therefore

$$q = q_o + q_c \qquad \text{(leakage flow is assumed negligible)}$$

where

$$q_o = A s X_o$$

and is that part of the flow which results in actuator motion;

also

$$q_c = \frac{\gamma'}{N} s p_L$$

and is that part of the flow through the valve orifice which does not result in actuator motion.

Therefore

$$q = A s X_o + \frac{\gamma'}{N} s p_L = C_\varepsilon \varepsilon - C_p p_L$$

or

$$C_\varepsilon \varepsilon = A s X_o + \left(C_p + \frac{\gamma'}{N} s\right) p_L \qquad \text{(II-20)}$$

where

A is the area of the actuator piston

γ' is the effective volume under compression

X_o is the actuator output position

ε is the system instantaneous error

p_L is the load induced pressure

N is the bulk modulus of the fluid

All the variables above are perturbation quantities. The detailed treatment of this part of the description is presented elsewhere in this volume.

The foregoing makes no attempt to justify completely the validity of the statements made. The reader is referred to Chapter III of this volume which treats this subject in greater detail. Specifically, the reader will need to understand what is meant by "the effective volume, γ'."

The concept of load impedance is again applied to compare this type of system with the positive displacement hydraulic transmission.

By definition,

$$Z_L = \frac{p_L}{q_o}$$

Since

$$q_o = AsX_o \quad ; \quad p_L = Z_L AsX_o$$

Substituting this value of p_L into Equation (II-20) gives:

$$C_\varepsilon \varepsilon = AsX_o + Z_L AsX_o\left(\frac{\gamma'}{N}s + C_p\right) \tag{II-21}$$

Writing this expression in the form of the open loop transfer function results in:

$$\frac{X_o}{\varepsilon}(s) = \frac{C_\varepsilon}{As} \frac{1}{1 + Z_L\left(\frac{\gamma'}{N}s + C_p\right)} \tag{II-22}$$

This may now be compared with the equivalent expression for the positive displacement hydraulic transmission:

$$\frac{\theta_o}{X}(s) = \frac{d_p \omega_d}{d_m s} \frac{1}{1 + Z_L\left(\frac{\gamma'}{N}s + L\right)} \tag{II-23}$$

The two expressions are identical in form, with the load dynamics isolated in each case. However, some very important differences exist. In (II-23), all the system parameters as given are constant and are fairly easy to evaluate.

These constants are:

$\frac{d_p \omega_d}{d_m}$ system gain term

γ_c volume of oil under compression

L leakage factor (which gives rise to system damping)

However, in the case of the valve controlled actuator device, none of the equivalent terms is a constant except over a very small operating range. Over any appreciable operating range, the problem is to assign reasonably accurate average values to C_ε , C_p , and γ'. Actually in practice it is fairly easy to establish a realistic value for C_ε. For conservative design the value of γ' for the piston at the midpoint of the stroke may be used since this is the point of maximum hydraulic compliance.

The most elusive parameter is the effective damping factor, C_p . No simple, direct method of evaluating this quantity, short of actually testing an existing device, is known to be completely satisfactory at this writing.

The reason for presenting the positive displacement hydraulic transmission and the valve controlled actuator in the manner in which this was done was to bring out the rather remarkable similarity of the two devices. Actual frequency response tests carried out on examples of the two types operating against similar loading and at the same power level yield very similar results. This is true in spite of the fact that in one case the system is linear throughout, and in the other case the system is very definitely non-linear.

CHAPTER III

ANALYSIS OF THE GENERALIZED HYDRAULIC SERVO ACTUATOR

SECTION 1 - INTRODUCTION

In this chapter, an analysis of the generalized hydraulic servo actuator shown in Figure III-1 is presented.

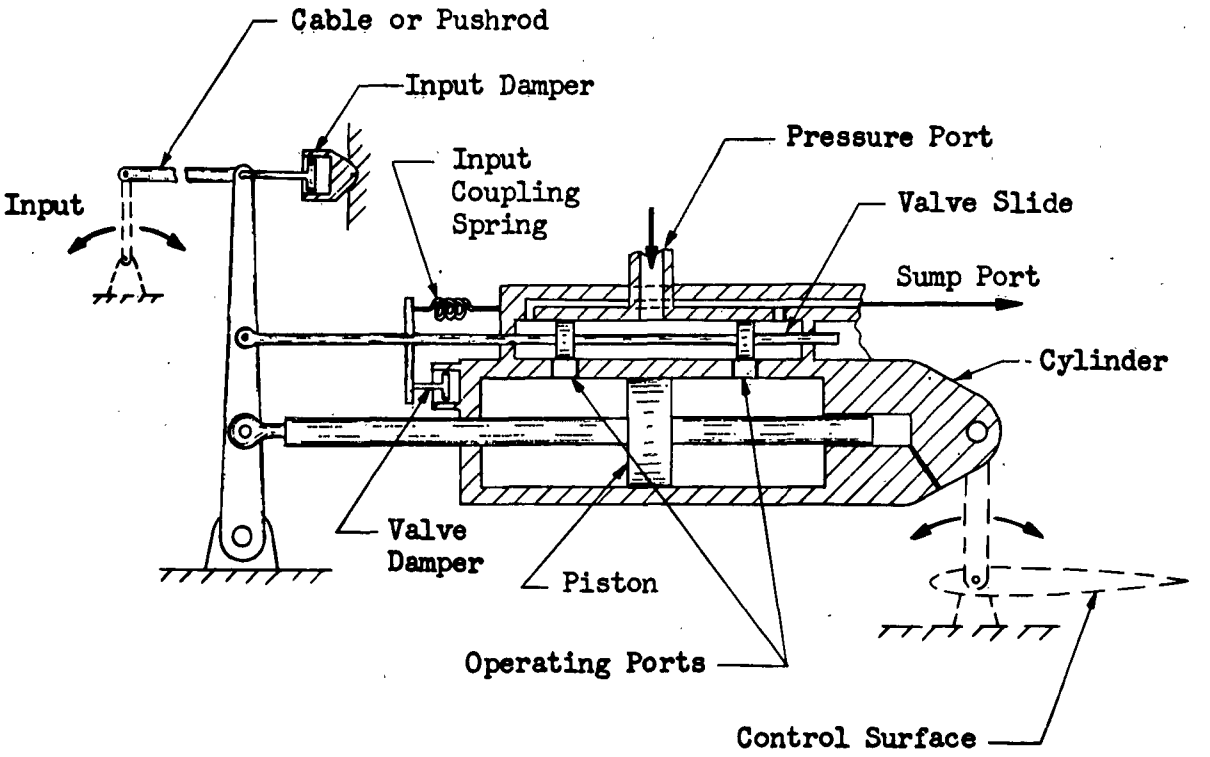

Figure III-1. The Generalized Hydraulic Servo Actuator

Since the input, or control member, is subject to only a portion of a static load on the control surface, the mechanism shown in the figure is a power boost actuator; that is, the hydraulic system provides only a portion of the energy necessary to move the output, or controlled member, against the imposed load. The rest of the necessary energy must be supplied by another source at the control end of the actuator. In an aircraft application, this

additional mechanism is either the human pilot or a flight controller servo-motor. The energy requirements for actuating aircraft control surfaces have increased steadily through the years, requiring the hydraulic system to provide an increasing proportion of the energy supplied. The limiting type — that in which the control member is not subject to any appreciable static load — is called the fully-powered actuator, and is of great importance at the present time. There remains, however, considerable interest in the power boost type. The mechanism of Figure III-1 has been selected so that the results of its analysis may be specialized to describe the behavior of a large percentage of the hydraulic servo actuators in current use.

The slide valve in Figure III-1 is of the conventional four-port type and is mounted integrally with the hydraulic cylinder. A more general actuator in which the valve housing is mounted on a linkage rather than directly attached to the cylinder would require additional flexible tubing, and the follow-up linkage would be likely to have considerable backlash. Because of these disadvantages, the more complicated system is of limited importance. The actuator of Figure III-1 may be regarded as typical of practice.

To accomplish its purpose of effectively duplicating input displacement in output displacement regardless of load, a positional actuator must have one or more feedback loops. The presence of the feedback makes an actuator a servo-mechanism and therefore makes an investigation of its stability a critical part of the analysis. The mechanism of Figure III-1 has more than one feedback loop, but the principal feedback is due to the integral mounting of valve and cylinder.

The valve may in general be one of the types broadly classified as "open center," "closed center," and "open center—closed center"; that is, the valve spool in a central position may fall short of covering the operating ports

leading to the cylinder, it may overlap these ports, or it may come very near to covering the ports exactly. The range of operation of a slide valve will in general include a central region of open center type behavior and adjacent regions of substantially closed center behavior. In the region of open center type behavior, the flow from an operating port to the cylinder, i.e., the flow tending to move the cylinder, is the difference of two flows — that from the pressure port past a valve spool land into the operating port and that from the operating port past the valve spool land to the sump port.

A hydraulic servo actuator which includes a predominantly open center type valve is characterized by considerable position error when operating under load. On the other hand, with an open center type valve, the fluid on each side of the cylinder is always under compression, minimizing the entrainment of air and the resultant reduction of oil rigidity. The "dead band" characteristic of a completely closed center type valve (one with overlap) is regarded as undesirable, and most present practice is a compromise, utilizing valves which are essentially of the closed center type, but which have a small central region of open center type behavior.

The analysis to be presented will be applicable to both a region of closed center type valve operation and a range of open center behavior, although the result of its application in the latter case will be only a good approximation, becoming less and less accurate as the range of open center behavior is made more extensive.

The mechanism under discussion is inherently nonlinear. Known mathematical techniques do not at present provide means for solving, in other than numerical form, the true nonlinear problem. However, a linearized treatment is sufficient basis for designing to meet most requirements, and the following analysis

is in terms of small increments, or "perturbations," about an operating point described by a fixed set of values of independent variables.

The plan of attack is as follows:

1. Derivation of flow equations of the hydraulic servo.
2. Derivation, under fairly general hypotheses, of the force and linkage equations of the servo.
3. Combination of (1) and (2) to secure a literal description of over-all servo behavior.

The following assumptions govern the analysis:

1. Linearity exists about operating points; i.e., the relationship between any two variables may be regarded as proportional within a sufficiently small range of values of the variables.
2. All masses and dampings can be replaced by lumped parameters.
3. The valve is essentially symmetrical; i.e., the valve spool and valve housing may assume such a relative position that all areas open to flow are approximately equal in magnitude and geometrically similar.
4. Both valve spool and valve housing are rigid.
5. The valve is designed in such a way that the rate of change of momentum of the fluid as it passes through the valve is negligible, resulting in the effective elimination of centering and decentering forces on the valve; or, equivalently, the numerical values assigned to an input coupling spring and a valve damper (see Figure III-1) are altered by the proper amounts to account for the valve forces.
6. The fluid in the cylinder is always compressed to the extent that cavitation is negligible.
7. The piston is double-ended.

8. Flows through ports connecting valve and cylinder are substantially equivalent.
9. The cylinder is rigid; or, equivalently, allowance is made for cylinder flexibility when considering oil compressibility.
10. There is no leakage past the piston.

SECTION 2 - FLOW EQUATIONS OF THE ACTUATOR

(a) VALVE ERROR

Referring to Figure III-1, it is evident that the flows from operating ports of the valve to the portions of the cylinder separated by the piston are primarily dependent on the position of the valve relative to its housing. It is desirable to introduce a variable to represent this relative position. In the following, this variable is called the "valve error." Since both the valve spool and valve housing are assumed rigid, no deflections of these structures need enter the definition of valve error.

If X_v is the displacement of an arbitrary point of the valve spool, and if X_o is displacement of an arbitrary point of the cylinder, both measured from a point on a fixed structure, a valve error E is defined as to form by the relationship $E \equiv X_v - X_o$. It remains only to choose a relative position of valve and cylinder which will be associated with a zero value of the error. A convenient choice for this purpose is usually the relative position which would be determined in test by capping the two operating ports with pressure gages, making supply and sump connections, and moving the valve spool relative to the housing until the operating port pressures match. For a symmetrical valve, a relative position determined in this way will be one for which all areas open to flow between valve and cylinder are equal in magnitude and geometrically

similar, and for which the common value of operating port pressures is one-half the sum of supply and sump pressures.

Let the perturbations of X_v, X_o, and E be x_v, x_o, and ε, respectively; then the error perturbation is given by

(III-1) $$\varepsilon \equiv x_v - x_o$$

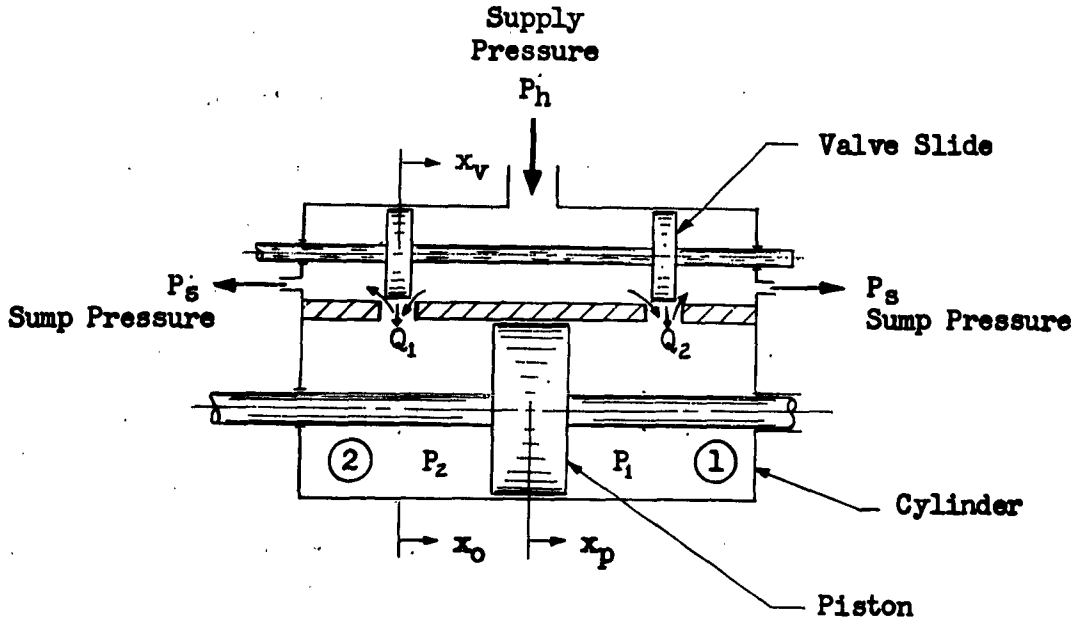

Figure III-2. Flow, Pressure, and Displacement Definitions

(b) FLOW FROM THE VALVE

Figure (III-2) shows flows Q_1 and Q_2, from operating ports into the cylinder. The flow Q_1 is of necessity a function of the supply pressure P_h, the sump pressure P_s, the valve error E, and the pressure P_1 in the cylinder volume on the right side of the piston. Similarly, Q_2 is a function of P_h, P_s, E, and the pressure P_2 in the cylinder volume to the left of the piston.

If the range of open center type operation of the valve is not extensive, there will be little interaction between the hydraulic actuator and either the supply or the sump systems; for this reason P_h and P_s are regarded as constants in the following analysis. This leaves Q_1 and Q_2 as functions of two variables: Q_1 is determined by P_1 and E ; and Q_2 , by P_2 and E .

To construct a simple, practical analysis of the actuator, it is desirable to reduce the number of quantities on which the flows depend. In particular it is preferable to restrict the analysis so as to permit the use of a single volumetric flow variable Q instead of the two flows Q_1 and Q_2 , and also a single load induced pressure variable P_L instead of the two pressures P_1 and P_2. The first requirement is met by restricting the mathematical model of the actuator so that the flows Q_1 and Q_2 are equal in magnitude:

$$Q_1 = -Q_2 \equiv Q \tag{III-2}$$

For the elimination of one of the pressure variables, the variable P_L is defined as the pressure differential across the piston:

$$P_L \equiv P_1 - P_2 \tag{III-3}$$

A rigorous correlation on the basis of the expressions (III-2) and (III-3) is not possible in general, and it is a matter for inquiry to determine what limitations the use of these expressions places on the actuator analysis. These limitations will now be illustrated for the case of a completely symmetrical valve, i.e., a valve in which all areas open to flow between valve and cylinder are equal in magnitude and geometrically similar at zero valve error.

The functional dependence of the flow on relevant parameters is obtained by use of the fundamental orifice equation for substantially incompressible flow:

$$Q = C_d \sqrt{\frac{2g\Delta P}{w}} \tag{III-4}$$

from which, using the definition (III-3),

$$(III\text{-}8) \qquad P_1 = \frac{(P_h^* + P_s^*) + P_L}{2}$$

and

$$(III\text{-}9) \qquad P_2 = \frac{(P_h^* + P_s^*) - P_L}{2}$$

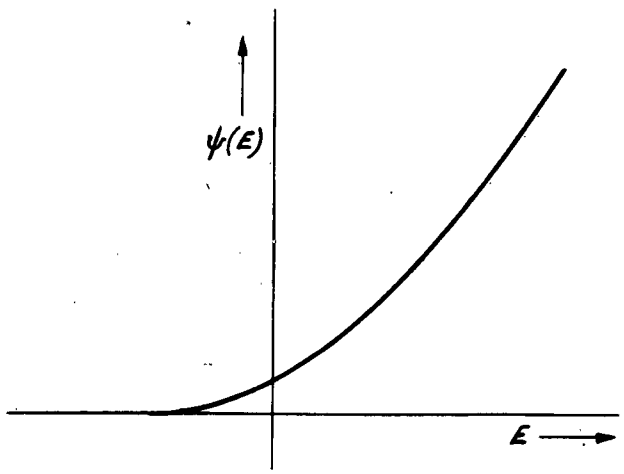

Figure III-3. General Form of the Error Coefficient of Flow Through a Single Orifice

If (III-2) is assumed valid, and the error is large enough in a positive sense so that $\psi(-E)$ is effectively zero, (III-7) is obtained, and (III-8) and (III-9) follow. Again, if the error is large enough in a negative sense so that $\psi(E)$ is effectively zero, (III-7), (III-8), (III-9) again apply.

From the above remarks, it appears that if (III-2) is valid and the valve is symmetrical, a correlation in P_L, rather than in P_1 and P_2, is possible in regions of closed center type valve operation and also in that part of the open center range of valve error where $Q = 0$. It may be shown that for intervening ranges of valve error a correlation in P_L alone is not possible, but that an analysis on the basis of (III-2) and (III-3) will yield an excellent

approximation when the region of open center type operation is not extensive.

The single flow equation for the case of the symmetrical valve is obtained from (III-2), (III-5), (III-6), (III-8), and (III-9):

$$(III\text{-}10) \qquad Q = \frac{\psi(E)}{\sqrt{2}}\sqrt{(P_h^* - P_s^*) - P_L} - \frac{\psi(-E)}{\sqrt{2}}\sqrt{(P_h^* - P_s^*) + P_L}$$

For a valve having a marked degree of asymmetry of behavior, a correlation in P_L becomes dubious. This is the motivation for Assumption 3 given in the introduction to this chapter.

All of the following analysis assumes the approximate validity of a correlation of flow behavior in terms of a single flow Q and the pressure difference P_L. An equation in perturbed quantities may then be written as:

$$(III\text{-}11) \qquad q = \frac{\partial Q}{\partial E}\varepsilon + \frac{\partial Q}{\partial P_L}p_L$$

Figure III-4 shows typical variations of net flow Q with pressure differential P_L, valve error E being held constant; and of Q with E, P_L being held constant.

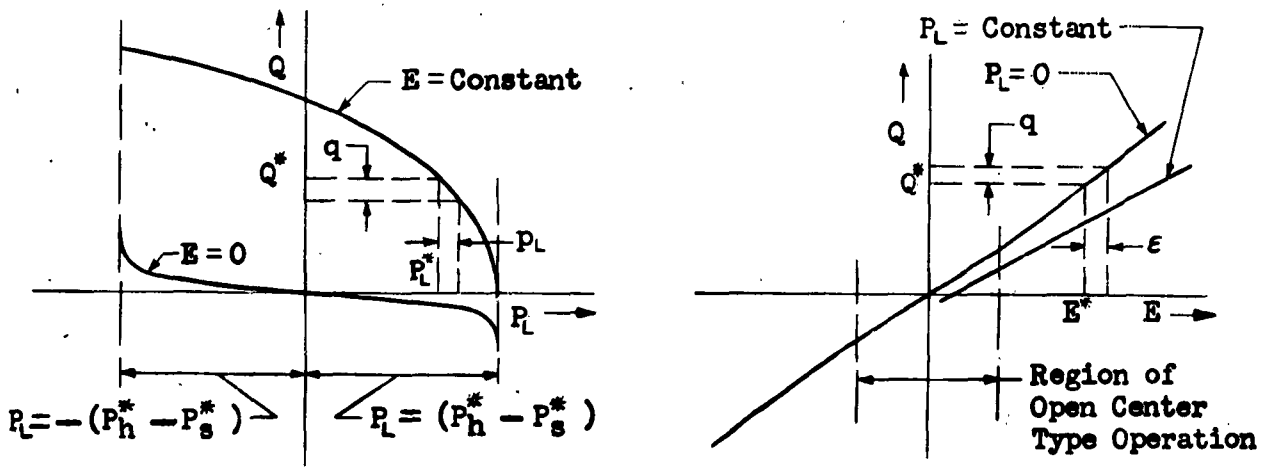

(a) Variation of Net Flow from Valve to Cylinder with Pressure Differential Across the Piston

(b) Variation of Net Flow from Valve to Cylinder with Valve Error

Figure III-4. Typical Variations of Net Flow

The figure also shows a typical operating point, the fixed values of the variables defining the operating point being Q^*, E^*, P_L^*, and indicates possible values of the perturbed quantities. The partial derivatives in (III-11) are the slopes of the curves evaluated at the operating point.

In Figure III-4, note that $\partial Q/\partial E$ is always positive and that $\partial Q/\partial P_L$ is always negative. It will be advantageous in the development that follows to make the normal signs of these quantities apparent; that is

$$q = C_\varepsilon \mathcal{E} - C_p P_L \qquad \text{(III-12)}$$

where

$$C_\varepsilon \equiv \frac{\partial Q}{\partial E}$$

$$C_p \equiv -\frac{\partial Q}{\partial P_L}$$

The term C_p is analogous to the slope of the torque-speed curve of a shunt motor and gives rise to a similar damping action. The term C_ε is analogous to the slope of the speed-field current curve of a shunt motor and produces a similar gain term in the over-all system.

C_p varies from a very small positive value to infinity as a function of E and P_L, the very small positive value occurring when the valve error is zero and no pressure differential exists across the piston, and the infinite value occurs at a stalled cylinder condition.

(c) FLOW INTO THE CYLINDER

It now becomes necessary to relate the flow from the valve to cylinder motion, piston motion, and pressure differential across the piston. In developing the equations for cylinder flow, the compressibility of the fluid will be taken into account.

The total mass of fluid to one side of the piston at any time t is

(III-13) $$m = \rho \gamma$$

where

γ is the volume occupied by the fluid mass

ρ is the fluid density at the time t, assumed independent of position within the volume

Then

(III-14) $$\frac{dm}{dt} = \rho \frac{d\gamma}{dt} + \gamma \frac{d\rho}{dt}$$

and the volumetric flow corresponding to this mass flow rate is

(III-15) $$Q = \frac{1}{\rho} \frac{dm}{dt} = \frac{d\gamma}{dt} + \frac{\gamma}{\rho} \frac{d\rho}{dt}$$

The compressibility of the fluid is characterized by the expression

(III-16) $$N = -\gamma \left. \frac{dP}{d\gamma} \right|_{m = constant} = \rho \frac{dP}{d\rho}$$

where

N is the bulk modulus of the fluid

ρ is the fluid density

P is the fluid pressure

By inserting this relation into (III-15):

(III-17) $$Q = \frac{d\gamma}{dt} + \frac{\gamma}{N} \frac{dP}{dt}$$

(III-17) applies to each of the regions of the cylinder separated by the piston (see Figure III-2).

(III-18) $$Q_1 = \frac{d\gamma_1}{dt} + \frac{\gamma_1}{N_1} \frac{dP_1}{dt}$$

$$(III\text{-}19) \qquad Q_2 = \frac{d\gamma_2}{dt} + \frac{\gamma_2}{N_2}\frac{dP_2}{dt}$$

If it is assumed that the instantaneous flow into one side of the cylinder is equal to the instantaneous flow out of the other side, i.e., $Q_1 = -Q_2 \equiv Q$, and if it is further assumed that the bulk modulus N is constant, and the same magnitude for both regions, (III-18) and (III-19) become:

$$(III\text{-}20) \qquad Q = \frac{d\gamma_1}{dt} + \frac{\gamma_1}{N_1}\frac{dP_1}{dt} = -\left(\frac{d\gamma_2}{dt} + \frac{\gamma_2}{N_2}\frac{dP_2}{dt}\right)$$

Since

$$\frac{d\gamma_1}{dt} = -\frac{d\gamma_2}{dt}$$

it follows that

$$(III\text{-}21) \qquad \gamma_1 \frac{dP_1}{dt} = -\gamma_2 \frac{dP_2}{dt}$$

Addition of the quantity $(\gamma_2\, dP_1/dt)$ to both sides of (III-21) gives:

$$(III\text{-}22) \qquad \frac{dP_1}{dt} = \frac{\gamma_2}{\gamma_1+\gamma_2}\frac{d}{dt}(P_1 - P_2) = \frac{\gamma_2}{\gamma_1+\gamma_2}\frac{dP_L}{dt}$$

where

$P_L \equiv P_1 - P_2$, the pressure differential across the piston

Further, the time rate of change of the volume on the high pressure side of the cylinder is

$$(III\text{-}23) \qquad \frac{d\gamma_1}{dt} = A\frac{d}{dt}(X_o - X_p)$$

where

X_o is the cylinder displacement relative to structure

X_p is the piston displacement relative to structure (non-rigid piston)

A is the cylinder area

By substituting the values of dP_1/dt and $d\gamma_1/dt$ from (III-22) and (III-23) into (III-20):

$$(III\text{-}24) \qquad Q = A\frac{d}{dt}(X_o - X_p) + \frac{1}{N}\left(\frac{\gamma_1\gamma_2}{\gamma_1+\gamma_2}\right)\frac{dP_L}{dt}$$

or

$$(III\text{-}25) \qquad Q = A\frac{d}{dt}(X_o - X_p) + \frac{\gamma'}{N}\frac{dP_L}{dt}$$

where

$\gamma' \equiv \frac{\gamma_1\gamma_2}{\gamma_1+\gamma_2}$, the effective oil volume*

It should be pointed out that this analysis is <u>strictly</u> applicable only when $\gamma_1 = \gamma_2$ or when the ports are blocked, since these are the only conditions where $d\gamma_1/dt = -d\gamma_2/dt$. However, the equation will represent an excellent approximation for any valve and cylinder where the flow through the valve ports due to compressibility is negligible, i.e., for any system where the valve decouples the effects of flow in the lines from flow into and out of the cylinder.

(III-25) is written in terms of total quantities, i.e., operating point values plus perturbations. The similar relation in terms of perturbed quantities is of the form:

$$(III\text{-}26) \qquad q = A\frac{d(x_o - x_p)}{dt} + \frac{(\gamma'^* + \Delta\gamma')}{N}\frac{dp_L}{dt} + \frac{1}{N}\left(\frac{dP_L}{dt}\right)^*\Delta\gamma'$$

where q, x_o, x_p, p_L, and $\Delta\gamma'$ are perturbations, and γ'^* and $(dP_L/dt)^*$ are values at the operating point.

The nonlinear term $(\Delta\gamma'/N)(dp_L/dt)$ is of higher order and may be ignored in a linear analysis. It is further assumed that $(dP_L/dt)^*$ is relatively small

* The physical representation of a column of oil as a spring also involves this same effective oil volume.

enough so that the term $(1/N)(dP_L/dt)^* \Delta\gamma'$ can be neglected. With these simplifications, the flow equation in perturbed quantities becomes:

$$q = A\frac{d(x_o - x_p)}{dt} + \frac{\gamma'^*}{N}\frac{dp_L}{dt} \qquad \text{(III-27)}$$

or, by designating s as the derivative operator, (d/dt):

$$q = As(x_o - x_p) + \frac{\gamma'^*}{N} s\, p_L \qquad \text{(III-28)}$$

To facilitate combining the flow and force equations, it is helpful to rewrite the coefficient γ'^*/N in a more usable form. Since γ'^* is a volume, and N a bulk modulus, it may readily be verified that the quantity γ'^*/N has the dimensions of an area squared over lb/in., that is, of an area squared over a linear spring constant. The relevant area in this case is the net piston area, A. If the equivalent spring constant is represented by the symbol k_o, (III-28) may then be rewritten as:

$$q = As(x_o - x_p) + \frac{A^2}{k_o} s\, p_L \qquad \text{(III-29)}$$

where $$k_o \equiv \frac{A^2 N}{\gamma'^*}$$

Thus the effect of compressibility of the oil appears as an equivalent spring rate.

By eliminating the perturbed flow q from (III-12) and (III-29) there results:

$$C_\varepsilon \varepsilon = As(x_o - x_p) + \left[\frac{A^2}{k_o} s + C_p\right] p_L \qquad \text{(III-30)}$$

This equation and the definition of the valve error, (III-1), are the basic relationships employed in the analysis which follows.

For the sake of simplicity, the preceding derivation of flow relationships has been limited in such a way that it rigorously applies only to an actuator

with a symmetrical, closed center valve, with equal volumes on each side of the cylinder, and with equal net areas on each side of the piston which operates through small displacements. The analysis is relatively insensitive to deviations from these conditions, however; and it scope of applicability is quite wide.

It should be mentioned that there are systems for which the analysis as presented here is not a sufficiently accurate description to permit useful application. The following are examples of conditions under which this statement may be true. If the valve is definitely an open center type, it is possible to have interaction between the actuator, and the tubing and pressure regulators of the supply system. Even if this interaction is taken into consideration for an open center valve, the analysis as given may lead to insufficiently accurate results because of the pronounced effect of neutral leakage. Space considerations sometimes demand that the piston have no blind rod or that the volumes on each side of the piston be markedly different for other reasons. There are some hydraulic fluids in use which display a constancy of bulk modulus only at fairly high pressures. The higher operating pressures can be obtained by purposely designing the valve to be asymmetrical. It is also possible to compensate for unequal net areas on the two sides of the piston or for preload (paired actuators) by designing the valve to be asymmetrical. In the case of unequal volumes on either side of the piston, this cannot be done, however. With any of the deviations from complete symmetry mentioned, non-linear behavior is accentuated; this leads to chopped and offset waves in the frequency response. In almost any case, it is possible to extract a linearized solution which predicts critical frequencies and stability, using in general a complete double set of parameters $C_p, C_\varepsilon, K_o, A$. This section has provided the initial basis for such a generalized development; however, it has not been carried through because of the specialized nature of its application. The analysis as presented is adequate for most design.

SECTION 3 - FORCE AND LINKAGE EQUATIONS OF THE ACTUATOR

(a) DISTRIBUTION OF PARAMETERS

In the development of the actuator analysis, it is convenient to regard the hydraulic servo actuator as being terminated by two linear springs, k_i and k_c. Linear motions of the ends of these springs represent inputs to the servo. Similarly, forces collinear with these motions are inputs. However, there must be an over-all dynamic balance of the forces acting on the system, so that one of them is not independent, and the linearized servo behavior may be described in terms of only three variables. One of the three variables must be a force, or convertible to a force. With these remarks in mind, the force and linkage relationships of the servo are assumed to be those implied by the schematic in Figure III-5. A comparison with Figure III-1 is suggested.

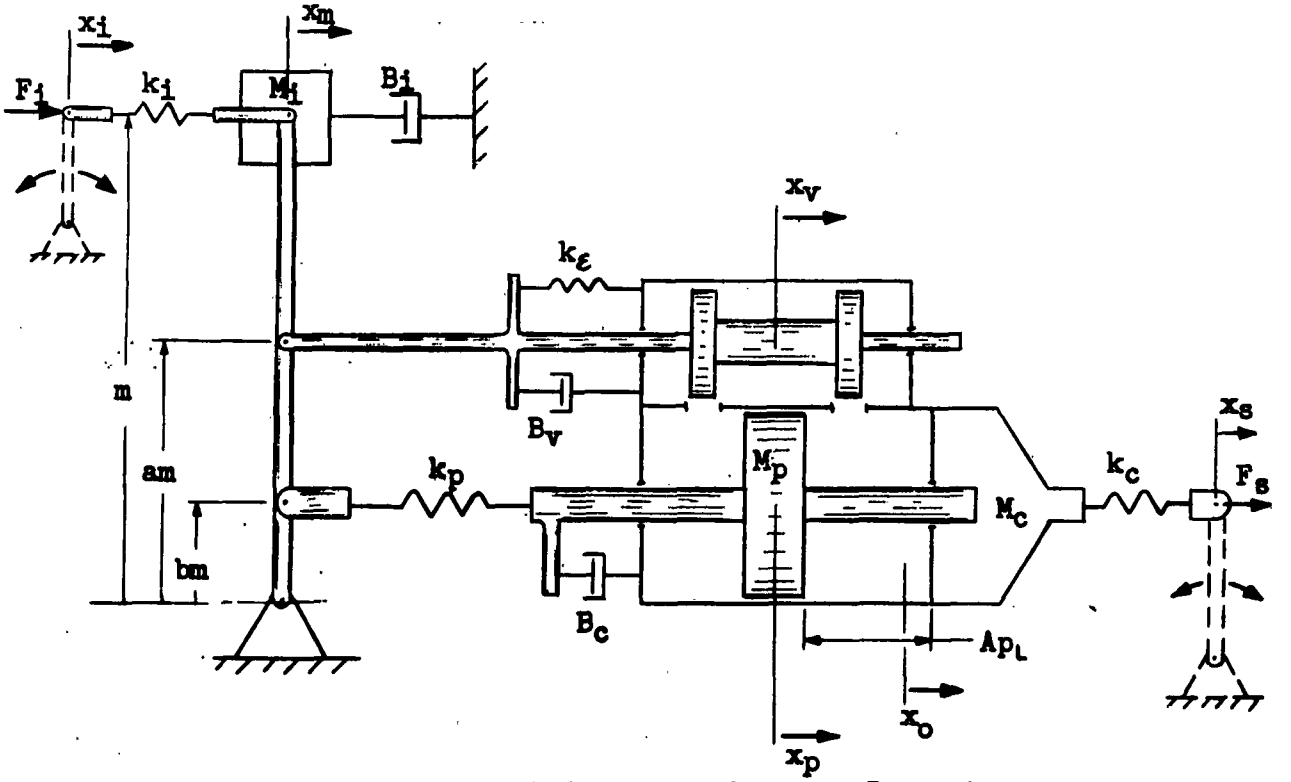

Figure III-5. Identification of Lumped Parameters

The vertical rod of length m is assumed to be rigid. The mass M_i, at the free end of the vertical rod, is a lumped equivalent of the mass of this rod, of the slide valve, of part of the piston rod, and of part of the cable or pushrod between the controlling element and the actuator. B_i is a viscous damping coefficient; it represents the effect of the damping in that part of the system associated with M_i, due to velocity relative to the fixed structure.

The magnitude m does not enter explicitly into the actuator equations; hence the radii from the fixed point of the vertical rod to the pivot points of actuator and valve are designated as the products of m by the dimensionless ratios b and a. The small error introduced by the fact that the motions of these pivot points are angular rather than linear is neglected.

B_v is a damping coefficient representing the effect of relative velocity between valve slide and cylinder. M_p is the equivalent mass of the piston, and M_c the equivalent cylinder mass. B_c is a damping coefficient representing the effect of relative velocity between piston and cylinder.

A force Ap_i on the piston and cylinder acts as shown in the diagram.

As a matter of terminology, points at which displacements such as x_i and x_s are measured will be called "nodes." The appropriateness of this terminology may be better appreciated after considering the mechanical network diagrams, or "nodal diagrams," used later in this chapter and throughout the remainder of the volume. For a more complete discussion of such diagrams, M. F. Gardner and J. L. Barnes, Transients in Linear Systems (John Wiley & Sons, N.Y., 1942), may be consulted.

The nodes x_i and x_s may be chosen so as to facilitate analysis of a larger system of which the servo actuator is only a part. It is to be noted that the selection of these nodes determines what are to be considered the coupling springs k_i and k_c. If numerical results of the hydraulic servo analysis are

to be supplied to another group, to be used in further, more comprehensive analyses, these nodes and consequently the springs should be definitely identified in the physical system; doing this imposes no restriction on the way in which adjacent sub-systems are analyzed. If, on the other hand, a wholly literal analysis of a more comprehensive system is to be performed, x_i and x_s may well be chosen at the terminal nodes of adjacent sub-systems.

In general, it will be necessary to increase the values of the quantities M_c , B_i , and M_i indicated in the preceding discussion to take into account distributed masses and dampings in coupling members.

The forces F_s and F_i each arise from inertias, dampings, and applied external forces associated with one or more degrees of freedom of an adjacent system.

(b) FORCE AND LINKAGE EQUATIONS

The equations of the force system of Figure III-5 are obtained by writing out the expressions for force and moment balances in a straightforward way; only the results are given here:

(III-31) $$F_s + k_c x_o = k_c x_s$$

(III-32) $$F_i + k_i x_m = k_i x_i$$

(III-33) $$(M_c s^2 + B_c s + k_c) x_o - B_c s x_p - (B_v s + k_\varepsilon)\varepsilon - A p_L = k_c x_s$$

(III-34) $$(M_p s^2 + B_c s + k_p) x_p - B_c s x_o - k_p b x_m + A p_L = 0$$

(III-35) $$(M_i s^2 + B_i s + k_i + b^2 k_p) x_m - b k_p x_p + a(B_v s + k_\varepsilon)\varepsilon = k_i x_i$$

(III-36) $$x_v = a x_m$$

SECTION 4 - COMBINATION OF FLOW, FORCE, AND LINKAGE EQUATIONS

(a) SIMPLIFICATION OF THE EQUATIONS

All of the equations defining behavior of the hydraulic servo actuator have now been derived: (III-1) defining the valve error, (III-30) describing flow behavior, and (III-31) through (III-36) expressing force and linkage relationships. In all, there are eight equations with ten variables F_s , F_i , x_o , x_p , x_m , x_v , x_s , x_i , p_L , and ε . All these equations are linear with coefficients which are algebraic functions of the derivative operator s . The over-all servo behavior can then be described by a single literal equation involving only three variables. When the equations are written in determinantal form, the coefficients in s may be manipulated in the same way as constants. However, if the equations are treated in the present form, the geometrical factors and flow coefficients make the reduction difficult. If the equations are changed to a form which can be easily expressed in a nodal diagram (mechanical-network diagram), the reduction is greatly facilitated.

An important simplification in the force and linkage equations (III-31) through (III-36) can be effected by relating the effects of masses, dampers, and springs acting at a radius αm , to those of equivalent quantities acting at some other radius βm ; for example, the equivalent mass, M', acting at a radius βm is equivalent to the original mass, M , at a radius αm multiplied by α^2/β^2 ; i.e., $M' = M(\alpha^2/\beta^2)$. This simplification also applies to the B's and k's . On the other hand, the displacement x' at a radius βm equivalent to x at αm is $\beta x/\alpha$.

The force and linkage equations (III-31) through (III-36) may then be simplified by the substitutions:

$$x_{mr} \equiv b x_m \quad , \quad x_{ir} \equiv b x_i \quad ,$$

$$M_{ir} \equiv \frac{M_i}{b^2} \quad , \quad B_{ir} \equiv \frac{B_i}{b^2} \quad , \quad k_{ir} \equiv \frac{k_i}{b^2}$$

Also, the node x_{ir} is easily eliminated by combining Equations (III-1) and (III-36). With these simplifications the set of equations (III-31) through (III-36) take the simpler forms:

(III-37) $$F_s + k_c x_o = k_c x_s$$

(III-38) $$\frac{F_i}{b} + k_{ir} x_{mr} = k_{ir} x_{ir}$$

(III-39) $$(M_c s^2 + B_c s + k_c) x_o - B_c s x_p - (B_v s + k_e)\varepsilon - A p_L = k_c x_s$$

(III-40) $$(M_p s^2 + B_c s + k_p) x_p - B_c s x_o - k_p x_{mr} + A p_L = 0$$

(III-41) $$(M_{ir} s^2 + B_{ir} s + k_{ir} + k_p) x_{mr} - k_p x_p + \frac{a}{b}(B_v s + k_e)\varepsilon = k_{ir} x_{ir}$$

(III-42) $$\varepsilon = \frac{a}{b} x_{mr} - x_o$$

The flow equation (III-30) may be rewritten as:

(III-43) $$A p_L = \frac{k_o\left[\left(\frac{AC_e}{C_p}\right)\varepsilon - \left(\frac{A^2}{C_p}\right) s (x_o - x_p)\right]}{\left[\left(\frac{A^2}{C_p}\right) s + k_o\right]}$$

It may be readily checked that AC_e / C_p has the dimensions of a spring constant (lb/in.) and that A^2/C_p has those of a viscous damping coefficient. These equivalent parameters of a force system are designated in the following as k_f and B_f, respectively. Equation (III-43) then becomes:

(III-44) $$(B_f s + k_o)\left(\frac{A p_L}{k_o}\right) + B_f s (x_o - x_p) - k_f \varepsilon = 0$$

where

$$k_f \equiv \frac{AC_e}{C_p} = -A \frac{\frac{\partial Q}{\partial E}}{\frac{\partial Q}{\partial P_L}} = +A \frac{\partial P_L}{\partial E}$$

$$B_f \equiv \frac{A^2}{C_p} = -\frac{A^2}{\frac{\partial Q}{\partial P_L}} = -A^2 \frac{\partial P_L}{\partial Q}$$

The nature of the "flow damping" B_f can be seen by rotating Figure III-4a through 90° clockwise. The "flow spring constant" k_f is the slope of the cross-plot shown in Figure III-6.

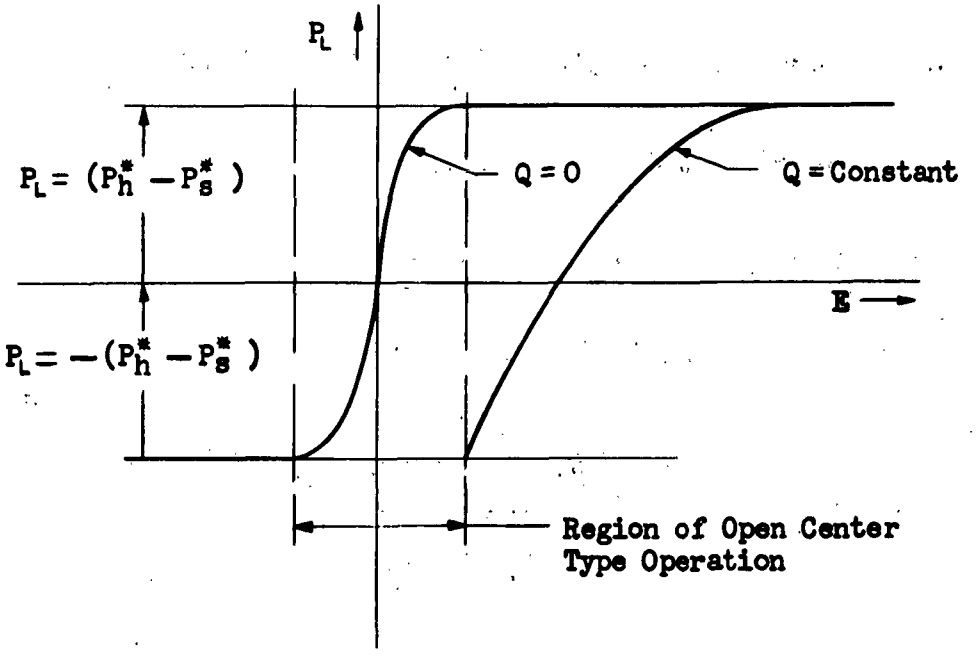

Figure III-6. Variation of Pressure Differential Across the Piston with Valve Error

The definition of the parameters k_o and B_f, expressing flow relationships, implies the presence of a physically important node associated with them. This node is located somewhere within the body of oil in the cylinder and can thus never be experimentally observed, but it is important in speeding the reduction of the actuator equations. The node x_f is defined by the relationship:

(III-45) $$x_f \equiv \frac{A p_L}{k_o} + x_o$$

With the introduction of x_f , (III-44) becomes:

(III-46) $$(B_f s + k_o)x_f - B_f s x_p - k_o x_o - k_f \varepsilon = 0$$

The force Ap_L is then given by:

(III-47) $$Ap_L = k_o(x_f - x_o) = B_f s(x_p - x_f) + k_f \varepsilon$$

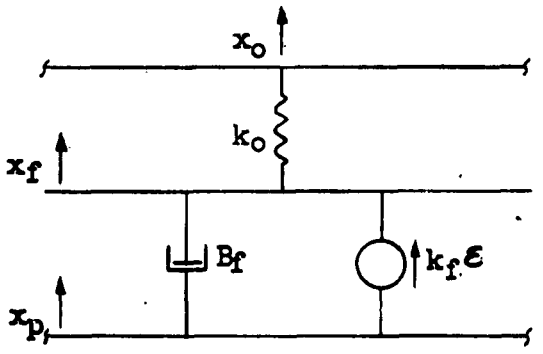

Figure III-7. Partial Nodal Diagram Expressing Flow Relationships

The partial nodal diagram shown in Figure III-7 may be constructed from Equation (III-46). The only node completely described by this diagram is the node x_f . This form may be used directly to express the flow behavior irrespective of linkage configuration. It is interesting to note that if p_L is zero, x_o and x_f are equivalent. The displacement x_f may then be considered as the output of an actuator subject to no external or internal loads. This nodal diagram is of particular use in the physical interpretation of the actuator as a force source driving x_o through a spring k_o . All of the parameters k_o , B_f , and k_f have physical values which can be measured by test.

The incorporation of (III-46) and (III-47) into the set (III-37) through (III-41) results in the following:

(III-48) $$F_s + k_c x_o = k_c x_s$$

(III-49) $$\frac{F_i}{b} + k_{ir} x_{mr} = k_{ir} x_{ir}$$

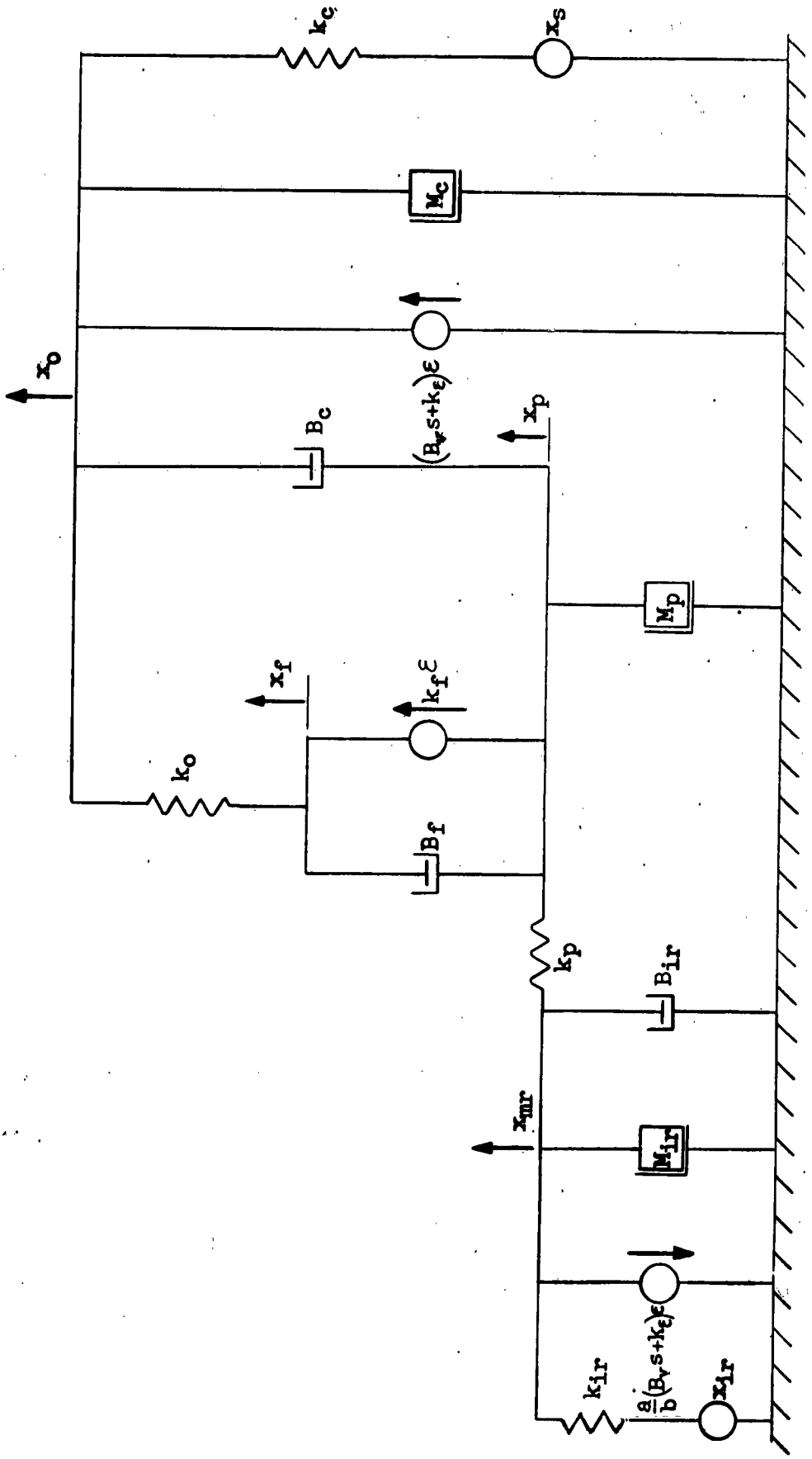

Figure III-8. Nodal Diagram of the Generalized Hydraulic Servo Actuator

$$(M_c s^2 + B_c s + k_o + k_c)x_o - B_c s x_p - k_o x_f - (B_v s + k_\varepsilon)\varepsilon = k_c x_s \quad \text{(III-50)}$$

$$[M_p s^2 + (B_c + B_f)s + k_p]x_p - B_c s x_o - B_f s x_f - k_p x_{mr} + k_f \varepsilon = 0 \quad \text{(III-51)}$$

$$(M_{ir} s^2 + B_{ir} s + k_{ir} + k_p)x_{mr} - k_p x_p + \frac{a}{b}(B_v s + k_\varepsilon)\varepsilon = k_{ir} x_{ir} \quad \text{(III-52)}$$

$$(B_f s + k_o)x_f - B_f s x_p - k_o x_o - k_f \varepsilon = 0 \quad \text{(III-53)}$$

Equations (III-50) through (III-53) are now all nodal in form (see Figure III-8), and the reduction is greatly expedited. The only force sources are in the valve error or its time derivative, where the valve error is defined:

$$\varepsilon - \frac{a}{b} x_{mr} + x_o = 0 \quad \text{(III-54)}$$

(b) REDUCTION OF THE EQUATIONS

The analysis presented in the following chapters depends on the reduction of the controlling equations of the actuator in such a manner as to isolate four relationships:

$$\text{(III-55)} \quad \begin{cases} F_s = \zeta_1(x_s, x_i) \\ F_i = \zeta_2(x_s, x_i) \\ x_o = \zeta_3(\varepsilon, x_s) \\ \varepsilon = \zeta_4(x_i, x_o, x_s) \end{cases}$$

The first three of the functional forms given above are unique. The fourth form will be determined in such manner as to facilitate physical interpretation of the results.

The determinant of the coefficients on the left of (III-50) through (III-54) is:

$M_c s^2 + B_c s + (k_o + k_c)$	$-B_c s$	0	$-k_o$	$-(B_r s + k_\varepsilon)$	
$-B_c s$	$M_p s^2 + (B_c + B_f) s + k_p$	$-k_p$	$-B_f s$	k_r	
0	$-k_p$	$M_{ir} s^2 + B_{ir} s + (k_{ir} + k_p)$	0	$\frac{a}{b}(B_r s + k_\varepsilon)$	
$-k_o$	$-B_f s$	0	$B_f s + k_o$	$-k_r$	
1	0	$-\frac{a}{b}$	0	1	

Solving (III-50) through (III-54) for x_o and x_{mr}, each in terms of x_s and x_{ir}, and substituting in (III-48) and (III-49),

$$(III\text{-}56) \qquad F_s = \frac{k_c x_s (\Delta_A - k_c A_{11}) - k_{ir} x_{ir} (k_c A_{31})}{\Delta_A}$$

$$(III\text{-}57) \qquad \frac{F_i}{b} = \frac{k_{ir} x_{ir} (\Delta_A - k_{ir} A_{33}) - k_c x_s (k_{ir} A_{13})}{\Delta_A}$$

where A_{ij} is the (signed) minor of the element in row i and column j of the system determinant, and Δ_A is the determinant itself. For purposes of discussion, it is convenient to have the above equations expressed in terms of operators which reduce to unity, or a good approximation thereof, when s equals zero. This is accomplished by dividing numerator and denominator of each equation by the product of major actuator springs $k_o k_p k_c k_{ir} k_f$, k_ε being omitted because it is small in comparison with k_f. The equations may now be rewritten:

$$(III\text{-}58) \qquad F_s = \frac{g_1 x_s - g_2 (a x_i)}{\left(\frac{g_5}{k_t}\right)}$$

$$(III\text{-}59) \qquad \frac{F_i}{b} = \frac{g_3 (a x_i) - g_4 x_s}{\left(\frac{g_5}{k_t}\right)}$$

where

$$\frac{1}{k_t} \equiv \frac{1}{k_c} + \frac{1}{k_f} + \frac{\left(\frac{a}{b}\right)}{k_{ir}} = \frac{1}{k_c} + \frac{1}{k_f} + \frac{ab}{k_l}$$

$$g_1 = \frac{(\Delta_A - k_c A_{11})}{k_o k_p k_f k_{ir}}$$

$$g_2 = \frac{\left(\frac{b}{a}\right)(A_{31})}{k_o k_p k_f}$$

$$g_3 = \frac{\left(\frac{b}{a}\right)(\Delta_A - k_{ir} A_{33})}{k_o k_f k_p k_c}$$

$$g_4 = \frac{A_{13}}{k_o k_p k_f}$$

$$\frac{g_5}{k_t} = \frac{\Delta_A}{k_o k_p k_c k_f k_{ir}}$$

g_1 , g_2 , g_3 , g_4 , and g_5 are polynominals in s , which reduce to unity when s equals zero if the input coupling spring k_c is much smaller than the flow spring k_f .

One additional operator of some use in later work may be derived from the system determinant. Equation (III-56) may be written in the form:

$$F_s = \left\{ k_c - \frac{k_c \left[\frac{A_{11}}{k_o k_p k_{ir} k_f} \right]}{\left(\frac{g_5}{k_t}\right)} \right\} x_s - \frac{g_2 (a x_i)}{\left(\frac{g_5}{k_t}\right)} \qquad \text{(III-60)}$$

An expression equivalent to this is

$$F_s = \left[k_c - \frac{\left(\frac{k_c}{k_{fi}}\right) g_6}{\left(\frac{g_5}{k_t}\right)} \right] x_s - \frac{g_2 (a x_i)}{\left(\frac{g_5}{k_t}\right)} \qquad \text{(III-61)}$$

where

$$\frac{1}{k_{fi}} \equiv \frac{1}{k_f} + \frac{\frac{a}{b}}{k_{ir}} = \frac{1}{k_f} + \frac{ab}{k_i}$$

$$g_6 = \frac{A_{11} k_{fi}}{k_o k_p k_{ir} k_f}$$

and g_6 is an expression in s which reduces approximately to unity when s equals zero. The third required relationship of (III-55) is derived by taking the determinant of the system of equations consisting of (III-50), (III-51) with the node x_{mr} eliminated by use of (III-54), and (III-53):

$$\begin{vmatrix} M_c s^2 + B_c s + k_o + k_c & -B_c s & -k_o \\ -\left(B_c s + \frac{b}{a} k_p\right) & M_p s^2 + (B_c + B_f)s + k_p & -B_f s \\ -k_o & -B_f s & B_f s + k_o \end{vmatrix}$$

The solution to this system of equations is given by:

$$(III\text{-}62) \qquad x_o = \frac{\left[\frac{(B_c s + k_c)B_{11} + \left(k_f - \frac{b}{a} k_p\right)B_{21} + k_f B_{31}}{k_o k_c k_p}\right] \epsilon + \left[\frac{B_{11}}{k_o k_p}\right] x_s}{\left[\frac{\Delta_B}{k_o k_c k_p}\right]}$$

where Δ_B is the determinant of this system and the B_{ij} its minors, as before.

The fourth functional form in (III-55) remains to be determined. If (III-50), (III-51), and (III-53) are added, there results:

$$(\text{III-63}) \qquad -(B_v s + k_\varepsilon)\varepsilon + M_p s^2 x_{mr} - (M_p s^2 + k_p)(x_{mr} - x_p) = k_c x_s - (M_c s^2 + k_c) x_o$$

The determinant of the system of equations (III-52), (III-54), and (III-63) is:

$$\begin{vmatrix} \frac{a}{b}(B_v s + k_\varepsilon) & M_{ir} s^2 + B_{ir} s + k_{ir} & -k_p \\ 1 & -\frac{a}{b} & 0 \\ -(B_v s + k_\varepsilon) & M_p s^2 & -(M_p s^2 + k_p) \end{vmatrix}$$

By solving these three equations for ε:

$$(\text{III-64}) \qquad \varepsilon = \frac{\left[\frac{\frac{b}{a} C_{11}}{k_p}\right](a x_i) - \left[\frac{(M_c s^2 + k_c) C_{31} - C_{21}}{k_p k_{ir}}\right] x_o + \left[\frac{\frac{b}{a} C_{31}}{k_p}\right] \frac{ab k_c x_s}{k_i}}{\left[\frac{\Delta_c}{k_p k_{ir}}\right]}$$

In expanding the determinants of this chapter it is worthwhile to exploit certain generally applicable relations between the parameters. Since the equivalent flow damping B_f is inversely proportional to the valve flow coefficient C_p, which remains quite small, B_f is always large in comparison with B_c, B_s, and B_v. Also, the input coupling spring k_ε will always be negligible in comparison with the flow spring k_f.

$$B_f >> B_c$$

$$B_f >> \frac{a}{(a-b)} B_s$$

$$B_f >> B_v$$

$$k_f >> k_e$$

The desired relations of (III-55) are now established.

The equations derived in this chapter are very general. In Chapter IV, these equations are restricted by imposing the load of an aircraft control surface on the hydraulic control system. Chapters V and VI consider two specific types of hydraulic surface actuator systems.

CHAPTER IV

A GENERALIZED HYDRAULIC CONTROL SYSTEM

SECTION 1 - SIMPLIFIED CONTROL SURFACE CHARACTERISTICS

A general analysis of control surface behavior is outside the scope of this volume, since this would require that the reader have a rather comprehensive knowledge of aeroelasticity in order to understand the complex interaction possible between non-rigid parent and control surfaces.

It is usually possible to represent control surface behavior fairly accurately by including with the actuator analysis a mass M_s and a coefficient of viscous damping B_s. These control surface parameters are referred to the line of action of the actuator cylinder. The control surface, regarded as a flexible structure, has some effective spring constant which expresses the flexibility between its effective mass center and the surface horn. The coupling spring k_c of the actuator analysis is conveniently taken as including this surface flexibility. The displacement x_s then becomes a node at the effective mass center of the surface. The nodal diagram is shown in Figure IV-1.

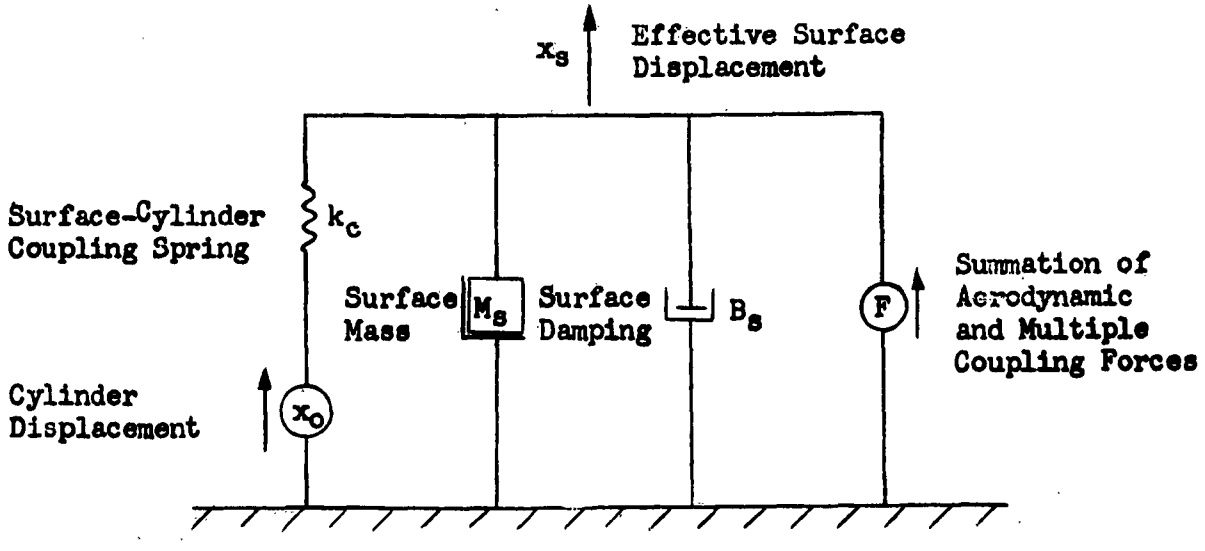

Figure IV-1. Nodal Diagram of Control Surface

The force F of Figure IV-1 is a quantity which is predominantly the aerodynamic moment acting on the control surface, referred to the line of action of the cylinder; however, this variable may also include terms expressing a coupling between multiple modes of vibration of control and parent surfaces. The equation corresponding to Figure IV-1 is

$$(M_s s^2 + B_s s + k_c)x_s - k_c x_o = F \tag{IV-1}$$

An equivalent relationship in terms of the force F_s existing in the coupling spring k_c is secured by use of Equation (III-48).

$$(M_s s^2 + B_s s)x_s + F_s = F \tag{IV-2}$$

It must be remembered here that the spring constant k_c is understood to include surface flexibility.

SECTION 2 - A GENERALIZED HYDRAULIC CONTROL SYSTEM

It is now proposed to consider the system composed of the hydraulic servo actuator of Figure III-8 and the simplified control surface of Figure IV-1. The final equations of Chapter III will be so combined with (IV-1) and (IV-2) as to permit investigation of the behavior of the system as a component, and also of the interaction through forces between the surface-actuator system and adjacent systems. The results of the combination will be a set of five relationships:

$$\begin{cases} F = Z_1(x_s, x_i) \\ F_i = Z_2(x_i, F) \\ x_o = Z_3(x_i, F) \\ x_o = Z_4(\varepsilon, F) \\ \varepsilon = Z_5(x_i, x_o, F) \end{cases} \tag{IV-3}$$

The first relationship of (IV-3) is of use in the investigation of a general flutter problem in which there is interaction between the control system as a servo and the aeroelastic behavior of control surface and parent surface. Part II of this volume is concerned with the statement of the flutter problem where there may be interaction with servos of the aircraft control chain. The relationship for F in terms of α_s and α_i will be expressed in three ways, each of which has some useful application to servo-flutter coupling interaction.

If the behavior of a system at the input end of the actuator is markedly affected by the force exerted on it by the actuator, there is force coupling, as well as displacement coupling, at the input end of the hydraulic control system. In this case it is necessary to use the second relationship of (IV-3).

The third, fourth, and fifth relationships of (IV-3) represent the behavior of the hydraulic control system as a positional servo. The over-all, or closed-loop behavior is given by α_o (which for convenience of comparison with test results is taken as the output of the system) in terms of α_i, the displacement input to the system, and F, the disturbing force. The fourth and fifth expressions of (IV-3) are functional forms of greater utility in the analysis than closed-loop expressions. Isolation of the critical variable ε, which is the valve error, gives rise to an open-loop transfer function when the disturbing force F can be regarded as negligible.

The relationships of Chapter III which can be combined with (IV-1) and (IV-2) to determine the first three relationships of (IV-3) are (III-58), (III-59), and (III-61). They are repeated here for convenience:

$$(IV\text{-}4) \qquad F_s = \frac{g_1 \alpha_s - g_2 (\Delta \alpha_i)}{\left(\frac{g_5}{k_t}\right)}$$

(IV-5) $$\frac{F_i}{b} = \frac{g_3(a x_i) - g_4 x_s}{\left(\frac{g_5}{k_t}\right)}$$

(IV-6) $$F_s = \left[k_c - \frac{\left(\frac{k_c}{k_{fi}}\right) g_6}{\left(\frac{g_5}{k_t}\right)}\right] x_s - \frac{g_2(a x_i)}{\left(\frac{g_5}{k_t}\right)}$$

where

$$\frac{1}{k_t} \equiv \frac{1}{k_c} + \frac{1}{k_f} + \frac{\frac{a}{b}}{k_{ir}} = \frac{1}{k_c} + \frac{1}{k_f} + \frac{ab}{k_i}$$

$$\frac{1}{k_{fi}} \equiv \frac{1}{k_f} + \frac{\frac{a}{b}}{k_{ir}} = \frac{1}{k_f} + \frac{ab}{k_i}$$

and g_1 , g_2 , g_3 , g_4 , g_5 are polynomials in s , each of which reduces to unity when s equals zero, if the input coupling spring k_ε is much smaller than the flow spring rate k_f . By elimination of F_s between (IV-2) and (IV-4),

(IV-7) $$F = \left[(M_s s^2 + B_s s) + \frac{g_1}{\left(\frac{g_5}{k_t}\right)}\right] x_s - \frac{g_2(a x_i)}{\left(\frac{g_5}{k_t}\right)}$$

By elimination of F_s between (IV-2) and (IV-6),

$$(IV\text{-}8) \qquad F = \left[(M_s s^2 + B_s s + k_c) - \frac{\left(\frac{k_c}{k_{fi}}\right) g_6}{\left(\frac{g_5}{k_t}\right)} \right] x_s - \frac{g_2 (a x_i)}{\left(\frac{g_5}{k_t}\right)}$$

By rearrangement of (IV-7),

$$(IV\text{-}9) \qquad F = \frac{\left[g_1 + (M_s s^2 + B_s s)\left(\frac{g_5}{k_t}\right) \right]}{\left(\frac{g_5}{k_t}\right)} x_s - \frac{g_2 (a x_i)}{\left(\frac{g_5}{k_t}\right)}$$

By elimination of x_s between (IV-5) and (IV-9)

$$(IV\text{-}10) \qquad F_i = \frac{b\left[\frac{k_t (g_1 g_3 - g_2 g_4)}{g_5} + (M_s s^2 + B_s s) g_3 \right] (a x_i) - b g_4 F}{\left[g_1 + (M_s s^2 + B_s s)\left(\frac{g_5}{k_t}\right) \right]}$$

By elimination of x_s between (IV-1) and (IV-9),

$$(IV\text{-}11) \qquad x_o = \frac{g_2 \left(\frac{M_s}{k_c} s^2 + \frac{B_s}{k_c} s + 1 \right) (a x_i) + \left(\frac{k_{fi} g_5}{k_t} - \frac{k_{fi} g_1}{k_c} \right) \frac{F}{k_{fi}}}{\left[g_1 + (M_s s^2 + B_s s)\left(\frac{g_5}{k_t}\right) \right]}$$

It is of interest at this point to examine the forms assumed by (IV-9) and (IV-11) when s is equal to zero:

$$(IV\text{-}11a) \qquad x_o \Big|_{s=0} = (a x_i) + \frac{F}{k_{fi}}$$

(IV-9a) $$x_g \Big|_{s=0} = (a x_i) + \frac{F}{k_t}$$

It can be seen from (IV-11a) that if the force F can be neglected, the control system is a servo with no steady-state position error; i.e., it has a single integration in the open-loop transfer function. The output displacement x_o attempts to follow the input displacement referred to the line of action of the valve slide. With F left undetermined, there is a position error determined by the spring k_{fl} from the input node x_i to the output node x_o. The spring k_{fl} is the series combination of the flow spring k_f and a modified input spring k_i/ab. If the power boost ratio $1/b$ is infinite, the spring k_{fi} becomes k_f. It is important to note that the servo action determines the steady-state behavior, and k_p and k_o are not involved. Equation (IV-9a) shows that in the steady state x_g, which is the displacement of the effective mass center of the control surface, behaves somewhat as the cylinder displacement x_o, except that the effective spring determining position error is now k_t, the series combination of k_{fi} and k_c. The position error due to a static force F is of course greater at x_g than at x_o.

The fourth expression of (IV-3) is obtained by combining Equations (III-50), (III-51) with the node x_{mr} eliminated by use of (III-54), (III-53), and (IV-1). The determinant is

$$\begin{vmatrix} M_c s^2 + B_c s + k_o + k_c & -B_c s & -k_o & -k_g \\ -B_c s - \frac{b}{a} k_p & M_p s^2 + (B_c + B_f) s + k_p & -B_f s & 0 \\ -k_o & -B_f s & B_f s + k_o & 0 \\ -k_c & 0 & 0 & M_g s^2 + B_g s + k_c \end{vmatrix}$$

The solution may be written:

$$(IV\text{-}12) \qquad x_o = \gamma_\varepsilon \varepsilon + \gamma_F F$$

where

$$\gamma_\varepsilon = \frac{\left[\frac{(B_v s + k_\varepsilon)\alpha_{11} + (k_f - \frac{b}{a}k_p)\alpha_{21} + k_f \alpha_{31}}{k_f k_o k_p k_c}\right]}{\left[\frac{\Delta_\alpha}{k_f k_o k_p k_c}\right]}$$

$$\gamma_F = \frac{\left[\frac{1}{k_f}\right]\left[\frac{-\alpha_{41}}{k_o k_p k_c}\right]}{\left[\frac{\Delta_\alpha}{k_f k_o k_p k_c}\right]}$$

The fifth and last expression of (IV-3) is obtained by using (III-52), (III-54), (III-63), and (IV-1). The determinant is

$$\begin{vmatrix} \frac{a}{b}(B_v s + k_\varepsilon) & M_{ir}s^2 + B_{ir}s + k_{ir} & k_p & 0 \\ 1 & -\frac{a}{b} & 0 & 0 \\ -(B_v s + k_\varepsilon) & M_p s^2 & -(M_p s^2 + k_p) & -k_c \\ 0 & 0 & 0 & M_s s^2 + B_s s + k_c \end{vmatrix}$$

The solution may be expressed in the form:

$$\text{(IV-13)} \qquad \varepsilon = Y_{eq}\left[Y_{\varepsilon i}(a\ddot{x}_i) - \ddot{x}_o + Y_{eF}F\right]$$

where

$$Y_{eq} = \frac{\left[\frac{(M_c s^2 + k_c)\beta_{31} - \beta_{21} + k_c\beta_{41}}{k_p k_c k_{ir}}\right]}{\left[\frac{k_i + a(a-b)k_\varepsilon}{k_i}\right]\left\{\frac{\Delta_\beta}{k_p k_c\left[k_{ir} + \frac{a(a-b)}{b^2}k_\varepsilon\right]}\right\}}$$

$$Y_{\varepsilon i} = \frac{\left[\frac{\frac{b}{a}\beta_{11}}{k_p k_c}\right]}{\left[\frac{(M_c s^2 + k_c)\beta_{31} - \beta_{21} + k_c\beta_{41}}{k_p k_c k_{ir}}\right]}$$

$$Y_{eF} = \frac{\left[\frac{ab}{k_i}\right]\left[\frac{-\frac{b}{a}\beta_{41}}{k_p k_c}\right]}{\left[\frac{(M_c s^2 + k_c)\beta_{31} - \beta_{21} + k_c\beta_{41}}{k_p k_c k_{ir}}\right]}$$

Equations (IV-12) and (IV-13) are the basis for the block diagram shown in Figure IV-2.

The quantity F of (IV-11), (IV-12), and (IV-13) in general includes terms which express a coupling between multiple modes of vibration of control surface and parent surface. If the magnitudes of these coupling terms are the same as,

or less than, that of the true aerodynamic force, the total F composed of aerodynamic force and coupling terms can usually be neglected without severely affecting the system analysis. If the coupling terms are large, however, the system analysis is incomplete, and the results of the actuator analysis must be combined with a more sophisticated formulation of the characteristics of control surface behavior. Such difficulties are often associated with unconventional control surface design, such as all-movable surfaces.

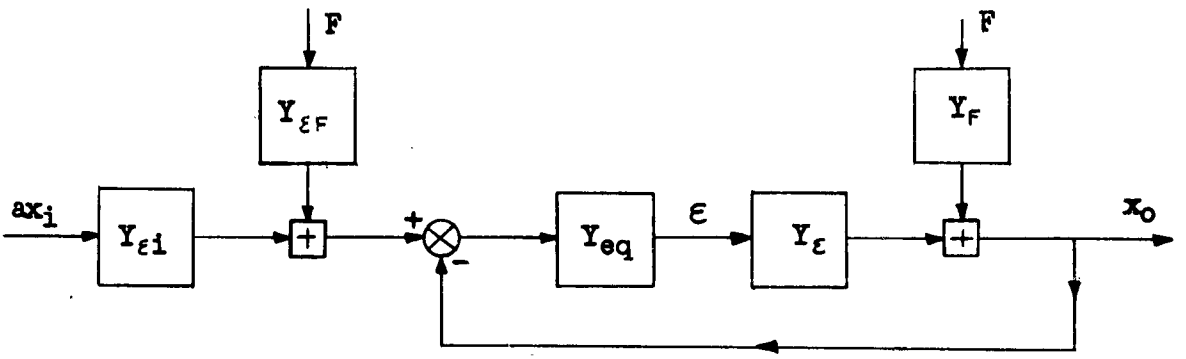

Figure IV-2. Block Diagram of the Generalized Hydraulic Control System

If the force F is considered negligible in Figure IV-2, the open-loop transfer function of the positional servo is given by the product of Y_{eq} and Y_ε. From an investigation of the frequency response of the open-loop transfer function one can form an excellent idea of the characteristics and limitations of various systems.

The following two chapters are concerned principally with the frequency response and stability of two systems. Chapter V deals with the case that the power boost ratio $1/b$ is infinite and the input ratio a is unity. Because of the wide use of the "fully-powered" system, portions of the material of Chapters III and IV are repeated, so that Chapter V may be read with little reference to earlier chapters. In Chapter VI analysis of the generalized power boost case is resumed.

CHAPTER V

THE FULLY-POWERED HYDRAULIC CONTROL SYSTEM

SECTION 1 - THE GENERALIZED SYSTEM

The purpose of this chapter is to present the equations governing the behavior of a fully-powered hydraulic control system and to investigate the effects of its various parameters upon frequency response and stability. The schematic diagram is shown in Figure V-1, and the corresponding nodal diagram is shown in Figure V-2. The form of this diagram is derived from Figure III-5 by assuming the power boost ratio $1/b$ to be infinite and the control input ratio a to be unity, and by adding the simplified surface characteristics discussed in Chapter IV.

The viscous damping coefficients B_v and B_i represent respectively the damping due to the relative velocity of the valve slide and the cylinder, and the damping in the cable and feel device. The mass M_i is the effective mass of the valve slide, the quadrant, and the cable. The spring constant k_e represents the effect of a springing action between the valve slide and the cylinder; and k_i represents the effect of the flexibility between the valve slide and a point of the controlling system having a displacement x_i, which is the actuating quantity of the control system.

For purposes of classification in this volume, a hydraulic control system of the general type shown in Figure III-5 is regarded as fully-powered whenever the power boost ratio $1/b$ is infinite. Strictly speaking, however, the damping B_v and the spring k_e cause a deviation from fully-powered operation in that a force may be transmitted from the control surface back to an initially controlling system, which may be the human pilot or an autopilot. If the behavior of the pilot or autopilot is markedly affected by a force transmitted from the control surface because the value of B_v or of k_e or of both is other than zero, there is a possibility that force coupling, in addition to displacement

coupling, exists between the initially controlling system and the hydraulic control system. With the human pilot, force coupling is probably not very important; however, with some autopilot installations, the effect might be appreciable. In most instances it is sufficient to consider only displacement coupling, and the following development is based on that assumption.

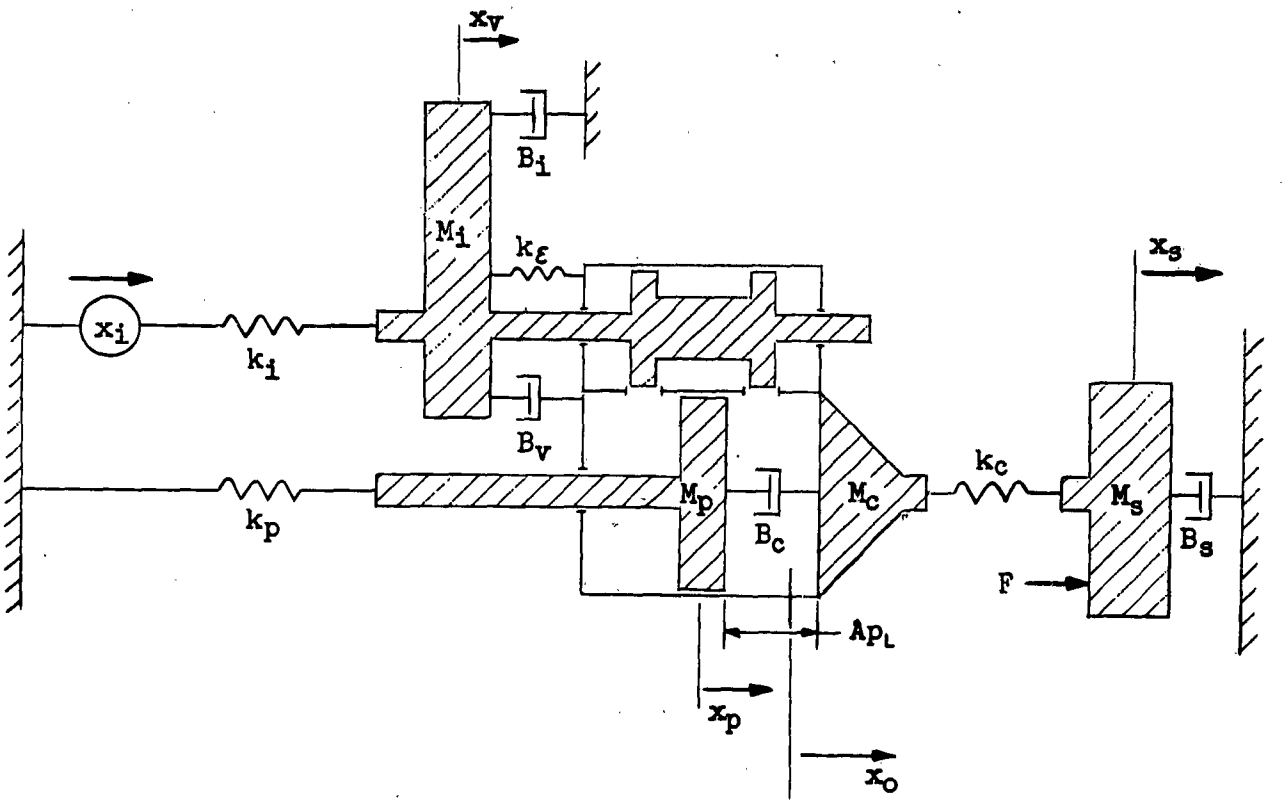

Figure V-1. Schematic Diagram of the Fully-Powered Hydraulic Control System

The controlling equations are easily written from Figure V-1 or Figure V-2:

(V-1) $$[M_c s^2 + (B_c + B_v)s + k_c + k_\varepsilon]x_o - B_c s x_p - B_v s x_v - k_c x_s - k_\varepsilon x_v = Ap_L$$

(V-2) $$(M_p s^2 + B_c s + k_p)x_p - B_c s x_o = -Ap_L$$

(V-3) $$(M_s s^2 + B_s s + k_c)x_s - k_c x_o = F$$

(V-4) $$[M_i s^2 + (B_i + B_v)s + k_i + k_\varepsilon]x_v - B_v s x_o - k_\varepsilon x_o = k_i x_i$$

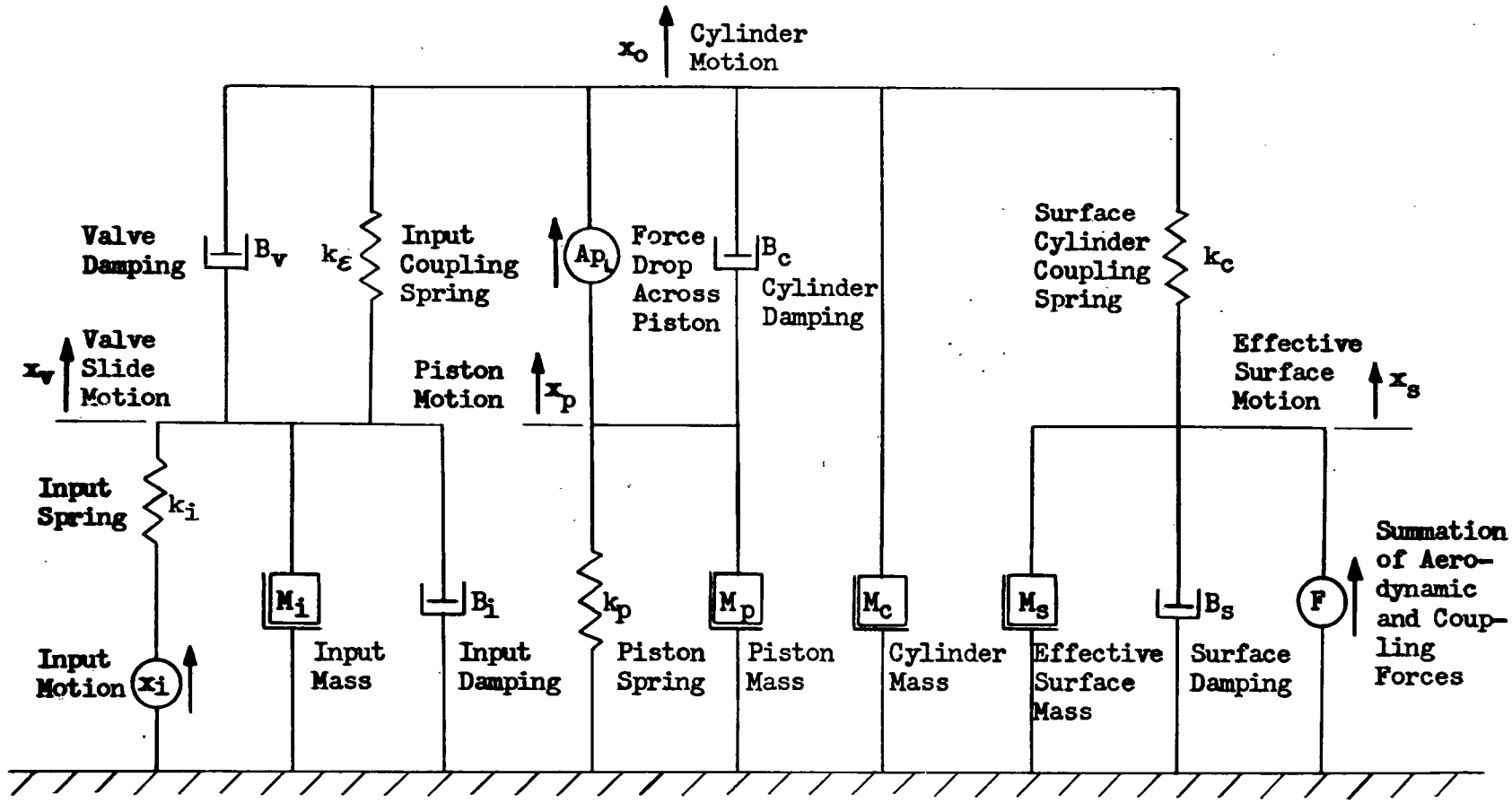

Figure V-2. Nodal Diagram of the Fully-Powered Hydraulic Control System

The flow relations governing the force differential across the piston, Ap_L, due to the pressure differential p_L, have been treated in detail in Section 2 of Chapter III. The equation for Ap_L is derived from Equation (III-30).

$$C_\varepsilon \varepsilon = A_s(x_o - x_p) + p_L\left(\frac{A^2}{k_o}s + C_p\right) \tag{V-5}$$

where

A is the net area of the piston

k_o is the spring rate due to oil compressibility

ε is the valve error, $\varepsilon = x_v - x_o$

and C_ε, C_p are experimentally determined coefficients of the net flow from valve to cylinder as a function of valve error ε and the pressure differential p_L across the operating ports, that is, across the piston. When multiplied by A/C_p, Equation (V-5) becomes

$$\left[\left(\frac{A^2}{C_p}\right)s + k_o\right]\left(\frac{Ap_L}{k_o}\right) - \left(\frac{AC_\varepsilon}{C_p}\right)\varepsilon + \left(\frac{A^2}{C_p}\right)s(x_o - x_p) = 0 \tag{V-6}$$

Using, for convenience, equivalent force parameters defined by:

$$k_f = \frac{AC_\varepsilon}{C_p}$$

$$B_f = \frac{A^2}{C_p}$$

the equation (V-6) takes the form

$$(B_f s + k_o)\left(\frac{Ap_L}{k_o}\right) + B_f s(x_o - x_p) - k_f \varepsilon = 0 \tag{V-7}$$

The incorporation of the valve error ε and (V-7) in the set (V-1) through (V-4) results in:

$$(M_c s^2 + B_c s + k_c)x_o - B_c s x_p - k_c x_s - k_o\left(\frac{Ap_L}{k_o}\right) = (B_v s + k_\varepsilon)\varepsilon \tag{V-8}$$

$$(V\text{-}9) \qquad \left(M_p s^2 + B_c s + k_p\right) x_p - B_c s x_o + k_o \left(\frac{A p_L}{k_o}\right) = 0$$

$$(V\text{-}10) \qquad \left(B_f s + k_o\right)\left(\frac{A p_L}{k_o}\right) + B_f s x_o - B_f s x_p = k_f \varepsilon$$

$$(V\text{-}11) \qquad \left(M_s s^2 + B_s s + k_c\right) x_s - k_c x_o = F$$

$$(V\text{-}12) \qquad \left[M_i s^2 + (B_i + B_v) s + k_i + k_e\right] \varepsilon + \left(M_i s^2 + B_i s + k_i\right) x_o = k_i x_i$$

A simple and readily interpreted result is obtained by solving (V-8) through (V-11) for x_o in terms of ε and F and Equation (V-12) for ε in terms of x_i and x_o. The system determinant of the first four equations is:

$$\begin{vmatrix} M_c s^2 + B_c s + k_c & -B_c s & -k_o & -k_c \\ -B_c s & M_p s^2 + B_c s + k_p & k_o & 0 \\ B_f s & -B_f s & B_f s + k_o & 0 \\ -k_c & 0 & 0 & M_s s^2 + B_s s + k_c \end{vmatrix}$$

This set of equations yields the following expression for the cylinder displacement x_o:

$$(V\text{-}13) \qquad x_o = \frac{\left[(B_v s + k_e) A_{11} + k_f A_{31}\right] \varepsilon + \left(-k_f A_{41}\right)\left(\frac{F}{k_f}\right)}{\Delta}$$

where Δ is the determinant shown above. The coefficients in (V-13) are polynomials in the derivative operator s. It is convenient for discussion and for forming of Bode plots to have the numerator coefficients in such a form that each reduces to unity, or very nearly so, when s is set equal to zero. This

is accomplished by dividing numerator and denominator by the product of the spring constants, $k_f\, k_o\, k_p\, k_c$. In symbolic form

$$\text{(V-14)} \qquad \pi_o = \gamma_\varepsilon\, \varepsilon + \gamma_F\, F$$

where

$$\gamma_\varepsilon = \frac{\left[\frac{(B_v s + k_\varepsilon) A_{11}}{k_f k_o k_p k_c} + \frac{A_{31}}{k_o k_p k_c}\right]}{\left[\frac{\Delta}{k_f k_o k_p k_c}\right]}$$

$$\gamma_F = \frac{\frac{1}{k_f}\left[\frac{-A_{41}}{k_o k_p k_c}\right]}{\left[\frac{\Delta}{k_f k_o k_p k_c}\right]}$$

When solved for the valve error ε, (V-12) becomes

$$\text{(V-15)} \qquad \varepsilon = \frac{k_i \pi_i - (M_i s^2 + B_i s + k_i)\pi_o}{\left[M_i s^2 + (B_i + B_v)s + k_i + k_\varepsilon\right]}$$

A functional form involving a unity feedback from the output π_o is desirable to facilitate interpretation of the results. The coefficient of π_o in (V-15) is then taken out as a multiplying factor.

$$\text{(V-16)} \qquad \varepsilon = \frac{(M_i s^2 + B_i s + k_i)}{\left[M_i s^2 + (B_i + B_v)s + k_i + k_\varepsilon\right]}\left[\frac{k_i \pi_i}{(M_i s^2 + B_i s + k_i)} - \pi_o\right]$$

If the static gain is isolated in (V-16):

$$\text{(V-17)} \qquad \varepsilon = \gamma_{eq}\left\{\frac{\pi_i}{\left[\frac{M_i}{k_i} s^2 + \frac{B_i}{k_i} s + 1\right]} - \pi_o\right\}$$

where

$$Y_{eq} = \left(\frac{k_i}{k_i + k_e}\right) \frac{\left[\frac{M_i}{k_i} s^2 + \frac{B_i}{k_i} s + 1\right]}{\left[\frac{M_i}{k_i + k_e} s^2 + \frac{B_i + B_v}{k_i + k_e} s + 1\right]}$$

(V-14) and (V-17) are readily combined into the functional block diagram shown in Figure V-3.

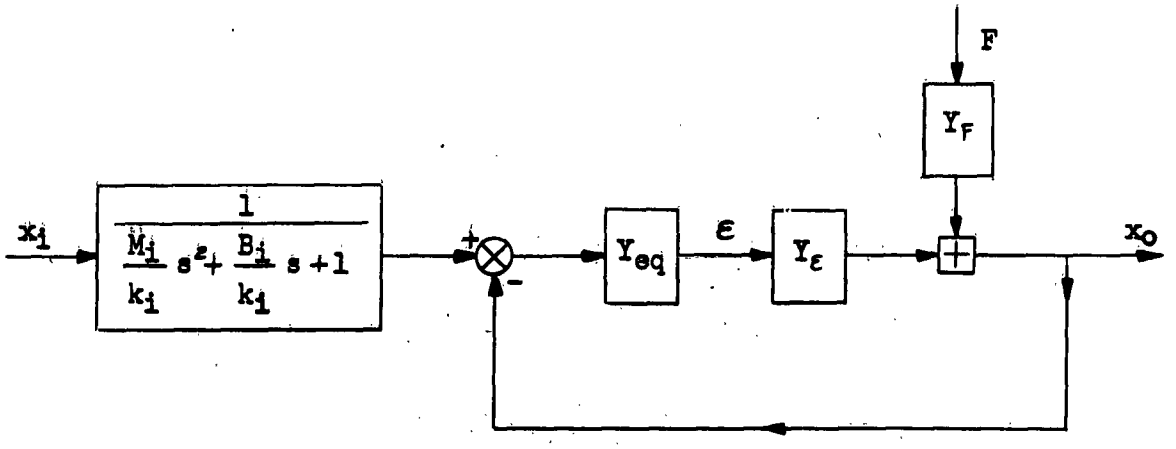

Figure V-3. Block Diagram of the Fully-Powered Hydraulic Control System

It is now necessary to consider the quantities involved in the expressions for Y_ϵ and Y_F. Certain of the relations between parameters are of such general validity as to justify basing all discussions on simplified expressions for these quantities. Since the equivalent flow damping B_f is inversely proportional to the small valve flow coefficient C_p, B_f is always large in comparison with the other damping coefficients B_c and B_s. Also, the control surface mass M_s will always be large in comparison with the cylinder mass M_c and also with the piston mass M_p. The input coupling spring k_ϵ will always be insignificant in comparison with k_f.

$$B_f \gg B_c$$

$$B_f \gg B_s$$

$$k_f \gg k_e$$

$$M_s \gg M_c$$

$$M_s \gg M_p$$

If the simplifications indicated by these relations are made, the expressions for Y_e and Y_F become less complex.

The numerator of Y_e is

(V-18)
$$\left[\frac{(B_v s + k_e)A_{11}}{k_f k_o k_p k_c} + \frac{A_{31}}{k_o k_p k_c}\right] \approx \left(\frac{M_s}{k_c}s^2 + \frac{Bs}{k_c}s + 1\right) \cdot$$
$$\left\{\left[\frac{B_v B_f M_p}{k_f k_o k_p}\right]s^4 + \left[\frac{B_v B_c B_f}{k_f k_o k_p} + \frac{B_v M_p}{k_f k_p} + \frac{k_e B_f M_p}{k_f k_o k_p}\right]s^3 + \left[\frac{B_v B_f}{k_f}\left(\frac{1}{k_o} + \frac{1}{k_p}\right)\right.\right.$$
$$\left.\left. + \frac{M_p}{k_p} + \frac{k_e B_c B_f}{k_f k_o k_p}\right]s^2 + \left[\frac{B_v}{k_f} + \frac{k_e B_f}{k_f}\left(\frac{1}{k_o} + \frac{1}{k_p}\right)\right]s + 1\right\}$$

The numerator of Y_F is:

(V-19)
$$\frac{1}{k_f}\left[\frac{-A_{41}}{k_o k_p k_c}\right] \approx \frac{1}{k_f}\left\{\left[\frac{B_f M_p}{k_o k_p}\right]s^3 + \left[\frac{B_c B_f}{k_o k_p} + \frac{M_p}{k_p}\right]s^2 + \left[B_f\left(\frac{1}{k_o} + \frac{1}{k_p}\right)\right]s + 1\right\}$$

The denominator of both Y_e and Y_f is:

$$(V\text{-}20)\qquad \left[\frac{\Delta}{k_f k_o k_p k_c}\right] \approx \frac{B_f}{k_f} s\left\{\left[\frac{M_c M_p M_s}{k_o k_p k_c}\right]s^6 + \left[\frac{B_s M_c M_p + B_c M_s (M_c + M_p)}{k_o k_p k_c}\right.\right.$$

$$\left. + \frac{M_c M_p M_s}{B_f k_p k_c}\right]s^5 + \left[\frac{M_p M_s}{k_p}\left(\frac{1}{k_o}+\frac{1}{k_c}\right) + \frac{M_c M_s}{k_c}\left(\frac{1}{k_o}+\frac{1}{k_p}\right) + \frac{B_c B_s (M_c + M_p)}{k_o k_p k_c}\right]s^4$$

$$+ \left[\frac{B_c M_s}{k_o}\left(\frac{1}{k_p}+\frac{1}{k_c}\right) + \frac{B_s M_p}{k_p}\left(\frac{1}{k_o}+\frac{1}{k_c}\right) + \frac{B_s M_c}{k_c}\left(\frac{1}{k_o}+\frac{1}{k_p}\right) + \frac{M_p M_s}{B_f k_p} + \frac{M_c M_s}{B_f k_c}\right]s^3$$

$$\left. + \left[M_s\left(\frac{1}{k_o}+\frac{1}{k_p}+\frac{1}{k_c}\right) + \frac{B_c B_s}{k_o}\left(\frac{1}{k_p}+\frac{1}{k_c}\right)\right]s^2 + \left[\frac{M_s}{B_f} + \frac{B_c}{k_o} + B_s\left(\frac{1}{k_o}+\frac{1}{k_p}+\frac{1}{k_c}\right)\right]s + 1\right\}$$

To sketch out the frequency response of the fully-powered system, approximate factors of the polynomials in Equations (V-18), (V-19), and (V-20) must be determined. These factorizations are obtained by taking into account relative magnitudes of parameters which are typical of practice.

An important parameter of the system is the surface mass M_s. To a large extent, general design considerations make it necessary that M_s be fairly large. The cylinder mass M_c and the piston mass M_p are always quite small in comparison with M_s; in addition, M_c is several times as large as M_p. The piston spring k_p and the flow spring k_f are each several times as large as the oil spring k_o. The surface coupling spring k_c is typically somewhat larger than k_o but still much smaller than k_p and k_f. The cylinder damping B_c, the surface damping B_s, the valve damping B_v, and the input damping B_i are all limited to a low range of values, and for purposes of factorization, they may

be regarded as approximately equal in magnitude. The input spring k_i is in general the spring constant of a long, light cable, and is usually very much smaller than k_o, k_c, k_p, and k_f. The input coupling spring k_ε which can be used is limited by the force which it is desirable to impose on the pilot or the autopilot, and may be considered to be either of the same magnitude as k_i, or less in magnitude than k_i.

If B_v and k_ε are negligible, the numerator of Y_ε, (V-18), reduces to:

$$\text{(V-21)} \qquad Num.\,Y_\varepsilon\Big|_{(B_v,\,k_\varepsilon=0)} = \left(\frac{M_g}{k_c}s^2 + \frac{B_g}{k_c}s + 1\right)\left(\frac{M_p}{k_p}s^2 + 1\right)$$

the quadratic containing M_p being effective only at a very high frequency. With B_v and k_ε large and k_p several times as large as k_o, a good approximation is

$$\text{(V-22)} \qquad Num.\,Y_\varepsilon \approx \left(\frac{M_g}{k_c}s^2 + \frac{B_g}{k_c}s + 1\right)\left(\frac{M_p}{k_o+k_p}s^2 + \frac{B_c}{k_o+k_p}s + 1\right) \cdot$$
$$\left\{\left[\frac{B_v B_f}{k_f}\left(\frac{1}{k_o}+\frac{1}{k_p}\right)\right]s^2 - \left[\frac{B_c}{k_o+k_p} - \frac{B_v}{k_f} - \frac{k_\varepsilon B_f}{k_f}\left(\frac{1}{k_o}+\frac{1}{k_p}\right)\right]s + 1\right\}$$

the last quadratic being characteristically non-minimum phase.

The numerator of Y_F, (V-19), has the approximate factors

$$\text{(V-23)} \qquad Num\,Y_F \approx \frac{1}{k_f}\left[B_f\left(\frac{1}{k_o}+\frac{1}{k_p}\right)s + 1\right]\left[\frac{M_p}{k_o+k_p}s^2 + \frac{B_c}{k_o+k_p}s + 1\right]$$

From (V-20) it is seen that the denominator of Y_ε and Y_F is composed of the factor $(B_f/k_f)s = (A/C_\varepsilon)s$ (which expresses the fundamental behavior of the control system as an integrating servo) and a sextic which consists of three quadratics in M_g, M_c, and M_p. In investigating this sextic, it is worthwhile to

consider first the undamped behavior with B_c and B_s each equal to zero and with B_f large. With typical magnitudes of the parameters, the approximate critical frequencies in this case are:

(IV-24)
$$\left[\begin{aligned} \omega_2 &= \sqrt{\frac{1}{M_s\left(\frac{1}{k_o}+\frac{1}{k_p}+\frac{1}{k_c}\right)}} \\ \omega_4 &= \sqrt{\frac{k_c+\frac{k_o k_p}{k_o+k_p}}{M_c}} \\ \omega_6 &= \sqrt{\frac{k_o+k_p}{M_p}} \end{aligned}\right.$$

Typically, $\omega_2 \ll \omega_4 < \omega_6$. Inclusion of the damping terms results in only minor modifications to these natural frequencies. From (V-21), (V-22), (V-23), and (V-24), it is seen that only a small amount of damping suffices to cause the effective cancellation of M_p quadratics in the numerator and denominator of Y_E and Y_F. An approximate expression for the cylinder displacement can then be written:

(V-25)
$$x_o \approx \frac{\left(\frac{s^2}{\omega_3^2}+\frac{2\zeta_3}{\omega_3}s+1\right)\left(\frac{s^2}{\omega_7^2}-\frac{2\zeta_7}{\omega_7}s+1\right)\varepsilon+\frac{1}{k_f}\left(\frac{s}{\omega_8}+1\right)F}{\frac{s}{\omega_1}\left(\frac{s^2}{\omega_2^2}+\frac{2\zeta_2}{\omega_2}s+1\right)\left(\frac{s^2}{\omega_4^2}+\frac{2\zeta_4}{\omega_4}s+1\right)}$$

The frequencies and coefficients of the middle terms of the quadratics in (V-25) are approximately as follows:

$$\omega_1 = \frac{k_f}{B_f}$$

$$\omega_2 = \sqrt{\frac{1}{M_s\left(\frac{1}{k_o} + \frac{1}{k_p} + \frac{1}{k_c}\right)}} \qquad \frac{2\zeta_2}{\omega_2} = \frac{M_s}{B_f} + \frac{B_c}{k_o} + B_s\left(\frac{1}{k_o} + \frac{1}{k_p} + \frac{1}{k_c}\right)$$

$$\omega_3 = \sqrt{\frac{k_c}{M_s}} \qquad \frac{2\zeta_3}{\omega_3} = \frac{B_s}{k_c}$$

$$\omega_4 = \sqrt{\frac{k_c + \frac{k_o k_p}{k_o + k_p}}{M_c}} \qquad \frac{2\zeta_4}{\omega_4} = \frac{B_c}{k_o + \frac{k_p k_c}{k_p + k_c}}$$

$$\omega_7 = \sqrt{\frac{k_f}{B_v B_f\left(\frac{1}{k_o} + \frac{1}{k_p}\right)}} \qquad \frac{2\zeta_7}{\omega_7} = \frac{B_c}{k_o + k_p} - \frac{B_v}{k_f} - \frac{k_e B_f}{k_f}\left(\frac{1}{k_o} + \frac{1}{k_p}\right)$$

$$\omega_8 = \frac{1}{B_f\left(\frac{1}{k_o} + \frac{1}{k_p}\right)}$$

SECTION 2 - THE SYSTEM WITHOUT INPUT COUPLING

If the damping B_v and the spring k_e in Figure V-1 have an appreciable magnitude, they effect a force coupling at the input. Section 3 of this chapter

discusses how these quantities can be used to stabilize the servo. If, however, these parameters are not deliberately augmented in design, their effect on stability is negligible, and the system where B_v and k_ε are effectively zero may be considered a basic case. Then Y_{eq} reduces to unity, and the block diagram takes the form shown in Figure V-4.

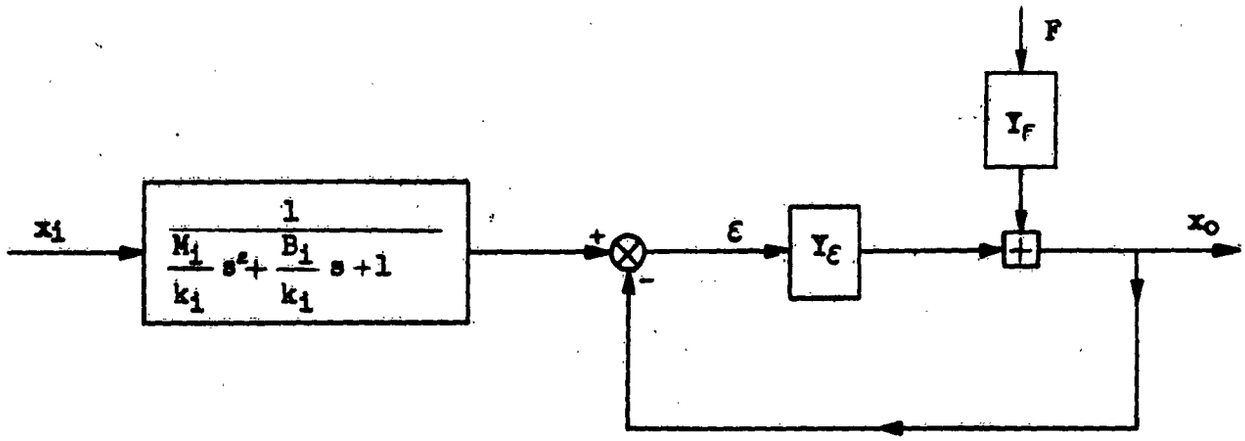

Figure V-4. The Fully-Powered System without Input Coupling

The effect of airload is always in the direction of greater stability and is almost always small. Moreover, it is necessary to design a system which is satisfactory on the ground or at low airspeed. The force F can therefore be neglected. An open-loop transfer function can then be written with the approximate factorizations of the preceding section:

$$x_o\Big|_{\substack{F=0\\B_v=0\\k_\varepsilon=0}} \approx \frac{\left(\frac{s^2}{\omega_3^2}+\frac{2\zeta_3}{\omega_3}s+1\right)e}{\frac{s}{\omega_1}\left(\frac{s^2}{\omega_2^2}+\frac{2\zeta_2}{\omega_2}s+1\right)\left(\frac{s^2}{\omega_4^2}+\frac{2\zeta_4}{\omega_4}s+1\right)} \tag{V-26}$$

where

$$\omega_1 = \frac{k_f}{B_f}$$

$$\omega_2 = \sqrt{\frac{1}{M_s\left(\frac{1}{k_o} + \frac{1}{k_p} + \frac{1}{k_c}\right)}} \qquad \frac{2\zeta_2}{\omega_2} = \frac{M_s}{B_f} + \frac{B_c}{k_o} + B_s\left(\frac{1}{k_o} + \frac{1}{k_p} + \frac{1}{k_c}\right)$$

$$\omega_3 = \sqrt{\frac{k_c}{M_s}} \qquad \frac{2\zeta_3}{\omega_3} = \frac{B_s}{k_c}$$

$$\omega_4 = \sqrt{\frac{k_c + \frac{k_o k_p}{k_o + k_p}}{M_c}} \qquad \frac{2\zeta_4}{\omega_4} = \frac{B_c}{k_o + \frac{k_p k_c}{k_p + k_c}}$$

A typical frequency response corresponding to (II-26) is shown in Figure V-5.

Inspection of (V-26) and Figure V-5 brings out several important facts. The only effective damping in the quadratic containing M_c is due to B_c, the damping coefficient pertaining to the relative motion of piston and cylinder. The damping ratio ζ_4 is not large, and there is a fairly sharp peak at ω_4 on the Bode plot. However, since the amplitude ratio is very low at this point, there is no danger of instability due to this peak. The damping ratio, ζ_4, will never be large enough to cause a large phase lag in the vicinity of ω_2 and ω_3. It is permissible, then, to disregard the quadratic in M_c and write:

(V-27)
$$x_o\Big|_{\substack{F=0\\B_v=0\\k_e=0}} \approx \frac{\left(\frac{s^2}{\omega_3^2} + \frac{2\zeta_3}{\omega_3}s + 1\right)\varepsilon}{\frac{s}{\omega_1}\left(\frac{s^2}{\omega_2^2} + \frac{2\zeta_2}{\omega_2}s + 1\right)}$$

where the frequencies are given in (V-26). The nature of the stability problem and the resultant limitation on performance are now evident. With ω_2 differing from ω_3, principally because the oil spring k_o is small, considerable damping ζ_2 is required to lower the resultant peak and thus prevent instability. The crossover frequency $\omega_1 = k_f/B_f = C_t/A$ principally determines the speed of response of the system. It is desirable to make this quantity as high as possible within some specified limit of overshoot in transient response. The magnitude of ω_1, the "gain" of the system, which is obtainable in practice is almost always limited by an incipient instability due to the separation of ω_2 from ω_3 mentioned above.

The characteristic equation corresponding to the open-loop transfer function (V-27) is

$$(V\text{-}28) \qquad 0 = 1 + \left[\frac{B_f}{k_f} + \frac{B_g}{k_c}\right]s + \left[M_g\left(\frac{1}{k_c} + \frac{1}{k_f}\right) + \frac{B_c B_f}{k_f k_o}\right.$$

$$\left. + \frac{B_g B_f}{k_f}\left(\frac{1}{k_o} + \frac{1}{k_p} + \frac{1}{k_c}\right)\right]s^2 + \left[\frac{B_f M_g}{k_f}\left(\frac{1}{k_o} + \frac{1}{k_p} + \frac{1}{k_c}\right)\right] s^3$$

Application of the Routh criterion to this relation yields the following necessary condition for stability:

$$(V\text{-}29) \qquad \frac{M_g}{k_f} + \frac{B_c B_f}{k_f k_o} + \frac{B_g B_f}{k_f}\left(\frac{1}{k_o} + \frac{1}{k_p} + \frac{1}{k_c}\right) > M_g\left(\frac{1}{k_o} + \frac{1}{k_p}\right)$$

A stable control system is not necessarily a satisfactory system. The overshoots in transient response may be too large or the time of response too long to meet operating requirements. This is, however, too much a matter of individual design to permit a generalization here.

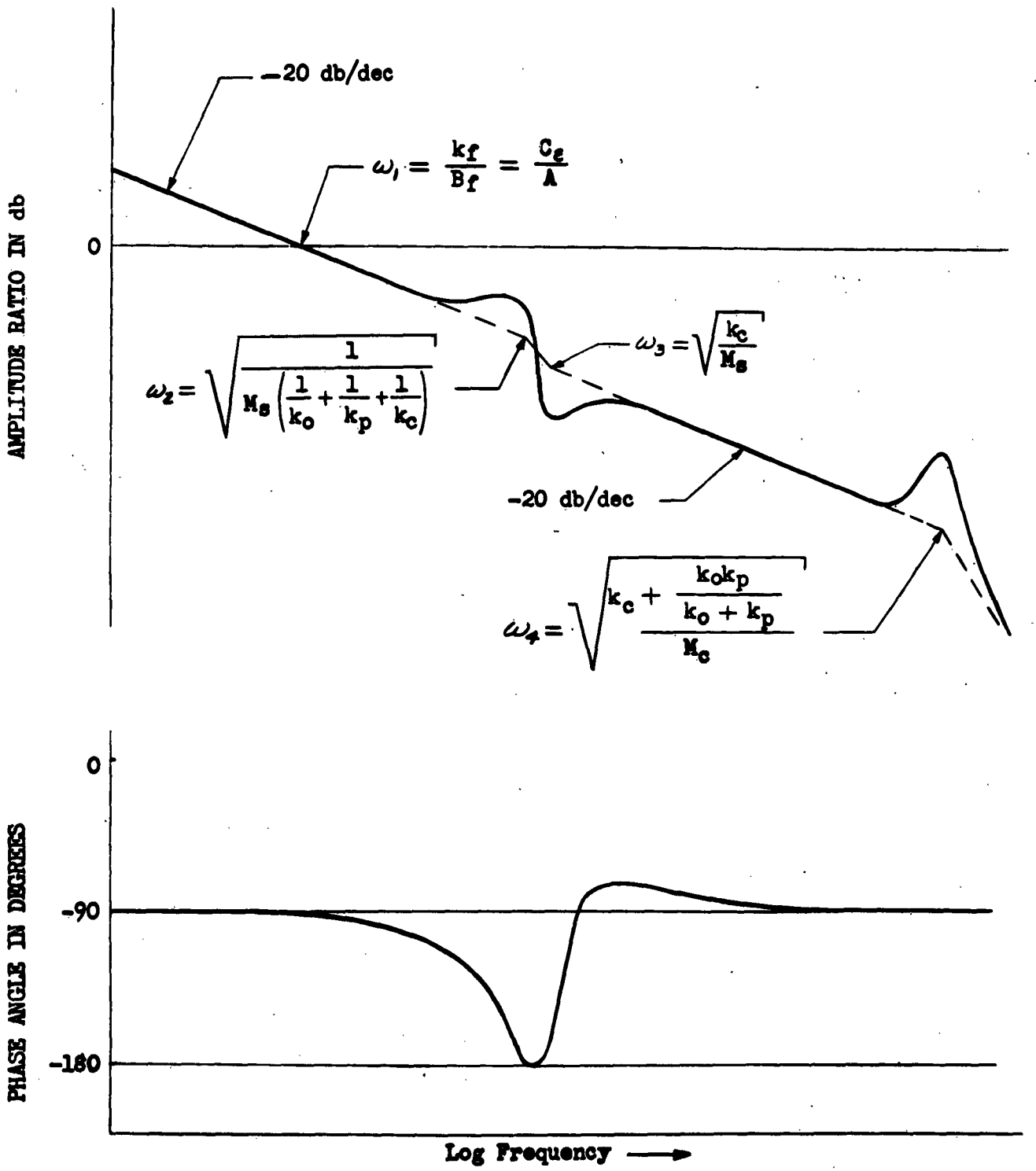

Figure V-5. Open-Loop Transfer Function Without Input Coupling and With No Appreciable Airload

If the damping ratio ζ_2 in (V-27) is sufficiently large, instability caused by the separation of ω_2 from ω_3 will not occur. The individual terms of $2\zeta_2/\omega_2$ thus become of definite interest in design. There is some small damping because B_f is finite. The surface damping, B_s, is more effective as a stabilizing parameter than the cylinder damping, B_c, since the former acts through a weaker spring.

It is important in view of weight and space limitations that requisite stabilization of the hydraulic control system be carried out with a minimum of design complication. Even though B_c must be increased by a large amount if it is to have much effect on stability, the cylinder damping is very important from the standpoint of simplicity of design. Considerable cylinder damping is obtained in the course of preventing leakage past the piston by use of O-rings. With piston diameter roughly established by general design considerations, B_c can be increased by inserting additional rings or by using pairs of rings with the intermediate region vented to the atmosphere. The latter technique increases the damping by increasing the pressure differential across each ring.

The surface damping B_s arises from several sources. First, there is some parasitic damping at the hinge and surface horn connections. Second, damping devices are sometimes inserted at the hinge line. The latter method is not altogether successful, since such devices usually take a heavy toll of weight and space allotments. A third source of surface damping is aerodynamic. With a fair degree of accuracy, the aerodynamic force acting on the control surface of an airplane in flight (F in Figure V-3 or Figure V-4) can be represented as the parallel combination of a spring and a damper. The effect of the airload spring on control system behavior is not great, and no account of this parameter has been taken so far in the analysis. However, the aerodynamic damping is simulated

as a part of B_s , the surface damping. This portion of B_s can be of appreciable magnitude, but it cannot be regarded as available for use in stabilizing the system, since the servo must be satisfactory on the ground.

It is appropriate at this point to discuss briefly the effect on servo behavior of the springing action of the airload on the control surface. The force F of Figure V-4 is assumed to take the form:

$$(V\text{-}30) \qquad -F = k_g x_g = \frac{\left(\frac{k_c k_g}{k_c + k_g}\right) x_o}{\left(\frac{M_g}{k_c + k_g} s^2 + \frac{B_g}{k_c + k_g} s + 1\right)}$$

The open-loop transfer is then approximately given by

$$(V\text{-}31) \qquad x_o \Big|_{\substack{B_v = 0 \\ k_\epsilon = 0}} \approx \left[\frac{M_g}{k_c} s^2 + \frac{B_g}{k_c} s + \frac{k_c + k_g}{k_c}\right] \epsilon \div \left\{\left[\frac{B_f M_g}{k_f}\left(\frac{1}{k_o} + \frac{1}{k_p} + \frac{1}{k_c}\right)\right] s^3 \right.$$

$$+ \left[\frac{M_g}{k_f} + \frac{B_c B_f}{k_f k_o} + \frac{B_g B_f}{k_f}\left(\frac{1}{k_o} + \frac{1}{k_p} + \frac{1}{k_c}\right) + \frac{k_g B_c B_f}{k_f k_o}\left(\frac{1}{k_c} + \frac{1}{k_p}\right)\right] s^2$$

$$\left. + \left[\frac{B_f}{k_f} + \frac{k_g B_f}{k_f}\left(\frac{1}{k_o} + \frac{1}{k_p} + \frac{1}{k_c}\right)\right] s + \frac{k_g}{k_f} \right\}$$

If the airload spring k_g is included, the fundamental character of the servo is disturbed to some extent, as is indicated by the last term in the denominator of (V-23). However, this additional term has little effect on servo behavior because a typical flow spring constant, k_f , is from 100 to 1000 times as

large as a typical airload spring constant, k_y . For all practical purposes, the extra term may be omitted. The frequency response then assumes the form:

$$(V\text{-}32) \qquad x_o\Big|_{\substack{B_w = 0 \\ k_\varepsilon = 0}} \approx \frac{\left(\frac{s^2}{\omega_3'^2} + \frac{2\zeta_3'}{\omega_3'}s + 1\right)\varepsilon}{\frac{s}{\omega_1'}\left(\frac{s^2}{\omega_2'^2} + \frac{2\zeta_2'}{\omega_2'}s + 1\right)}$$

where

$$\omega_1' = \left(\frac{k_f}{B_f}\right)\left(\frac{k_c + k_s}{k_c}\right)\left[\frac{1}{1 + k_s\left(\frac{1}{k_o} + \frac{1}{k_p} + \frac{1}{k_c}\right)}\right]$$

$$\frac{2\zeta_2'}{\omega_2'} = \left[\frac{\frac{M_s}{B_f} + \frac{B_c}{k_o} + B_s\left(\frac{1}{k_o} + \frac{1}{k_p} + \frac{1}{k_c}\right) + \frac{k_s B_c}{k_o}\left(\frac{1}{k_c} + \frac{1}{k_p}\right)}{1 + k_s\left(\frac{1}{k_o} + \frac{1}{k_p} + \frac{1}{k_c}\right)}\right]$$

$$\omega_2' = \sqrt{\frac{1}{M_s\left(\frac{1}{k_o} + \frac{1}{k_p} + \frac{1}{k_c}\right)} + \frac{k_s}{M_s}}$$

$$\frac{2\zeta_3'}{\omega_3'} = \frac{B_s}{k_c + k_s}$$

$$\omega_3' = \sqrt{\frac{k_c + k_s}{M_s}}$$

If a system with the airload spring is compared, on the basis of the same open-loop gain, with a system where this spring is negligible, the following remarks regarding the effect of k_s may be made. The damping ratios of both numerator and denominator quadratics are virtually unchanged. The frequencies ω_2 and ω_3 are increased, but their difference, $\omega_3 - \omega_2$, is slightly decreased. There is then a slight stabilizing effect due to the airload spring, and thus calculations which ignore the airload spring are somewhat conservative as far as stability is concerned. A further justification for omitting the airload spring in analysis is that it becomes weak at low airspeeds.

The steady-state servo response, including k_s, is given by

$$\text{(V-33)} \qquad \frac{x_o}{x_i} = \left(\frac{k_f - k_s}{k_f} \right)$$

Since k_s is normally much smaller than k_f, the position error is small.

The hydraulic control system must ultimately be considered as a component of a larger system including the airframe. In typical practice the hydraulic control component is coupled to the more comprehensive system only at very low frequencies. It is then possible to view in isolation the question of stability of the hydraulic control system. If the hydraulic control system itself is stable, its behavior as a component of the larger system can usually be simplified.

If the numerator and denominator quadratics are deleted from (V-27), the open-loop characteristic is that of a perfect integrating servo:

$$\text{(V-34)} \qquad \frac{x_o}{\varepsilon} = \frac{k_f}{B_f s} = \frac{C_\varepsilon}{A s}$$

The closed-loop behavior is then

$$\text{(V-35)} \qquad \frac{x_o}{x_i} = \frac{1}{\frac{B_f}{k_f} s + 1} = \frac{1}{\frac{A}{C_\varepsilon} s + 1}$$

For purposes of illustration, the values of the time constant $(B_f/k_f)=(A/K_g)$ may be considered as extending from .05 to .025, with the latter value running into a range where it is sometimes difficult to stabilize the system.

SECTION 3 - THE EFFECT OF INPUT COUPLING

The stabilizing means considered in Section 2 are rather limited in effectiveness. If the hydraulic control system must be very fast, more effective means of stabilization are desirable. The additional means considered in this volume use the combination of a force and a relatively weak spring to secure compensating displacements at some point of the system. There are, of course, numerous variations possible in physical application of this idea. The material presented in Section 1 facilitates discussion of some of these possibilities.

Consider now a case where the valve damping B_v or the input coupling spring k_c, or both, and also the input damping B_i are augmented by physical changes in a system with a high gain valve. The block diagram in Figure V-3 then applies. With F set equal to zero, the operator Y_ϵ is written from (V-25):

$$(V\text{-}36) \qquad Y_\epsilon \approx \frac{\left(\frac{s^2}{\omega_3^2}+\frac{2\zeta_3}{\omega_3}s+1\right)\left(\frac{s^2}{\omega_7^2}+\frac{2\zeta_7}{\omega_7}s+1\right)}{\frac{s}{\omega_1}\left(\frac{s^2}{\omega_2^2}+\frac{2\zeta_2}{\omega_2}s+1\right)\left(\frac{s^2}{\omega_4^2}+\frac{2\zeta_4}{\omega_4}s+1\right)}$$

where

$$\omega_1 = \frac{k_f}{B_f}$$

$$\omega_2 = \sqrt{\frac{1}{M_s\left(\frac{1}{k_o}+\frac{1}{k_p}+\frac{1}{k_c}\right)}} \qquad \frac{2\zeta_2}{\omega_2} = \frac{M_s}{B_f}+\frac{B_c}{k_o}+B_s\left(\frac{1}{k_o}+\frac{1}{k_p}+\frac{1}{k_c}\right)$$

$$\omega_3 = \sqrt{\frac{k_c}{M_c}} \qquad \frac{2\zeta_3}{\omega_3} = \frac{B_c}{k_c}$$

$$\omega_4 = \sqrt{\frac{k_c + \frac{k_o k_p}{k_o + k_p}}{M_c}} \qquad \frac{2\zeta_4}{\omega_4} = \frac{B_c}{k_o + \frac{k_p k_c}{k_p + k_c}}$$

$$\omega_7 = \sqrt{\frac{k_f}{B_v B_f \left(\frac{1}{k_o} + \frac{1}{k_p}\right)}} \qquad \frac{2\zeta_7}{\omega_7} = \frac{B_c}{k_o + k_p} - \frac{B_v}{k_f} - \frac{k_e B_f}{k_f}\left(\frac{1}{k_o} + \frac{1}{k_p}\right)$$

The frequency ω_7 of the typically non-minimum phase quadratic in the numerator drops sharply with an increase in valve damping B_v; however, the decrease is offset by a high gain k_f / B_f. This quadratic can fall inside the denominator frequency ω_4, but it is improbable that it should ever reach the neighborhood of ω_2 and ω_3. With ζ_7 characteristically a small negative damping, there is little phase lag at important frequencies. The quantity Y_ε can then be assumed to have the same form as (V-27) of Section 2:

$$(V\text{-}37) \qquad x_o\big|_{F=0} \approx \frac{\left(\frac{s^2}{\omega_3^2} + \frac{2\zeta_3}{\omega_3} s + 1\right)\varepsilon}{\frac{s}{\omega_1}\left(\frac{s^2}{\omega_2^2} + \frac{2\zeta_2}{\omega_2} s + 1\right)}$$

Interest now centers on the modifying term Y_{eq}; see (V-17):

$$(V\text{-}38) \qquad Y_{eq} = \left(\frac{k_i}{k_i + k_e}\right) \frac{\left[\frac{M_i}{k_i} s^2 + \frac{B_i}{k_i} s + 1\right]}{\left[\frac{M_i}{k_i + k_e} s^2 + \frac{B_i + B_v}{k_i + k_e} s + 1\right]}$$

The spring constant k_i usually expresses the flexibility of a long, light cable, and is generally fairly small. The input mass M_i is kept low by weight considerations, and is normally of about the same magnitude as M_p, the piston mass. If the product $k_i M_i$ is sufficiently small, the quadratics of (V-38) can be split into first order factors by increasing B_i and B_v. In this case, an equalizer might take the form:

$$\text{(V-39)} \qquad Y_{eq} \approx \left(\frac{k_i}{k_i + k_e}\right) \frac{\left[\frac{B_i}{k_i} s + 1\right]}{\left[\frac{B_i + B_v}{k_i + k_e} s + 1\right]}$$

Equation (V-39) suggests several possibilities, which will be briefly sketched in the following paragraphs.

If B_i and k_e are small, and B_v / k_i is large,

$$\text{(V-40)} \qquad Y_{eq} \approx \frac{1}{\left[\frac{B_v}{k_i} s + 1\right]}$$

In this case, valve damping combines with a weak input spring to form a lag factor in the open-loop response.

If k_e is small, and B_v / k_i is large, and B_i is fairly large,

$$\text{(V-41)} \qquad Y_{eq} \approx \frac{\left[\frac{B_i}{k_i} s + 1\right]}{\left[\frac{B_i + B_v}{k_i} s + 1\right]}$$

The modifying factor in this equation is a lag-lead. The lead would probably be too high to affect stability, but the introduction of B_i makes a lag at low frequency more easily realizable.

If B_v is small and B_i / k_i and k_ε are large,

$$\gamma_{eq} \approx \left(\frac{k_i}{k_i + k_\varepsilon}\right) \frac{\left[\frac{B_i}{k_i} s + 1\right]}{\left[\frac{B_i}{k_i + k_\varepsilon} s + 1\right]} \qquad \text{(V-42)}$$

A lead-lag modifier can be realized if the gain of the valve is increased to compensate for the decrease in gain in the equalizer.

The spring constant k_i is to some extent a fixed factor in design; however, it varies considerably between control systems in different aircraft and also between the several control channels in the same aircraft. If modifying devices of the types discussed above are used for stabilization, they must be "tailor-made" for the specific installation. This is not too serious a drawback, because aircraft control systems in general do not permit much standardization.

The effect of a lag stabilizer on an unstable system is shown in Figure V-6, and the effect of the lead-lag equalizer is shown in Figure V-7.

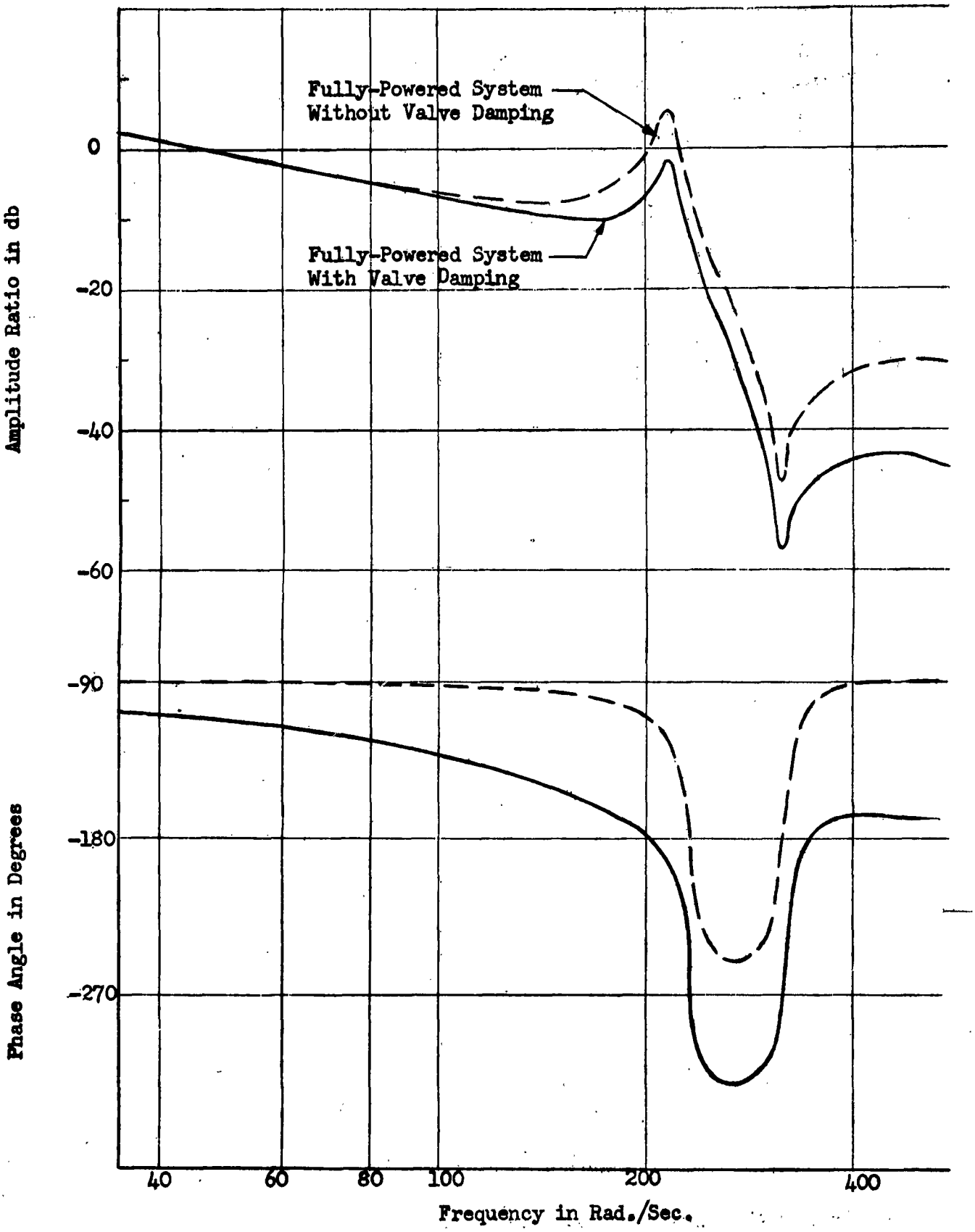

Figure V-6. The Effect of Valve Damping on Fully-Powered System

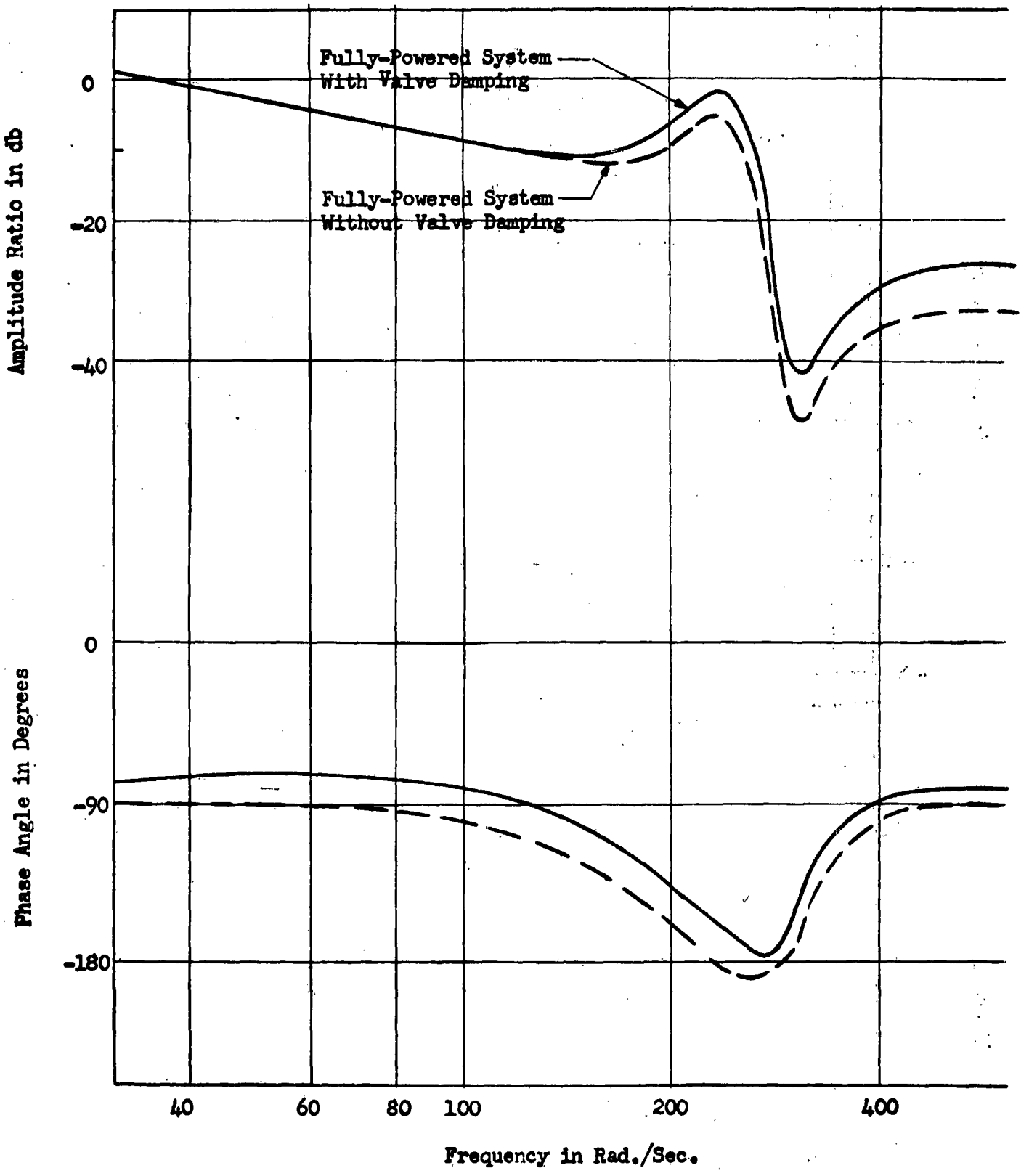

Figure V-7. Lead-Lag Modification of the Fully-Powered System

CHAPTER VI

THE POWER BOOST HYDRAULIC CONTROL SYSTEM

The material of this chapter is a continuation of Chapter IV. It is primarily concerned with the evaluation and the approximate factorization for the power boost case of the expressions occurring in Equations (IV-12) and (IV-13), which are repeated here for convenience:

$$\text{(VI-1)} \qquad x_o = Y_\varepsilon \varepsilon + Y_F F$$

$$\text{(VI-2)} \qquad \varepsilon = Y_{eq}\left[Y_{\varepsilon i}(\partial x_i) - x_o + Y_{\varepsilon F} F\right]$$

The corresponding block diagram is shown in Figure IV-2.

In Chapter V, it has been shown that the effects of the force F are always stabilizing and usually small in the fully-powered case if the behavior of the control surface can be effectively expressed by use of the single node x_s. Moreover, it is necessary to design the control system to insure stable operation at low airspeeds or on the ground. An analysis of the fully-powered case with F taken as zero thus yields conservative conclusions as to stability if coupling of multiple modes of vibration of control surface and parent surface is negligible. The situation in the power boost case is in general somewhat different. As will be shown later in the chapter, it is possible, by a suitable choice of the power boost ratio $1/b$, to adjust frequencies of the open-loop transfer function $Y_{eq} Y_\varepsilon$ so as to eliminate a stability problem arising in ground operation of the power boost system. A consequence of the pronounced effect of the power boost ratio on stability is that the aerodynamic force F may be either stabilizing or destabilizing, depending on the value of b. If b is small, however, the conclusions of Chapter V regarding the effect of aerodynamic force on stability are equally valid in the power boost case, and in the

following analysis it is assumed that the quantity F is zero.

(VI-3) $$x_o = Y_\varepsilon \varepsilon$$

(VI-4) $$\varepsilon = Y_{eq} \left[Y_{\varepsilon i} (a x_i) - x_o \right]$$

These relationships are illustrated schematically in Figure VI-1.

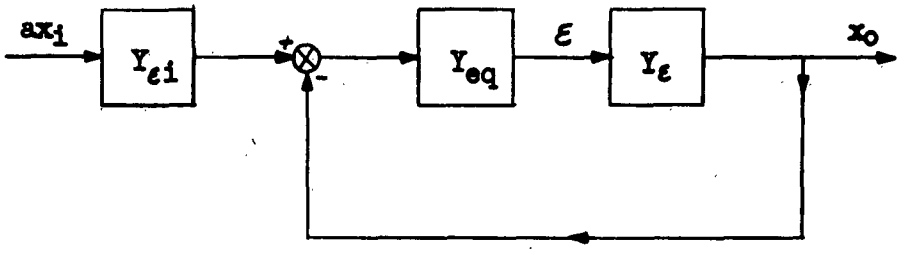

Figure VI-1. The Power Boost Hydraulic Control System with Negligible Airload

The quantities Y_ε, Y_{eq}, and $Y_{\varepsilon i}$ of Figure VI-1 are obtained from the determinants associated with (IV-12) and (IV-13). Writing of these results is simplified by assuming relative magnitudes of parameters, as was done in Chapter V.

$$B_f >> B_c \qquad M_s >> M_c$$

$$B_f >> \left(\frac{a}{a-b}\right) B_s \qquad M_s >> M_p$$

$$k_f >> k_e$$

$$\frac{M_s}{k_c} >> \frac{M_p}{k_p} \qquad M_{ir} >> M_p$$

$$\frac{M_{ir}}{k_{ir}} >> \frac{M_p}{k_p} \qquad M_{ir} >> \frac{a}{b} M_c$$

$$k_p M_{ir} M_s >> B_s B_{ir} M_p$$

The numerator of Y_ε takes the form:

(VI-5)
$$Num_{Y_\varepsilon} \approx \left(\frac{M_s}{k_a} s^2 + \frac{B_s}{k_c} s + 1\right)\left\{\left[\frac{B_v B_f M_p}{k_f k_o k_p}\right] s^4 + \left[\frac{B_v B_c B_f}{k_f k_o k_p} + \frac{B_v M_p}{k_f k_p} + \frac{k_e B_f M_p}{k_f k_o k_p}\right] s^3 + \left[\frac{B_v B_f}{k_f}\left(\frac{1}{k_o} + \frac{1}{k_p}\right) + \frac{M_p}{k_p} + \frac{k_e B_c B_f}{k_o k_f k_p} + \frac{\left(\frac{b}{a}\right) B_c B_f}{k_f k_o}\right] s^2 + \left[\frac{B_v}{k_f} + \frac{k_e B_f}{k_f}\left(\frac{1}{k_o} + \frac{1}{k_p}\right) + \frac{\left(\frac{b}{a}\right) B_f}{k_f}\right] s + 1\right\}$$

The denominator of Y_ε becomes:

(VI-6)
$$Den_{Y_\varepsilon} \approx \frac{\left(\frac{a-b}{a}\right) B_f}{k_f} s \left\{\left\{\frac{\left(\frac{a}{a-b}\right) M_c M_p M_s}{k_o k_p k_a}\right\} s^6 + \left\{\frac{\left(\frac{a}{a-b}\right) M_c M_p M_s}{B_f k_p k_c} + \frac{\left(\frac{a}{a-b}\right)\left[B_s M_c M_p + B_c (M_c + M_p) M_s\right]}{k_o k_p k_c}\right\} s^5 + \left\{\frac{\left(\frac{a}{a-b}\right) M_p M_s}{k_o k_p} + \frac{\left(\frac{a}{a-b}\right) M_c M_s}{k_o k_a} + \frac{\left(\frac{a}{a-b}\right) B_c B_s (M_c + M_p)}{k_o k_p k_c} + \frac{\left(\frac{a}{a-b}\right)(M_c + M_p) M_s}{k_p k_c}\right\} s^4 + \left\{\frac{\left(\frac{a}{a-b}\right)(B_c M_s + B_s M_p)}{k_o k_p} + \frac{\left(\frac{a}{a-b}\right) M_c M_s}{B_f k_a} + \frac{\left(\frac{a}{a-b}\right) M_p M_s}{B_f k_p} + \frac{B_c M_s + \left(\frac{a}{a-b}\right) B_s M_c}{k_o k_c} + \frac{\left(\frac{a}{a-b}\right) B_s (M_c + M_p)}{k_p k_c}\right\} s^3$$

$$+\left\{M_s\left[\frac{\left(\frac{a}{a-b}\right)}{k_o}+\frac{\left(\frac{a}{a-b}\right)}{k_p}+\frac{1}{k_c}\right]+\frac{B_c B_s}{k_o}\left[\frac{\left(\frac{a}{a-b}\right)}{k_p}+\frac{1}{k_c}\right]\right\}s^2$$

$$+\left\{\frac{\left(\frac{a}{a-b}\right)M_s}{B_f}+\frac{B_c}{k_o}+B_s\left[\frac{\left(\frac{a}{a-b}\right)}{k_o}+\frac{\left(\frac{a}{a-b}\right)}{k_p}+\frac{1}{k_c}\right]\right\}s+1\Bigg]$$

In a typical system the piston mass M_p is small, and the piston spring k_p is several times larger than either the oil spring k_o or the cylinder-surface coupling spring k_c. Numerator and denominator of Y_ε then each have a quadratic factor at the approximate high frequency $\sqrt{k_p/M_p}$. With these quadratics effectively cancelling out, a good approximate factorization of Y_ε is:

(VI-7)
$$Y_\varepsilon \approx \frac{\left(\frac{s^2}{\omega_3^2}+\frac{2\zeta_3}{\omega_3}s+1\right)\left(\frac{s^2}{\omega_7^2}+\frac{2\zeta_7}{\omega_7}s+1\right)}{\frac{s}{\omega_1}\left(\frac{s^2}{\omega_2^2}+\frac{2\zeta_2}{\omega_2}s+1\right)\left(\frac{s^2}{\omega_4^2}+\frac{2\zeta_4}{\omega_4}s+1\right)}$$

where

$$\omega_1=\frac{\left(\frac{a}{a-b}\right)k_f}{B_f}$$

$$\omega_2=\sqrt{\frac{1}{M_s\left[\frac{\left(\frac{a}{a-b}\right)}{k_o}+\frac{\left(\frac{a}{a-b}\right)}{k_p}+\frac{1}{k_c}\right]}}$$

$$\frac{2\zeta_2}{\omega_2}=\frac{\left(\frac{a}{a-b}\right)M_s}{B_f}+\frac{B_c}{k_o}+B_s\left[\frac{\left(\frac{a}{a-b}\right)}{k_o}+\frac{\left(\frac{a}{a-b}\right)}{k_p}+\frac{1}{k_c}\right]$$

$$\omega_3=\sqrt{\frac{k_c}{M_s}}$$

$$\frac{2\zeta_3}{\omega_3}=\frac{B_s}{k_c}$$

$$\omega_4 = \sqrt{\frac{k_c + \frac{\left(\frac{a-b}{a}\right) k_o k_p}{(k_o + k_p)}}{M_c}} \qquad \frac{2\zeta_4}{\omega_4} = \frac{B_c}{k_o + \frac{\left(\frac{a}{a-b}\right) k_p k_c}{\left(\frac{a}{a-b}\right) k_c + k_p}}$$

$$\omega_7 = \sqrt{\frac{k_f}{B_f\left[B_v\left(\frac{1}{k_o} + \frac{1}{k_p}\right) + \frac{\left(\frac{b}{a}\right) B_c}{k_o}\right]}} \qquad \frac{2\zeta_7}{\omega_7} = \frac{B_f}{k_f}\left[\frac{B_v}{B_f} + \left(\frac{b}{a}\right) + k_\varepsilon\left(\frac{1}{k_o} + \frac{1}{k_p}\right) - \frac{k_f}{B_f}\frac{B_c}{(k_o + k_p)}\right]$$

It should be noted that the expression (VI-7) for Y_ε is identical in form with the expression for the fully-powered case, (V-25), with $F = O$. If the power boost ratio $1/b$ is less than infinite, there is a slight increase in the gain ω_1 and a reduction of the frequencies ω_2, ω_4, and ω_7. From an examination, on the basis of typical parameters, of the frequencies ω_4 and ω_7, it can be stated that the quadratic containing M_c can be neglected because it lies at very high frequency; if the power boost ratio is high, i.e., if the system approaches a fully-powered system, the quadratic at ω_7 is out of the range of interest. The transfer function Y_ε may then be rewritten in the fairly simple form:

(VI-8) $$Y_\varepsilon \approx \frac{\left(\frac{s^2}{\omega_3^2} + \frac{2\zeta_3}{\omega_3} s + 1\right)}{\frac{s}{\omega_1}\left(\frac{s^2}{\omega_2^2} + \frac{2\zeta_2}{\omega_2} s + 1\right)}$$

where the frequencies and the middle terms of the quadratics are as given in (VI-7).

The effects of the small masses M_c and M_p on the quantities γ_{eq} and γ_{ei} can be entirely neglected, and these transfer functions become:

$$\gamma_{eq} = \frac{\left[\frac{k_i}{k_i + a(a-b)k_\varepsilon}\right]\left[\left(\frac{M_s}{k_c}s^2 + \frac{B_s}{k_c}s + 1\right)\left(\frac{M_i}{k_i}s^2 + \frac{B_i}{k_i}s + \frac{k_i + abk_c}{k_i}\right) - \frac{abk_c}{k_i}\right]}{\left(\frac{M_s}{k_c}s^2 + \frac{B_s}{k_c}s + 1\right)\left[\frac{M_i}{k_i + a(a-b)k_\varepsilon}s^2 + \frac{B_i + a(a-b)B_v}{k_i + a(a-b)k_\varepsilon}s + 1\right]} \tag{VI-9}$$

$$\gamma_{ei} = \frac{\left(\frac{M_s}{k_c}s^2 + \frac{B_s}{k_c}s + 1\right)}{\left(\frac{M_s}{k_c}s + \frac{B_s}{k_c}s + 1\right)\left(\frac{M_i}{k_i}s^2 + \frac{B_i}{k_i}s + \frac{k_i + abk_c}{k_i}\right) - \frac{abk_c}{k_i}} \tag{VI-10}$$

The latter quantity is, of course, unimportant in a determination of stability.

The open-loop transfer function of the positional servo is the product $\gamma_{eq}\gamma_\varepsilon$. By examining (VI-8) and (VI-9), it is seen that the control surface quadratic at ω_3 cancels in the product. It would be desirable in order to insure stability that the numerator of γ_{eq} be such as to cancel the denominator quadratic of γ_ε. The numerator of γ_{eq} can be factored to obtain this cancellation if the following conditions are met:

$$\begin{cases} \dfrac{k_i + abk_c}{M_i} \gg \dfrac{k_c}{B_s} \\ B_s \longrightarrow 0 \\ B_i \longrightarrow 0 \\ b(a-b) = \dfrac{k_i(k_o + k_p)}{k_o k_p} \end{cases} \tag{VI-11}$$

The determination of b in accordance with the last condition may be in conflict with other considerations of control system design. For a particular aircraft, the force to which the pilot or autopilot is thus subjected may be

too large or too small for proper operation.

If the conditions of (VI-11) are satisfied, the block diagram of the servo is as shown in Figure VI-2.

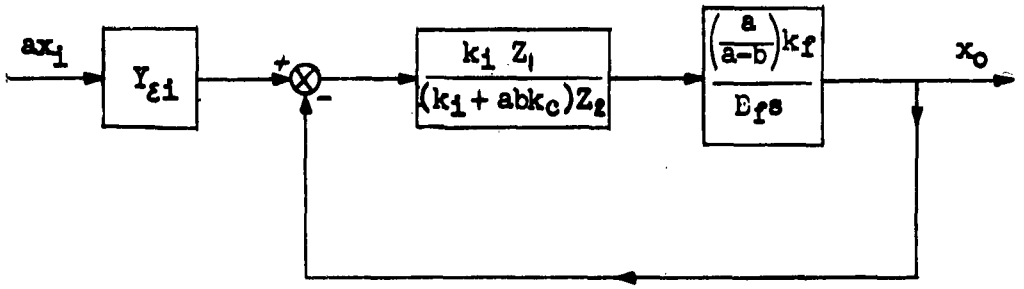

$$Z_1 = M_i s^2 + B_i s + (k_i + abk_c)$$

$$Z_2 = M_i s^2 + \left[B_i + a(a-b)B_v\right]s + \left[k_i + a(a-b)k_\varepsilon\right]$$

Figure VI-2. Power Boost System with Power Boost Ratio Adjusted to Stabilize the System

The valve damping B_v and the coupling spring k_ε were shown in Chapter V to be of value in stabilizing the fully-powered system. In the power boost case these effects are masked by the force feedback which arises because b is greater than zero. It is desirable, then, to keep these parameters as small as possible in the power boost system.

The discussions of the fully-powered system in Chapter V and the power boost system in Chapter VI have necessarily been brief, but it is hoped that they will have provided the reader with some insight into the behavior of hydraulic control systems and into the problems of reconciling a rapid response with stability.

CHAPTER VII

SPECIAL CONSIDERATIONS IN HYDRAULIC CONTROL SYSTEM DESIGN AND ANALYSIS

SECTION 1 - INTRODUCTION

The purpose of this chapter is to consider several special topics in the design and analysis of hydraulic control systems. The material presented here is to be regarded as supplementary to the discussion and analysis of Chapters III through VI.

Section 2 is concerned with forces acting between valve slide and valve housing due to inertia of the hydraulic fluid. It is shown that the effects of such forces are well represented by adjusted values of parameters already considered in Chapter III.

Section 3 discusses the hydraulic actuator with a three-way valve and how it differs from the more conventional four-way arrangement. The analysis of previous chapters is applicable with only small alterations.

Sections 4 and 5 deal briefly with additional means for stabilizing a hydraulic control system. The results are comparable with those of the methods discussed in Section 3 of Chapter V and in Chapter VI. Gain adjustment through the use of an auxiliary linkage is the subject of Section 6. In Section 7 the recently developed electrically operated transfer valves are described.

SECTION 2 - LONGITUDINAL FORCES ON CONTROL VALVE SPOOLS*

In the design of the hydraulic control valve for a high performance servo system, some knowledge of the force required to operate the valve spool is necessary. In addition to the inertial and frictional forces which can to a

*This section is largely an adaptation of Shih-Ying Lee and John T. Blackburn, "Axial Forces on Control-Valve Pistons," Meteor Report No. 65, Dynamic Analysis and Control Laboratory, Massachusetts Institute of Technology, Cambridge, Massachusetts, June 1950.

degree be calculated or which can be estimated on the basis of previous design experience, two other axial forces which are functions of flow through the valve exist. The more easily recognizable of these two forces is the so-called Bernoulli (or centering) force. This force is a nearly linear function of the volumetric flow rate through the valve. Hence for a linear flow valve, the force is proportional to valve spool displacement. The force displacement gradient is thus similar to an equivalent spring constant. The remaining force is proportional to the rate of change of flow rate through the valve. This is equivalent then to an additional valve damping term. The total forces involved are those accounted for earlier in Chapter III, specifically the valve damping B_v and the valve spring constant k_ε. In general, each of these two forces can be either positive or negative. The Bernoulli force in the usual valve design is positive; i.e., it resists motion of the valve spool in a direction which increases the flow rate through the valve. This gives rise to the misnomer "centering" force.

Because these two forces are functions of the geometry of the valve spool and sleeve configuration, the designer has some control over these forces. A well-designed valve will be of such a configuration that the Bernoulli force is minimized and the spool damping effect is positive.

Three main assumptions are made at this point:

1. The fluid is considered to be incompressible and non-viscous.
2. The peripheral width of the orifice is assumed to be large in comparison with its length so that the flow can be considered two-dimensional.
3. The flow is considered to be irrotational in the adjacent region upstream of the orifice.

For small valve spool displacements, the first two assumptions are reasonably accurate. The third assumption is not true throughout most of the hydraulic circuit but is fairly accurate in the small region of interest.

Consider the figure below which shows an element of a control volume made up of a square land valve spool and the sleeve in which it operates.

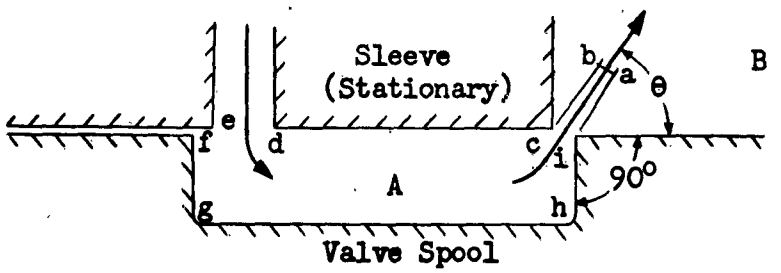

Figure VII-1. An Element of a Control Volume

The force existing on the valve spool is the axial component of the net rate of efflux of momentum through the control volume boundary a-b-c-d-e-f-g-h-i-a, The area a-b of the vena contracta of the jet is much smaller than the area d-e where the fluid enters the upstream chamber A. Since the velocities are inversely proportional to the respective areas involved, the influx of momentum through d-e is considered to be negligibly small compared to the efflux of momentum at a-b, Therefore, the net axial force is

(VII-1) $$F_{A-B} = QU\rho \cos\theta$$

where

Q is the total rate of flow ($in.^3$ $sec.^{-1}$)

U is the velocity at the vena contracta (in. $sec.^{-1}$)

ρ is the fluid density (lb. $in.^{-4}$ $sec.^2$)

For the configuration shown with sharp edged orifices and very small radial clearance, the angle Θ is 69 degrees. This value has been determined analytically and verified experimentally. Since Θ is always less than 90° for the configuration shown, the force F_{A-B} of (VII-1) is always positive and tends to center the valve spool. This is true regardless of the direction of flow. In either case it is the configuration of the downstream chamber that determines the force.

Because it is the downstream chamber that determines the force, there exists the possibility of shaping the downstream chamber of a port in such a way as to produce a negative (decentering) force. If such a configuration is used for one port of a four-way valve, the negative force can be made to cancel the effect of the positive force existing at the other port.

In the negative force port configuration, the axial component of the efflux of momentum from the downstream chamber is made greater than the influx. Therefore a negative or decentering force at one of two ports is generated. The configuration of such a port is shown in the figure below.

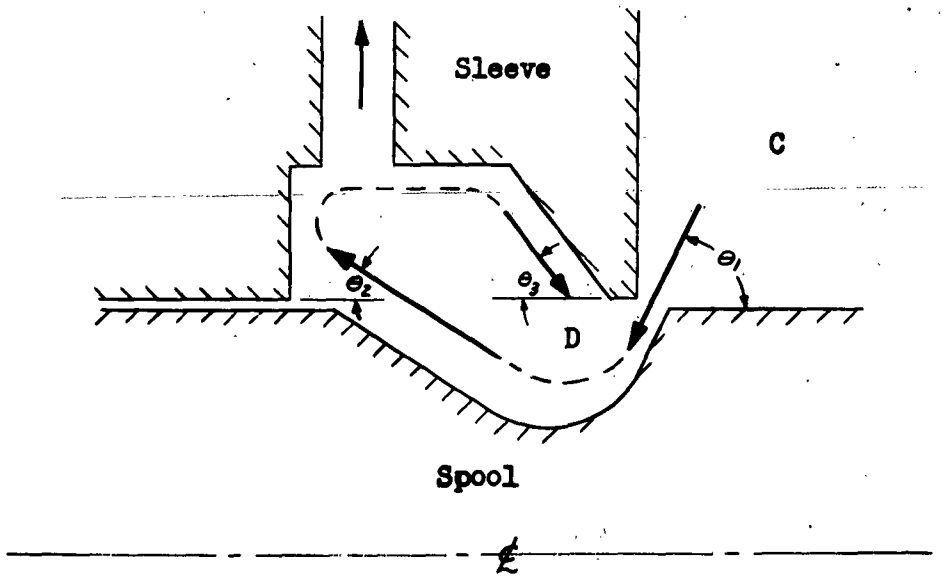

Figure VII-2. A Negative Force Port Configuration

In Figure VII-2, the chamber in the spool is shaped somewhat like a turbine bucket with the sleeve relieved to form an extension of the downstream chamber. The force existing on the spool is

(VII-2) $$F_{c-D} = QU\rho(\cos\theta_1 - \cos\theta_2)$$

This force is negative since $\cos\theta_2$ is considerably larger than $\cos\theta_1$. In addition, the eddy re-entering the chamber D at the angle θ_3 further increases the negative force. A four-way valve with force compensation is shown below.

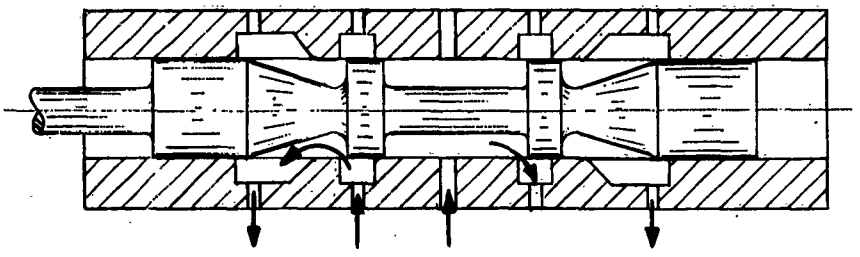

Figure VII-3. A Four-Way Valve With Force Compensation

The total force on the valve spool (exclusive of inertial and frictional effects) is developed in the referenced report (see footnote, page VII-1). The total axial force is

(VII-3) $$F_x = \rho Q u_2 + \rho(x_2 - x_1)\frac{dQ}{dt}$$

where

$$u_2 = -C_u\sqrt{\frac{2\Delta p}{\rho}}\cos\theta$$

$$Q = C_q \omega x'\sqrt{\frac{2\Delta p}{\rho}}$$

and

$$\frac{dQ}{dt} = C_g \omega \sqrt{\frac{2\Delta p}{\rho}} \frac{dx'}{dt}$$

Δp is the pressure drop across the orifice

x' is the linear opening of the orifice

ω is the peripheral width of the orifice

C_g is the orifice discharge coefficient (approximately .65)

C_u is the velocity coefficient (approximately .98)

Therefore,

$$F_x = -\left[2C_g C_u (\cos\theta)\omega\Delta p\right]x' + \left[C_g \omega \sqrt{2\Delta p \rho}\; L\right]\frac{dx'}{dt} \qquad \text{(VII-4)}$$

where $L = x_2 - x$, of the figure below.

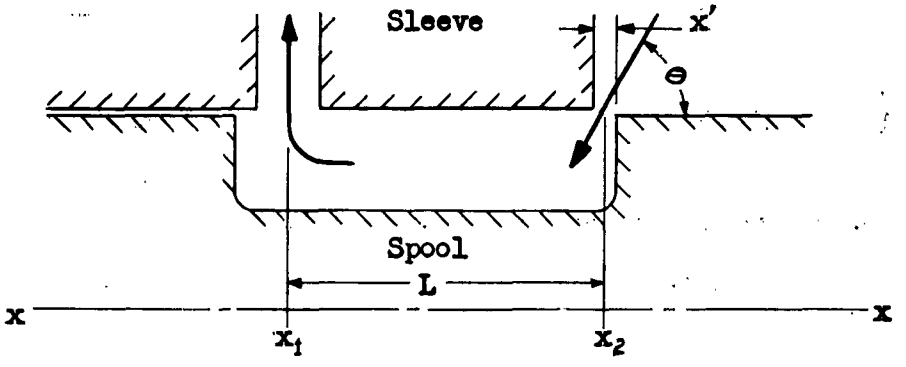

Figure VII-4. Flow Into the Annular Chamber of the Valve Spool

For the direction of flow as shown with the jet discharging into the annular chamber of the valve spool, $L = x_2 - x$, and is positive. This results in a negative damping coefficient in the force equation. If the flow is reversed and is from the annular chamber out through the orifice, the damping is positive. In a multi-orifice valve, the positive damping must be greater than the negative damping to prevent valve instability.

SECTION 3 - ACTUATORS WITH THREE-WAY VALVES

(a) COMPARISON OF ACTUATORS WITH THREE-WAY AND WITH FOUR-WAY VALVES

In the discussion so far concerning control valves and actuators, only the symmetrical four-way valve and balanced area actuator have been considered. The typical configuration is repeated below.

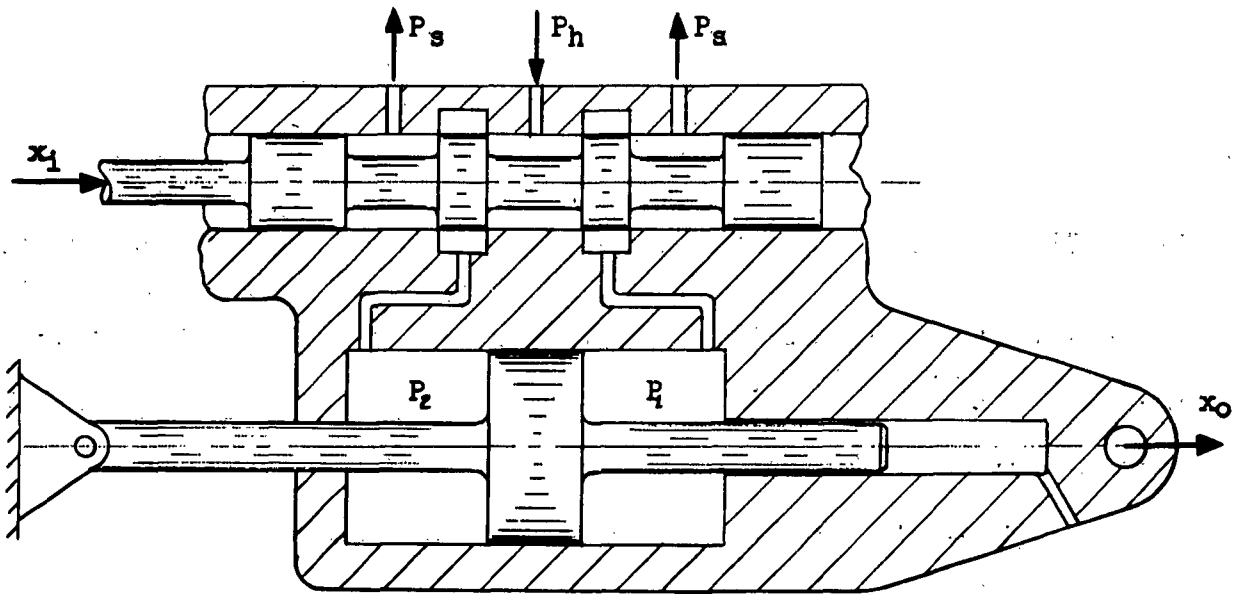

Figure VII-5. A Four-Way Valve and Balanced Area Actuator

The operation of this device has been described in more detail elsewhere in this volume. In general, there are two equal pressure drops at the two valve ports, and assuming an incompressible fluid, there are two equal volumetric flow rates into and out of the respective cylinder volumes.

(VII-5) $$\Delta P_1 = P_h - P_1 = P_2 - P_s = \Delta P_2$$

and the load induced pressure

(VII-6) $$P_L = P_1 - P_2$$

This can be illustrated by a bridge circuit shown in Figure VII-6.

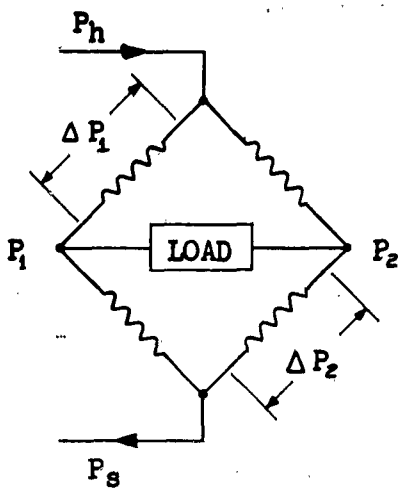

Figure VII-6. Bridge Circuit Analogous to Hydraulic Servo of Figure VII-5.

At this point, it appears desirable to describe another type of valve and actuator that is somewhat simpler in operation. Because the valve is simpler in construction, the device becomes attractive as far as design is concerned. A typical configuration of the three-way valve and differential area actuator is shown in Figure VII-7.

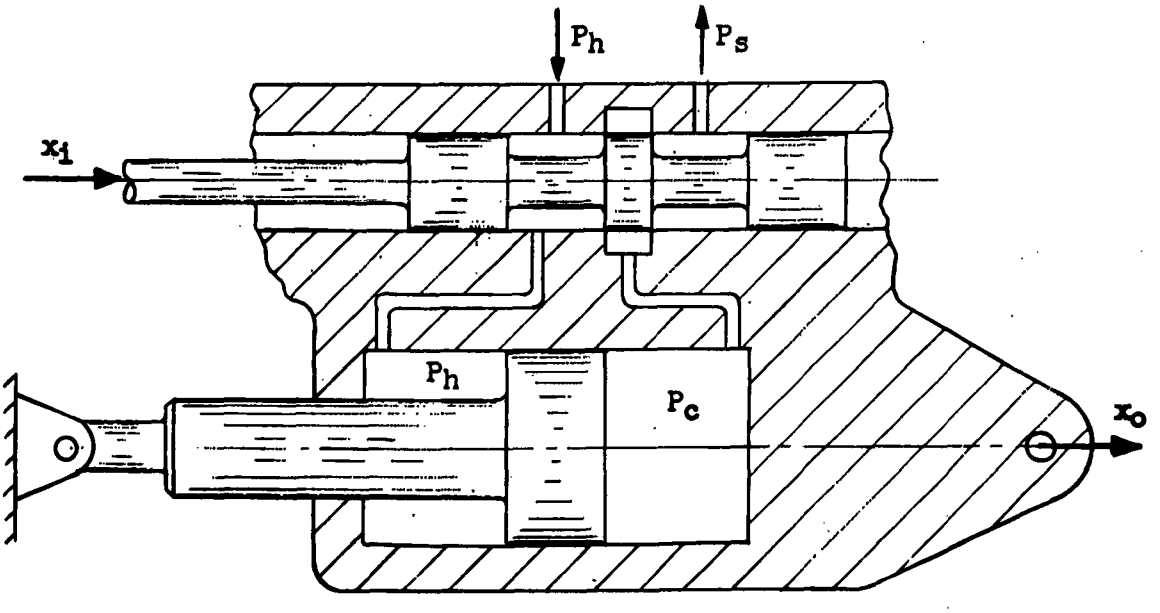

Figure VII-7. A Three-Way Valve and Differential Area Actuator

Here the actuator piston is constructed so that the areas of the two sides of the piston head, subjected to pressure, have a ratio of two to one. To compare equivalent systems, suppose that the smaller area is equal to the area presented by either side of an equivalent balanced area piston. This smaller area chamber communicates directly to the high pressure supply (P_h). For the actuator to be in a state of static equilibrium under no load conditions, the pressure (P_c) in the larger area chamber must be maintained at a value of one-half the high pressure supply. Therefore, control of the actuator resolves itself into controlling the pressure and flow into (or out of) one chamber of the actuator. Because of this, only one controllable orifice within the valve is required.

The actuator is operated by controlling the magnitude of a variable force against which a constant force operates. For the configuration shown, the same maximum force in either direction is available and is equal to the respective maximum force attainable in either direction by an equivalent balanced area actuator.

Both types require the same amount of supply volume per cycle. However, the differential area actuator delivers twice the volume to the return line over a half cycle than does the balanced area actuator. Over the other half cycle, the differential area actuator delivers zero volume to the return line. In addition, the piston diameter of the differential area actuator is larger than that of an equivalent balanced area actuator.

In concluding the discussion of the two types of valves and actuators, it should be pointed out that at the mid-point of the stroke, the hydraulic compliances of the two types are equal. However, in the case of the balanced area actuator, controlled by a four-way valve, the effective spring constant of the oil within the cylinder increases as the actuator departs from the mid-stroke

position. In the case of the differential area actuator controlled by a three-way valve, the compliance is proportional only to the volume of oil trapped in the larger area chamber. Therefore, the hydraulic compliance of such a device is minimum at one extreme of actuator stroke and maximum at the other. Also, in the case of the three-way valve actuator, since the small area side of the actuator is directly connected to system supply pressure, pronounced variations in system pressure are more apt to affect the actuator output position. Actuator output motions under load perturbations are also proportional to the actuator hydraulic compliance.

In the discussion, a two-to-one area relationship was assumed in the case of the differential area actuator. Because it is convenient in the design of an actuator to incorporate O-rings for sealing means, it may not always be feasible to provide a precise two-to-one area relationship. Under such conditions the actuator response will not be truly symmetrical about a no-load operating point. In general, if the actual area relationship is within 10% of the idealized two-to-one relationship, it becomes difficult to detect any asymmetry in the actuator output.

Similar comments apply in the case of the balanced area actuator where the areas at both sides of the piston head are not precisely equal. A typical case is where it is not desirable to balance the areas with the actuator blind shaft extension.

A lack of area balance in either type actuator causes a slight departure from symmetrical response. The operation is similar to that which would be caused by a moderate load bias, which is a fairly common operating condition for any type actuator.

(b) ANALYSIS OF ACTUATORS WITH THREE-WAY CONTROL VALVES

Since the piston areas of this actuator are unbalanced, it might appear that analysis is more difficult; however, this is not the case. For this type of actuator, the flow is metered across two lands of the valve rather than across four lands as in the four-way transfer valve. If the port connecting the supply pressure to the small area side of the piston is large in comparison with the metering ports of the valve, and the supply pressure is assumed constant, it can be seen that the analysis of flow equations need only be concerned with the flow in and out of the large area side of the piston, since the small area side of the piston can be assumed to do nothing more than supply a constant force. If the large area is twice the small area, the expression for the load induced pressure P_L will be:

(VII-7) $$P_L = P_1 - \frac{P_s}{2}$$

For purposes of computing the oil spring the volume of oil under compression is only the oil on the large side of the piston; therefore, the analysis should always be carried out for a position of the cylinder where the large area side of the piston has its greatest volume, since this will be the point where the oil spring is the weakest. This is the extended position for the actuator shown in Figure VII-7. With the small changes mentioned above, analysis is then carried out by the methods of Chapter 3.

SECTION 4 - EQUALIZATION BY HYDRAULIC MEANS

Chapter III of this volume describes a typical valve-controlled servo element. If the piston rod spring constant k_p is very large and the piston mass M_p is very small, (III-44) can be approximated by:

(VII-8) $$x_o = \frac{k_f}{B_f s}\left[\varepsilon - \left(\frac{B_f}{k_o}s + 1\right)\left(\frac{A p_L}{k_f}\right)\right]$$

Assume that the complete set of performance specifications has been made available and that the actuator size has been selected. Therefore, for a predetermined value of system supply pressure P_h, the piston area A has been established, and the effective volume of fluid under compression γ' is approximately determined. The servo designer has no control over the load induced pressure p_L or the fluid bulk modulus N.

The only design parameters over which the servo designer has any effective control are the slopes C_ε and C_p of the valve flow curves. Further, because of the difficulty of evaluating C_p, the servo designer has only one design parameter by which he may optimize his design. This design parameter is C_ε which is essentially a gain term.

Suppose then that the designer has selected a value of C_ε which seems to be satisfactory. After fabrication of a prototype, certain indications of incipient instability become apparent. The designer then can reduce the value of C_ε. However, with the servo gain diminished, the system may not be able to satisfy the design requirements. Another solution is to provide such devices as heavy valve damping or a bleed across the cylinder parts. However these devices are also performance inhibitors and are generally unsatisfactory.

The problem now resolves itself into one of equalization, of providing methods of utilizing elements with essentially fixed characteristics in order to achieve a type of behavior that is in no way inherent in the valve controlled servo element itself.

An equalization means which is widely used for electrical networks is the R-C lead network. This network, which is shown in Figure VII-8, is put in series with the control element and effectively modifies the signal to the control element (in this case the servo valve) in a particular manner. The result is that the servo can operate at a higher gain in the forward loop (with a higher value

of C_ε) without resulting instability. This is due to the positive phase shifting characteristics of the network.

The basic lead network is shown below

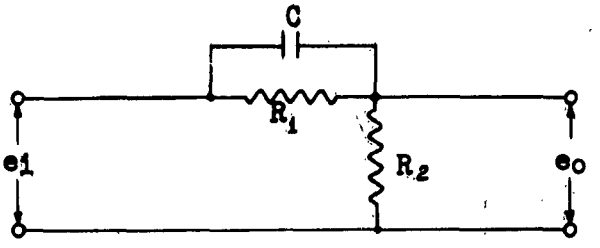

Figure VII-8. Basic Lead Network

The relationship of the voltage out e_o to the voltage in e_i is

$$\frac{E_o}{E_i} = \frac{(\alpha \tau s + 1)}{\alpha(\tau s + 1)} \qquad \text{(VII-9)}$$

where

$$\alpha = \frac{R_1 + R_2}{R_2}$$

$$\tau = \frac{R_1 R_2 C}{R_1 + R_2}$$

Such a network is of little interest to the hydraulic servo designer unless of course the control valve happens to be positioned by some electromagnetic device. The remaining portion of this section will discuss means by which hydraulic and mechanical elements may be used to provide an equivalent effect.

One possible way of achieving the desired equalization is shown in Figure VII-9.

In Figure VII-9 the main valve and actuator are exactly the same as those described in Chapter V. The auxiliary valve, the auxiliary piston, and the floating link are added. All hydraulic components are located in a common housing.

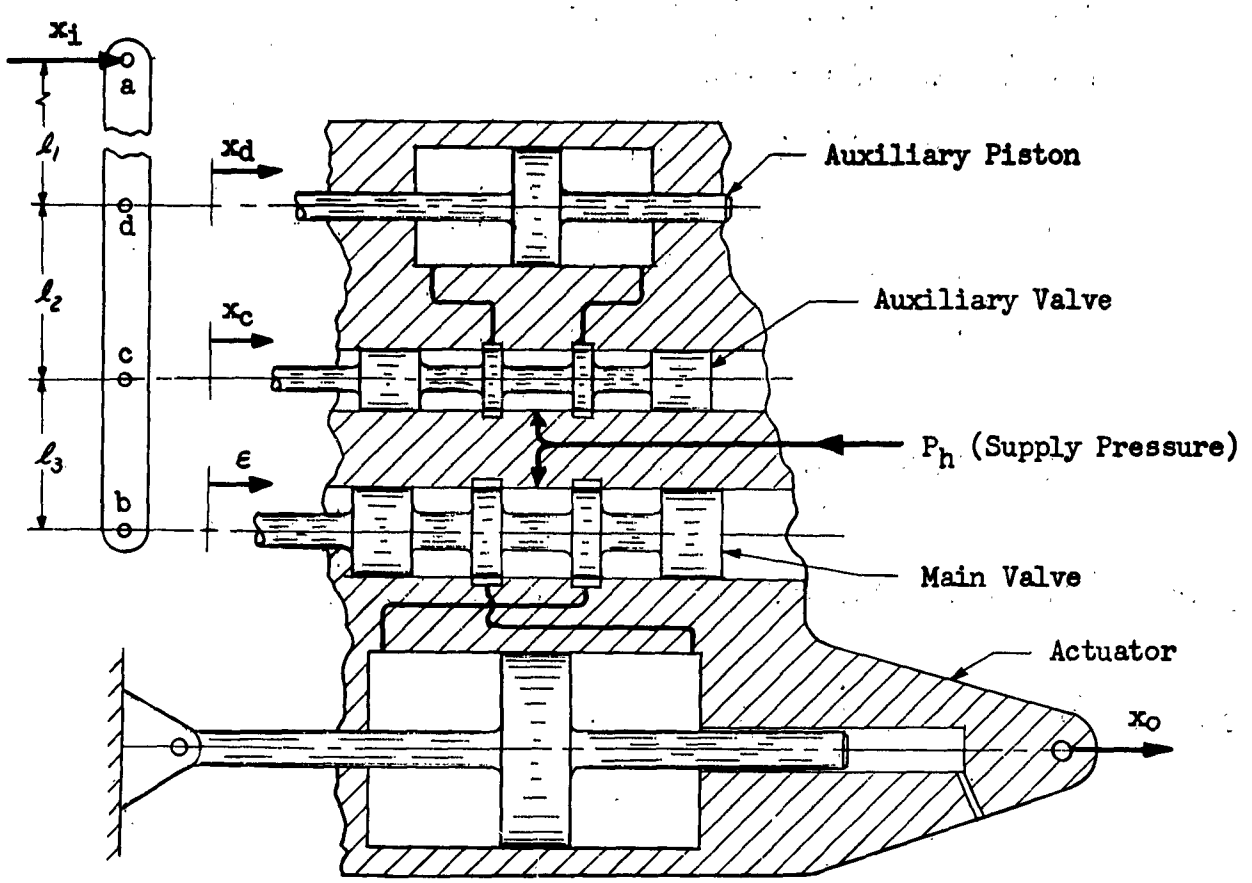

Figure VII-9. Typical Hydraulic Actuator with Equalization

Therefore the input signal x_i and the actuator output position x_o are measured relative to a fixed reference. The displacements x_d of the auxiliary piston, x_c of the auxiliary valve spool, and ϵ of the main valve spool are measured relative to the movable actuator housing.

First consider the system at rest as shown in the figure. Suppose a step input x_i displaces to the right point "a" on the linkage. Initially then, the link rotates in a clockwise direction about point "d" as an instantaneous center. This results in a displacement x_c of the auxiliary valve spool and a proportional displacement ϵ of the main valve spool. Both of these valve displacements are towards the left. The results are that the auxiliary piston moves to the right

relative to the movable housing and the main actuator moves to the right. As the main actuator moves to reduce the error to zero, the auxiliary valve spool, because of the linkage geometry, crosses its neutral point before the main valve spool reaches its respective neutral position. Thus the auxiliary piston, the auxiliary valve spool, and the main valve spool all simultaneously are returned to their respective neutral positions as the system error reduces to zero.

The figure below shows the link in two positions. Figure VII-10(a) shows the angular position of the link immediately following the introduction of a step displacement of x_i, before the actuator has changed position in response to the signal. Figure VII-10(b) shows the link as the actuator approaches synchronism with the signal. Note that in (b) the auxiliary valve spool has crossed its neutral position and that the auxiliary piston has reversed its direction of motion, returning to its neutral position. The heavy arrows show the direction of motion and velocity of the points indicated.

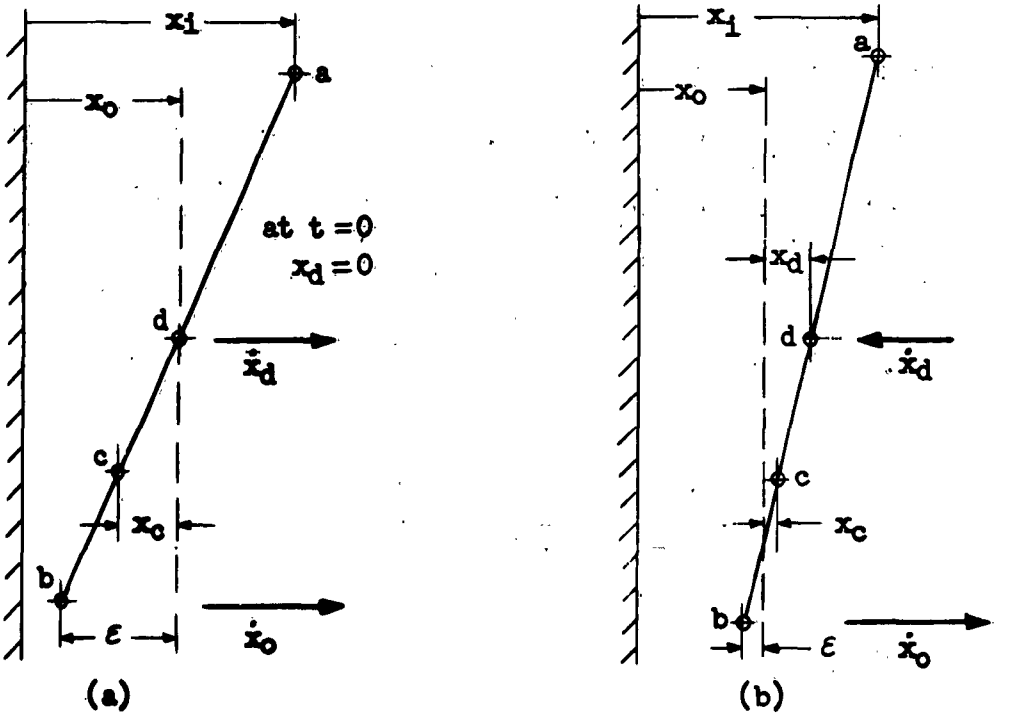

Figure VII-10. Link Displacement

From the linkage geometry it is possible to write two equations for the link instantaneous angular position Θ:

$$\text{(VII-10)} \qquad \Theta = \frac{x_i - x_o - x_d}{l_1} = \frac{x_d - x_c}{l_2}$$

and

$$\text{(VII-11)} \qquad \Theta = \frac{x_i - x_o - x_d}{l_1} = \frac{x_d - \varepsilon}{l_2 + l_3}$$

also

$$\text{(VII-12)} \qquad -x_c = \frac{s x_d}{k_1}$$

where k_1 is the auxiliary system gain. Equation (VII-12) is valid if the auxiliary actuator is unloaded; that is, if B_v and k_c are very small.

$$\text{(VII-13)} \qquad x_o = -\gamma_\varepsilon \varepsilon$$

where γ_ε is the transfer function of Chapter V.

The minus signs indicate that valve displacement to the left results in actuator motion to the right. Combining (VII-10) and (VII-12)

$$\text{(VII-14)} \qquad l_2(x_i - x_o - x_d) = l_1\left(x_d + \frac{s x_d}{k_1}\right)$$

from which

$$\text{(VII-15)} \qquad x_d = \frac{l_2(x_i - x_o)}{\left[(l_1 + l_2) + \frac{l_1 s}{k_1}\right]}$$

Equation (VII-11) may be rewritten as:

$$\text{(VII-16)} \qquad (x_i - x_o)(l_2 + l_3) = (l_1 + l_2 + l_3)x_d - l_1 \varepsilon$$

Substituting (VII-15) in (VII-16) and solving for $\mathcal{E}$:

$$(VII\text{-}17) \qquad \mathcal{E} = -(x_i - x_o)\left[\frac{l_3}{l_1 + l_2}\right]\left[\frac{\frac{(l_2 + l_3)}{l_3 k_1}s + 1}{\frac{l_1}{(l_1 + l_2)k_1}s + 1}\right]$$

or

$$\mathcal{E} = -\gamma_{eq}(x_i - x_o)$$

Equation (VII-17) may be combined with (VII-13) to form the same type of block diagram as that developed in Chapter V which is repeated here.

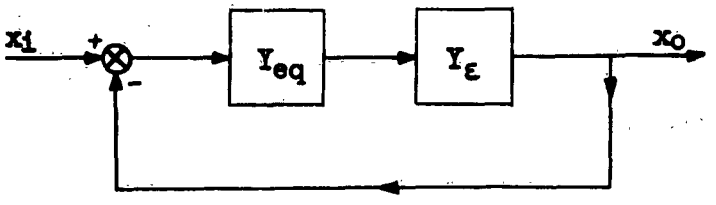

Figure VII-11. Block Diagram of Actuator With Hydraulic Equalizer

It is desirable that the equalization term γ_{eq} be equivalent to that given in (VII-9). Therefore,

$$(VII\text{-}18) \qquad \frac{(\alpha\tau s + 1)}{\alpha(\tau s + 1)} = \left[\frac{l_3}{l_1 + l_2}\right]\left[\frac{\frac{(l_2 + l_3)}{l_3 k_1}s + 1}{\frac{l_1}{(l_1 + l_2)k_1}s + 1}\right]$$

For (VII-18) to be true, the linkage equation $l_1 = l_2 + l_3$ must be true; then

$$(VII\text{-}19) \qquad \alpha = \frac{l_1 + l_2}{l_3} \quad , \quad \tau = \frac{l_1}{(l_1 + l_2)k_1}$$

The corresponding quantities of the electrical equalizer are:

$$(VII\text{-}20) \qquad \alpha = \frac{R_1 + R_2}{R_2}$$

(VII-21) $$\tau = \frac{R_1 R_2 C}{R_1 + R_2}$$

Other methods for providing equalization can be used. For instance, a floating valve spool which is not directly connected to the pilot's mechanical input motion may be employed. In this case the control valve spool is not positioned by the system instantaneous error but rather by some particular function of this error. By selection of the particular function of the error by which the control valve is positioned, the type of equalization is determined. This is by no means limited to an analogy of the electrical R-C network selected in the foregoing. By the exercise of some ingenuity in the hydraulic curcuit design, a wide variety of equalization characteristics is made possible.

In general, the proper application of equalization techniques will greatly improve the stability characteristics of a given servo system throughout a critical frequency region. In many designs the normally critical design parameters such as valve gain, represented by the slope of the valve flow curve, becomes relatively less important.

In addition, because most hydraulic equalization means employ an internal feedback loop around the contol valve itself, or a functional equivalent of such a feedback loop, the normal non-linear action of the valve becomes obscured. This also results in the fact that the device instantly responds within itself to the effects of load perturbations without error perturbations necessarily resulting. Further, the steady state load error can be made zero in most designs.

SECTION 5 - EQUALIZATION BY STRUCTURAL FEEDBACK

The principal problem in hydraulic control system design is to find means of de-emphasizing the incipient instability arising because of the large mass

of the control surface and the low rigidity of the oil in the cylinder. Force feedback, operating in conjunction with a fairly weak spring, is remarkably effective in this respect, as has been shown in Section 3 of Chapter V and in Chapter VI. However, the effectiveness of methods discussed to this point depends on the magnitude of flexibility in the input link (cable or pushrod), and the design must be tailored to a given control channel. The application of such methods often requires numerous time-consuming tests. Merely as a matter of speeding design, there is some practical need for a means of force feedback stabilization in which the dependence on input dynamics is not pronounced. In the following there is a brief discussion of a method which has acquired the name "structural feedback." *

Consider the simplified system shown schematically in Figure VII-12.

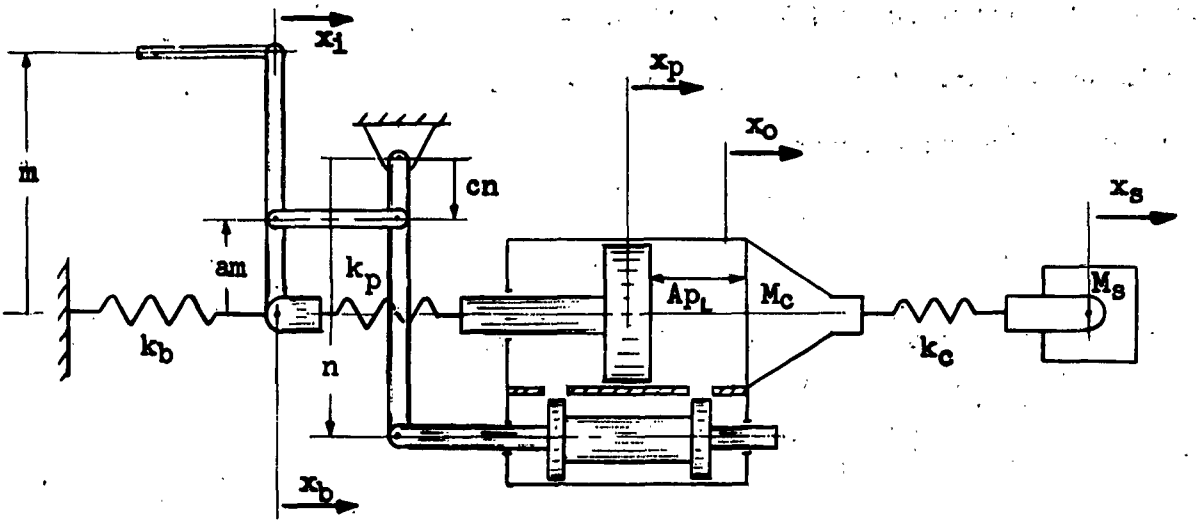

Figure VII-12. Fully-Powered System with Structural Spring and Multiplying Link

The quantities B_v, k_ε, M_i, B_i, B_c, and B_s are considered zero for purpose

* Rahn, J. J., and Kangas, E. W., Improvement of Power Surface Control Systems by Structural Deflection Compensation, BuAer Report No. AE-61-5-III: Report of the Second Piloted Aircraft Flight Control System Symposium, June 2, 3, 4, and 5, 1952.

of illustration. The pivot point of the input arm is in this case not considered fixed, but as being on a "weak bracket" with spring constant k_b. At some point of the input arm with dimensionless radius a, motion due to both the immediate input x_m and the deflection x_b of the pivot point is fed to a multiplying link. The valve error then becomes:

$$\text{(VII-18)} \qquad \varepsilon = \left(\frac{a}{c}\, x_i\right) + \frac{(1-a)}{c}\, x_b - x_o$$

It should be pointed out that derivation of this equation tacitly assumes that the input arm does not translate as a whole in response to load, as is approximately the case if the input arm is a quadrant with preloaded cable and the bracket spring k_b is less than infinite. The immediate connection between the input system and the input arm of the actuator is now taken as a pushrod, in which case the equation (VII-18) applies.

With no aerodynamic force F, the cylinder displacement x_o can be expressed as a function of the valve error ε.

$$\text{(VII-19)} \qquad x_o = \gamma_\varepsilon\, \varepsilon$$

where, for the simplified case shown in Figure VII-12,

$$\text{(VII-20)} \qquad \gamma_\varepsilon = \frac{\left(\frac{s^2}{\omega_3^2} + 1\right)}{\frac{s}{\omega_1}\left(\frac{s^2}{\omega_2^2} + \frac{2\zeta_2}{\omega_2}\, s + 1\right)}$$

where

$$\omega_1 = \frac{k_f}{B_f}$$

$$\omega_2 = \sqrt{\frac{1}{M_s\left(\frac{1}{k_a} + \frac{1}{k_c} + \frac{1}{k_b} + \frac{1}{k_p}\right)}}$$

$$\omega_3 = \sqrt{\frac{k_c}{M_s}}$$

$$\frac{2\zeta_2}{\omega_2} = \frac{M_s}{B_c}$$

A force balance on the cylinder yields the equation

(VII-21) $$k_b x_b + k_c(x_o - x_s) = 0$$

The valve error is obtained as a function of x_o and ax_i/c by combining (VII-18), the equation about the surface node (IV-1), and the equation expressing the force balance on the actuator (VII-21).

(VII-22) $$\epsilon = \gamma_{eq}\left[\gamma_{ei}\left(\frac{ax_i}{c}\right) - x_o\right]$$

where

$$\gamma_{eq} = \frac{\left(\frac{s^2}{\omega_g^2} + 1\right)}{\left(\frac{s^2}{\omega_3^2} + 1\right)}$$

$$\gamma_{ei} = \frac{\left(\frac{s^2}{\omega_3^2} + 1\right)}{\left(\frac{s^2}{\omega_g^2} + 1\right)}$$

$$\omega_3 = \sqrt{\frac{k_c}{M_s}}$$

$$\omega_g = \sqrt{\frac{1}{M_s\left[\frac{1}{k_c} + \frac{(1-a)}{ck_b}\right]}}$$

The block diagram of the servo is shown in Figure VII-13.

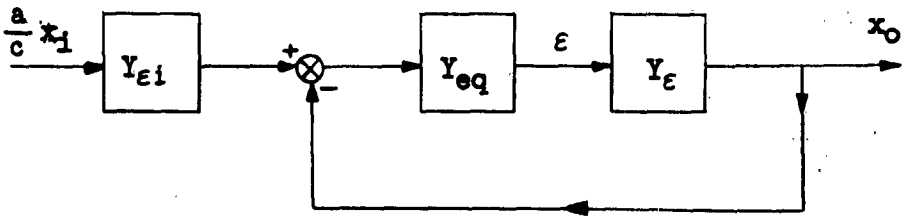

Figure VII-13. Block Diagram of Fully-Powered System with Structural Spring and Multiplying Link

From a comparison of Y_{eq} and Y_ε it is seen that if the frequency of the numerator quadratic of Y_{eq} is the same as that of the denominator quadratic of Y_ε, the control surface dynamics cancel and the open loop transfer function becomes $k_f / B_f s$. The cancellation requires that:

$$\text{(VII-23)} \qquad \frac{k_b + k_c\left(\frac{1-a}{c}\right)}{k_b k_c} = \frac{1}{k_o} + \frac{1}{k_c} + \frac{1}{k_b} + \frac{1}{k_p}$$

or simplifying, and assuming $k_p >> k_o$,

$$\text{(VII-24)} \qquad \frac{1-a-c}{c} = \frac{k_b}{k_o}$$

The choice of a and c is restricted by the fact that the ratio a/c enters as an initial gain.

If the multiplying link is not present, c is unity, and (VII-24) becomes:

$$\text{(VII-25)} \qquad -a = \frac{k_b}{k_o}$$

The utilization for stabilization of structural feedback without a multiplying link thus requires that the input x_i be reversed. It is assumed here that the spring k_b represents added flexibility in every case.

It is by no means easy to design a bracket for strength and flexibility at the same time. If structural feedback is to be used for purposes of stabilization, the design process may be expected to be largely cut and try.

SECTION 6 - MECHANICAL GAIN ADJUSTMENT

A common fault found with the integral valve-cylinder actuators used as illustrative examples earlier in this volume is the difficulty in changing gain, since the gain is chiefly the slope of the flow curve. Figure VII-14 shows a simple actuator where the open-loop gain is dependent upon the mechanical advantage of the linkage operating the valve.

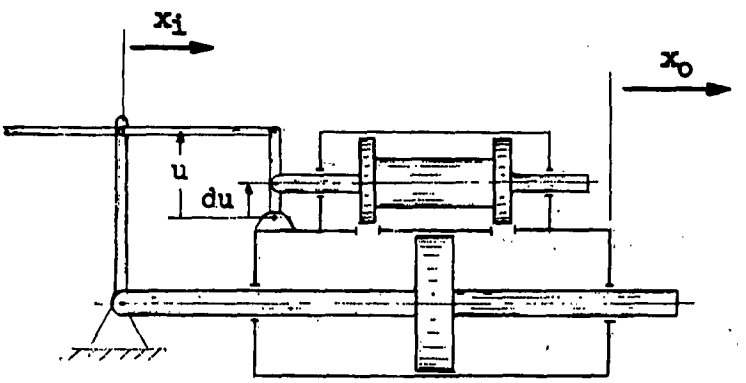

Figure VII-14. Simple Hydraulic Actuator

The valve error for the actuator shown in Figure VII-14 is defined as:

(VII-26) $$\varepsilon = d(x_i - x_o)$$

If (VII-26) is written in the form presented in Chapters V and VI, the form would be

(VII-27) $$\varepsilon = \gamma_{eq}(x_i - x_o)$$

where

$$\gamma_{eq} = d$$

Since the transfer function $x_o/\mathcal{E} = Y_\varepsilon$ remains unchanged, the block diagram for the system is shown in Figure VII-15.

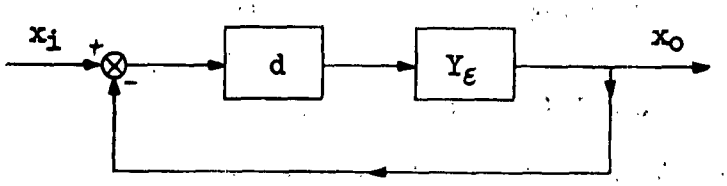

Figure VII-15. Block Diagram of a Simple Hydraulic Acutator

It can be seen from Figure VII-15 that the factor d directly effects the open loop gain of the system. A change in gain by a factor of two can be easily realized by this means, but ratios larger than two may be difficult to obtain due to the length of the linkage arms involved.

It can be seen from Figure VII-15 that the leading effect of valve friction on an input mechanism is reduced if d is smaller than one. This may be desirable in case an autopilot actuator is used as an input device.

SECTION 7 - ELECTRICALLY CONTROLLED TRANSFER VALVE

A type of control valve that has become widely used in recent years with hydraulic actuators is the electrically controlled transfer valve. It has not as yet been used for primary surface actuators on piloted planes because of its relative unreliability compared with manual control valves. However, it is widely used on missiles and a few autopilot installations. It is desirable, therefore, to have an analysis which will cover this type of valve.

The valve analysis presented in Chapter III assumes that two variables P_L and $\mathcal{E}$ are sufficient to define the behavior of the valve. The same analysis could be extended if a transfer function could be found between valve spool error of the electric transfer valve and the electric signal supplied to the valve, for instance the current. However, for most valves used today, the dynamics of

this transfer function occur at such high frequencies that the relation between valve error and current may be regarded as a constant. Figures VII-16(a), b, and (c) show the experimental flow curves for one electrically operated four-way transfer valve in use today.

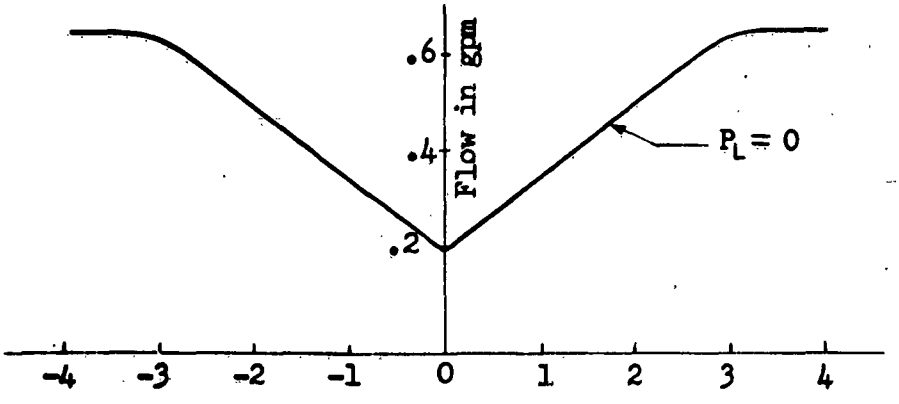

(a)

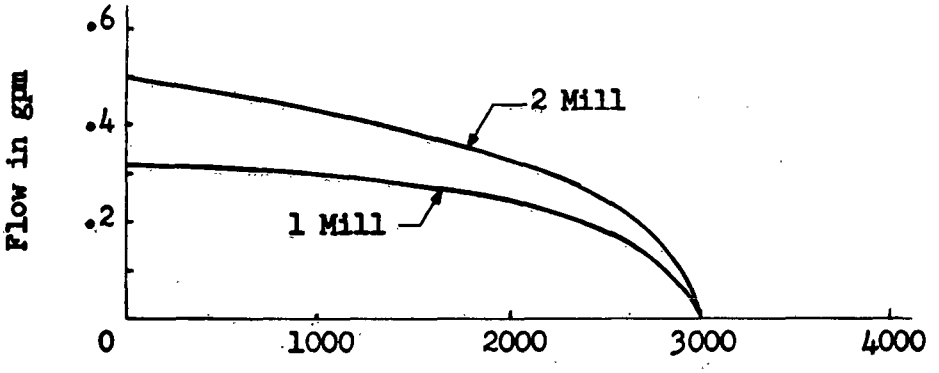

(b)

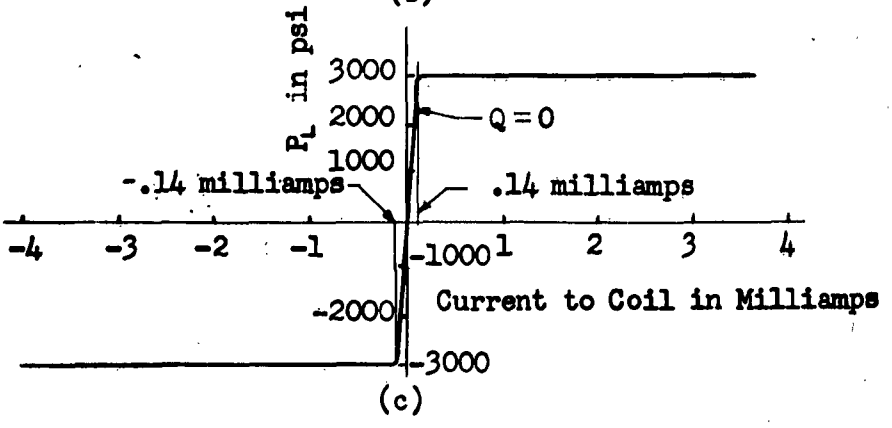

(c)

Figure VII-16. Flow Curves for Typical Electric Transfer Valve

It can be seen that these curves compare very closely with the curves presented in Figures III-4 and III-6 of Chapter III for a manually controlled valve. Therefore, the analysis presented in Chapter III can be used if the current to the valve is substituted for valve error. The transfer function x_o/i may then be obtained. The rest of the servo loop, exclusive of equalization, consists of feedback potentiometer and amplifier as shown in Figure VII-17 and can therefore be handled directly by standard servo techniques.

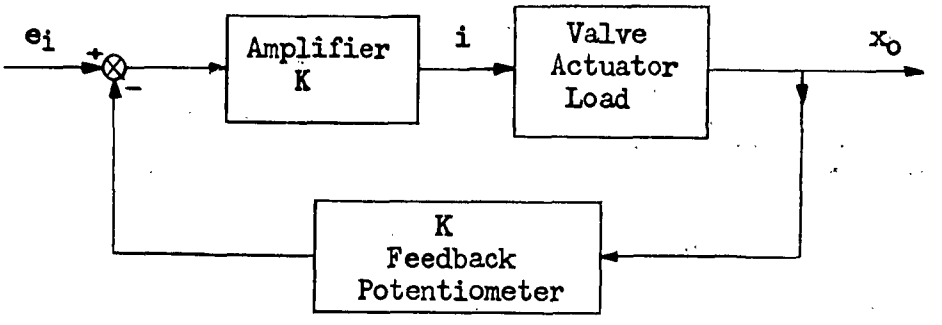

Figure VII-17. Block Diagram for Positional Servo Using an Electrically Operated Valve

One effect that has been neglected in this analysis is hysteresis. The normal, manually controlled valve has a negligible hysteresis loop; however, this may not be the case for the electrically controlled valve. If the hysteresis loop is not negligible, the analysis is more complicated.* Also, if the dynamics of the valve fall within the frequency regime of interest, the transfer function x_o/i will have to be broken up as previously mentioned and these dynamics included.

Electrically operated valves could be built as a three-way valve; however, analysis would still be similar.

* See Chapter VI, "Non-Linearities," Methods of Analysis and Synthesis of Piloted Aircraft Flight Control Systems, BuAer Report No. AE-61-4 I, Northrop Aircraft, Inc., Hawthorne, California, 1952.

CHAPTER VIII

COMPONENT DESIGN FACTORS

SECTION 1 - INTRODUCTION

It is the purpose of this chapter to summarize pertinent component design factors and to show how the design of the control surface actuator is integrated into the over-all design of the airplane, i.e., how the hydraulic actuator design influences and is influenced by the design of other airplane components. Most of the discussion is confined to fully-powered actuators incorporating substantially closed-center valves; however, the presentation includes mention of some of the problems associated with other types of systems. The discussion has been kept quite general, although at several points specific magnitudes or relative magnitudes of parameters are quoted as being typical and/or desirable. It should be pointed out that individual design problems may present difficulties which are not completely covered in the sections to follow. It is hoped that the chapter will at least provide a starting point.

SECTION 2 - ACTUATOR SELECTION

A primary consideration in the hydraulic system design is the type of actuator that will be used. The actuator may be a moving cylinder type with a separately mounted valve or a moving piston type. Most of this volume has been concerned with the moving cylinder type of actuator, with integrally mounted valve. This combination provides inherent servo follow-up, as well as minimization of line lags between valve and cylinder; it also results in the simplest operating linkage and consequently little backlash in the feedback path. Disadvantages of the combination are that the moving cylinder "sweeps out" more airframe structure than does the fixed cylinder moving piston type, and the follow-up linkage is not as readily adjusted for necessary "fixes" in the later design phases.

It may be desirable to employ two hydraulic actuators rather than a single actuator. This is particularly true on multi-engine airplanes where the two actuators may be furnished hydraulic power from separate pumps on different engines. The dual hydraulic system has obvious advantages from a vulnerability and reliability standpoint provided, of course, that the aircraft can still execute simple maneuvers with a single actuator operative. Another advantage of the dual system is that the two actuators may be preloaded against one another, thereby eliminating dangerous backlash under otherwise critical surface flutter conditions. The preload is accomplished by displacing the valves so that when the control surface is faired, the actuator cylinders tend to move in opposite directions.

Many modifications are possible in the actuator configurations. Examples are "gain" changers, hydraulic equalization, and complex feedback linkages. These complications of design should be used only when necessary. The prime effort must be to keep the design as simple as possible, and yet fulfil system performance requirements and stay within airframe structural and space limitations.

SECTION 3 - SYSTEM PRESSURE SELECTION

Another consideration which must be established early in the hydraulic actuator design is the system pressure. To minimize cylinder size and weight, it is usually desirable to use as high a system pressure as possible. The advantages thus gained must be balanced against the disadvantages of providing extra engine power to drive a heavier and more costly pump. A high system pressure also complicates the problem of leakage from hydraulic lines and couplings.

At the present time most hydraulic components and hardware are qualified for a pressure of 3000 psi. A pressure of 5000 psi is considered the optimum

pressure for minimum size and weight of the over-all hydraulic system of a present-day high speed aircraft, but procurement of complete sets of high-pressure components and hardware is not currently possible. Within the next few years higher qualification pressures will be realized as airplane speed and hinge moment requirements increase.

SECTION 4 - ACTUATOR-SURFACE GEOMETRY

The values of certain basic parameters are available to the designer of hydraulic control systems prior to the establishment of the control system configuration. These data are:

1. Maximum hinge moment on surface due to air loads.
2. Surface deflection limits.
3. Surface rate or maximum velocity.

Assuming a certain system pressure, it is easily shown that the total cylinder oil volume must remain constant, irrespective of the surface horn radius (or actuator stroke) selected. To obtain the same maximum hinge moment, the cylinder area must, of course, be varied; this results in an altered compressibility of the cylinder oil even though the volume remains fixed. In many cases the dominant flexibility of the combined actuator-surface system is due to the compressible oil, yet the resultant natural frequency of the surface acting through this oil spring also remains unchanged for various horn radii when the same hinge moment and surface deflection are required.

Lengthening the surface horn radius has the advantages of relaxing the positioning accuracy requirements of a given hydraulic servo and of minimizing the effects of backlash at all bearing, or attach, points. A disadvantage is that the actuator stroke is correspondingly increased, and consequently the actuator assembly may require a large space between extremes of its travel within the

parent surface structure. If, further, the servo valve travel limits are kept fixed, in addition to hinge moment, surface deflection, and surface rate, the hydraulic actuator gain is also increased; that is, the first order time constant of the servo is decreased, giving rise to a stability problem. In most instances, space limitations severely limit actuator surface geometry, thus making many theoretical considerations purely academic.

SECTION 5 - VALVE DESIGN

Most present-day fully-powered actuator designs include modified "closed center" servo valves. These valves are constructed in such a manner that a small amount of fluid ("neutral leakage") is allowed to flow from the pressure line to the return line through the valve ports when the valve is in a neutral, or centered, position as shown in the figure below.

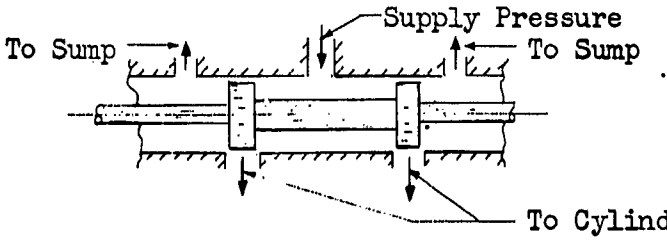

With this arrangement, even when the cylinder is not carrying external loads, the pressure in the fluid on either side of the piston is very high (approximately one-half system pressure). Any air which is entrained within the fluid has negligible effect on the compressibility of the oil. The controlled leakage feature of the valve also produces an "open-center" servo operation over a very small range of valve travel; in this range the pressure differential across the cylinder piston is primarily a function of valve displacement. Thus any movement of the valve will result in a pressure differential across the piston. In most valve designs, full system pressure differential is available to the cylinder when the valve has been displaced approximately 5% of its full travel. The complete system usually is designed in such a manner that full valve travel

corresponds to two degrees or less at the control surface. Since a pressure differential on the order of 2% of system pressure is normally required to overcome cylinder friction, it is evident that any "flat-spot" in the plot cylinder velocity as a function of valve displacement is about 0.002 degrees. Care should be taken that the neutral leakage flow is relatively small since there may be a number of similar valves operating on a single hydraulic power source. The sum of the neutral leakage flows may become excessively large for the case of wind milling engines, at which time the hydraulic pumps are operating well below their rated capacity.

The slope of the flow curve, i.e. flow valve displacement, is the most important parameter of a closed center valve, since it, together with the cylinder area, determines the gain of the hydraulic actuator, or the time constant of the servo system.* A hydraulic system time constant of 0.05 seconds is usually sufficient for present-day fighter aircraft. In the case of an open-center valve design, the slope of the flow curve does not necessarily dictate the system time constant.

The design of the actual valve orifice depends a great deal upon the maximum oil flow required, which in turn is fixed by the required surface speed. On many airplanes of the past, the surface speed has been fixed by a rule of thumb: "full surface travel in one second." In general this rule leads to surface speeds that are much higher than necessary. The flight condition which usually dictates the maximum surface speed is the landing condition, where the hinge moment is low but rapid surface corrections are necessary. It is worthwhile to carry out an investigation to determine the actual maximum surface velocity to maintain good control of the airplane. One approach is to assume a two-degree-of-freedom airframe and solve for the time required to reach a given change in airplane

* See Chapter V.

attitude as a function of surface velocity. The input is assumed to be a chopped ramp (Figure VIII-1); i.e., the surface has a constant speed to its limiting travel and then stays at that position. The time-velocity curve resulting from this approach will have the form shown in Figure VIII-2.

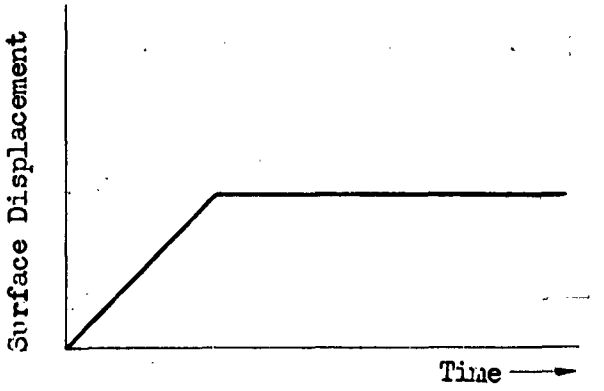

Figure VIII-1. Input to Surface

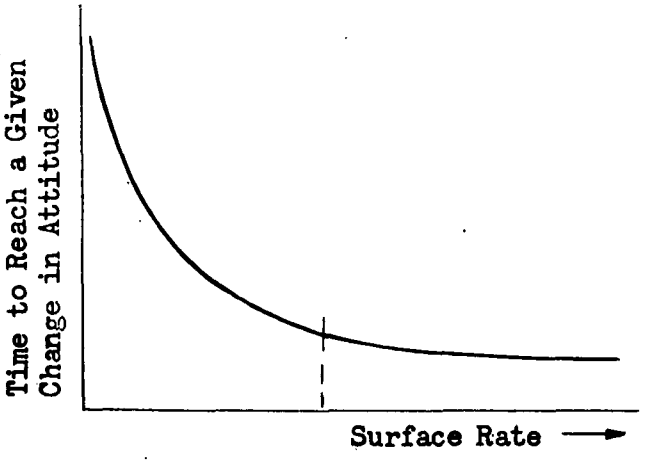

Figure VIII-2. Response of Surface

It can be seen that beyond the dotted line of Figure VIII-2, increasing surface speed does very little toward increasing a response of the airplane. NACA reports have shown that satisfactory landings can be made with surface speeds as low as

10 degrees per second if the pilot is not aware that the surface is actually moving that slowly. Any reduction in surface velocity is reflected as a considerable weight saving due to the smaller pump required to drive the hydraulic system.

In certain valve designs, the flow of fluid through the valve results in pressure drops which produce forces on the valve spool. These forces normally tend to return the valve to the neutral or centered position. Poorly designed valves can give rise to erratic valve centering forces which are objectionable to pilots and might cause system instability. For these reasons, attempts are made to minimize the effects by designing the valves in such a manner that the flow into and out of the valve is normal to the axis of the valve spool. The flow through the valve may be broken into a series of flow patterns where at maximum valve displacement the majority of the flow is in a region where dynamic centering forces cannot be applied to the valve spool. With this type of design, centering forces may be reduced to small values.

Valve friction, even if rather small in magnitude, is very objectionable to a pilot from the standpoint of the character of the force. The coulomb friction component is constant in magnitude, but takes the sign of the spool velocity. However, the coulomb effect upon the pilot is most pronounced during motion reversals, while, on the other hand, valve "stiction" (or break-away friction) appears at the stick only when motion is initiated from a rest position. As a result, both of these valve forces feel to the pilot as though the system has high inertia. Also, a sluggish feel results if the viscous friction component of the total valve friction is too high. Maximum acceptable valve friction is approximately 2 lbs.; values less than this can only be obtained in sealed valve designs by reducing "O" ring squeeze, reducing valve spool diameters, etc. Where fluid leakage is no problem, simple lapping of the spool and sleeve

(or spool housing) produces relatively low valve friction forces.

Adequate filters must be provided in as close proximity to the valve as possible. Further precautionary filters may be integrated in the valve body itself. The possibility that foreign materials such as filings and chips might get into the fluid and jam the servo valve is a real problem. An additional safety measure which may be incorporated is a design of the valve and sleeve such that, rather than providing one large-area orifice, or slot, which might easily be jammed by a particle, a series of small diameter metering holes are uncovered in sequence by a sharp-edged valve spool land. The valve spool and sleeve are hardened to Rockwell C-55 to C-58. As a result, large particles cannot enter, and the particles which can are small enough to be sheared off by forces developed on the spool by the pilot. Certain flight controller servos can also develop enough force to provide the necessary shearing action.

It is desirable in valve design to provide a valve sleeve which floats on "O" rings within the valve housing. The radial clearance between the sleeve and the housing should be great enough that no binding of the sleeve will occur under extreme temperature conditions. The "O" rings also isolate the closely lapped sleeve and spool from external stresses which may exist due to mechanical mounting means. To further eliminate external forces on the sleeve, the valve spool travel stops should be on the housing rather than on the sleeve. The floating sleeve arrangement also allows easy servicing of the valve, since the sleeve and spool may be removed without disturbing the housing and its attached plumbing.

SECTION 6 - ACTUATOR DESIGN

Several spring constants which may affect system operation are inherent in the cylinder and piston design. Two very important sources of flexibility are

the piston rod and the extension, or coupling spring, between the cylinder body and the surface horn. A reasonable criterion for these two spring constants is that they each be at least ten times greater than the spring constant of the oil within the cylinder. The axial flexibility of the cylinder body itself may be disregarded if a neutral leakage type valve is employed. The reason for this is that the sum of the pressures on each side of the piston remains approximately constant, even with load variations, thus yielding the equivalent effect of a pre-loaded spring. It is common practice to insure long cylinder life by inserting a steel cylinder sleeve which is smaller than, but concentric with, the cylinder body; the sleeve is supported by appropriate mountings on both ends. The sleeve should not be so thin that its radial expansion under pressure will materially reduce the effective spring constant of the cylinder oil. The equivalent spring constant of this sleeve should be at least twenty times as large as the oil spring constant. In every case, the piston and cylinder assemblies must be designed for rigidity and not merely for strength.

When the servo valve is mounted separately from the actuator, rigid tubing must be employed between valve and cylinder, the use of flexible hose in this application dangerously reduces the series combination spring constant of the oil and lines. The calculation of the total oil under compression must also include that in the interconnect lines for the remote valve configuration.

An additional spring constant, which is a very important system parameter, is the combined series spring constant of the surface horn, the torque tube between horn and surface (if such exists), and the inherent flexibility of the surface itself. This spring is dependent on the structural design of the surface and is not under the direct control of the hydraulic designer. The structural designer should be aware that rigidity of the surface is an extremely

important parameter in the design of the hydraulic actuator system. The effective spring constant of the surface is difficult to evaluate since the surface is a distributed parameter system and as such has many oscillatory modes. It is usually sufficient to evaluate the surface spring from the derived or measured value of its fundamental torsional frequency as seen from the horn. The bending modes are usually relatively unimportant since most surfaces are supported at several points along the hinge line. Parent surface bending if very great does not permit the simplification suggested above. Also, on recent airplane designs all-movable surfaces have been employed in which the bending modes are much more dominant than the torsional modes.

There is one more design item over which the designer has limited control. This parameter is the effective damping coefficient between cylinder and piston due to O-ring installation. The O-rings are, of course, used to prevent piston rod leakage as well as load induced leakage past the piston from one side of the cylinder to the other. The introduction of the necessary O-rings into the design entails non-linear damping, the effective viscous equivalent of which is difficult to evaluate. Data on O-ring damping for various cylinder pressures and degrees of O-ring "squeeze" are contained in Air Force Technical Report No. 5997. The use of a single grooved piston sometimes results in O-ring roll which resembles backlash in the output motion of the cylinder (or piston) as the load pressure reverses sign. This O-ring roll may be minimized by providing two O-rings per piston and venting the peripheral area between the two to atmospheric pressure. In this fashion the force on either ring due to pressure in the cylinder never reverses sign.

SECTION 7 - STABILITY ANALYSIS

A brief review of a typical hydraulic actuator will now be presented to illustrate the effect upon system stability of the design parameters that have

just been discussed. The case which will be taken is the fully-powered actuator of Section 2 of Chapter V.

In general, stability analyses of hydraulic control systems are made for a grounded condition of the aircraft, i.e., when there is no airload on the surface. This is usually the most adverse condition from the standpoint of stability since airloads entail additional surface damping and an additional restraining spring on the surface. It is a well-known fact that although many hydraulic control actuactors have been subject to ground chatter or buzz, they have proved perfectly stable in flight. Ground chatter also prevents checkout of the manual and automatic modes of the flight control system.

With aerodynamic force on the control surface assumed negligible, the open-loop transfer function of the typical example is approximately given by (V-27), which is repeated here for convenience:

(VIII-1)
$$\left.\frac{x_o}{\varepsilon}\right|_{\substack{F=0\\ B_s=0\\ k_c=0}} \approx \frac{\left(\frac{s^2}{\omega_3^2}+\frac{2\zeta_3}{\omega_3}s+1\right)}{\frac{s}{\omega_1}\left(\frac{s^2}{\omega_2^2}+\frac{2\zeta_2}{\omega_2}s+1\right)}$$

where

$$\omega_1 = \frac{k_f}{B_f}$$

$$\omega_2 = \sqrt{\frac{1}{M_s\left(\frac{1}{k_o}+\frac{1}{k_p}+\frac{1}{k_c}\right)}} \qquad \frac{2\zeta_2}{\omega_2} = \frac{M_s}{B_f}+\frac{B_c}{k_o}+B_s\left(\frac{1}{k_o}+\frac{1}{k_p}+\frac{1}{k_c}\right)$$

$$\omega_3 = \sqrt{\frac{k_c}{M_s}} \qquad \frac{2\zeta_3}{\omega_3} = \frac{B_s}{k_c}$$

The frequency response plot of this transfer function is shown in Figure VIII-3.

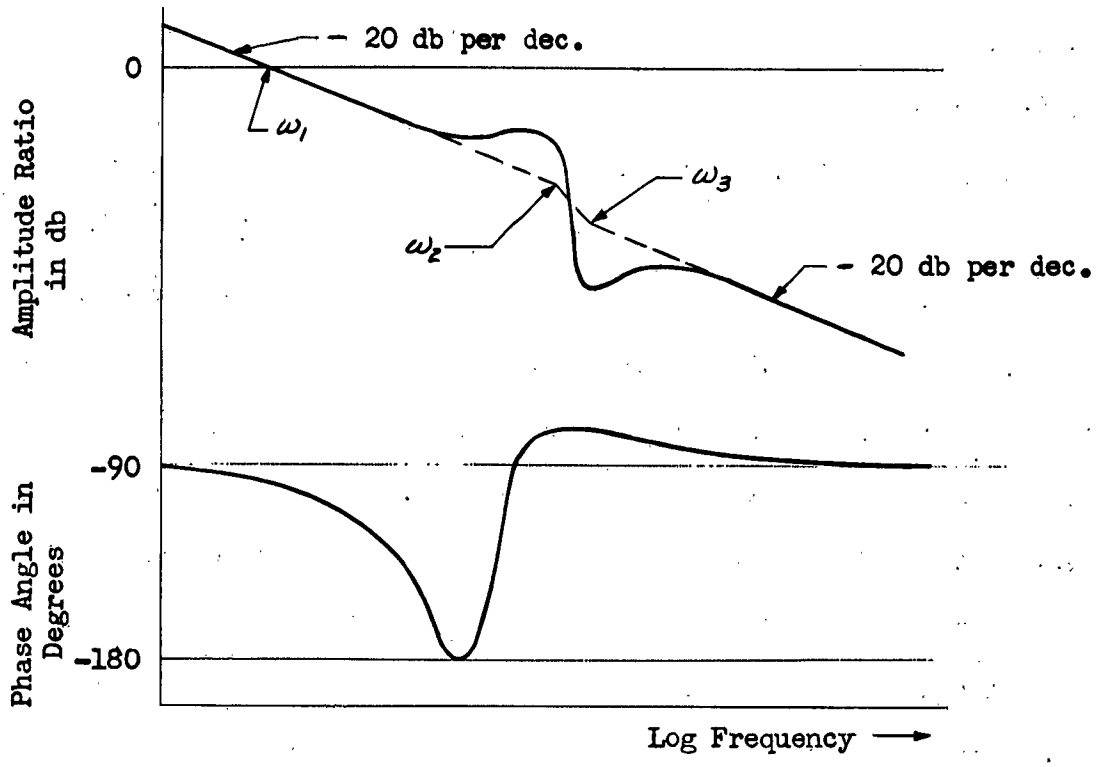

Figure VIII-3. Typical Open-Loop Frequency Response

The most important parameters which place upper limits on the system gain are those which are contained in the damping and natural frequency terms of the denominator quadratic. It is seen that the frequency ω_2 is dependent upon all the springs in the system as seen by the surface mass. It is important to keep this frequency as high as possible since it is relatively lightly damped; otherwise the system gain term, or zero gain line, must be adjusted at the expense of optimum performance. The preliminary analysis should indicate whether the design will be adequate, i.e., completely stable, yet with sufficient gain to yield a satisfactory time constant.

The design criteria which have been set forth in previous sections of this chapter establish the cylinder oil spring and the inherent surface spring as the dominant springs in the system. The predetermined hinge moment, surface displacement, and surface rate requirements render the oil spring constant essentially

introduced through an autopilot is limited; therefore, it becomes important that the combined phase curve of the autopilot, hydraulic system, and airframe allow the gain to be adjusted to give good control of the airplane. Since the airframe frequency response is dictated by the designed configuration, it is unalterable, and since the phase lead introduced by the autopilot is limited, the hydraulic actuator must be good enough to make the combined system satisfactory. Therefore, if an autopilot is to be used in conjunction with an airframe, it is essential that the autopilot designers be consulted to determine what time constant is necessary for the hydraulic system.

The second problem, low threshold, is important since the autopilot actuator will be required to make a great many small corrections because it cannot distinguish between phugoid and short period oscillations of the airframe. If the threshold is high, the autopilot hydraulic actuator airframe system will tend to have a limit cycle oscillation that the pilot will find objectionable. In conjunction with the low threshold requirement, it is necessary to maintain a satisfactory time constant for very small input amplitudes. Many hydraulic systems tend to have a higher time constant for smaller amplitudes because sufficient care was not taken in the valve design. This effect will again tend to produce limit cycle oscillations in the combined system.

Other hydraulic system parameters that affect autopilot design are loads imposed upon the autopilot actuator by the hydraulic system and velocity limiting of the hydraulic cylinder. For a fully-powered system, the only load imposed upon the autopilot actuator by the hydraulic system is the valve operating force. Assuming that Bernoulli forces have been designed to be small, the larger part of this force is coulomb friction. Since most autopilot actuators are electric motors whose torque error curve may have a low slope, this coulomb friction can

PART II

HYDRAULIC ACTUATORS IN FLUTTER SYSTEMS

CHAPTER IX

THE INFLUENCE OF SERVOMECHANISMS ON THE FLUTTER OF SERVO CONTROLLED AIRCRAFT *

SECTION 1 - INTRODUCTION TO SERVO-FLUTTER INTERACTION

The extensive application of servomechanisms in the control of aircraft has been both cause and result of some of the most important recent advances in aircraft design. To a greater degree than was formerly the case it has become necessary to examine the controlled aircraft system as an integrated whole. In particular, the introduction in high speed aircraft of complex control systems embracing several servomechanisms is making it a necessary part of design to study in some detail the dynamic interaction between the control system and the aeroelastic airplane.

This chapter is concerned with the modification of classical flutter theory to account for the effect of a complex control system. Since control systems are highly variable in content and layout, a considerable portion of the chapter is devoted to control system elements which are likely to be present in practice. The material presented here is not to be regarded as a ready-made expression of any problem in servo-flutter interaction which may arise, but rather as a systematic organization of the considerations which the design engineer must take into account in order to set down his problem.

The central consideration in the study of dynamic interaction between the aeroelastic airplane and a complex control system including, in general, several servomechanisms is that there are present in the control system energy sources which may either promote or retard a tendency toward flutter of the overall system. Most of present day airplanes have powered controls, at least

* Portions of the material contained in this chapter appeared previously in Air Force Technical Report #6287. Special permission for its use here has been granted by Wright Air Development Center.

system having three degrees of freedom (torsion, bending, and surface rotation) and acted upon by two-dimensional aerodynamic flow forces. Each degree of freedom of the mechanical system is characterized by self-inertias, dampings and springs, and by coupling terms (via inertia, damping, or springs), with the other degrees of freedom. These self and coupling terms are all mechanical reaction forces, and the mathematical models describing their behavior (with zero applied aerodynamic forces) are linear differential equations with constant coefficients.

The mathematical model of the applied aerodynamic forces cannot be expressed in the same way. Basically, the forces are considered as the effects of two-dimensional flows and are usually described in terms of the results obtained by solving Laplace's equation for a particular two-dimensional configuration. The mathematical models of the aerodynamic flow forces are therefore functions of the mechanical degrees of freedom and of time. To put the aerodynamic forces into a usable form (or even to solve Laplace's equation), it is necessary to assume a steady state oscillation of the three mechanical degrees of freedom. Since the forces also depend upon the speed of the airflow about the particular two-dimensional configuration, the oscillation frequency is "non-dimensionalized," and referred to as the "reduced frequency," $b\omega/v$. On the basis of this assumption, the aerodynamic forces are expressed as a linear combination of functions of the three mechanical degrees of freedom but with the coefficients as functions of the reduced frequency. It is this complication, with the attendant special methods of solution, that has necessitated the creation of a special field for considering the dynamics of flutter.

With this background, the mathematical model describing a typical classical flutter system is given in (IX-1), (IX-2), and (IX-3), where the constant coefficient mechanical reaction forces are on the left and the frequency dependent

aerodynamic forces are on the right. The equations are written for the two dimensional case with zero structural damping and no tab.

Surface Rotation Equation:

$$(IX\text{-}1) \qquad \left[I_\beta \ddot{\beta} + C_\beta \beta\right] + \left[I_\beta + b(c-a)S_\beta\right]\ddot{\alpha} + S_\beta \ddot{h} = T'$$

Torsion Equation:

$$(IX\text{-}2) \qquad \left[I_\beta + b(c-a)S_\beta\right]\ddot{\beta} + \left[I_\alpha \ddot{\alpha} + C_\alpha \alpha\right] + S_\alpha \ddot{h} = M'$$

Bending Equation:

$$(IX\text{-}3) \qquad S_\beta \ddot{\beta} + S_\alpha \ddot{\alpha} + \left(M\ddot{h} + C_h h\right) = L$$

where

a is the coordinate of axis of rotation

α is the instantaneous value of local torsional angular displacement of airfoil

b is the semi-chord of entire airfoil

β is the instantaneous value of control surface rotational displacement

c is the arbitrary damping coefficient

C_α is the torsional stiffness of parent surface about elastic axis per unit span

C_β is the torsional stiffness of control surface restraint about control surface hinge axis per unit span

C_h is the bending stiffness of parent surface about elastic axis per unit span

h is the instantaneous value of local bending displacement

aerodynamic forces are on the right. The equations are written for the two dimensional case with zero structural damping and no tab.

Surface Rotation Equation:

$$(IX\text{-}1) \qquad \left[I_\beta \ddot{\beta} + C_\beta \beta\right] + \left[I_\beta + b(c-a)S_\beta\right]\ddot{\alpha} + S_\beta \ddot{h} = T'$$

Torsion Equation:

$$(IX\text{-}2) \qquad \left[I_\beta + b(c-a)S_\beta\right]\ddot{\beta} + \left[I_\alpha \ddot{\alpha} + C_\alpha \alpha\right] + S_\alpha \ddot{h} = M'$$

Bending Equation:

$$(IX\text{-}3) \qquad S_\beta \ddot{\beta} + S_\alpha \ddot{\alpha} + \left(M\ddot{h} + C_h h\right) = L$$

where

- a is the coordinate of axis of rotation
- α is the instantaneous value of local torsional angular displacement of airfoil
- b is the semi-chord of entire airfoil
- β is the instantaneous value of control surface rotational displacement
- c is the arbitrary damping coefficient
- C_α is the torsional stiffness of parent surface about elastic axis per unit span
- C_β is the torsional stiffness of control surface restraint about control surface hinge axis per unit span
- C_h is the bending stiffness of parent surface about elastic axis per unit span
- h is the instantaneous value of local bending displacement

I_{α} is the moment of inertia of parent surface per unit span about elastic axis

I_{β} is the moment of inertia about hinge line of control surface per unit length

L is the total aerodynamic lift on entire airfoil per unit span

M is the total oscillatory aerodynamic moment acting on parent surface about its quarter-chord point per unit span

M' is the total aerodynamic moment acting on entire airfoil about its elastic axis per unit span

S_{α} is the static moment of entire airfoil per unit span about elastic axis

S_{β} is the static moment per unit length of control surface about hinge line

T' is the total aerodynamic torque acting on control surface per unit length about hinge line.

These classical equations are complete in themselves if no further energy sources are present and if the description of the reaction forces is accurate. However, when a fully-powered or power-boosted surface control system is added, two different types of modifications to the classical equations are in general required.

The first of these types of modifications deals with one degree of freedom vibration and is made necessary by the fact that the mechanical reaction forces described by the flutter equations no longer describe the physical situation. In this instance, the self-reaction forces in (IX-1), $I_{\beta}\ddot{\beta} + C_{\beta}\beta$, representing effectively a spring (for example, torsion springs and a pushrod) and the surface inertia, require modification to describe the presence of the hydraulic actuator having no input valve motion. The nature of this entire modified self-reaction

force may be found by looking back into the surface actuator system. Since the first approximation is still an inertia and a spring term, with the inertia essentially I_β, the entire system may be considered almost the same as the conventional system for sufficiently low frequencies. However, for high frequencies the spring term must be considered complex. This type of modification is considered later in detail.

The second type of modification to the classical flutter system deals with systems of two or more degrees of freedom. In this case, one of the flutter system motions α, β, or h, or a function of one of these motions, causes an input to the actuator and hence additional coupling of β with torsion or bending. As examples of this type of coupling, consider:

1. The case where rotation of the surface bends the fuselage, stretching one portion of a cable system more than another, resulting in valve motion which changes the surface rotation, etc., or
2. The case where the torsional displacement, α, causes a change in moment on the aircraft, in turn resulting in a change in load factor which is picked up by an accelerometer in a stability augmenter (or by a bobweight in a feel system), which then gives rise to a stability augmenter motion, a valve motion, and consequent surface rotation.

The changes to the flutter system model in Case 2 above are obviously much more complicated, depending upon the characteristics of the stability augmenter and upon the characteristics of the feedback of a flutter system motion to the stability augmenter sensor. In the following portions of this chapter, stability augmenter characteristics are reviewed, and a method of handling this sort of feedback is presented. The types of feedback from a flutter system motion to various stability augmenter sensors are discussed, but nothing definitive can be said about exact forms.

In summary, the presence of the surface actuator makes it necessary to consider two types of modification to the flutter system:

1. A fairly simple change in effective surface dynamics (with no input to the actuator).
2. Much more complicated couplings due to the fact that the subsidiary systems cause surface actuator inputs.

It should be stated at this point that a special instance of this second modification, which may be of great value in future designs, is the case where a function of a flutter system motion is picked up by a sensor, specifically installed for this purpose, which then moves the control surface in such a way that the influence of undesirable couplings is reduced; such a sensor is a flutter system stability augmenter. This sort of device could become quite important in future designs because it would make possible the use of certain airplane configurations now considered unsatisfactory because of flutter. It would also be particularly helpful as a remedial measure in alleviating trouble caused by unexpected flutter and as a safety device for flutter testing.

(b) MODIFICATION OF THE CLASSICAL SYSTEM

The purpose of this subsection is to indicate the general form taken by the flutter equations when a surface actuator is added to the system. The modifying terms are expressed as transfer functions which are operators relating input and output quantities.* The procedure will be to assume that all possible feedbacks to the surface exist, and then to show how the general flutter equations are modified. Later sections discuss in detail the actual forms of the general feedbacks assumed here. The reason for including this section at this

* See: Methods of Analysis and Synthesis of Piloted Aircraft Flight Control Systems, BuAer Report No. AE-61-41, Northrop Aircraft, Inc., Hawthorne, California, 1952.

point is to supply a better background for certain of the more detailed analyses given later.

A general surface actuator has the defining equation: *

(IX-4) $$M_F = \gamma_s \beta + \gamma_i x_i$$

where M_F is the net moment due to the combined effect of β (and its derivatives) and the effect of any input x_i to the servo device. The moment component $\gamma_i x_i$ implies the existence of surface rotation through feedback coupling involving α, β, or h which produce x_i. In terms of the flutter equations,

(IX-5) $$M_F = T' - [I_\beta + b(c-a)S_\beta]\ddot{\alpha} - S_\beta \ddot{h}$$

Note that in the classical flutter case the actuator system is not considered, and $\gamma_s \beta = I_\beta \ddot{\beta} + C_\beta \beta$. Equation (IX-5) then becomes identical to (IX-1).

Physically, $\gamma_s \beta$ is the moment component due to surface rotation, and $\gamma_i x_i$ is the moment component due to an actuator input.

If the input to the actuator, x_i, is a function of α, β, or h (due to the presence of coupling stability augmenters, autopilots, structural feedbacks directly in the actuator, etc.), the form of x_i becomes

(IX-6) $$x_i = \gamma_\alpha \alpha + \gamma_\beta \beta + \gamma_h h$$

where γ_α is the total transfer function from the torsion angle α, to actuator input x_i, etc.

In general, the γ_α, γ_β, γ_h transfer functions are combinations of various feedback paths and contain portions which are functions of $b\omega/v$ as well as portions which are functions only of ω. Since the transfer function concept allows

* It is assumed that the surface actuator applies no forces that directly cause torsion or bending.

the analyst to effectively lump degrees of freedom, complex feedback paths can be handled readily in this fashion if the feedbacks are functions only of ω. When portions of the transfer functions become properties of $b\omega/v$, it is desirable to consider certain of the degrees of freedom as additional ones to the three used thus far as examples, without lumping all the feedback degrees of freedom as transfer functions. This case is discussed in Chapter X. In this chapter, the examples used are considered to be functions only of ω and are selected to illustrate the fact that feedback terms modify the conventional flutter terms. The equations used in this section would be general in nature if the $Y(\omega)$'s are replaced by $Y(b\omega/v)$'s. This is undesirable as far as actually solving the general flutter system problem is concerned.

Combining (IX-4), (IX-5), and (IX-6),

$$(IX\text{-}7) \qquad Y_s\beta + Y_i(Y_\alpha \alpha + Y_\beta \beta + Y_h h) = T' - [I_\beta + b(c-a)S_\beta]\ddot{\alpha} - S_\beta \ddot{h}$$

The modified surface rotation equation then becomes (for sinusoidal α, β, and h):

$$(IX\text{-}8) \qquad [Y_s(\omega) + Y_i(\omega)Y_\beta(\omega)]\beta + \{[I_\beta + b(c-a)S_\beta](-\omega^2) + Y_i(\omega)Y_\alpha(\omega)\}\alpha + \{-\omega^2 S_\beta + Y_i(\omega)Y_h(\omega)\}h = T'$$

In general, $Y_s(\omega) = \{-I_\beta \omega^2 + C_\beta + C'_\beta(\omega)\}$

so

$$(IX\text{-}9) \qquad [-I_\beta \omega^2 + C_\beta + C'_\beta(\omega) + Y_i(\omega)Y_\beta(\omega)]\beta + \{[I_\beta + b(c-a)S_\beta](-\omega^2) + Y_i(\omega)Y_\alpha(\omega)\}\alpha + \{-\omega^2 S_\beta + Y_i(\omega)Y_h(\omega)\}h = T'$$

The extent to which the flutter system is affected by any modifying system is measured by comparison of the values of the additive terms relative to the

corresponding classical terms (e.g., $Y_i(\omega)Y_h(\omega)$ relative to $-\omega^2 S_\beta$). In this instance, if $-\omega^2 S_\beta >> Y_i(\omega)Y_h(\omega)$ at the frequency of interest, the contribution of the additional bending coupling will be negligible.

In a formal fashion, the entire problem of servo systems and flutter is described by (IX-2), (IX-3), and (IX-9) if the $Y(\omega)$'s are replaced by $Y(b\omega/v)$'s. In the practical case, the forms of the additive quantities and detailed methods of analytically handling the additions are important. The sections that follow consider these aspects in detail.

Section 3 discusses the forms of Y_δ and Y_i due to hydraulic surface actuating systems. A simple fully-powered case is taken as an example. While only hydraulic surface actuators are considered in detail, the use of electrical actuators leads to essentially the same results. Section 4 discusses the portions of Y_α , Y_β , and Y_h due to stability augmenter systems. Section 5 discusses the portions of Y_α , Y_β , and Y_h due to cable systems and bobweights. Section 6 discusses the portions of Y_α , Y_β , and Y_h due to feedback of a flutter motion to a stability augmenter sensor, a bobweight, etc. With these "component" characteristics established, the combination of individual characteristics established, the combination of individual characteristics into the total modifying terms C_β , $Y_i Y_\alpha$, $Y_i Y_\beta$, and $Y_i Y_h$ is discussed in Section 7.

SECTION 3 - SURFACE ACTUATOR SYSTEMS

Hydraulic surface actuators are in common use in current piloted aircraft. In the case of missiles, the surface load and speed requirements and the missile airframe response requirements permit the use of a greater variety of surface actuator types, e.g., electrically powered units, pneumatic units, and electro-hydraulic units, as well as hydraulic actuators. The dynamical characteristics of all surface actuators are of essentially the same form, i.e., expressible by

similar generic transfer functions with interchange of certain basic system parameters.

With the above facts in mind, the system chosen for illustrative treatment is the fully-powered type formed by simplifying the system shown in Figure III-5. The power boost ratio $1/b$ is taken as infinite, and the input mass M_i, input damping B_i, valve damping B_v, and input coupling spring constant k_c are each taken as zero. The system is then truly fully-powered; i.e., the input member is subjected to no force at any time.

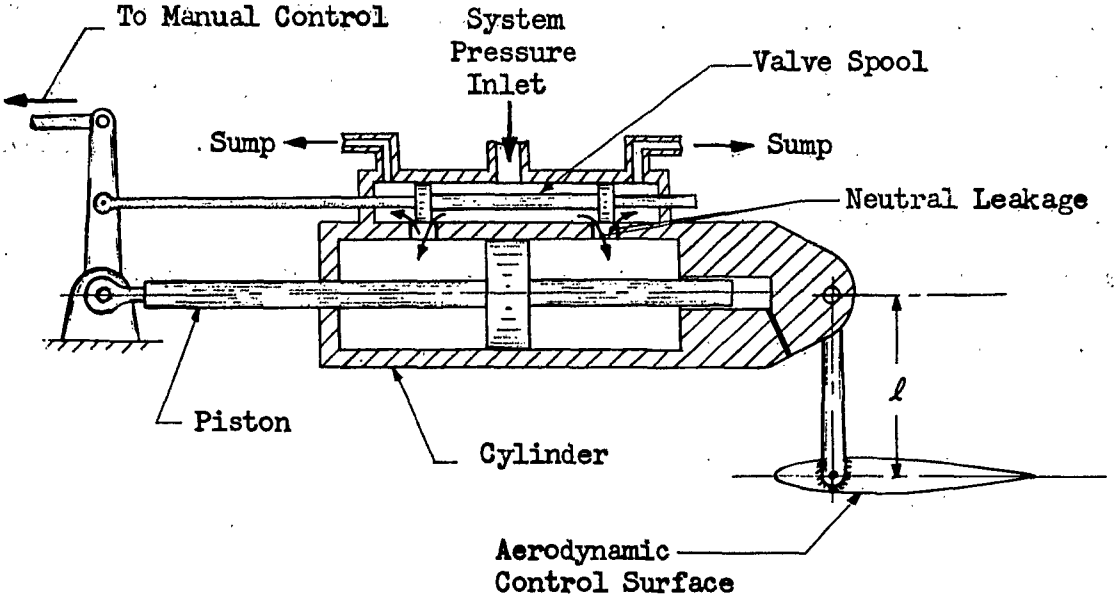

Figure IX-1. The Fully-Powered Hydraulic Servo Actuator

If ℓ is the surface horn radius in Figure IX-1 and d is the surface span served by the hydraulic actuator, there exists a simple relationship between the force F of Chapter IV and the moment M_F of (IX-5):

$$M_F = \frac{\ell}{d} F \qquad \text{(IX-10)}$$

The displacement x_s and parameters M_s and B_s of Chapter IV are given in rotational terms:

$$\text{(IX-11)} \qquad \begin{cases} x_s = l\beta \\ M_s = \dfrac{d}{l^2} I_\beta \\ B_s = \dfrac{d}{l^2} B_\beta \end{cases}$$

where β and I_β are the same as in (IX-1). The parameter B_β is a damping of control surface rotation which is seldom used in flutter analysis, since in this case it does not simulate any part of the aerodynamic force, and any remaining damping is usually negligible.

Equations (IV-7), (IV-8), (III-58), and (III-61) are easily specialized to apply to the truly fully-powered system under discussion:

$$\text{(IX-12)} \qquad F = \left[(M_s s^2 + B_s s + k_c) - \frac{\left(\frac{k_c}{k_f}\right) g_6}{\left(\frac{g_5}{k_t}\right)} \right] x_s - \frac{g_2 (a x_i)}{\left(\frac{g_5}{k_t}\right)}$$

$$\text{(IX-13)} \qquad F = \left[(M_s s^2 + B_s s) + \frac{g_1}{\left(\frac{g_5}{k_t}\right)} \right] x_s - \frac{g_2 (a x_i)}{\left(\frac{g_5}{k_t}\right)}$$

where

$$\frac{1}{k_t} = \frac{1}{k_c} + \frac{1}{k_f}$$

$$g_1 = \frac{\Delta_{\xi} - k_c \xi_{11}}{k_o k_p k_f}$$

$$g_2 = \frac{-\xi_{41}}{k_o k_p k_f}$$

$$\left(\frac{g_5}{k_t}\right) = \frac{\Delta_\xi}{k_o k_c k_p k_f}$$

$$g_6 = \frac{\xi_{11}}{k_o k_p}$$

and the ξ determinant is

$$\begin{vmatrix} M_c s^2 + B_c s + k_o + k_c & -B_c s & -k_o & 0 \\ -B_c s & M_p s^2 + (B_c + B_f)s + k_p & -B_f s & k_f \\ -k_o & -B_f s & B_f s + k_o & -k_f \\ 1 & 0 & 0 & 1 \end{vmatrix}$$

The g's given above are polynomials in s which reduce to unity if s equals zero.

Equations (IX-10), (IX-11), (IX-12), (IX-13) are combined to form:

(IX-14) $$M_F = \gamma_\beta \beta + \gamma_i x_i$$

where

$$\gamma_\beta = I_\beta s^2 + B_\beta s + C_{\beta TOTAL}$$

$$C_{\beta TOTAL} = C_\beta + C'_\beta$$

$$C'_\beta = \frac{-\frac{\ell^2}{d}\left(\frac{k_c}{k_t}\right) g_6}{\left(\frac{g_5}{k_t}\right)}$$

$$C_{\beta} \equiv \frac{\ell^2}{d} k_c$$

$$C_{\beta TOTAL} = \frac{\frac{\ell^2}{d} g_1}{\left(\frac{g_5}{k_t}\right)}$$

$$Y_i = \frac{-\frac{\ell}{d} a g_2}{\left(\frac{g_5}{k_t}\right)}$$

The expansion of C_{β}' , $C_{\beta TOTAL}$, and Y_i is simplified by taking the flow damping B_f as large in comparison with the cylinder damping B_c , as is always the case. In the typical case, the piston mass M_p is quite small, and the piston spring k_p is several times as large as either the oil spring k_o or the cylinder-surface coupling spring k_c . The polynomials g_1 , g_2 , g_5/k_t , and g_6 then each have high frequency quadratic factors at the approximate frequency $\sqrt{k_p/M_p}$. These factors effectively cancel out of C_{β}' , $C_{\beta TOTAL}$, and Y_i , which may be written:

(II-15) $$C_{\beta}' \approx \frac{-\frac{\ell^2}{d}\frac{k_c^2}{(k_c+k_f)}\left(\frac{s}{\omega_x}+1\right)}{\left(\frac{s}{\omega_x}+1\right)\left(\frac{s^2}{\omega_x^2}+\frac{2\zeta_x}{\omega_x}s+1\right)}$$

(II-16) $$C_{\beta TOTAL} \approx \frac{\frac{\ell^2}{d}\frac{k_c k_f}{(k_c+k_f)}\left(\frac{s}{\omega_{III}}+1\right)\left(\frac{s^2}{\omega_{IV}^2}+\frac{2\zeta_{IV}}{\omega_{IV}}s+1\right)}{\left(\frac{s}{\omega_{II}}+1\right)\left(\frac{s^2}{\omega_x^2}+\frac{2\zeta_x}{\omega_x}s+1\right)}$$

(II-17) $$Y_i \approx \frac{-\frac{\ell}{d} a \frac{k_c k_f}{(k_c+k_f)}}{\left(\frac{s}{\omega_{II}}+1\right)\left(\frac{s^2}{\omega_x^2}+\frac{2\zeta_x}{\omega_x}s+1\right)}$$

where

$$\omega_I = \frac{1}{B_f\left(\frac{1}{k_o} + \frac{1}{k_p}\right)}$$

$$\omega_{II} = \frac{k_f\left(\frac{1}{k_f} + \frac{1}{k_c}\right)}{B_f\left(\frac{1}{k_o} + \frac{1}{k_c} + \frac{1}{k_p}\right)}$$

$$\omega_{III} = \frac{k_f}{B_f}$$

$$\omega_{IV} = \sqrt{\frac{1}{M_c\left(\frac{1}{k_o} + \frac{1}{k_p}\right)}} \qquad \frac{2\zeta_{IV}}{\omega_{IV}} = \frac{B_c}{k_o}$$

$$\omega_V = \sqrt{\frac{k_c + \frac{k_o k_p}{(k_o + k_p)}}{M_c}} \qquad \frac{2\zeta_V}{\omega_V} = \frac{B_c}{k_o + \frac{k_c k_p}{(k_c + k_p)}}$$

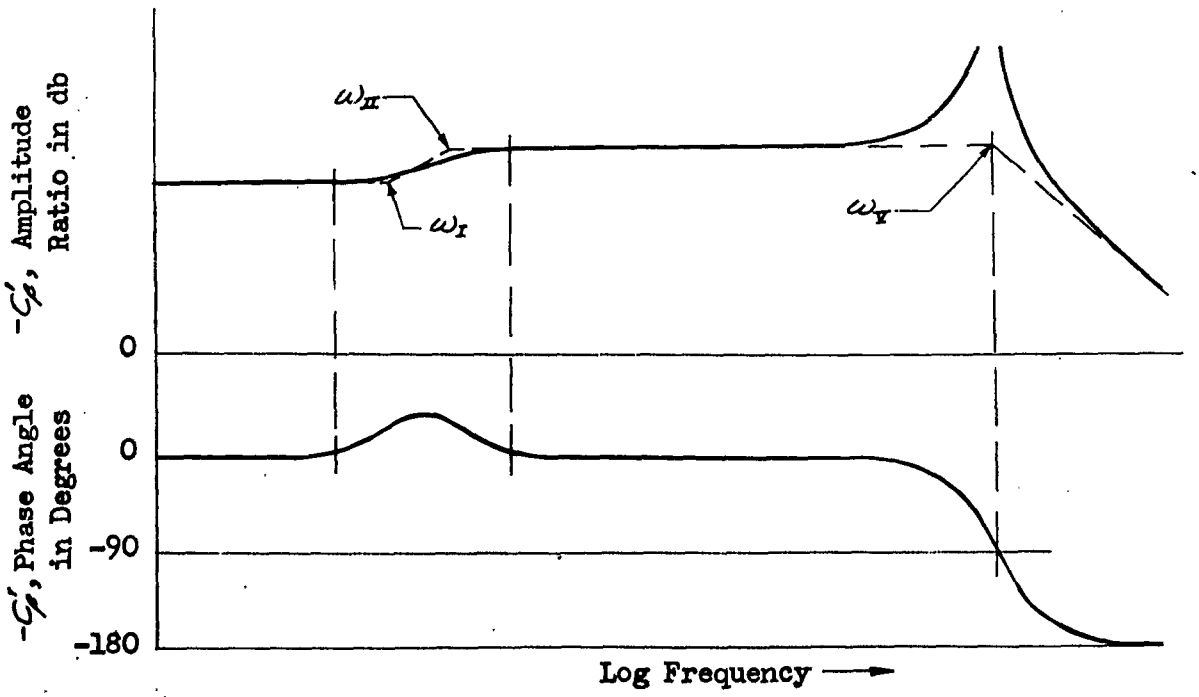

Figure IX-2. Frequency Response of Corrective Term $-C'_\beta$

Figure IX-2 shows a generic frequency response of the corrective term $-C_{\beta}'$. This quantity acts to alter the effective rotational stiffness of the control surface from $C_{\beta} = (\ell^2/d)k_c$, which would be the stiffness if the actuator cylinder did not move under load. The actual stiffness at any given frequency is the complex quantity obtained by adding C_{β} and C_{β}'. It should be noted that the servo action is effective at zero frequency, in which case $C_{\beta}' = -(\ell^2/d)(k_c^2/k_c + k_f)$ The dynamics in Figure IX-2 are limited to a very low frequency range and a very high frequency range. For the simple case used as an example, thereis a broad intermediate region where there is no phase correction. This is the range of usual interest in flutter. However, the correction is not as simple with more complicated actuators.

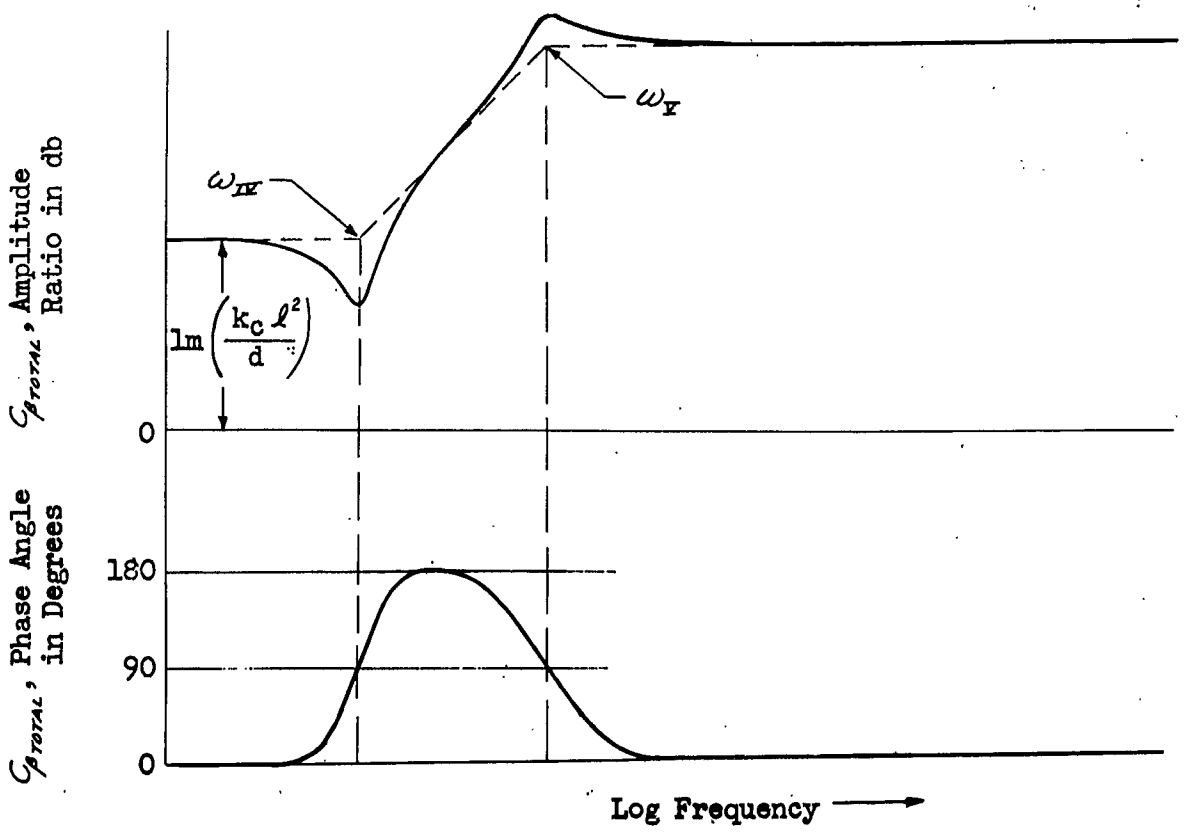

Figure IX-3. Typical Frequency Response of Total Complex Spring $C_{\beta_{TOTAL}}$

In Figure IX-3 it is assumed that ω_{II} and ω_{III} are practically equivalent; i.e., $(1/k_f)=(1/k_o)+(1/k_p)$. This is true if the oil spring k_o is sufficiently high or the flow spring k_f is sufficiently low. The figure graphically demonstrates the fact that when the two frequencies ω_{II} and ω_{I} approach coincidence (which is the case for $k_o >> k_c$), the complex spring becomes for all frequencies a pure spring, its value being very nearly that of the coupling spring $C_\beta = (\ell^2/d)\,k_c$. Although the plot shows the value of the complex spring at zero frequency to be $C_\beta = (\ell^2/d)\,k_c$, this is not precisely true. If will be noted that the complete analytical expression for the complex stiffness at zero frequency is

$$C_{\beta TOTAL}\,|_{\omega \to 0} = \frac{\ell^2}{d}\,\frac{k_c k_f}{(k_c + k_f)} \qquad \text{(IX-18)}$$

Then at sufficiently low frequencies, i.e., those approaching static or steady-state load conditions $C_{\beta TOTAL}$ becomes a pure spring formed by the series linkage of the coupling spring $(\ell^2/d)k_c$ and the effective hydraulic servo spring $(\ell^2/d)k_f$. The approximate relationship $C_{\beta TOTAL}|_{\omega \to 0} \approx (\ell^2/d)\,k_c$ holds true if $k_f >> k_c$, which is the case for a very high gain, closed-center hydraulic servo.

The range of frequencies higher than the frequency peak indicated by ω_I on Figure IX-3 may also be examined. The exact value of $C_{\beta\,TOTAL}$ in this range cannot be obtained in general terms. However, numerical calculations for typical systems have substantiated the physical reasoning that the equivalent spring is essentially the series spring combination that would be obtained if the hydraulic system were viewed as a passive network. In other words, at sufficiently high frequencies the servo action of the system is greatly suppressed, and the effective spring at frequencies above ω_I is

$$C_{\beta TOTAL}\,|_{\omega >> \omega_I} = \frac{\ell^2}{d}\left(\frac{k_c k_o k_p}{k_c k_o + k_c k_p + k_o k_p}\right)$$

It should be emphasized that normal static tests (e.g., loading the surface and measuring its deflections) will not provide a satisfactory means for obtaining the above spring constant.

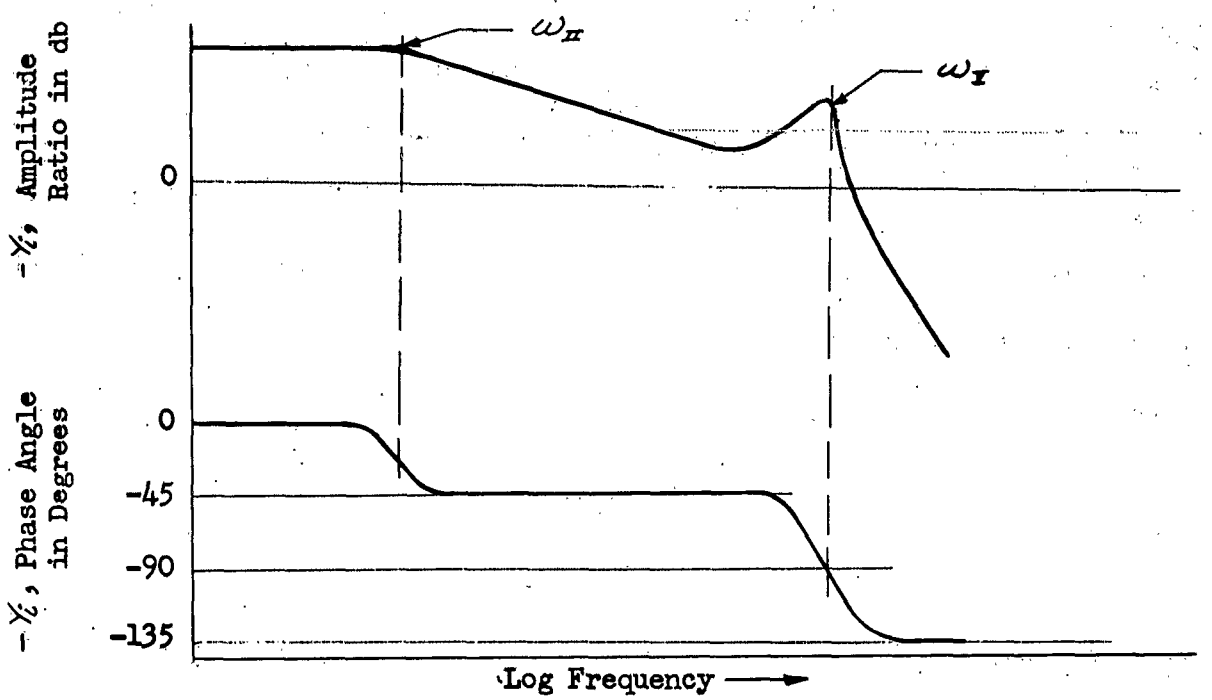

Figure IX-4. Frequency Response of $-\gamma_i$

The typical frequency response of $-\gamma_i$ is shown in Figure IX-4. The moment compenent $\gamma_i \alpha_i$ (see IX-14 and IX-5) due to an actuator input requires additional consideration. The transfer function γ_i cannot be classified as a complex spring in the same sense as $C_{\beta\ TOTAL}$, even though it has the dimensions of a spring. The servo input must first be known as a function of α, β, or h before the complex stiffness concept can be extended to include γ_i.

The expressions (IX-15), (IX-16), and (IX-17) were obtained by consideration of a very simple type of hydraulic actuator. Many hydraulic servos fit into the pattern of Figure III-5, and the results of Chapters III and IV are available for use in investigation of more complicated cases.

The validity of the linear analysis in the high frequency region near ω_α and ω_x in Figures IX-3, IX-4, and IX-5 is to be questioned, and if unusually high flutter frequencies are encountered a purely analytical study of the modified flutter system is probably useless. The linear analysis fails at high frequency because of the increased importance of distribution of mass and damping.

The discussion concerning the incorporation of hydraulic system data in flutter calculation can be summarized as follows:

1. Both general and approximate relationships have been presented as transfer functions, or portions thereof, which relate surface dynamics, hydraulic servo dynamics, coupling moments due to $\ddot{\alpha}$ and $\ddot{h}$, and the total aerodynamic moment on the surface.
2. A complex spring stiffness concept has also been developed, thus providing a convenient means for analytical or graphical inclusion in the normal flutter solution techniques.
3. The reductions of the complex stiffness term and the moment-input transfer function to effectively pure springs in certain frequency regimes have been presented merely to give the reader a keener physical insight into the servo-flutter problem. The frequency variant expressions must be employed in the usual analysis.

SECTION 4 - STABILITY AUGMENTER SYSTEMS

A stability augmenter may be defined as a device which augments or creates desirable airplane stability characteristics by applying proper control surface motions and hence proper stabilizing forces and moments to the aircraft. Examples of physical stability augmenters are the pilot-artificial feel-airframe

system, yaw damper systems, sideslip stability augmenter system, and automatic pilots.

For a stability augmenter to function in the desired way, i.e., to control a "controlled element," several distinct elements are required.

The first is the "controlled element," which in this instance will always be the airframe. The controlled element is characterized by inputs to obtain control (via control deflections) and outputs generated by the input (such as changes in speed, angle of attack, and rate of pitch). Since the controlled element portion of a stability augmenter does not figure prominently at this point of the discussion, it will not receive detailed treatment here.

The second element required in a stability augmenter is a device to supply a surface rotation. This is usually a positional servomechanism, either driving the surface directly or, more commonly at present, driving the input member of a surface actuating servomechanism. The latter element is discussed in Section 3.

The third important element required in a stability augmenter is the sensor. This is a device capable of detecting a particular motion of the controlled element and of transmitting a signal proportional to this motion. The sensors which are important in flight control system work and which may also be important in the modified flutter problem are:

1. Rate gyros
2. Accelerometer or force pick-ups
3. Stabilized gyros

The characteristics of these elements are summarized in later portions of this section.

The fourth important element in a stability augmenter is the equalization. Equalization includes all the means required (including physical connections)

to modify the performance of any of the system elements and of the over-all system to achieve satisfactory system operation. This definition is rather general, but, from a dynamic standpoint at least, equalization in stability augmenters usually takes the form of a rate circuit and an amplification. This element will also be discussed in this section.

With the four prime elements of a stability augmenter defined, it is possible to establish a fairly general pictorial representation of a stability augmenter system.

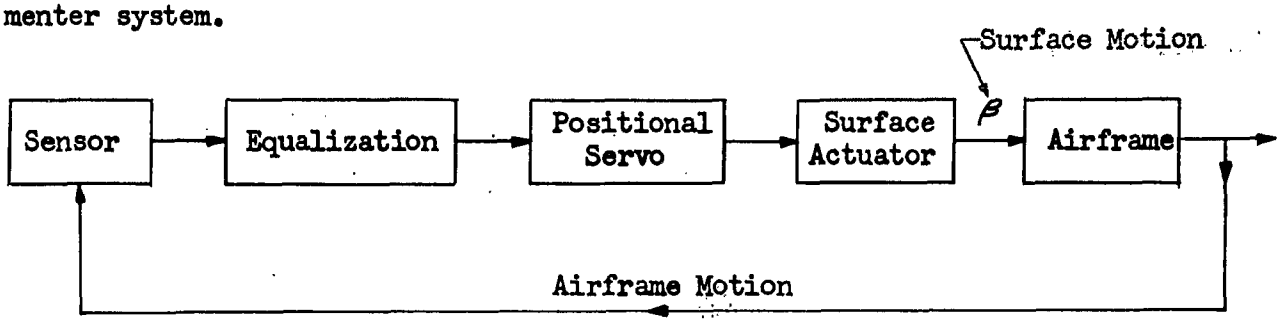

Figure IX-5. Block Diagram of a General Stability Augmenter

From the standpoint of modifying classical flutter analysis, the presence of the stability augmenter creates the possibility that the sensor may pick up some function of a flutter motion α, β, or h in addition to the "rigid" airframe motion it is expected to sense. In these instances, the flutter motion signal can result in motion of the surface, thereby creating the coupling of the second type mentioned in Section 2(b).

With this information on stability augmenters as a background, it can now be stated that the purpose of this section is to consider in detail the mathematical model of that portion of the stability augmenter system from sensor input to positional servo output. These input-output relationships will be developed in terms of the transfer functions of each block, with the end result being expressions containing positional servo output motions and sensor inputs.

(a) SENSORS

. RATE GYROS

A rate gyro is a gyroscopic element restrained to move in only one degree of freedom. If the wheel is spinning at an angular velocity ω_y and has a moment of inertia about the spin axis, I_y ; an angular velocity Ω_x about the x axis results in a precessing torque about the z axis as shown in Figure IX-6. This torque is given by the equation:

(IX-19) $$L_z = I_y \omega_y \Omega_x$$

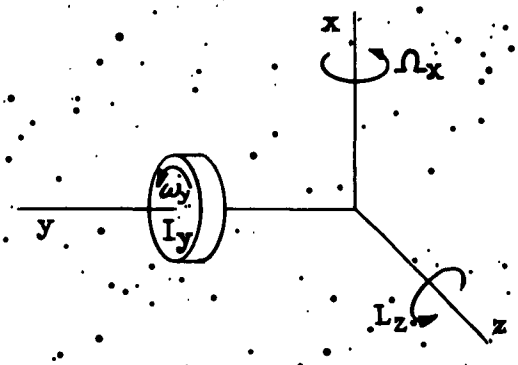

Figure IX-6. Rate Gyro Relationships

For small precession angles, where the gyro is restrained about the z axis with a spring and with coulomb and viscous dampers,

(IX-20) $$L_z = (I_y \omega_y)\Omega_x = I_z \ddot{\theta} + B_z \dot{\theta} + k_z \theta + T_g \, SGN \, \dot{\theta}$$

The symbol θ is not to be confused with the θ used in later portions of this report as an airframe angular rotation.

The gyro then has a transfer function

(IX-21) $$\frac{\theta}{\Omega_x} = \frac{\left(\frac{I_y \omega_y}{k_z}\right)}{\left(\frac{s^2}{\omega_{ng}^2} + \frac{2\zeta_g}{\omega_{ng}} s + 1\right)}$$

where

$$\omega_{n_g} = \sqrt{\frac{k_z}{I_z}}$$

and

$$\zeta_g = \frac{B_z}{2\omega_{n_g} I_z}$$

If some sort of pickoff is then attached to give a linear electrical output signal, V_g, for a given precession angle θ,

$$\frac{V_g}{\Omega_x} = \frac{\left(\frac{k_g}{k_z}\right)(I_y \omega_y)}{\left(\frac{s^2}{\omega_{n_g}^2} + \frac{2\zeta_g}{\omega_{n_g}} s + 1\right)} \qquad \text{(IX-22)}$$

It will be noted that a minimum detectable input angular rate due to the gyro construction itself exists, and is given by

$$\Omega_{x_{MIN.}} = \frac{T_g}{I_y \omega_y} \qquad \text{(IX-23)}$$

Resolution of potentiometers or thresholds of other types of pickoffs must be added to this minimum signal to obtain the total minimum detectable signal.

Since a rate gyro gives an output proportional in the steady state to angular rates, the airframe motions roll rate, p, pitch rate, q, and yaw rate, r, can be directly measured by properly mounted rate gyros.

It must be mentioned at this point that considerable portions of the effective angular velocity presented to the rate gyro could conceivably be due to an elastic motion of the airframe itself in creating local angular velocities different from those of the "rigid airframe." This possibility is usually minimized by proper mounting of a rate gyro. It is obvious that the location of the airplane and also the frequency of any disturbing influences are of the

utmost importance in considering any modification to flutter analysis. This same conclusion is valid for the remaining stability augmenter sensors considered. It should also be noted that a certain minimum amount of feedback is required to actuate the sensor.

ACCELEROMETERS OR FORCE PICKUPS

Because most sensing elements used in aircraft stability work require an unbalanced force or moment to change some motion or other quantity of the sensing mechanism, they are in reality force or moment pickups. However, the unbalanced force on an object may be a function of a velocity or displacement, etc., or may be made proportional to a displacement or velocity, etc., over some frequency range. As an example, consider the simple second order system shown schematically in Figure IX-7. (Since most accelerometers have equivalent network diagrams, this diagram will suffice for all the accelerometers considered here.)

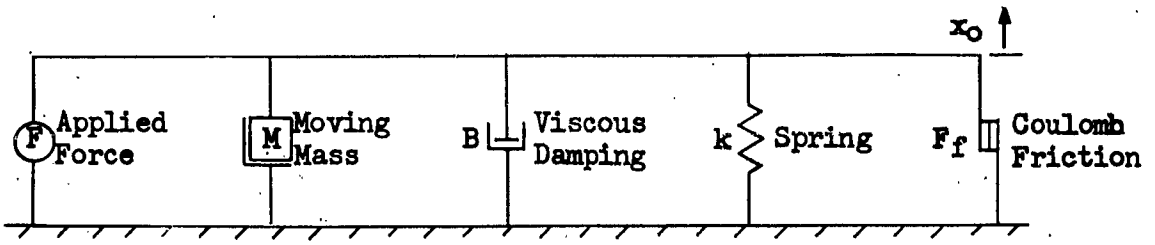

Figure IX-7. Network Diagram of Accelerometer

The mechanical system shown has the equation:

$$F = M\ddot{x}_o + B\dot{x}_o + kx_o + F_f \, SGN \, \dot{x}_o \tag{IX-24}$$

or

$$\frac{F}{M} = \ddot{x}_o + 2\zeta_a \omega_{n_a} \dot{x}_o + \omega_{n_a}^2 x_o + \frac{F_f}{M} SGN \, \dot{x}_o \tag{IX-25}$$

;

$$\zeta_a = \frac{B}{2\omega_{n_a} M} \quad ; \quad \omega_{n_a}^2 = \frac{k}{M}$$

giving a transfer function when $F_f = 0$,

$$\text{(IX-26)} \qquad \frac{x_o}{F} = \frac{1}{K\left(\frac{s^2}{\omega_{n_a}^2} + \frac{2\zeta_a}{\omega_{n_a}} s + 1\right)}$$

At various forcing frequencies, the system acts as follows:

$$\text{(a)}\ \omega >> \omega_{n_a} : \frac{x_o}{F/-\omega^2} \approx \frac{\omega_{n_a}^2}{K}$$

$$\text{(IX-27)}\ \text{(b)}\ \omega \approx \omega_{n_a} : \frac{x_o}{F/j\omega} \approx \frac{\omega_{n_a}}{2\zeta_a K}$$

$$\text{(c)}\ \omega << \omega_{n_a} : \frac{x_o}{F} \approx \frac{1}{K}$$

It is clear from (IX-27) that the displacement x_o is a measure of displacement, velocity, and acceleration; that is, for

$\omega >> \omega_{n_a}$, the system is a displacement pickup.

$\omega \approx \omega_{n_a}$, the system is a velocity pickup.

$\omega << \omega_{n_a}$, the system is an acceleration pickup.

Since the primary concern at present relates to the use of an accelerometer, it is evident that the approximation of (IX-27c) will be of most concern; that is, the natural frequency should be higher than frequencies of interest in the system.

With a suitable pickup for the motion of the mass, the accelerometer transfer function becomes:

$$\text{(IX-28)} \qquad \frac{V_a}{a_i} = \frac{K_a}{\omega_{n_a}^2\left(\frac{s^2}{\omega_{n_a}^2} + \frac{2\zeta_a}{\omega_{n_a}} s + 1\right)}$$

where V_a is the accelerometer output signal and a_i is the input acceleration.

The minimum detectable acceleration is given by:

$$\text{(IX-29)} \qquad \left.\frac{F}{M}\right|_{MIN.} = \frac{F_f}{M} = a_{i\,MIN.}$$

To this minimum detectable value must be added the resolution or threshold of the pickup.

Here again, the sensor is capable of picking up only the local input, which can easily be a function of a flutter motion.

STABILIZED GYROS

Stabilized gyros, as normally used in aircraft controllers, establish reference planes fixed in inertial space. In the case of a vertical gyro, this is achieved by utilizing the gyro-torqueing system as an extremely low natural frequency filter for a vertical sensor (basically a two degree of freedom pendulum or accelerometer). Gyro-torqueing is employed as a similar filter for a magnetic field (or other reference) detector in the case of a directional gyro. From a vertical-direction gyro system, the airplane roll, pitch, and yaw angles can be measured directly when airframe displacements from essentially straight and level flight occur.

For all practical purposes, a properly designed gyro system has a constant for a transfer function for fairly low airframe speeds:

$$\text{(IX-30)} \qquad \frac{V_{GYRO}}{\phi,\ \psi,\ \text{OR}\ \theta} = K_g$$

As mentioned above, the vertical gyro is actually nothing more than a filter for a pendulum, mercury switch, or other force detector, and since phugoid periods in seconds are about one-fifth the airspeed in mph, the dynamics of

the gyro-erecting system may become important. Therefore, for this case,

$$(IX\text{-}31) \qquad \frac{V_{GYRO}}{a_{z\,TOTAL}} = \frac{K_g\left(\frac{1}{\omega_{ngy}^2}\right)}{\frac{s^2}{\omega_{ngy}^2} + \frac{2\zeta_{gy}}{\omega_{ngy}}s + 1}$$

or

$$(IX\text{-}32) \qquad \frac{V_{GYRO}}{\theta, \phi} = \frac{K_g'\left(\frac{s^2}{\omega_{ngy}^2}\right)}{\frac{s^2}{\omega_{ngy}^2} + \frac{2\zeta_{gy}}{\omega_{ngy}}s + 1}$$

Some instances of possible gyro-erection system coupling with the phugoid are already on record for high speed aircraft exhibiting phugoid periods of the order of 120 seconds. For all flutter modification considerations, however, the transfer function is a constant.

As discussed above, stabilized gyros normally measure roll, pitch, and yaw angles. These angles are always the local angles at the gyro mounting, and hence the non-rigid airplane motions could affect the output of the gyro. Mounting is, again, all important as a detail consideration.

(b) POSITIONAL SERVO SYSTEMS

Two types of positional servo systems are important in stability augmenting systems. These are the electrohydraulic and the electromechanical. The electrohydraulic servo system utilizes an electrical input signal in conjunction with torque motors or hydraulic amplification or both to position a hydraulic valve. The hydraulic valve meters flow to a cylinder or to a rotary hydraulic motor. An electrical follow-up unit is added to provide feedback. The device operates in a fashion similar to the fully-powered surface actuator discussed in Chapter

V and has a transfer function from input signal to output motion which is very similar to the low frequency approximation of the fully-powered surface actuator:

$$\text{(IX-33)} \qquad \frac{x_o}{x_i} = \frac{K_{PS}}{T_h s + 1}$$

The second type is the conventional electric motor with follow-up. As is well known, this type of system is approximated by:

$$\text{(IX-34)} \qquad \frac{x_o}{x_i} = \frac{K_{PS}}{\frac{s^2}{\omega_{PS}^2} + \frac{2\zeta_{PS}}{\omega_{PS}} s + 1}$$

(c) EQUALIZATION

The equalization normally required in any stability augmenter, even in the most complex case, is usually derived from an electrical or mechanical rate circuit and amplification. The transfer function of such a device is given by:

$$\text{(IX-35)} \qquad \frac{x_i}{V} = K_a \frac{T_1 s + 1}{T_2 s + 1}$$

(d) THE SENSOR-EQUALIZATION-POSITIONAL SERVO COMBINATION

Combining the characteristics of the sensor, equalization, and positional servo of a stability augmenting system gives a total open loop transfer function of the form:

$$\text{(IX-36)} \qquad \frac{x_o}{\Omega, a_i \text{ or } \theta} = \underbrace{\left\{ \left[K_{SENSOR} \right] \text{ or } \left[\frac{K_{SENSOR}}{\frac{s^2}{\omega_{SENSOR}^2} + \frac{2\zeta_{SENSOR}}{\omega_{SENSOR}} s + 1} \right] \right\}}_{\text{SENSOR}} \cdot \underbrace{\left[\frac{K_a (T_1 s + 1)}{(T_2 s + 1)} \right]}_{\text{EQUALIZATION}} \cdot \underbrace{\left\{ \left[\frac{K_{ELEC.}}{\frac{s^2}{\omega_{SERVO}^2} + \frac{2\zeta_{SERVO}}{\omega_{SERVO}} s + 1} \right] \text{ or } \left[\frac{K_{HYD}}{T_{SERVO} s + 1} \right] \right\}}_{\text{POSITION SERVO}}$$

If $j\omega$ is substituted for s, the transfer function becomes a frequency response. The entire transfer function can then be changed into a real and an imaginary part:

$$\text{(IX-37)} \qquad \frac{x_o}{\Omega \text{ , } a_i \text{ OR } \Theta}(\omega) = R_{AUGMENTER} + jI_{AUGMENTER} = \sqrt{R^2 + I^2}\, e^{j\tan^{-1}\frac{I}{R}}$$

In servo work, the "amplitude ratio," $(R^2 + I^2)^{\frac{1}{2}}$, is usually converted into decibels for plotting purposes by taking $20\log_{10}(R^2 + I^2)^{\frac{1}{2}}$. The phase, $\tan^{-1} I/R$, is used directly. The plot of typical cases of (IX-37) would look like Figure IX-8. The real and imaginary parts, R and I, can be easily obtained from such a Bode plot.

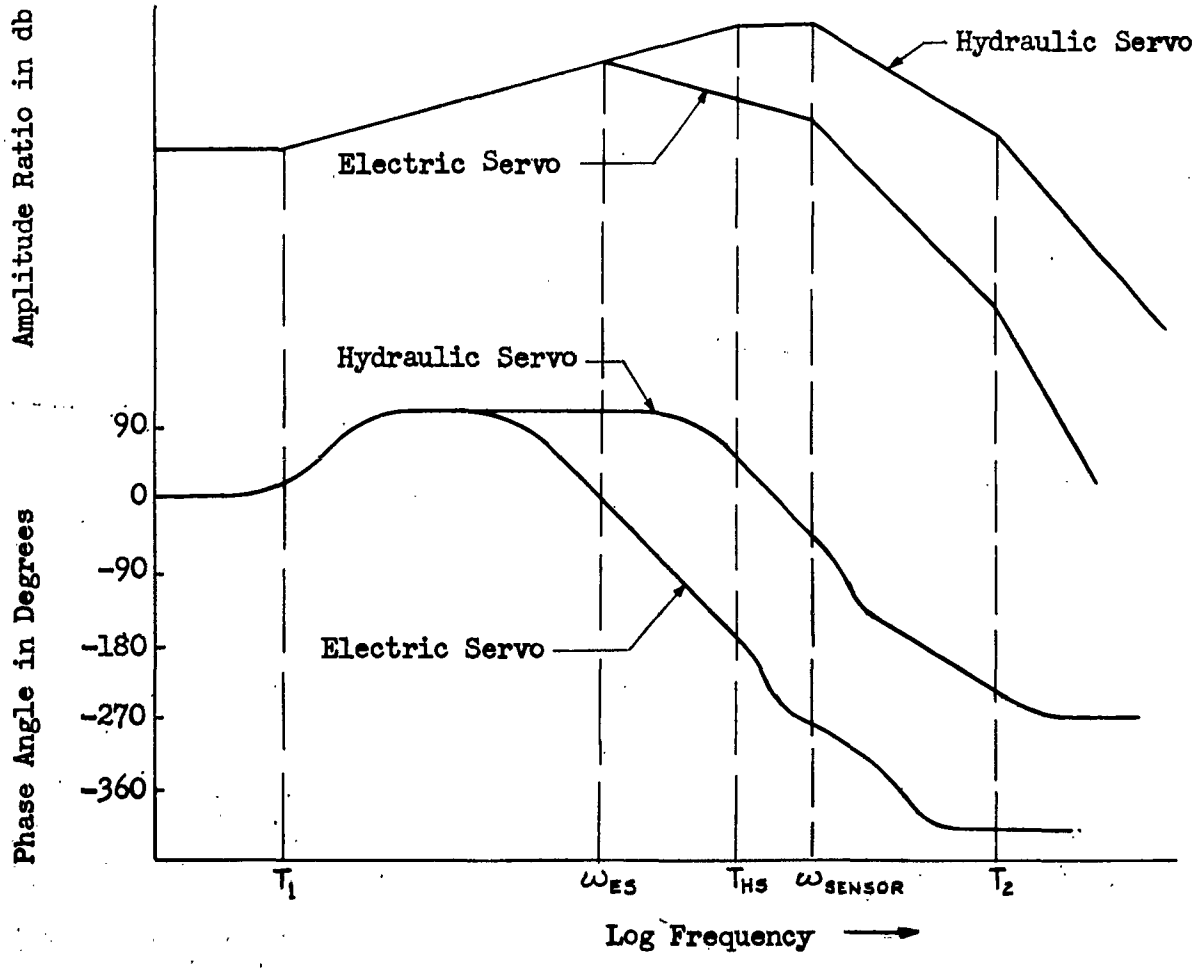

Figure IX-8. Frequency Response of Sensor-Equalization-Positional Servo Combination

SECTION 5 - UNBALANCED CONTROL SYSTEM INERTIAS AND CABLE SYSTEMS

The control systems of missiles and airplanes (particularly piloted aircraft) contain certain masses or inertias which are subject to forces as a result of accelerations. These forces usually arise from the rigid body dynamics of the airframe, say, in the longitudinal case, the short period oscillations of the airplane. A bobweight installed as a part of an artificial feel device is usually the most effective element for producing surface actuator input signals via a flexible cable system. The stick assembly inertia is another important element in the control system. In any event, the combination of rigid-body acceleration sensitive masses, system frictions, and cable or feel system flexibilities may be lumped together into a single second order system,

$$\text{(IX-38)} \qquad \frac{x_i}{n} = \frac{K_B \frac{M_B}{k}}{\left(\frac{-\omega^2}{\omega_T^2} + 1 + j2\zeta_T \frac{\omega}{\omega_T}\right)}$$

where

x_i is the surface actuator servo input displacement.

n is the local normal acceleration.

M_B is the unbalanced mass subject to the acceleration.

K_B is the mechanical advantage between the unbalanced mass displacement and the servo input displacement.

k is the effective centering spring for the unbalanced mass.

ζ_T is the effective system damping ratio.

$\omega_T = (k/M_T)^{\frac{1}{2}}$, where M_T is the total effective mass of the control system.

Another case where a surface actuator input can occur via a control system element is when rotation of the surface bends or twists the fuselage, stretching one portion of the cable system more than another. The transfer function relating the surface rotation β and the resultant displacement of some portion of

the cable system will be discussed later.

The particular transfer function characteristics under consideration at this point are those caused by cable system dynamics when excited by a local cable input x_i' . A functional relationship may be developed between the displacement x_i' and the displacement of the mass or inertia center, x_T , of the complete control (cable) system. This transfer function also may be represented as a second order expression:

$$(IX\text{-}39) \qquad \frac{x_i'}{x_T} = \frac{K}{\left(\frac{(-\omega)^2}{\omega_T^2} + 1 + j2\zeta_T\frac{\omega}{\omega_T}\right)}$$

Since a mechanical advantage K_i usually exists between the cable system and the surface actuator input point, the final desired transfer function is:

$$(IX\text{-}40) \qquad \frac{x_i}{x_T} = \frac{K_i}{\left(\frac{(-\omega)^2}{\omega_T^2} + 1 + j2\zeta_T\frac{\omega}{\omega_T}\right)}$$

SECTION 6 - FEEDBACK OF A FLUTTER MOTION TO A STABILITY AUGMENTER SENSOR, BOBWEIGHT, ETC.

The previous discussion of stability augmenters, bobweights, etc., has treated one phase of description of possible flutter couplings due to a flutter motion detected by a sensor and actuating the surface. Before anything definite can be said about these couplings, the possibility that sensors might pick up some function of the flutter motion must be explored. As previously pointed out, the analytical formulation of this link is dependent almost entirely upon the installation of the sensor in the airframe, and upon the flutter motion transmitting characteristics of the elastic airframe. Therefore, this section cannot take all possible couplings into account. The possibility that any one

feedback may occur must be a subject for individual study on each aircraft considered, but in many cases, proper sensor mounting could obviate the necessity of considering some of these links. (Proper sensor mounting would be defined, for this consideration, as the process of placing a sensor where it picks up only those quantities desired for the particular device).

The quantities required are expressions for sensor input in terms of flutter motions, i.e.,

$$\text{(IX-41)} \qquad \frac{\Omega\,,\ a_i\,,\ \theta}{\beta\,,\ \alpha\,,\ h} = R_f + jI_f$$

This expression can then be combined with the transfer characteristics of the stability augmenter to form a complex number representation of the particular coupling:

$$\text{(IX-42)} \qquad (R_f + jI_f)(R_a + jI_a) = R + jI$$

The result can then be examined by the methods outlined in Section 7 of this chapter to determine whether a particular coupling is important.

(a) COUPLING WITH SURFACE ROTATION

All stability augmenters are coupled with surface rotation through the "rigid" body motions of the airframe. The airframe transfer functions for such cases are very well known* and need only be repeated here. Normally, the frequency response of the augmenter-airframe combination is concentrated in such a low frequency region that the effect on all but the lowest frequency flutter is negligible.

Of more direct concern at present, is the coupling of the surface rotation and the "elastic" motions of the airframe through the stability augmenter.

* See, for example, "Aircraft Controller Design," Northrop Report SMD-31A, Northrop Aircraft, Inc., Hawthorne, California, October, 1952.

For example, consider the case where an elevator rotation, by increasing the horizontal tail load, bends the fuselage of the aircraft. This phenomenon can easily move one portion of a cable system, produce a local component of effective angular velocity sensed by a rate gyro, create a load force on an accelerometer, or cause other similar effects. Any of these effects can ultimately result in input signals to the surface actuator system and thereby affect surface motion. The transfer characteristic would have a first approximation as a second order system, with the natural frequency being that of the first fuselage bending mode.* In any situation where fuselage bending is an important mode, the possibility of such a coupling should not be overlooked.

Summarizing the transfer functions of importance:

1. "Rigid Body" Airframe (Longitudinal Axis only)

$$\text{(IX-43)} \qquad \frac{n}{\beta} = \frac{K_{n_\beta}(j\omega)\left[T_{n_1}(j\omega)+1\right]\left[T_{n_2}(j\omega)+1\right]\left[-T_{n_3}(j\omega)+1\right]}{\left(\frac{-\omega^2}{\omega_p^2}+\frac{2\zeta_p}{\omega_p}(j\omega)+1\right)\left(\frac{-\omega^2}{\omega_{sp}^2}+\frac{2\zeta_{sp}}{\omega_{sp}}(j\omega)+1\right)}$$

$$\text{(IX-44)} \qquad \frac{\theta}{\beta} \text{ or } \frac{q/s}{\beta} = \frac{K_{\theta_\beta}\left[T_{\theta_1}(j\omega)+1\right]\left[T_{\theta_2}(j\omega)+1\right]}{\left(\frac{-\omega^2}{\omega_p^2}+\frac{2\zeta_p}{\omega_p}(j\omega)+1\right)\left(\frac{-\omega^2}{\omega_{sp}^2}+\frac{2\zeta_{sp}}{\omega_{sp}}(j\omega)+1\right)}$$

2. Elastic Airframe (Fuselage Bending)

$$\text{(IX-45)} \qquad \frac{\frac{n}{g^2} \text{ OR } \frac{q}{g} \text{ OR } \theta}{\beta} = \frac{K_{FB}}{\left(\frac{-\omega^2}{\omega_{FB}^2}+\frac{2\zeta_{FB}}{\omega_{FB}}(j\omega)+1\right)}$$

* The basic assumption here is that the aerodynamic forces are of a quasi-steady nature; i.e., they are not functions of $b\omega/v$ as such.

where K_{FB} is the static amount either of upward displacement (in the case of the accelerometer or bobweight) or angular displacement (in the case of the rate gyro or vertical gyro), etc., per unit of surface rotation.

(b) COUPLING WITH TORSION

A change in the twist, α, of a tail surface causes a change in the local angle of attack and hence in pitching moment and tail load. The tail load change is nearly instantaneous, and consequently fuselage bending effects analogous to those considered above are possible. The tail load and moment change can also excite the sensors through the airplane rigid body motions which, of course, are of fairly low frequency.

(c) COUPLING WITH BENDING

An excellent example of possible bending coupling is given in the case of an elevon controlled airplane with a normal force stability augmenter. The first wing bending mode can be of very low frequency (particularly with pods or stores), and is almost invariably picked up by the normal accelerometer or bobweight. The transfer characteristic is again approximated by a second order system, with the natural frequency in this case given by that of the first wing bending mode. This type of coupling could be quite serious in cases of elevon flutter.

Another example is that of asymmetrical bending of a horizontal stabilizer giving rise to fuselage torsion, which is picked up by either a roll rate or roll gyro. In some cases this coupling is probably not serious, especially where torsional frequencies are very high, and the sensor will usually be used to control the ailerons. However, the downwash is changed by aileron rotation, so a very complex coupling of asymmetrical bending-roll gyro-aileron-downwash-stabilizer could conceivably occur.

No summary of possible bending-sensor transfer functions will be given here, since the form depends very intimately upon the actual configuration.

SECTION 7 - TYPICAL FLUTTER SYSTEM MODIFYING TERMS

In this section, the previously developed component characteristics are combined into the total flutter-servo system modifying terms for a typical case.

For illustrative purposes, assume that the total system is composed of:

1. The conventional flutter system.
2. A pitch rate stability augmenter using an electrical servo and no equalization other than a gain.
3. A fully-powered hydraulic surface actuator.

In addition, assume that the only feedbacks are:

1. A rigid body feedback due to β.
2. An elastic feedback due to fuselage bending caused by β.
3. A rigid body feedback due to α.
4. An elastic feedback due to fuselage bending caused by α.

Physically, α and β produce airloads on the parent surface and on the control surface respectively. These loads cause the airframe to execute rigid body oscillations and fuselage bending, both of which are detected and transmitted by the pitch rate sensor.

The airframe augmenter system under discussion can be represented as shown in Figure IX-9. The block labeled "airframe" will be different depending on whether the pitch rate is caused by α or β and whether the mode of motion under consideration is a rigid body mode or a fuselage bending mode.

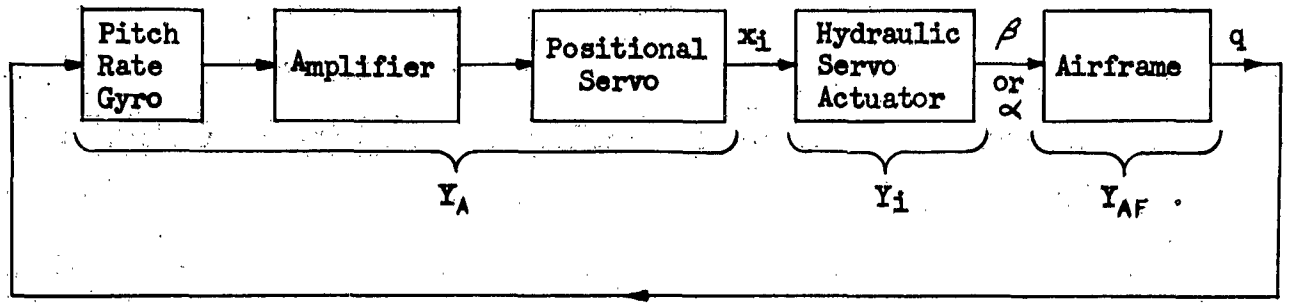

Figure IX-9. Block Diagram of a Typical Stability Augmenter

For the case where the rigid body feedback is due to β, the modifying term has the form:

(IX-46) $$Y_i Y_{\beta_1} = Y_i Y_A Y_{AF}$$

(IX-47) $$Y_i Y_{\beta_1} = \frac{K_{HYD}}{(T_{HYD}s+1)} \frac{K_{RG}}{\left(\frac{s^2}{\omega_{n_{RG}}^2} + \frac{2\zeta_{RG}}{\omega_{n_{RG}}}s + 1\right)} \frac{K_{SERVO}}{\left(\frac{s^2}{\omega_{SERVO}^2} + \frac{2\zeta_{SERVO}}{\omega_{SERVO}}s + 1\right)}$$
$$\frac{K_{\theta\beta}(T_{\theta_1}s+1)(T_{\theta_2}s+1)s}{\left(\frac{s^2}{\omega_p^2} + \frac{2\zeta_p}{\omega_p}s + 1\right)\left(\frac{s^2}{\omega_{sp}^2} + \frac{2\zeta_{sp}}{\omega_{sp}}s + 1\right)}$$

By substituting $j\omega$ for s, (IX-47) becomes a frequency response, and can be represented as:

(IX-48) $$Y_i(\omega) Y_{\beta_1}(\omega) = R(\omega) + jI(\omega)$$

A Bode plot of (IX-47) is shown in Figure IX-10.

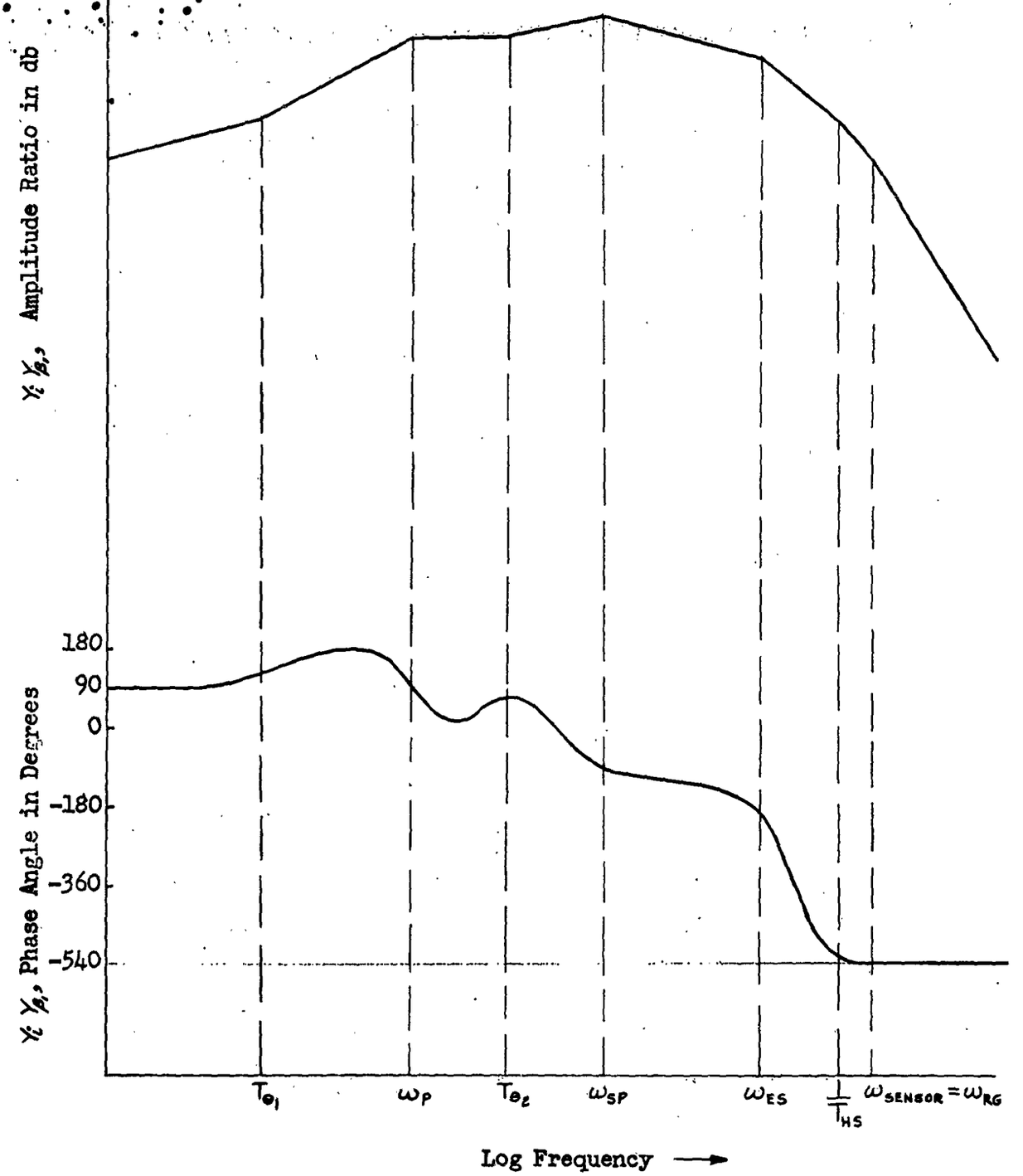

Figure IX-10. Frequency Response of Modifying Term $Y_i Y_{\beta_1}$

At frequencies of concern in flutter analysis, the phugoid is not important. The rigid body feedback representation can then be approximated by Figure IX-11.

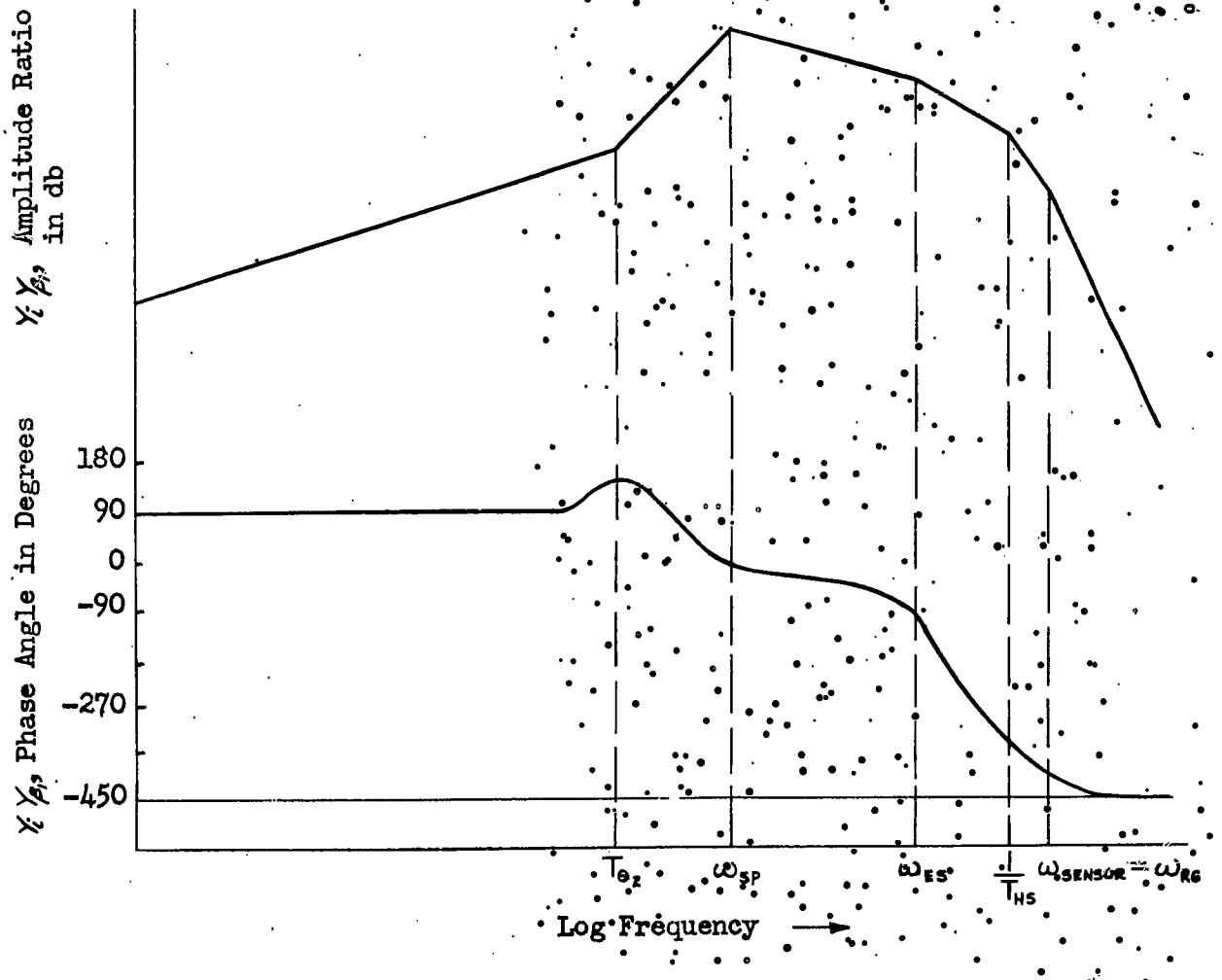

Figure IX-11. Simplified Frequency Response of Modifying Term $Y_i Y_{\beta_1}$

For the case of the fuselage bending feedback due to β, the airframe portion of (IX-47) can be replaced by the fuselage bending transfer function. Thus:

$$(IX\text{-}49) \qquad Y_i Y_{\beta_2} = \frac{K_{HYD}}{(T_{HYD}\, s + 1)} K_A \frac{K_{RG}}{\left(\frac{s^2}{\omega_{RG}^2} + \frac{2\zeta_{RG}}{\omega_{RG}} s + 1\right)} \cdot \frac{K_{SERVO}}{\left(\frac{s^2}{\omega_{SERVO}^2} + \frac{2\zeta_{SERVO}}{\omega_{SERVO}} s + 1\right)} \cdot \frac{s \cdot K_{FB}}{\left(\frac{s^2}{\omega_{FB}^2} + \frac{2\zeta_{FB}}{\omega_{FB}} s + 1\right)}$$

As in the previous case, the substitution of $j\omega$ for s allows the transfer function to be separated into its real and imaginary parts. A Bode plot of (IX-49) is shown in Figure IX-12.

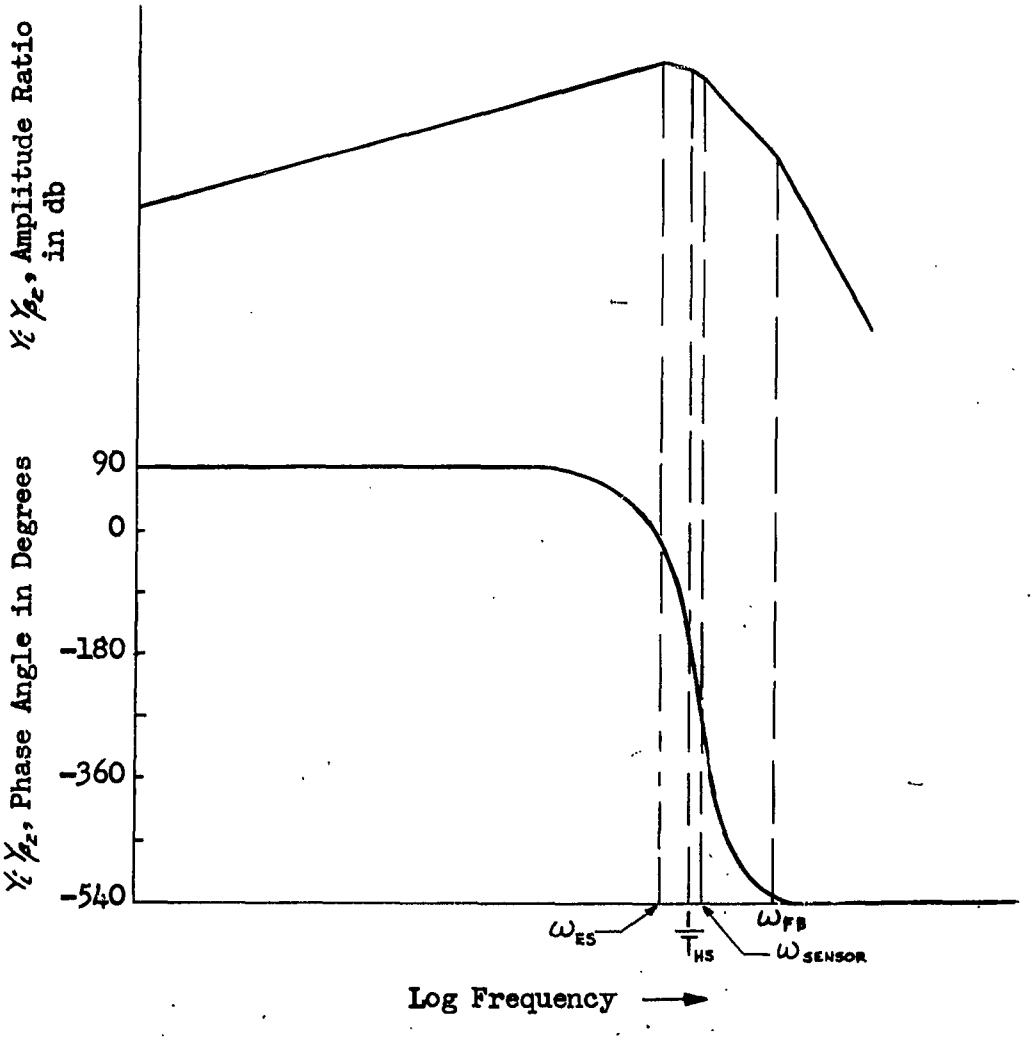

Figure IX-12. Frequency Response of Modifying Term $Y_i Y_{\beta_2}$

The Bode plots shown in Figures IX-11 and IX-12 are complete except for the zero db line which establishes the system gain. The over-all system gain is a direct function of the gain of each of the component transfer functions.

These gains are of course functions of the dynamical characteristics of the particular system being investigated. In the general case, the gain can only be approximated.

In the typical case under consideration in this section, the Bode plots for the rigid body feedbacks due to α and β differ only by the location of the zero db line; that is, the motion caused by a given deflection of either the parent surface or the control surface will be the same except for the amplitude. This is also true for the case of the fuselage bending feedback. Thus $Y_i(\omega)Y_{\beta_1}(\omega)$, $Y_i(\omega)Y_{\alpha_1}(\omega)$, $Y_i(\omega)Y_{\beta_2}(\omega)$, and $Y_i(\omega)Y_{\alpha_2}(\omega)$ can be evaluated for a particular frequency from Figures IX-11 and IX-12 with the appropriate zero db lines. Once the real and imaginary parts of these terms have been determined, they can be included in (IX-9). The magnitude of these modifying terms compared to the classical flutter terms determines the influence of the stability augmenter system on the flutter system.

The generic forms of the Bode plots for stability augmenter-flutter systems using other types of sensors can be inferred by inspection of Figures IX-10 and IX-11. For instance, a system using a stabilized gyro rather than a pitch rate gyro would sense pitch angle instead of pitch rate. In the case of either the rigid body or the fuselage bending feedback, the plots in Figures IX-10 and IX-11 would be altered by the addition of a slope of -6 db per octave to each of the asymptotes, and the entire phase curve would be shifted -90°. For example, the Bode plot of Figure IX-12 altered to pertain to a system using a stabilized gyro would appear as shown in Figure IX-13.

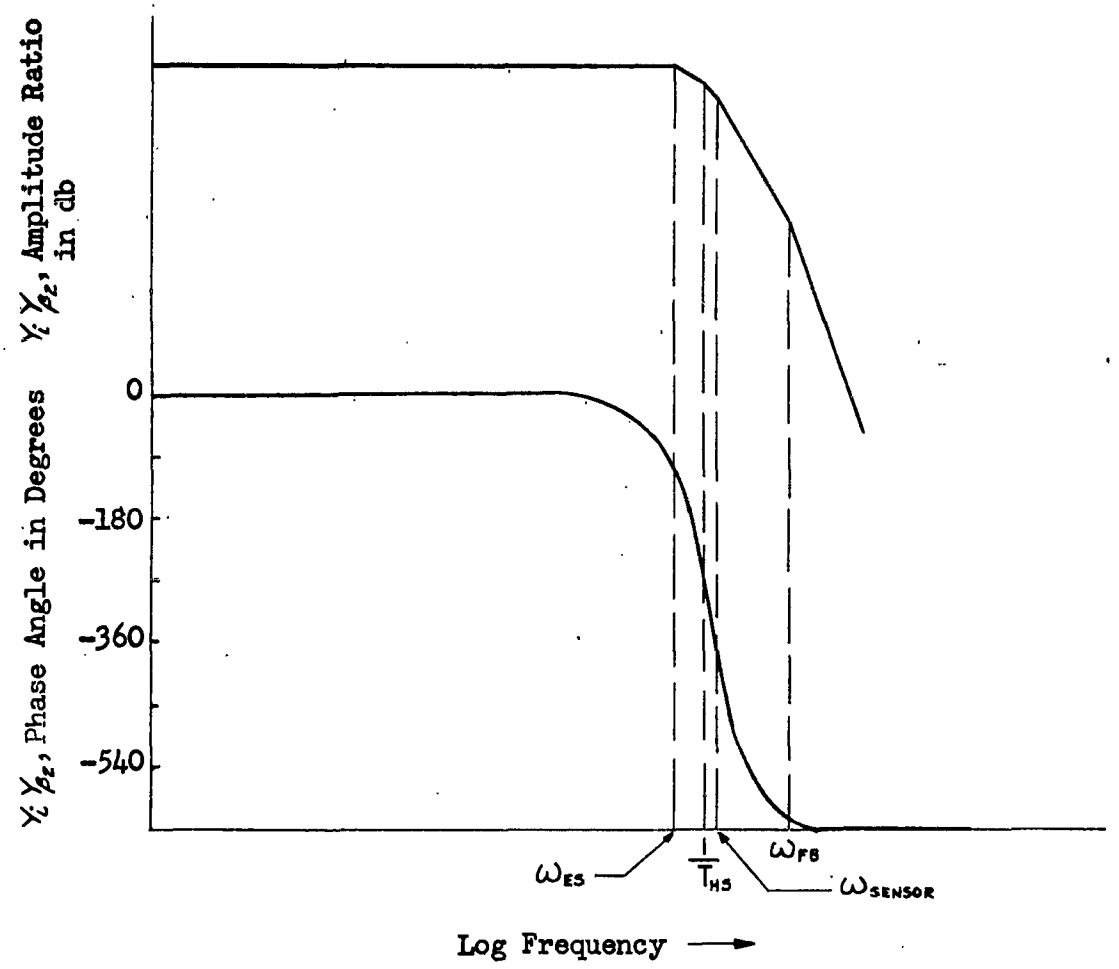

Figure IX-13. Frequency Response of Modifying Term $Y_i Y_{\beta_z}$ for a System Using a Stabilized Gyro

Expressions that account for other types of feedbacks, such as hydraulic valve motion due to cable system movement, can be developed in the manner used in deriving (IX-9).

The technique of modifying the classical flutter equations to account for the presence of complex servomechanism systems has been presented. Chapter X will develop the mechanics of solving these modified flutter equations, i.e., the methods of handling $R(\omega) + jI(\omega)$ modifying terms. The cases where feedback path transfer functions become functions of $b\omega/v$, thereby requiring additional degrees of freedom, will also be discussed.

CHAPTER X

METHODS OF ANALYSIS OF SERVO-FLUTTER INTERACTION*

SECTION 1 - INTRODUCTION

This chapter considers the theoretical determination of the flutter characteristics of a coupled servo-airframe system. The method of attack is the successive consideration of three increasingly complex systems. This approach is chosen as being of particular value in gaining an insight into the manner in which the servomechanism affects the characteristics of a flutter system. It is believed that the method to be used here yields a practical approach to this problem, without departing too radically from conventional methods of flutter analysis. By progressing from a simple system to ones in which more complex problems of interaction exist, a physical feel for the mutual influences of the servo and the flutter system may be obtained.

The three type of systems to be considered are:

1. Single degree of freedom, no structural feedback to servo input.
2. More than one degree of freedom, no structural feedback to servo input.
3. More than one degree of freedom, with structural feedback to servo input.

In (1), the only degree of freedom to be considered is the rotation of the control surface; no deformations of the control surface, the parent surface, or other structures are taken into account.

In (2), the system is to be regarded as having, besides a degree of freedom associated with control surface rotation, additional degrees of freedom which express any combination of the following: Parent surface bending and torsion, fuselage bending and torsion, and control surface torsion. None of the

*Portions of the material contained in this chapter appeared previously in Air Force Technical Report #6287. Special permission for its use here has been granted by Wright Air Development Center.

additional degrees of freedom are to cause any appreciable input to the servo.

In (3), the system is of the type mentioned under (2), but modified by structural feedback which provides an additional input to the servo, with no specification as to how or where the feedback originates.

SECTION 2 - BASIC CONCEPTS

The flutter characteristics of a coupled servo-airframe system may differ considerably from those of a conventional flutter system. A physical understanding of these differences is facilitated by the introduction of three relatively new concepts:

1. Frequency Dependent Restraint
2. "Complex Stiffness"
3. "Feedback Uncoupling"

In addition to their usefulness as aids to intuitive thinking, these concepts have a basic utility in analysis. It is worthwhile, then, to begin the development of methods of analysis with a discussion of these very important concepts.

(a) FREQUENCY DEPENDENT RESTRAINT

In the conventional flutter system, the resistance offered by the control system to control surface rotation is considered to be that provided by a spring of fixed stiffness. The definition of the control system is somewhat arbitrary. It has, in general, several inputs, one of which is the control surface rotation. The determination, either experimentally or by analysis, of a spring constant to be used in the flutter analysis involves some sort of specification of all control system inputs except the control surface rotation. Once the spring constant is established, it is considered to be applicable for any frequency at which flutter may occur. The control surface thus has only one natural frequency of rotation, and this natural frequency is invariant with the frequency of a forced oscillation of the control surface.

For the more complex servo-actuator control system, this simplification is generally not valid; in this case the effective stiffness becomes a complex function of frequency. Why this is true can be seen as follows: Consider that the control surface is removed and that the actuator is grasped at its connection to the control surface horn and its output shaft oscillated with some fixed amplitude and at a fixed frequency. The servo will attempt to hold its output position fixed against the action of this load disturbance. However, due to the nature of the servo system components (electric motors, hydraulic fluid, distributed and concentrated masses and springs), and to the fact that the servo is an error-operated, closed-loop device, the force output of the servo will differ from the disturbance both in amplitude and phase.

In general, the amplitude and phase of the servo response under the above conditions will be functions of the frequency with which the load disturbance oscillates. This indicates that the restraint applied by the servo system to the control surface cannot be adequately represented by the fixed spring of the conventional flutter analysis.

As an example of the possibly serious errors which might be introduced into a flutter analysis when the frequency dependence of restraint is not taken into account, consider the following:

Suppose that a single value of rotational frequency is measured for a given servo actuator--control surface combination, and that this is used in a conventional flutter analysis. Then, unless the resultant flutter frequency is very close to the measured natural frequency, the restraint provided by the servo system at the flutter frequency will not be of the correct amplitude nor in the correct phase to afford adequate control of the surface at this frequency. It may actually occur that although calculations based on this single measured frequency indicate stable flutter characteristics, the

system becomes unstable in practice at some other frequency. This will be the case if the control system restraint of the surface at this other frequency is sufficiently reduced, or if its phase is markedly changed, by the frequency dependence.

It will be noted that both amplitude and phase changes as a result of varying frequency were mentioned in the preceding discussion. If only the amplitude were affected, the servo-actuator system could be regarded as merely a variable spring constant. However, the mention of variation in phase with load disturbance frequency implies that damping (positive or negative) occurs; that is, that the system contains an energy dissipating or an energy producing device. The magnitude of the energy absorbed, or supplied, will also in general vary with frequency.

(b) "COMPLEX STIFFNESS"

The second concept to be introduced is that of the "complex stiffness" of the control system. This is a quantity which can be used to describe the properties of the control system from its input (or inputs) to the point at which the actuator is connected to the control surface. It may be defined as the steady-state reaction on the control surface, exerted by the control system, due to control surface motion at fixed amplitude and at a fixed frequency. It is assumed in this definition that there is no input to the control system other than that due to the surface load disturbance. Since the servo itself is an error-actuated, closed-loop device, it will have an output to counteract this load disturbance, but this will in general differ in amplitude and phase from the disturbance. The complex stiffness thus has a real and an imaginary part, each of which is a function of the frequency with which the surface is oscillated.

The complex stiffness of the control system can be experimentally determined on the ground with the control system actuated only by the control surface motion.

Control surface inertia and aerodynamic forces play no part in determining the complex stiffness. By using the concept of complex stiffness, analyses of conventional and of servo control systems can be performed in the same general way. The stiffness characteristics of the control system can be evaluated in a routine manner. With conventional control systems, the natural frequency can be measured. With the servo type system, a single measurement of natural frequency is not sufficient, but the characteristic for this type can be determined by a frequency response test. Calculated or measured stiffness characteristics can then be supplied to the flutter specialist in much the same way that basic weight or stiffness data are now supplied.

With the approach discussed above, the servo engineer need not become a flutter expert, and the flutter engineer need not become a specialist in calculating the effective stiffness of a control system of either conventional or servo type. Each can concentrate on his own phase of the theoretical investigation and use his experience in his own field efficiently. Their activities correspond to regions of the physical system which join at the connection of actuator and control surface.

(c) "FEEDBACK UNCOUPLING"

The third concept concerns a method of attack for the case where feedback arising from other degrees of freedom may, through the servo actuator, result in control surface response. The input to the actuator may result from elastic deformation of cables or bellcranks, from inertia forces due to concentrated masses, or from the response of sensing devices and servo transducers. Actuator inputs may thus attend an elastic or rigid body degree of freedom in flutter. Hence, if a certain actuator input results from a given degree of freedom, whether it is wing first bending or airplane yaw, this particular input is associated with a fixed shape of the deflection distribution over the airframe,

which in general does not include control surface rotation. The result is that the control surface, because of its fixed position (i.e., $\beta = 0$), is subjected to actuator imposed forces (or moments) as a consequence of feedback. The forces which thus arise from a given degree of freedom (such as wing torsion) are then capable of doing work in the control surface degree of freedom. This is analogous to structural coupling between two generalized coordinates.

To achieve what is in effect feedback uncoupling, it is necessary to consider the previously mentioned wing torsion degree of freedom as including control surface rotation of such relative magnitude and phase as would be determined by the condition that the actuator force applied to the control surface is zero.

Figure X-1 shows simple systems which exhibit these characteristics. Motion is restricted to control surface rotation and parent surface bending (or translation).

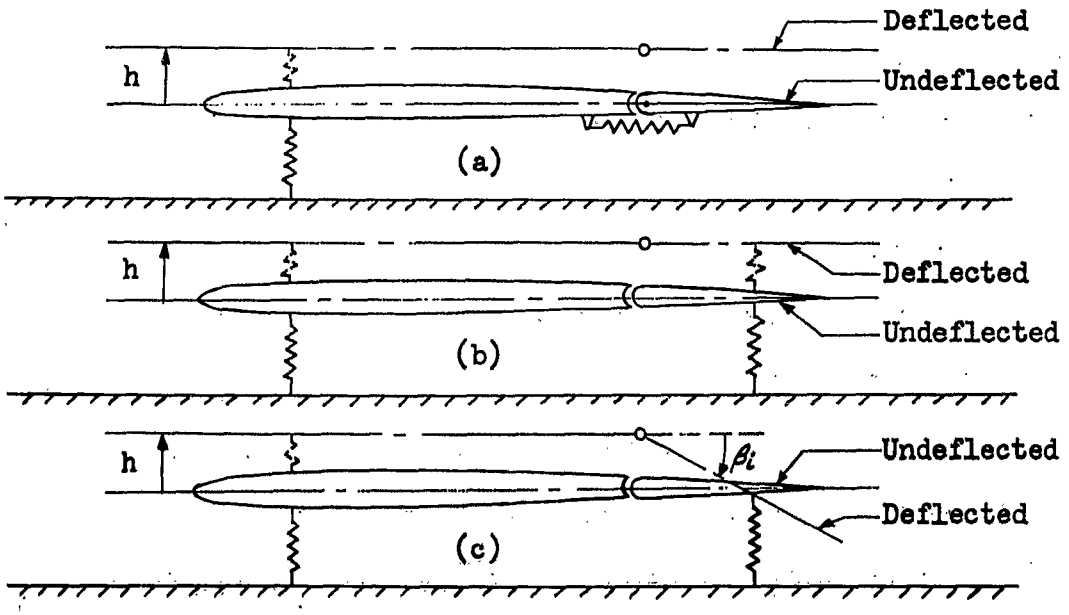

Figure X-1. Simple Systems

Figure X-1(a) represents the general case of a more conventional system, or, more explicitly, the case where the control surface is not subjected to internal

forces (or moments) due to bending of the parent surface. In this degree of freedom, there is no rotation β. It should be noted that this system is also representative of the case of a servo actuator with no feedback.

Figure X-1(b) illustrates the effect of feedback. As a normal consequence of the conventional type of bending mode h (no rotation β), the control surface is subjected to an internal moment due to the stretching of the attached spring. This is similar to the case where bending motion results in actuator inputs, and hence actuator imposed moments on the surface.

Figure X-1(c) illustrates the case shown in Figure X-1(b) except that the bending degree of freedom h is altered to include a proportionate amount of rotation β_i such that the attached spring does not stretch. Hence, no spring (or feedback) coupling occurs in the adjusted bending degree of freedom.

In the simple case shown, there is no phase angle between the bending motion h and the rotation β_i for the directions indicated as positive in Figure X-1. Also, the ratio of β_i to h is a constant and is independent of the frequency of oscillation. However, in the case of a practical servo system, due to the nature of the mechanical, electrical, hydraulic, and structural elements between the source of the feedback and the control surface proper, both the amplitude ratio and the phase angle between the degree of freedom which causes feedback and the "induced" control surface rotation β_i are in general functions of the frequency of oscillation.

In general, then, associated with a given degree of freedom q_i is a control surface rotation β_i , which is determined by the condition that the internal force applied to the control surface is zero. Hence, $\beta_i = R_i q_i$, where R_i is a complex function of frequency.

It should be noted that, in accordance with current techniques of flutter analysis, the q_i degree of freedom (e.g., wing second symmetrical torsion) is

fixed insofar as the shape of its deflection distribution is concerned and is assumed to contribute to the flutter mode, regardless of the flutter frequency, without changing its shape. Therefore, use of this concept implies the need for determining the relationship between the rotation β_i and the deflection q_i for a fixed mode shape and any required frequency. This is not a difficult problem if the major contribution to the servo input is from a single sensing device, such as an accelerometer, because the result of acceleration at the sensor location can be either calculated or measured. However, when the feedback is the result of combined inertia, elastic, and electrical effects and is dependent on both the deflection distribution and the frequency, experimental determination of the physical phenomenon represented by the symbol R_i is difficult.

As an example, consider the case where R_i due to an elastic degree of freedom, say wing bending, is to be determined in a ground test. The control surface is removed to meet the necessary condition of zero force at the horn. The servo actuator is then connected to a light weight link which does not restrict motion of the actuator extension. With proper instrumentation, the actuator extension B_i and the bending motion at a reference point on the wing can be measured. However, except at the natural frequency of the wing bending mode, it is not possible to excite the structure at frequencies much different from this natural frequency and still retain the same wing bending mode shape. Yet, this is required if compatibility is to be achieved between the resultant flutter frequency and the feedback contribution at the flutter frequency.

The difficulty mentioned above, however, does not necessarily restrict the use of this method of attack insofar as the application of experimental results is concerned. Experimental measurements can be made at and near resonant frequencies, and a combination of calculations and engineering judgment can be used to arrive at the character of R_i at frequencies above and below the measured frequency.

The conditions of fixing the mode shape (if the feedback system is dependent on it) and varying the frequency of oscillation can probably be realized in a completely analytical approach to the determination of R_i as a function of frequency.

In the event that there are pressure sensing devices which influence the servo action, and hence the amount of feedback resulting from a given degree of freedom, it may be necessary to determine the function R_i as a function of dynamic pressure, in addition to frequency. In this case, there is the additional complication that compatibility must be achieved between the dynamic pressure at flutter and the feedback associated with the flutter conditions. To determine R_i experimentally in a ground test, it may be necessary to measure B_i at each frequency for each of several typical pressures applied to the sensing device.

SECTION 3 - ANALYTICAL PROCEDURES

The basic concepts discussed in Section 2 are used in the following analytical treatments of the three systems described in Section 1.

(a) ONE DEGREE OF FREEDOM FLUTTER (NO FEEDBACK)

The one degree of freedom flutter case involving only rigid control surface rotation will be considered. Structural twist of the surface is most conveniently handled by considering it as a separate degree of freedom. This is discussed in Section 3(b).

In a manner similar to that employed in current flutter practice, a fictitious damping will be assumed to exist at the control surface horn. The amount of this damping required to maintain steady state oscillations will be determined. A negative value of this damping corresponds to an excitation, i.e., to the presence of a fictitious "energy providing" device. When negative values result, it means that an exciter is necessary to maintain steady state motion. Hence, lacking this exciter, motion would decay. If positive values result, a

damper would be required. Hence, without this required damper, divergence will occur. A zero value of this fictitious damping indicates that the system is capable of constant amplitude flutter without the benefit of either of these fictitious devices.

Consider the case shown in Figure X-2:

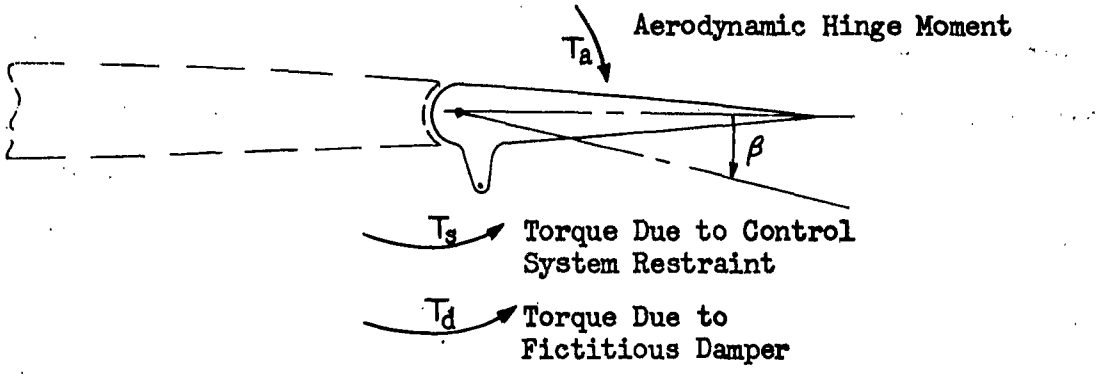

Figure X-2. One Degree of Freedom Case with Fictitious Damper

The torque due to the restraint of the servo control system as a result of constant amplitude oscillatory displacements β can be expressed (in the linear range) as

$$T_s = K\beta \qquad \text{(X-1)}$$

It is important to note that T_s is the reaction supplied by the control system as a result of motion imposed at the control surface. Any servo input that may result would occur due to reflection through the input system as a result of control surface driving motion. The influence of any feedback that may result due to control surface rotation only, for example, feedback through a sensing element attached to control surface, would be integrated within the complex stiffness discussed in Section 2(b).

The complex stiffness K^* is in general made up of real and imaginary parts. Hence,

$$(X\text{-}2) \qquad K = \frac{T_G}{\beta} = K_R + jK_I$$

where

$$(X\text{-}3) \qquad \begin{cases} K_R = K_R(\omega) \\ K_I = K_I(\omega) \end{cases}$$

The torque due to the fictitious damper can be considered proportional to the amplitude β and, in the sense shown, leading it by 90°. Hence,

$$(X\text{-}4) \qquad T_d = j\beta c$$

where c is some arbitrary constant.

If it is desired to consider the damping action as viscous, and the torque, therefore, proportional to velocity, it should be noted that for steady state harmonic motion, $j\beta c$ is replaced by $j\omega\beta c'$. Thus, $c = \omega c'$.

Inasmuch as the object is to find the value of c required for steady state oscillatory motion, the resultant flutter frequency will allow a value of c' to be readily obtained. In addition, here, the realistic case is considered to hold for $c = 0$; hence, also for $c' = 0$. Therefore, the concept of a damping force proportional to amplitude rather than velocity (whether it is structural damping or viscous damping), as employed in classical flutter analysis, need not be considered restrictive. It can be thought of as a convenient artifice employed to obtain equations of a form which can be solved more readily without necessarily sacrificing physical significance.

*For the hydraulic actuator treated in Section 3 of Chapter 9, this complex stiffness is denoted by $C_\beta + C_\beta' = C_{\beta\,TOTAL}$

The aerodynamic hinge moment due to β motion only is obtained from page 34 of Reference . Integrated over the span, for constant β distribution, the total aerodynamic hinge moment is

(X-5) $$T_a = \beta \omega^2 Q$$

where

$$Q = \pi \rho \int b^4 \left[T_\beta - (P_\beta + T_x)(c - e') + P_x (c - e)^2 \right] dx$$

The equation for the one degree flutter case is obtained by the use of Lagrange's equations,

where $\beta = \beta_o e^{j\omega t}$

Kinetic energy $= \frac{1}{2} \dot{\beta}^2 \int I_\beta dx$

Potential energy = 0 (Due to the absence of structural deformation in this degree of freedom)

Work done by external forces due to virtual displacement, δ_β , is $(T_a - T_s - T_d)\delta_\beta$

The resultant equation is

(X-6) $$-\omega^2 \beta \int I_\beta dx - T_a + T_s + T_d = 0$$

or, substituting (X-1), (X-2), (X-4), and (X-5) into (X-6),

(X-7) $$-\omega^2 \beta \int I_\beta dx + \beta (K_R + j K_I) + j \beta c - \beta \omega^2 Q = 0$$

A different measure of the fictitious damping will be introduced for convenience. The relationship between this new damping g_o and c is

(X-8) $$g_o \equiv \frac{c}{K_R}$$

It should be noted that for $K_R > 0$, the quantity g_o has the same physical meaning as has c.

Substituting (X-8) into (X-7) and dividing by $\omega^2\beta$, the equation for the one degree case becomes

$$(X\text{-}9) \qquad I_{\beta_T} - \frac{K_R}{\omega^2}(1 + j g_\beta) + Q = 0$$

where

$$I_{\beta_T} \equiv \int I_\beta \, dx$$

$$g_\beta \equiv \frac{K_I}{K_R} + g_o$$

Equation (X-9) is, of course, essentially no different from the more familiar control surface one degree of freedom equation (see page 63 of Air Corps Technical Report No. 4798), inasmuch as a concentrated real spring of stiffness K_R is equivalent to writing $\omega^2_\beta I_{\beta_T}$. Also, for $g_o = 0$, K_I/K_R is equivalent to the available structural damping.

A solution of (X-9) is accomplished by solving for values of K_R/ω^2 and g_β that are required at each value of $v/b\omega$. From a knowledge of the character of K_R as a function of ω, the compatible value of ω results. From this value of ω, g_o can be obtained by subtracting the available amount of damping (i.e., K_I/K_R) from the required value g_β. The corresponding airspeed is obtained at each $v/b\omega$ by using the compatible value of ω. By taking enough values of $v/b\omega$, a plot of g_o vs. V can be made in the usual manner.

The flutter speed will occur when $g_o = 0$. The detailed procedure is described below:

1. Obtain plots of K_R/ω^2 vs. ω and K_I/K_R vs. ω by calculation, measurement, or any other means desired.

2. Select a value of $v/b\omega$. This fixes the complex number $Q = Q_R + jQ_I$.

3. Compute the required value of K_R/ω^2 from (X-9). This value is equal to $I_{\beta_r} + Q_R$. Compute required value of g_β from (X-9).

4. From plot of K_R/ω^2 vs. ω , pick off value of ω at which the required value of K_R/ω^2 is provided. (If more than one solution exists, obtain each value of ω. In general, there will probably be an odd number of solutions.)

5. Using this value of ω , read the value of K_I/K_R that is available from the plot of K_I/K_R vs. ω .

6. Using this value of K_I/K_R and the required value of g_β , compute g_o .

7. Obtain corresponding value of V from $V/b\omega$, b , and ω .

8. Plot the values of V and g_o on a plot of g_o vs. V . If step (4) resulted in 3 solutions, there will be three points on this plot.

9. Repeat steps (2) through (8) for several values of $v/b\omega$.

10. Pick off flutter speed from plot of g_o vs. V at point corresponding to $g_o = 0$ in the usual manner. At speeds corresponding to negative values of g_o , the system is stable. At speeds corresponding to positive values of g_o , divergent flutter will result.

(b) TWO DEGREE OF FREEDOM FLUTTER (NO FEEDBACK)

The one degree of freedom flutter case discussed in Section 3(a) will be extended to include any other elastic degree of freedom. (Note: The addition of a rigid body degree of freedom, e.g., airplane pitching, does not necessitate a change in the character of the solution for the one degree case.)

The method of solution of the flutter case involving more than two elastic degrees of freedom (no feedback) is discussed in Section 3(c).

The two degree case treated here will consist of:

a. Control surface rotation (as a rigid body) due to control system elasticity (i.e., servo elasticity).

b. Any other elastic degree of freedom, such as parent surface (or fuselage) bending or torsion or control surface structural torsion. It is assumed that deformations in this degree of freedom do not give rise to servo inputs. The feedback case is discussed in Section 3(d).

It should be noted that attempting to account for control surface structural torsion by combining it with control surface rotation as a coupled degree of freedom is not recommended for the following reason:

The implicit assumption made in using the coupled degree of freedom is that the ratio of the magnitude of the structural torsion degree of freedom to the magnitude of the rotational degree of freedom is constant for all (flutter) frequencies. This assumption does not hold for the general case and could lead to more erroneous results for the servo case than for the conventional case, depending on the nature of the frequency dependent stiffness characteristic of the control system.

However, sufficient experience with practical systems may lead to the general conclusion that a coupled degree of freedom can be employed in an analysis involving a servo with a tolerable error in results. Until such time, however, it appears that a theoretical investigation of a flutter mode which may involve a variation in β along the span of the aerodynamic control surface, arising from structural torsion of the control surface,* is more likely to yield realistic results if the structural effects are included as a separate degree of freedom (i.e., rigid control system).

* This is to be distinguished from the well known phenomenon of a variation in β resulting from structural torsion of the parent surface alone. This effect can be included in the usual manner.

A parent surface bending degree of freedom will be added to the one degree case of Section 3(a) with the understanding that the analytical procedure that follows is general for any additional flexible degree of freedom. Then, from page 61 of Air Corps Technical Report No. 4798 the following two equations result:

$$\underline{\bar{A}}\, h_0 + \underline{\bar{C}}\, \beta_0 e^{j\phi_\beta} = 0$$

$$\underline{\bar{G}}\, h_0 + \underline{\bar{I}}\, \beta_0 e^{j\phi_\beta} = 0$$

where, from page 63 of referenced report, for $n = 0$, and $f_\beta \equiv 1$,

(X-10) $$\underline{\bar{A}} = \left[1 - \left(\frac{\omega_h}{\omega}\right)^2 (1 + j g_h)\right] \int_0^L M f_h^2\, dx + \pi\rho \int_0^L L_h b^2 f_h^2\, dx$$

(X-11) $$\underline{\bar{C}} = \int_{L_1}^{L_4} S_\beta f_h\, dx + \pi\rho \int_{L_1}^{L_4} \left[L_\beta - L_z (c - e)\right] b^3 f_h\, dx$$

(X-12) $$\underline{\bar{G}} = \int_{L_1}^{L_4} S_\beta f_h\, dx + \pi\rho \int_{L_1}^{L_4} \left[T_h - P_h (c - e)\right] b^3 f_h\, dx$$

and, for the case considered here, $\underline{\bar{I}}$ is given by (X-9):

(X-13) $$\underline{\bar{I}} = I_{\beta_T} - \frac{K_R}{\omega^2}(1 + j g_\beta) + Q$$

For the determinant to vanish, it is required that

(X-14) $$\underline{\bar{I}} = \frac{\underline{\bar{G}}\, \underline{\bar{C}}}{\underline{\bar{A}}}$$

Now, for a given airframe, and at a fixed value of $v/b\omega$, the following terms can be represented by fixed vectors. Then, letting

(X-15) $$V_1 = I_{\beta_T} + Q$$

(X-16) $$V_2 = \bar{G}\,\bar{C}\,\frac{1}{\int_0^L M f_h^2\,dx}$$

(X-17) $$V_3 = -\left[1 + \frac{\pi\rho\int_0^L L_h\, b^2 f_h^2\,dx}{\int_0^L M f_h^2\,dx}\right]$$

and substituting (X-10), (X-11), (X-12), (X-13), (X-15), (X-16), and (X-17) in (X-14),

(X-18) $$\frac{K_R}{\omega^2} = (1 + jg_\beta) = V_1 + \frac{V_2}{\left(\frac{\omega_h}{\omega}\right)^2(1 + jg_h) + V_3} = V_4$$

The solution to (X-18) is obtained by finding the frequency ω, at which compatibility is achieved between the required value of K_R/ω^2, represented by the real part of the vector V_4 and the available value of K_R/ω^2. Then, in the same manner as for the one degree of freedom flutter case discussed in Section 3(a), the required value of g_β is compared to the available value of K_I/K_R at this compatible frequency. The difference between g_β and K_I/K_R represents a measure of the stability or instability at this value of $v/b\omega$; and, hence, at the associated airspeed.

Now, for a given value of ω_h, and a selected value of g_h, (both being fixed characteristics of the known airframe) the right hand side of (X-18) (i.e., the vector V_4) would be a function of ω. Also, the available value of K_R, in general, would be a function of ω. Therefore, it is clear that, unless K_R can be conveniently expressed in terms of ω, the required solution will involve either a trial and error procedure or a graphical procedure.

Furthermore, if ω_h is not definitely established (e.g., during the early design stages or for a general study), or if the nature of K_R changes as the design progresses, it may be necessary to repeat a major portion of the work for each change of ω_h or K_R. With this in mind, it would be desirable to obtain results which are essentially independent of the magnitude of ω_h or of the nature of K_R vs. ω_h and which, for a minimum of additional labor, could be translated into results corresponding to a specified value of ω_h or a specified character of K_R.

The following procedure, which consists of three steps, is presented as one manner in which the above might be achieved.

Step 1

For a given value of $v/b\omega$, and at an assumed or specified value of structural damping, g_h, calculate the vector V_4 for several values of ω_h/ω from (X-18). This could be accomplished in more than one way. A graphical method could employ the Bleakney circle which is discussed in Air Corps Technical Report No. 4798. The real part of V_4 represents the required value of K_R/ω^2, and the imaginary part of V_4 divided by the real part of V_4 represents the required value of g_β necessary for constant amplitude flutter to occur at each value of ω_h/ω. Repeat for as many values of $v/b\omega$ as deemed necessary.

These results are then plotted as shown in Figure X-3 where curves representing results for two values of $v/b\omega$ are shown.

These plots of required values of K_R/ω^2 and g_β, once obtained, are fixed.

The second step is independent of the first step and is limited to the determination of the complex stiffness as a function of ω.

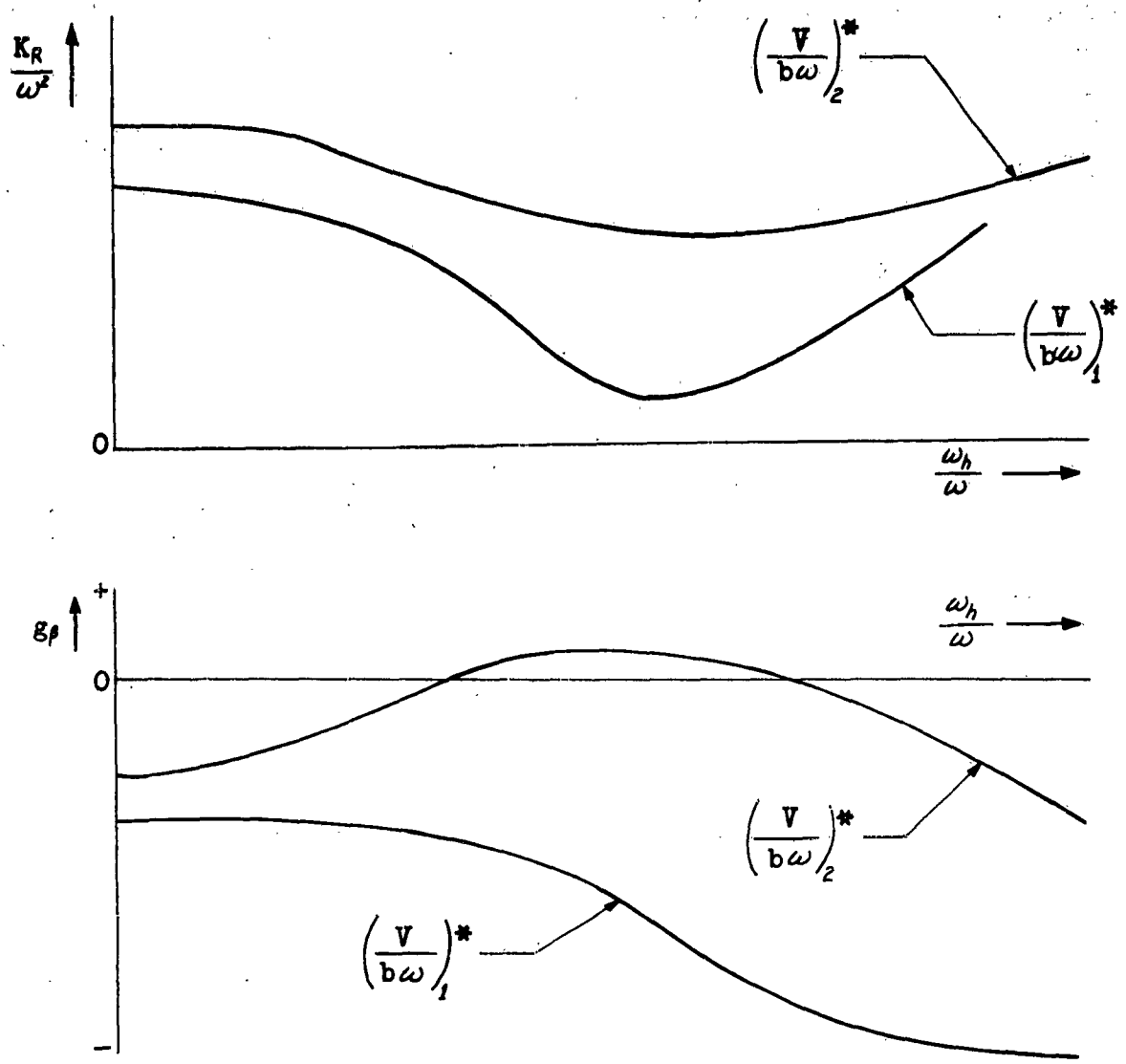

Figure X-3.

Step 2

Determine K_R/ω^2 and K_I/K_R as functions of ω. These characteristics of the control system might be determined by analysis, ** by experimental means, estimated, assumed, etc. In any event, these functions, which are

---

* Numerical subscripts denote particular values of $V/b\omega$.

** The expression for the complex stiffness for a typical hydraulic actuator is developed in Section 3 of Chapter IX.

then plotted as shown in Figure X-4, are intended to represent the available values of K_R/ω^2 and K_I/K_R .

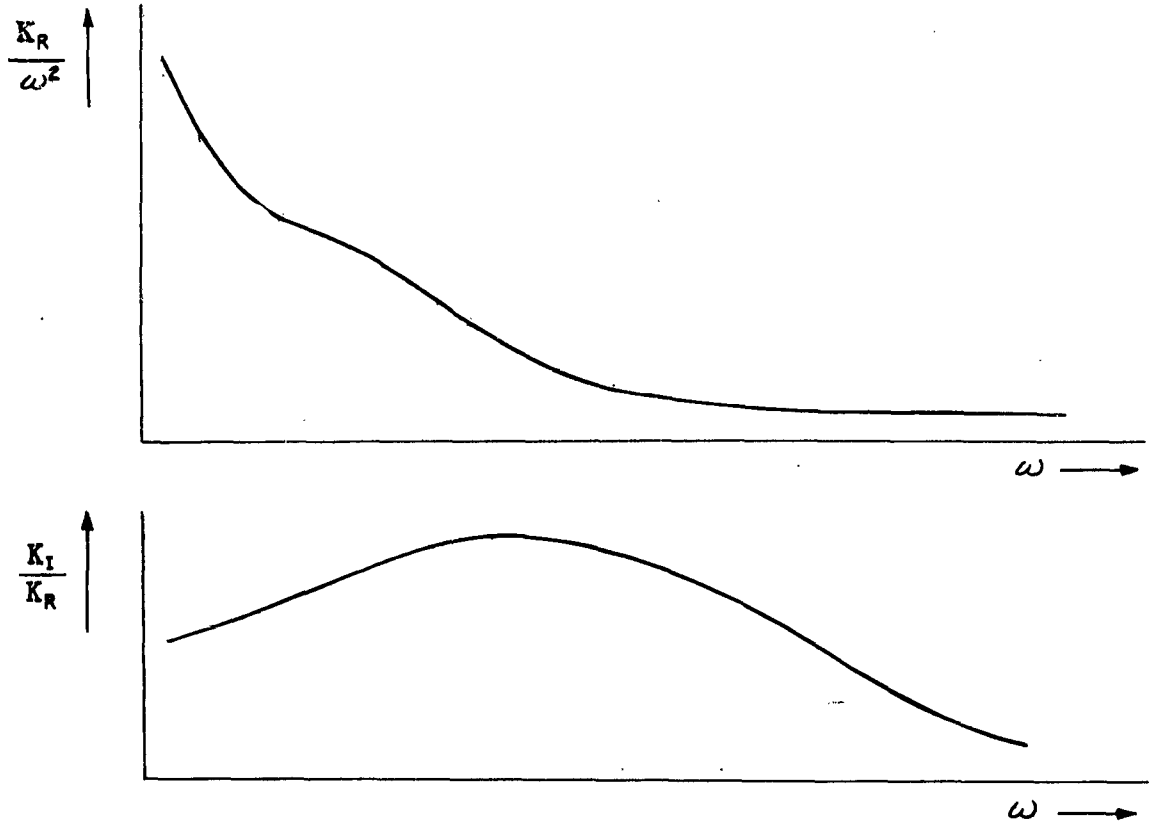

Figure X-4.

Step 3

In the third step, the plots resulting from Step 1 and those obtained in Step 2 are combined in one special chart. This chart allows for the necessary compatibility to be realized between the required value of K_R/ω^2, the available value of K_R/ω^2, the associated value of ω, and any specified value of ω_h. The corresponding values of q_β, K_I/K_R, and V are read directly from this chart.

This chart is made up of four basic types of curves as illustrated in Figure X-5. These are as follows:

Type (1) curves are shown as solid lines. They are dependent only on the ordinate scale, and consist of:

1. A single hyperbolic curve which is a plot of ω vs. $1/\omega$. This is shown in the left center part of the chart.
2. Straight lines, each of which represents a fixed value of ω_h . These are located in the right center part of the plot. (Only one is shown in Figure X-5 but any number may be drawn). The tangent of the angle between this line and the vertical is equal to ω_h multiplied by a constant which is determined by the relative scales of the ω_h/ω and $1/\omega$ ordinates.

Type (2) curves are shown as solid lines. These are results of solving (X-18) (i.e., plots obtained from Step 1). One of each of the following 3 curves for each value of $v/b\omega$. (Only one set is shown in Figure X-5, but curves from all values of $v/b\omega$ may be drawn on the same chart).

1. Curve of (K_R/ω^2) vs. (ω_h/ω) . These are located in the upper right hand part of the chart.
2. Curve of g_p vs. (ω_h/ω) . These are located in the lower right hand part of the chart.
3. Straight line of V vs. ω . These are located in the left center part of the chart.

Type (3) curves are shown as dashed lines. These are characteristics of the control system (i.e., plots obtained from Step 2):

1. Curve of (K_R/ω^2) vs. ω . This is shown in the upper left hand part of the chart.

2. Curve of K_I/K_R vs. ω. This is shown in the lower left hand part of the chart.

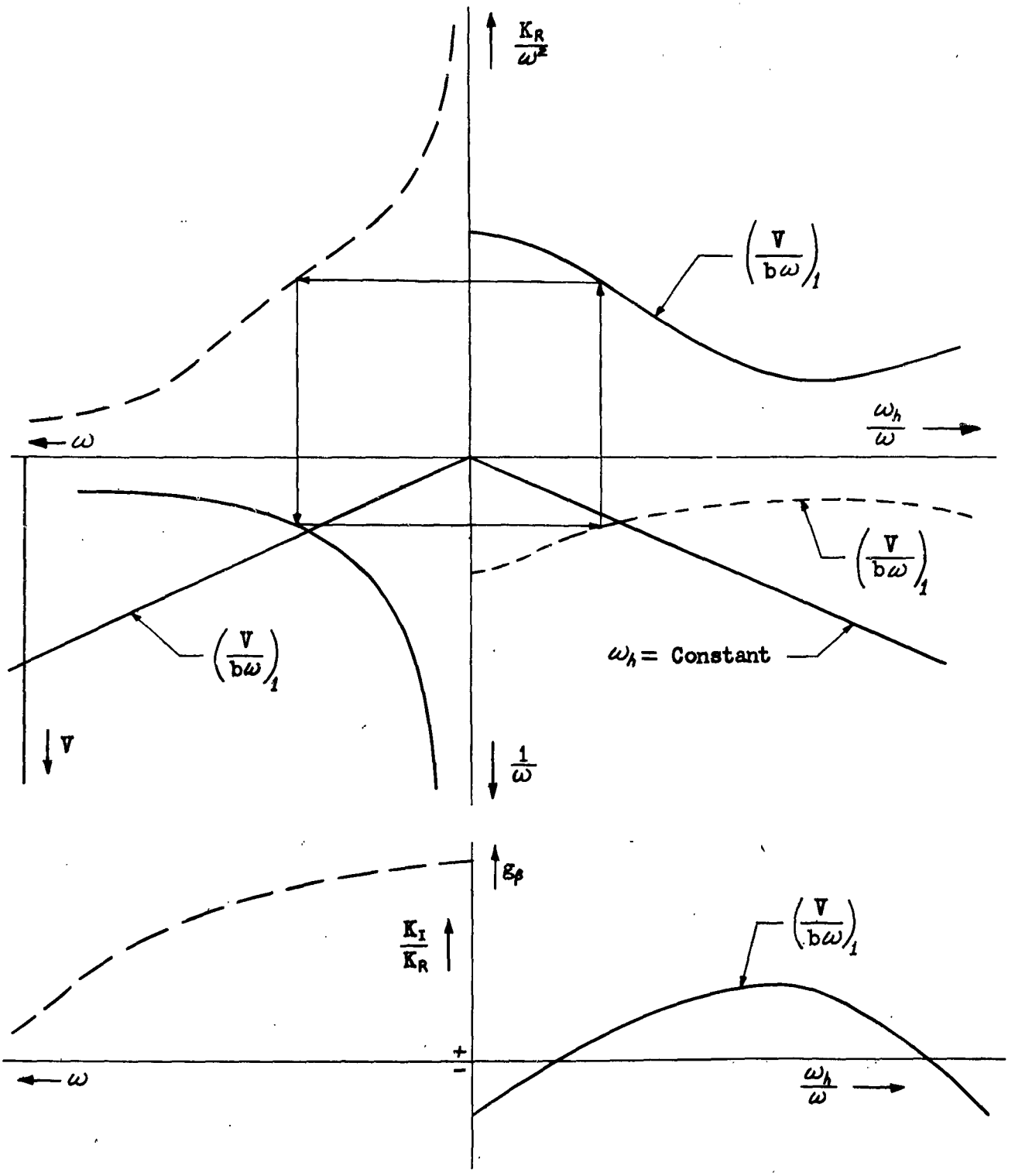

Figure X-5. Chart Showing Procedure for Constructing "Compatibility Curves"

Type (4) curves are shown as dashed lines. These are "compatibility curves", one for each value of $v/b\omega$, and are located in the right center part of chart. (Only one is shown):

1. Curve of (ω_h/ω) vs. $(1/\omega)$. A point, the locus of which describes this curve, is located by straight line projections which form an imaginary rectangle between the (K_R/ω^2) required curve, the (K_R/ω^2) available curve, the hyperbolic curve, and the point in question. An example of the procedure followed in locating any one point on this curve is shown in Figure X-5.

The procedure which, for a given value of ω_h, yields values of the airspeed V, the required damping g_β, the available damping K_I/K_R, and the associated frequency ω, for each value of $v/b\omega$ for which compatibility is achieved, is as follows: (Note: There may be more than one solution as mentioned in Section 3(a).)

For curves corresponding to $v/b\omega$, (see Figure X-6).

1. First proceed along line corresponding to desired value of ω_h to intersection with "compatibility curve" shown as point "a" on Figure X-6.
2. Project vertically down to intersection of g_β curve (point "b"). Read value of g_β.
3. From point "a", project horizontally left to intersection of hyperbolic curve (point "c"). From point "c" up, read ω.
4. From point "c" down to K_I/K_R curve (point "d"). Read available K_I/K_R value.
5. From point "c" down to airspeed (straight) line (point "e"). Read value of V.

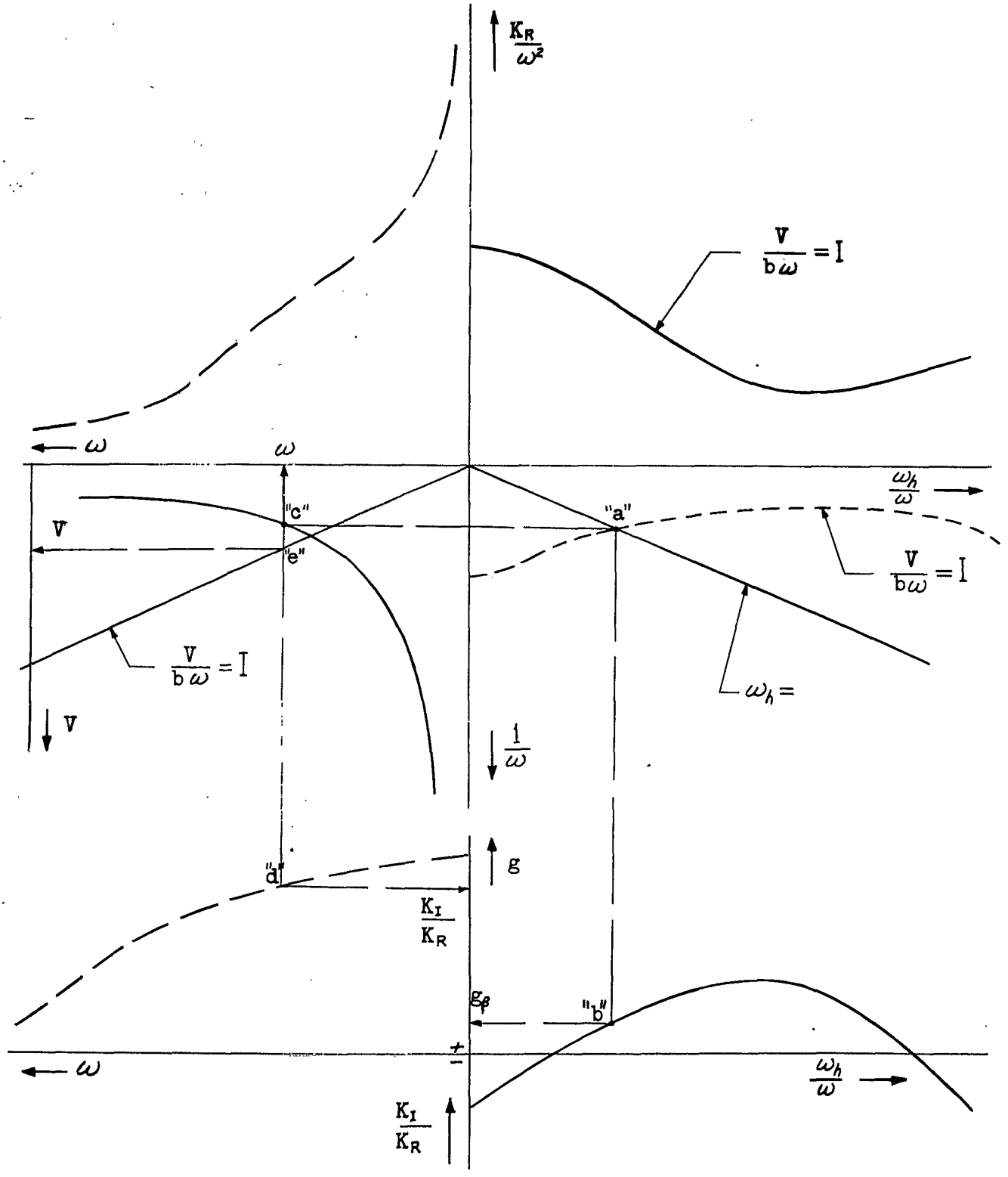

Figure X-6. Chart Showing Procedure for Obtaining Results Corresponding to a Unique Value of ω_h

Repeat steps (1) thru (5) for curves corresponding to $(v/b\omega)_2$, $(v/b\omega)_3$, etc.

Now, for each value of $v/b\omega$, corresponding values of V , g_β , K_T/K_R , and ω have been obtained. As previously mentioned, more than one set of these values are possible for any single value of $v/b\omega$.

The fictitious damping, g_o , is found from (X-9) to be

$$g_o = g_\beta - \frac{K_T}{K_R}$$

At this point a plot of V vs. g_o (for fixed value of ω_h) can be made as shown below.

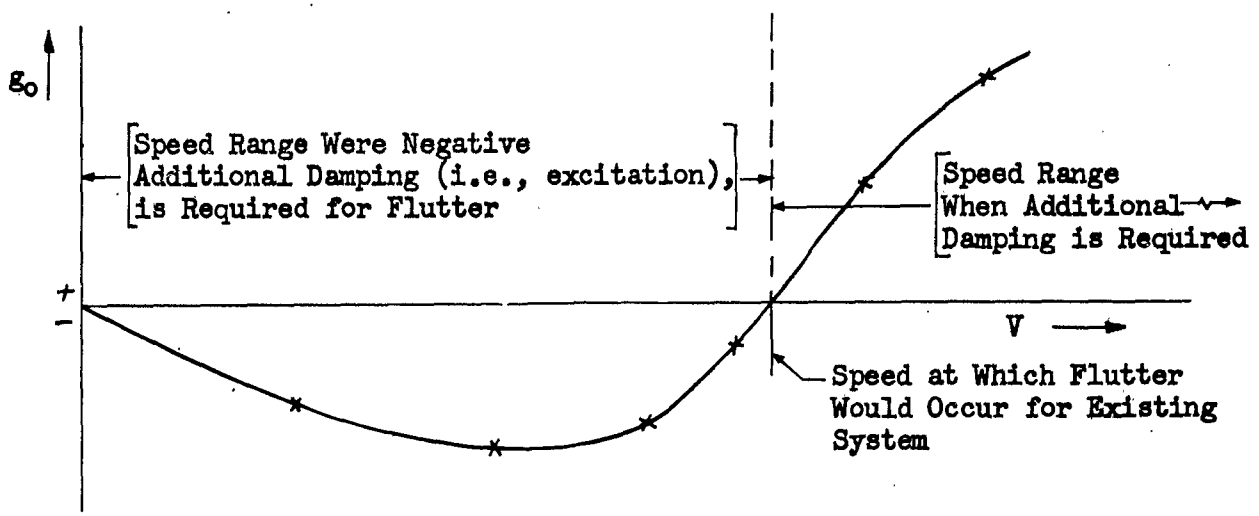

Figure X-7.

It should be noted that:

1. An arbitrary change in the value of ω_h requires a relatively small amount of labor to obtain a corresponding V vs. g_o curve.

2. A change in the nature of the K_R (available) curve requires the construction of new "compatibility" curves, but the curves resulting from the analyses remain unchanged. In this way, several prints of the chart in which Type (3) and Type (4) curves are excluded could be made. Then the effect of changes in the nature of the complex stiffness (i.e., K_R and K_I) could be obtained graphically from these charts with a minimum of effort.

(c) THREE (OR MORE) DEGREES OF FREEDOM (NO FEEDBACK)

The three degree of freedom flutter case is a normal extension of the two degree case discussed in Section 3(b). The additional labor required to include the third degree of freedom here is comparable to that required in adding a third degree of freedom to a conventional Bleakney circle analysis.

A parent surface torsional degree of freedom will be added to the two degree case of Section 3(b) with the understanding that any flexible degree of freedom may be added and the same procedure would still apply.

Page 61 of Air Corps Technical Report No. 4798 gives the following three equations:

$$\underline{\bar{A}} h_o + \underline{\bar{B}} \alpha_o e^{j\phi_\alpha} + \underline{\bar{C}} \beta_o e^{j\phi_\beta} = 0$$

$$\underline{\bar{D}} h_o + \underline{\bar{E}} \alpha_o e^{j\phi_\alpha} + \underline{\bar{F}} \beta_o e^{j\phi_\beta} = 0$$

$$\underline{\bar{G}} h_o + \underline{\bar{H}} \alpha_o e^{j\phi_\alpha} + \underline{\bar{I}} \beta_o e^{j\phi_\beta} = 0$$

Page 63 of the same reference gives the equations for $\underline{\bar{A}}$, $\underline{\bar{B}}$, $\underline{\bar{C}}$, $\underline{\bar{D}}$, $\underline{\bar{E}}$, $\underline{\bar{F}}$, $\underline{\bar{G}}$, and $\underline{\bar{H}}$. These will not be repeated here. The equation for $\underline{\bar{I}}$ is given by (X-13).

For the determinant to vanish, it is required that,

$$(X\text{-}19) \qquad I = \frac{\bar{G}\bar{C}}{\bar{A}} - \frac{\left(\bar{H} - \frac{\bar{G}\bar{B}}{\bar{A}}\right)\left(\bar{F} - \frac{\bar{D}\bar{C}}{\bar{A}}\right)}{\left(\bar{E} - \frac{\bar{D}\bar{B}}{\bar{A}}\right)}$$

This is a more complex form of (X-14). However, by specifying values for g_h , g_α , and (ω_h/ω_α), (X-19) can be written as follows:

$$(X\text{-}20) \qquad \frac{K_R}{\omega^2}\left[1 + j g_\beta\right] = V_s$$

where, for a fixed value of $(V/b\omega)$, the vector V_s becomes a function of (ω_h/ω) or (ω_α/ω), whichever is desired. Then from this point on, the procedure is identical to that outlined in Section 3(b) for the two degree case. The essential difference is that the evaluation of V_s is more laborious. One graphical method of computing V_s is by the extension of the Bleakney circle method to include the third degree of freedom whereby the term (see (X-19))

$$\frac{\left(\bar{H} - \frac{\bar{G}\bar{B}}{\bar{A}}\right)\left(\bar{F} - \frac{\bar{D}\bar{C}}{\bar{A}}\right)}{\left(\bar{E} - \frac{\bar{D}\bar{B}}{\bar{A}}\right)}$$

becomes a vector which is added to the vector obtained from the Bleakney circle plot for a given value of (ω_h/ω) or (ω_α/ω). This is a well known method of solution for a case of this type and will not be discussed in detail here.

The extension to more than three degrees of freedom is, of course, even more laborious, but the same procedure will still apply.

The foregoing has been concerned with the case where specified magnitudes of the structural frequencies were not required until the major portion of the work was completed. In this section, however, the ratios of structural frequencies relative to each other are necessary. In the event that all of the

structural frequencies are known prior to any analyses, the chart would not be required, and the solution would become somewhat more direct.

(d) THE FLUTTER SYSTEM WITH FEEDBACK

The equations for the system in which motion in a degree of freedom other than the control surface degree of freedom results in feedback coupling through the control system are developed by employing the concept of "feedback uncoupling" discussed in Section 2(c).

The feedback terms, i.e., $\mathcal{R}_i$, employed in this treatment are taken as those which do not involve aerodynamic couplings; hence there is no functional dependence on the reduced frequency $v/b\omega$. As an example, consider the two cases described in Section 1 of Chapter IX. In the second of these cases, torsion, α, causes a change in the aerodynamic moment on the aircraft and hence accelerations which are detected by a sensor and in turn result in actuator inputs. If the α degree of freedom involves no motion of the fuselage (e.g., cantilever torsion of wing or stablilizer) and if the accelerometer or bobweight is located within the fuselage, then no actuator input is directly associated with the α degree of freedom. However, if the α mode is a free-free symmetric mode involving fuselage pitching or a coupled mode involving any fuselage motion, there is a direct relationship between accelerations at the sensor and the torsion α. Then, any actuator input arising from sensing elements within the fuselage is associated with zero airspeed modes involving fuselage motion (i.e., airplane rigid body pitching, translation, or roll, fuselage flexible modes). Also, if a sensing element is in the wing, any actuator input resulting from sensor excitation is associated with only those degrees of freedom involving wing motion.

Associated with some degree of freedom (e.g., fuselage side bending) is a control surface rotation β_i which is determined by the condition that zero torque is transmitted to the control surface by the actuator.

The magnitude of β_i due to the feedback which arises from this fuselage side bending mode is not influenced by control surface inertia effects. (Note: In actual practice, the feedback terms could as readily be obtained, either analytically or experimentally, with the control surface attached. However it would then be necessary to exercise care in order to eliminate certain of the inertia coupling terms in the final flutter equations.) With this in mind, a procedure for analytically determining the R_i functions from the transfer functions discussed in Section 2 of Chapter IX would be as follows:

Equation (IX-4) is

$$M_F = \gamma_\beta \beta + \gamma_i x_i \tag{X-21}$$

Equation (IX-9) states that, in general,

$$\gamma_\beta(\omega) = \left[-I_\beta \omega^2 + C_\beta + C'_\beta(\omega)\right] \tag{X-22}$$

Equation (IX-6) is written here for only the h degree of freedom,

$$x_i = \gamma_h h \tag{X-23}$$

In accordance with the requirements for R_i (i.e., $M_F = 0$ and no surface inertia effects) the above three equations, when combined, yield the following expression:

$$\frac{\beta}{h} = \frac{\beta_h}{h} = -\frac{\gamma_i \gamma_h}{C_\beta + C'_\beta(\omega)} = R_h \tag{X-24}$$

where, the γ_h function required to obtain the R_h function is not dependent upon $v/b\omega$.

(e) TWO DEGREE OF FREEDOM FLUTTER WITH FEEDBACK

The two degree case considered in Section 3(b) will be used as an example. The additional complication due to feedback is that the bending degree of freedom is allowed to include some control surface rotation β_h , such that

(X-25) $$\beta_h = R_h h_o$$

(Note: β_h is a constant along the span of the control surface.)

The total angle, β_T , due to these two degrees of freedom becomes

(X-26) $$\beta_T = R_h h_o + \beta_o$$

Now, in lieu of proceeding through the mathematical derivation of the flutter equations here, they will be obtained by inductive means. This procedure will often allow equations (or flutter determinant elements) for systems with more degrees of freedom to be obtained more readily.

Referring to (X-10), (X-11), (X-12) and (X-13) and writing them in determinant form as follows:

(X-27)

Work Done by: h		β Degree of Freedom
Work Done in:		
h	$\bar{A}$	$\bar{C}$
Degree of Freedom β	$\bar{G}$	I

$$= 0$$

It can be seen that each element represents the total work done in a particular degree of freedom by a particular degree of freedom (e.g., $\bar{C}$ represents total work done in the h degree of freedom due to forces arising as a

result of β motion.)

Now, $\underline{\bar{I}}$ represents the work done by

1. Inertia torque
2. Aerodynamic torque
3. Actuator restraining torque (i.e., strain energy)

By separating (1) and (2) from (3), $\underline{\bar{I}}$ can be written as,

(X-28) $$\underline{\bar{I}} = I' - S$$

where from (X-13),

(X-29) $$I' = I_{\beta_T} + Q$$

and

(X-30) $$S = \frac{K_R}{\omega^2}(1 + jg_\beta)$$

Hence, I' represents the work done by the inertia and aerodynamic torques only.

Now, inasmuch as the "adjusted" bending mode due to feedback consists of

1. The bending mode as represented in (X-27)

plus

2. β motion equal to $R_h h_o$.

and, inasmuch as this β motion does not include any actuator restraining torque (due to required condition that this torque be zero), it follows that the work done in the "adjusted" bending degree of freedom by the "adjusted" bending degree of freedom would include a term, $R_h^2 I'$. This term arises from work done by the β component of h_{adj} in the β portions of the h_{adj} degree of freedom. Similarly, the work done by the β component of h_{adj} in the h_o

portion of h_{adj} would be represented by $R_h \bar{\underline{C}}$ (see X-27). Also, work done by the h_o component of h_{adj} in the β portion of h_{adj} is expressed by $R_h \bar{\underline{G}}$, etc.

Extension of this reasoning allows the determinant elements for the case represented by (X-27) with the addition of feedback to be written as

$$(X\text{-}31) \qquad \left[\begin{array}{c|c} \bar{\underline{A}} + R_h(\bar{\underline{C}} + \bar{\underline{G}}) + R_h^2 I' & \bar{\underline{C}} + R_h I' \\ \hline \bar{\underline{G}} + R_h I' & I' - S \end{array}\right] = O$$

For $R_h = O$, the above determinant becomes identical with the "no feedback" case represented by (X-27).

It is worthy of note that the determinant elements for the case with feedback can be written by combining the elements for the "no feedback" case as shown in (X-27) and (X-31). This is advantageous in that if the determinant elements (for a given value of $v/b\omega$) have been calculated for a "no feedback case", the additional work necessitated by the inclusion of the "induced" β, due to feedback, is not prohibitive (for a specified value of R_h).

Consideration will be given to three special cases of a system represented by (X-31), each of which requires a different procedure for solution. These are as follows:

1. R_h does not vary with frequency, ω.
2. The general case where R_h is a function of frequency, ω.
3. The case where flutter of the two degree of freedom system represented by (X-27) exists, and a "beneficial feedback," sufficient to stabilize this flutter mode, is desired.

For the case where R_h (a complex number, in general) does not vary with frequency, a solution can be obtained by following the procedure of Section 3(b). The essential difference is that the determinant elements on the right hand side of (X-14) would be replaced by those shown in (X-31). For a known value of R_h, the additional terms can be readily evaluated.

This case can be thought of as a control surface which is geared to parent surface bending by a linkage with a (complex) gear ratio = R_h. The chart discussed in Section 3(b) would be applicable here.

The general case in which the magnitude and/or phase angle of the vector R_h may vary with the frequency of oscillation requires that an additional condition be satisfied; namely, that compatibility be achieved between the frequency associated with the value of R_h used in an analysis and the frequency resulting from said analysis.

Three slightly different procedures for solution are presented. They are all similar in that they require more computations than do any of the previously discussed systems. Each of these proposed methods requires that different combinations of three of the following five characteristics of the structure be known prior to solving the flutter determinant for the remaining two characteristics. These five characteristics are:

1. The real part of the available complex stiffness (i.e., K_R) as a function of ω.
2. The imaginary part of the available complex stiffness (i.e., K_I) as a function of ω.
3. Both the real and imaginary parts (or the magnitude and phase angle) of R_h as a function of ω.
4. The value of the bending frequency, ω_h.
5. The value of the available structural damping coefficient, g_h.

Method 1.

Here, it is required that characteristics (3), (4), and (5) be known. The object is to solve (X-31) for the value of S (i.e., K_R/ω^2 and q_β) required to sustain constant amplitude flutter. The procedure is as follows:

1. Select a value of $v/b\omega$. Compute aerodynamic terms.
2. Select a value of ω . (Note: This fixes $\bar{A}$ and R_h .)
3. The only unknown left in (X-31) is S . Solving for S yields the value of K_R/ω^2 and the value of q_β required.
4. For the same value of $v/b\omega$, repeat Steps 2 and 3 for several values of ω .
5. Repeat Steps 1 thru 4 for several values of $v/b\omega$.
6. Plot the results as curves of K_R/ω^2 vs. ω and q_β vs. ω for each value of $v/b\omega$ (see Figure X-8).

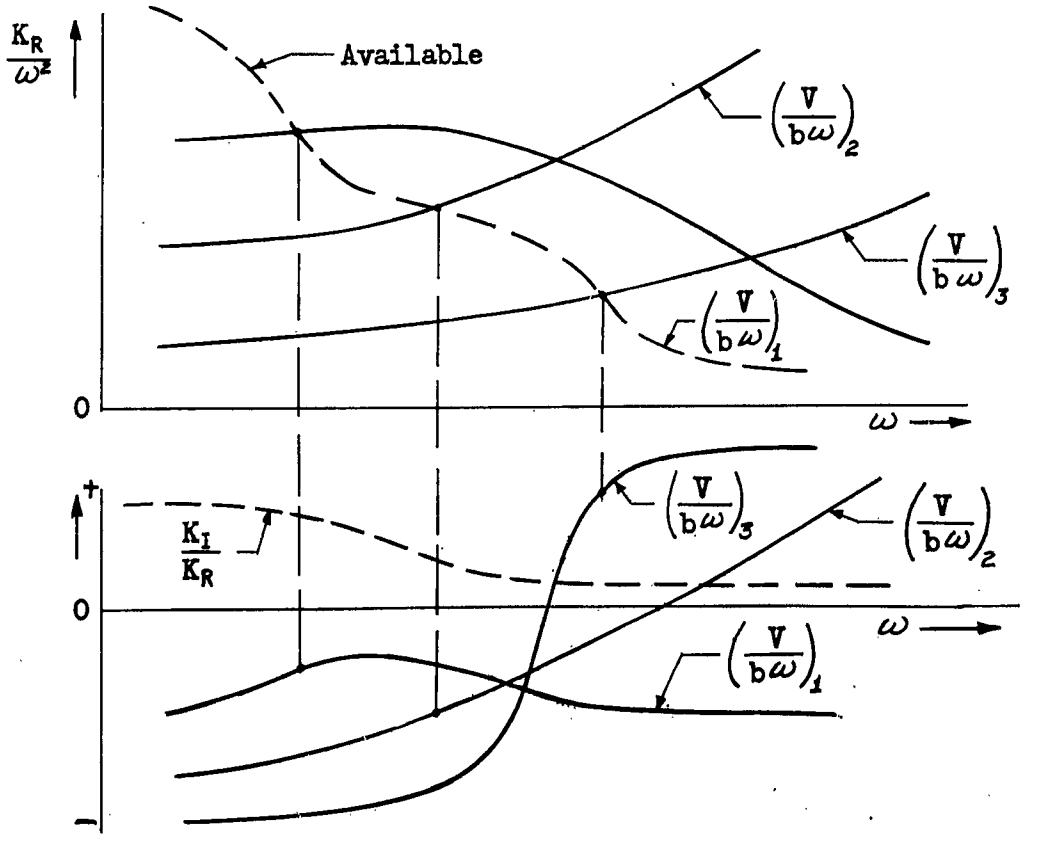

Figure X-8.

7. When characteristics (1) and (2) are obtained, either by analysis, measurement, estimation, etc., plot them as shown in Figure X-8 (shown as dashed curves). Intersection of the curve of available K_R/ω^2 with the curves required K_R/ω^2 determine points at which compatibility exists. Associated values of g_s are obtained from corresponding curves of g_s required.

8. From the resultant values of $\omega(\therefore V)$, g_s required, and K_I/K_R available a plot of g_o (see (X-9)) vs. V can be made in the usual manner.

One advantage of this method over the following two methods is that the effect on the flutter characteristics due to arbitrary variations of K_R (available) and/or K_I (available) can be found with a small amount of additional work.

Method 2.

Here it is required that characteristics (1), (2), and (3) be known. The object is to solve for the values of ω_h and g_h required for flutter to occur. For this method, the fictitious damping, g_o, is not allowed to exist. Hence, $g_s = (K_I/K_R)$ or

$$S = \frac{K_R}{\omega^2}\left(1 + j\frac{K_I}{K_R}\right)$$

The procedure follows:

1. Select a value of $v/b\omega$. Compute aerodynamic terms.
2. Select a value of ω. (Note: This fixes S and R_h).
3. The only unknowns left in (X-31) are ω_h and g_h. Find values of ω_h and g_h required for the determinant to vanish.
4. For the same value of $v/b\omega$, repeat Steps 2 and 3 for several values of ω.
5. Repeat Steps 1 thru 4 for several values of $v/b\omega$.
6. Plot the results as curves of ω_h vs. ω and g_h vs. ω for each value of $v/b\omega$. (See Figure X-9).

7. For a fixed value of ω_h (shown by single dashed line in figure shown below), the resulting intersections with the curves of required ω_h yield compatible values of ω. Associated values of g_h are obtained from corresponding curves of g_h required.
8. From the resultant values of $\omega(\therefore V)$ and g_h required, a plot of g_h vs. V can be made. Intersection of this curve with the available value of g_h indicates the flutter speed in the usual manner.

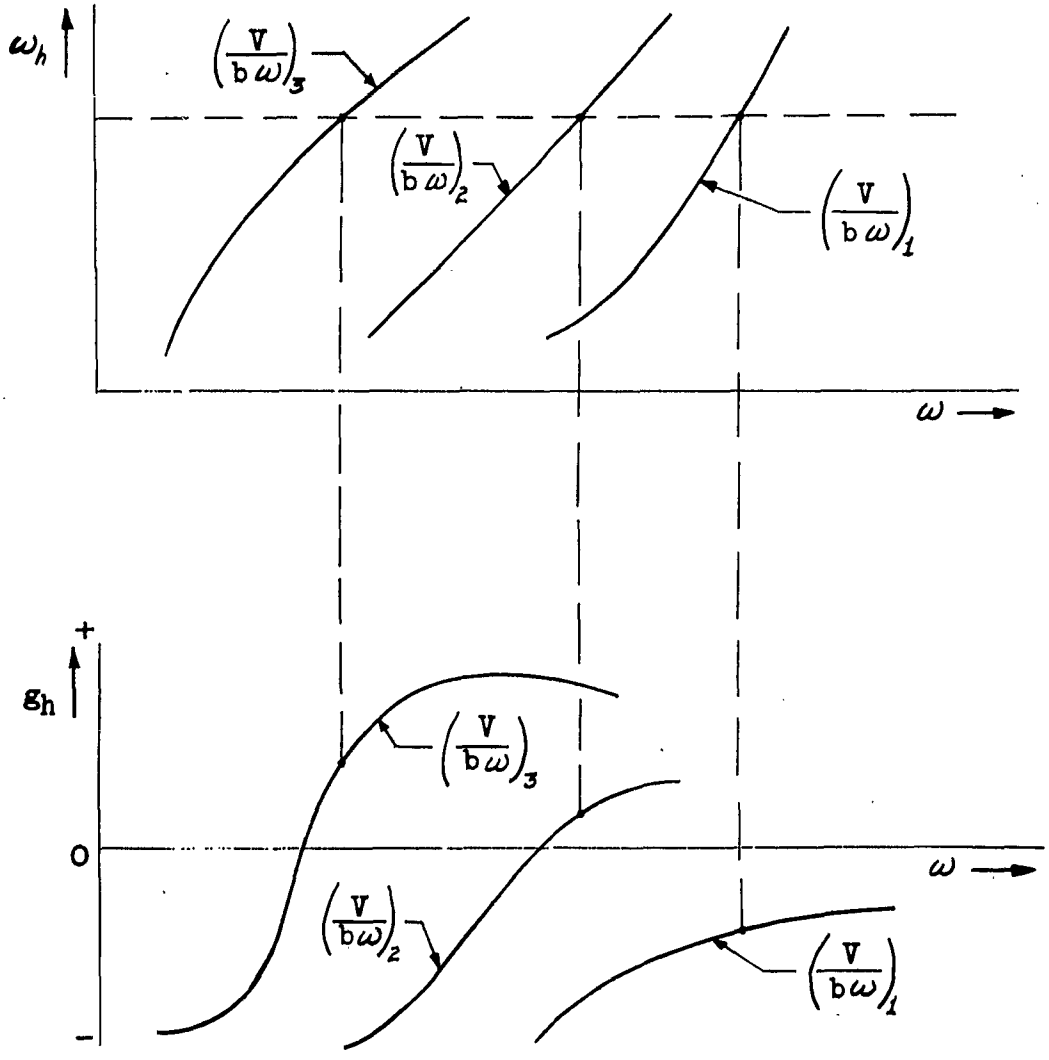

Figure X-9.

One advantage of Method 2 over Method 1 is that the variation of flutter speed with bending frequency (for the same bending mode shape) can be found without too much effort. In practice, however, this is not likely to prove very useful for this type of problem unless a preliminary study is being made wherein R_h , K_R , and K_I functions are estimated.

Method 3.

Here, it is required that characteristic (3) be known. In addition, the ratio of characteristic (1) to characteristic (4) is necessary (i.e., K_R/ω_h^2 as a function of ω). Also g_β and g_h are each represented by g_r . Let

(X-32) $$g_h = g_\beta = g_r$$

(X-33) $$S = \left(\frac{K_R}{\omega_h^2}\right)\left(\frac{\omega_h}{\omega}\right)^2(1 + jg_r)$$

The object is to solve for the values of ω_h/ω and g_r required for flutter to occur. (This is similar to the Material Center Method of Air Corps Technical Report No. 4798.) The procedure is as follows:

1. Select a value of $v/b\omega$. Compute aerodynamic terms.
2. Select a value of ω . (Note: this fixes K_R/ω_h^2 and R_h .)
3. Now, the terms $\bar{A}$ and S (see (X-10), (X-31), (X-32), and (X-33)) each contain the unknown vector, $(\omega_h/\omega)^2(1 + jg_r)$. Solve for the values of ω_h/ω and g_r .
4. For the same value of $v/b\omega$, repeat Steps 2 and 3 for several values of ω .
5. Repeat Steps 1 thru 4 for several values of $v/b\omega$.
6. Plot the results as curves of ω/ω_h vs. ω and g_r vs. ω for each value of $v/b\omega$. (See Figure X-10).

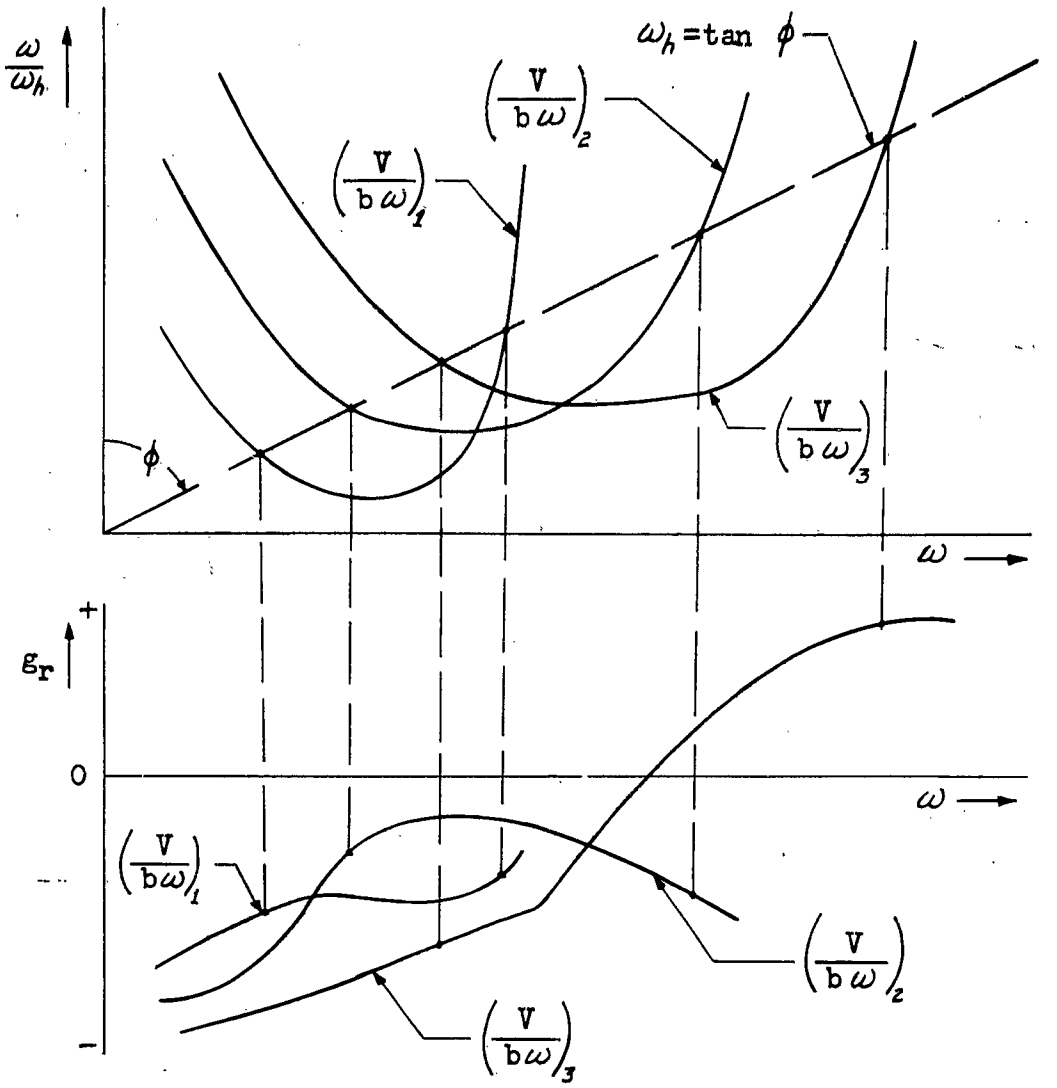

Figure X-10.

7. A straight line drawn from the origin of co-ordinates at an angle, ϕ, from the vertical (see above figure) represents a given value of ω_h (note: $\omega_h = TAN\ \phi$). The intersections of this line (shown as a dashed line in above figure) with the curves obtained from Step 6 represent solutions for this value of ω_h. At these intersections, values of ω (and, therefore V) are obtained. Associated values of g_r are obtained from the corresponding curves of g_r vs. ω.

8. Plot V vs. g_r . The intersection of this curve with g_r equal to the minimum available value of K_I/K_R or g_r equal to the available value of g_h , whichever is less, should yield a conservative flutter speed. It should be noted that if the available value of K_I/K_R , for all practical frequencies, is not approximately equal to the available structural damping, g_h , then either of the first two methods may be more satisfactory insofar as obtaining results that are not unduly conservative.

One advantage of this method over the first two methods is that, for a fixed character of the K_R/ω_h^2 vs. ω curve, the effect of scaling both K_R and ω_h^2 (by the same factors), up or down, can be found in a few minutes.

In Section 1 of Chapter IX, mention is made of a flutter system stability augmenter. This augmenter would be "designed into" the airplane so as to stabilize an otherwise unstable flutter mode by providing, in effect, a source of "beneficial feedback". The design of a device which would be capable of providing a given amount of feedback that is required is another problem.

One possible method of determining the required amount of "beneficial feedback" will be discussed briefly.

Suppose a two degree of freedom system (represented by (X-27)) exhibits divergent flutter for a certain airspeed range and at associated flutter frequencies. The required value of feedback could be found as follows:

1. Allow the existence of some feedback, R_h .
2. Equation (X-27) would then appear as (X-31).
3. From the divergent speed range and associated flutter frequencies, select a value of V and the corresponding value of ω . This fixes the value of $\bar{v}/b\omega$.

4. Let g_h and g_β be sufficiently negative. (At most, less than the available values).
5. The only unknown then left in (X-31) is R_h. Solve for R_h. This is the amount of feedback which, for constant amplitude flutter to occur, now requires more negative amounts of g_h and g_β than are available. Therefore, the available damping would cause motion to decay.
6. Using this amount of feedback, establish that this mode, and all other possible flutter modes, are sufficiently stable by using one of the methods associated with Figures X-8, X-9, or X-10. It should be noted that determination of R_h vs. ω will be necessary before this step can be satisfactorily accomplished. This requires a knowledge of the "beneficial feedback" path from sensing element to control surface.

If this "beneficial feedback" has an adverse influence on a different, and otherwise stable, flutter mode, it would be necessary to relocate the "built in" source of this feedback (e.g., a sensor) in order to obtain an optimum condition.

Experimental verification of this desired feedback might later be realized on the ground by measuring R_h.

(f) THREE DEGREE OF FREEDOM FLUTTER WITH FEEDBACK

For the three degree of freedom flutter case wherein each of the two structural degrees of freedom has a certain amount of feedback associated with it, the equations for the determinant elements will be obtained by an extension of the method employed in Section 3(e).

The three degree case will consist of:

1. Any degree of freedom, p.
2. Any other degree of freedom, q.
3. A control surface rotational degree of freedom, β.

Now for this system without feedback, the flutter determinant would have the following form:

(X-34)

$$\begin{array}{c|c|c|c} & p & q & \beta_o \\ \hline p & A & B & C \\ \hline q & D & E & F \\ \hline \beta_o & G & H & I'S \end{array} = 0$$

where, the equations for each of the determinant elements, A thru H would be obtained in conventional fashion. $I'S$ remains unchanged.

The existence of feedback due to p and q results in control surface rotations β_p and β_q, such that

(X-35) $$\beta_p = R_p p$$

(X-36) $$\beta_q = R_q q$$

Then the total rotational angle, β_T, becomes

(X-37) $$\beta_T = R_p p + R_q q + \beta_o$$

The "adjusted" degrees of freedom can be considered as

(X-38) $$\begin{cases} p_{adj} = p + \beta_p \\ q_{adj} = q + \beta_q \end{cases}$$

Hence, each of the "adjusted" degrees of freedom is composed of motion represented by the original mode shapes (i.e., p and q) and some β motion. Now, by considering each "adjusted" degree of freedom to be composed of two parts (see (X-38)), the determinant elements for the feedback case can be written by properly combining the elements for the "no feedback" system given in (X-34).

As an example, the correction terms to the B element of (X-34) will be obtained. The desired determinant element represents work done in the p_{adj} degree of freedom due to forces and moments arising from motion in the q_{adj} degree of freedom. This can be divided into four parts as follows (see (X-38)):

1. Work done in p due to q motion.
2. Work done in p due to β_q motion.
3. Work done in β_p due to q motion.
4. Work done in β_p due to β_q motion.

From (X-34), it can be seen that

Work done in p due to β_o motion $= C(p\beta_o)$

Work done in β_o due to q motion $= H(q\beta_o)$

Work done in β_o due to β_o motion $= (I' - S)(\beta_o\beta_o)$

Therefore, inasmuch as β_o , β_q , and β_p motions are identical except for amplitude, the above four portions of the "adjusted" element become

$$B(pq) = B(pq) = B(pq)$$

$$C(p\beta_q) = C(pR_q q) = CR_q(pq)$$

$$H(q\beta_p) = H(qR_p p) = HR_p(pq)$$

$$I'(\beta_p\beta_q)^* = I'(R_p p\, R_q q) = I'R_pR_q(pq)$$

* Note: S does not appear in this element.

and the complete determinant element is

$$\left[B + R_q C + R_p H + R_p R_q I'\right](pq)$$

Similar corrections to each of the other affected elements of (X-34) result in the following flutter determinant for the feedback case.

$$\text{(X-39)} \qquad \left[\begin{array}{c|c|c} A + R_p(C+G) + R_p^2 I' & B + R_q C + R_p H + R_p R_q I' & -C + R_p I' \\ \hline D + R_p F + R_q G + R_p R_q I' & E + R_q(F+H) + R_q^2 I' & F + R_q I' \\ \hline G + R_p I' & H + R_q I' & I' - S \end{array}\right] = 0$$

The same reasoning can be applied to cases with more than three degrees of freedom.

It should be noted that for a case in which a system (possibly not a true servo) exhibits irreversible characteristics (i.e., complex stiffness approaches an infinite value) and yet is, by some device, able to sense motion elsewhere in the structure and convert it into a physical motion of the control surface.

Equation (X-39) would include only the four elements corresponding to the p and q degrees of freedom. However, the influence of the induced β motion in each degree of freedom is introduced by the correction terms which are added to the A, B, C, D, and E elements.

The methods presented in Section 3(e) for solving the two degree of freedom case with feedback are applicable to the case represented by (X-39) with the following minor changes (note that both R_p and R_q as functions of ω must be known).

Method 1.

Here it is required to know the natural frequencies and coefficients of structural damping for each of the p and q degrees of freedom (i.e., ω_p, ω_q, g_p, and g_q must be fixed).

Method 2.

Here, let $g_p = g_q = g_r$

Fix, ω_p / ω_q

Solve for ω_p (or ω_q) and g_r.

Method 3.

Here, let $g_p = g_q = g_\beta = g_r$

Fix, ω_p / ω_q as well as K_R / ω_p^2

Solve for ω_p / ω and g_r.

The procedure given in Section 3(e) for solving for a "beneficial feedback" can be applied to the three degree of freedom case. Here, either an R_p or R_q (not both) would be obtained in order to stabilize an otherwise unstable flutter mode.